THE UNIVERSITY OF CHICAGO

HOW TO PAINT A BUTTERFLY?
DEVELOPMENTAL INSIGHTS INTO HELICONIUS EMBRYOLOGY, COLOR PATTERNING, AND PIGMENTATION

A DISSERTATION SUBMMITTED TO

THE FACULTY OF THE DIVISION OF THE BIOLOGICAL SCIENCES

AND THE PRITZKER SCHOOL OF MEDICINE

IN CANDIDACY FOR THE DEGREE OF

DOCTOR OF PHILOSOPHY

GRADUATE PROGRAM IN INTEGRATIVE BIOLOGY

BY

ERICK XAVIER BAYALA RODRIGUEZ

CHICAGO, ILLINOIS

JUNE 2022

TABLE OF CONTENTS

LIST OF FIGURES ..... **v**

LIST OF TABLES ..... **vii**

ACKNOWLEDGEMENTS ..... **viii**

DISSERTATION ABSTRACT ..... **x**

1. GENERAL INTRODUCTION AND BACKGROUND **1**

1.1 *Heliconius* butterflies as a model system for understanding the developmental basis of color patterning 2

1.2 Elucidating the developmental basis of white and yellow variation in *Heliconius* butterflies 4

1.3 Outline for the Dissertation and Experimental Highlights 5

1.4 Result Highlights 6

1.5 Figures 6

2 FROM THE FORMATION OF EMBRYONIC APPENDAGES TO THE COLOR OF WINGS: CONSERVED AND NOVEL ROLES OF ARISTALESS1 IN BUTTERFLY DEVELOPMENT **9**

2.1 Abstract 9

2.2 Introduction 10

2.3 Results 13

2.3.1 *al1* knockouts switch white scales to yellow and black scales to brown but have no effect on yellow scales 13

2.3.2 Al1 staining in embryos recapitulates the previous known role of Al with respect to proper appendage extension 14

2.3.3 Al1 accumulates in future white and black scale cell precursors, but not yellow scale cell precursors 15

2.3.4 Al1 CRISPR knockouts and RNA interference knockdowns reduce levels of Al1 and recapitulate the white to yellow color switch 17

2.3.5 Ommochrome pathway genes are differentially expressed between white and yellow wings 18

2.3.6 Wnt signaling acts as an upstream positive regulator of Al1 19

2.4 Discussion 21
2.5 Methods 26
2.6 Figures 33

3 COMPARATIVE VIEW OF ARISTALESS1 AND ARISTALESS2 EXPRESSION AND FUNCTION ACROSS BUTTERFLY EMBRYOLOGY AND WING DEVELOPMENT **58**

3.1 Abstract 58
3.2 Introduction 59
3.3 Results 62
3.3.1 Al1 and Al2 expression patterns are temporally distinct but still associated with embryonic appendages 62
3.3.2 Al1 accumulates dorsally in developing embryos 62
3.3.3 Al1 and Al2 localization is tightly linked with spines growth and development 63
3.3.4 High Al1 localization is associated with pupal wings scale cell precursors but don't seem to co-localize with nuclei 63
3.4 Discussion 64
3.5 Methods 66
3.6 Figures 68

4 GENERAL DISCUSSION **75**

4.1 Functional differences between Al and Al2 within their role in appendage extension. 80
4.2 Regulatory qualities of Al and Al2 and possible protein interactions 83
4.3 Extranuclear localization of Al1 84
4.4 Finding the functional link between appendages and wing coloration 85

5 APPENDIX 1: APPLICATION OF NOVEL IN VIVO IMAGING TECHNIQUES FOR THE STUDY OF PIGMENTATION IN HELICONIUS BUTTERFLIES. **90**

5.1 Abstract 90
5.2 Introduction 90
5.3 Results 92
5.3.1 White *Heliconius cydno* pigmentation features 92
5.3.2 Yellow *Heliconius cydno* pigmentation features 93
5.3.3 UV light and confocal microscopy can be used to study other features of terminal pigmentation 93

5.4 Discussion 94
5.5 Methods 95
5.6 Figures 97

6 APPENDIX 2: BUILDING A BUTTERFLY WIDE DATABASE FOR THE ANALYSIS OF SCALE ULTRASTRUCTURAL MORPHOLOGY: DISENTANGLING THE WEIGHT OF COLOR IDENTITY AND PHYLOGENY **102**

6.1 Abstract 102
6.2 Introduction 103
6.3 Results 104
6.3.1 Morphological measurements 104
6.3.2 Building a dataset of butterfly scale ultrastructure 105
6.3.3 Preliminary data analyses 105
6.4 Future Directions: 106
6.5 Methods 107
6.6 Figures 108

7 REFERENCES **139**

List of Figures

Chapter 1:

1- *Heliconius* butterfly development outline……7

2- Summary of *Heliconius* wing pattern development…….8

Chapter 2:

3- Wild type and *al1* CRISPR/Cas9 knockout forewings of white and yellow *H. cydno*……34

4- Immunodetection of Aristaless1 in wild-type and -Al1 CRISPR *Heliconius cydno* Embryos……35

5- Immunodetection of Aristaless1 in white and yellow *Heliconius cydno* pupal Forewings…….37

6- Immunodetection of Aristaless1 at the boundary between black and yellow scales in *Heliconius cydno* pupal forewing imaginal discs (3 Days APF)……..39

7- Immunodetection of Aristaless1 in *al1* CRISPR knockout pupal wings of white *Heliconius* cydno forewings (3 Days APF)……..40

8-Analysis of candidate pigmentation genes that may act downstream of Aristaless1……41

9- Aristaless1 is regulated by Wnt signaling……43

10-Graphical model for the role of Al1 in the specification *H. cydno* wing color……...45

11- Detection of aristaless1 by mRNA *in situ* hybridization and Al1 specific antibodies in white *H. cydno*……...46

12- Dot blot test to determine the specificity of the Al1 antibodies…….47

13- Temporal and spatial differences in Al1 protein localization between white and yellow……...48

14-Immunodetection of Aristaless1 in melanic scales for both white and Yellow……...49

15- Immunodetection of Aristaless1 in white *Heliconius cydno* pupal forewings (between 2-3 days APF) across several control setups……50

16- Showcase of the clones variation in Al1 CRISPR adults……...52

17- Showcase of the clones variation by immunodetection in Al1 CRISPR pupal wings (48 to 72 APF)……...53

18- Immunodetection of Aristaless1 in *al1* RNAi knockdown pupal forewings of white *Heliconius cydno* (3 Days APF)……55

19- Downstream ABC transporters qPCR expression analysis between

white and yellow *H. cydno* butterflies……..56

Chapter 3:

20- Immunodetection of Aristaless1 and Aristaless2 in wild-type *Heliconius cydno* embryos early in development……69

21- Immunodetection of Aristaless1 and Aristaless2 in wild-type *Heliconius cydno* embryos late in development……...……...70

22- Immunodetection of Aristaless1 highlighting the dorsal domain of expression in wild-type *Heliconius cydno* embryos across development…….71

23- Immunodetection of Aristaless1 and Aristaless2 in *Heliconius cydno* spines across embryonic development……..72

24- Immunodetection of Aristaless1 and Aristaless2 in *Heliconius cydno* day 1 white pupal wings…….73

25- Schematic representation of Al1 and Al2 Immunodetection across embryonic Development……...74

Appendix 1:

36- Developmental time series of the terminal pigmentation steps of White *Heliconius cydno* pupa……...98

27- Developmental time series of the terminal pigmentation steps of yellow *Heliconius cydno* pupa……...99

28- Yellow *Heliconius cydno* pupa on the last 3 hours of pupation……..100

29- Time series analysis during terminal pigmentation of yellow *Heliconius cydno* pupa under UV light……....101

Appendix 2:

30- Scheme of scales ultrastructure components and details of measured morphological features……....109

31- Preliminary analysis of scale ultrastructure and their relationship with specific color fates……....110

List of Tables

Chapter 2:

T1- qPCR gene primers and efficiency tests……57

Appendix 2:

T2- Meta-data details on measurements on scale ultrastructural morphology across butterflies……113

T3- Selected species, references, and average measurements done for both wildtype and mutant butterflies……...…..114

T4- Raw data table of all the measurements across all our datasets for wild type butterfly scales……116

T5- Data on genetically modified or chemically altered butterfly scales……...135

ACKNOWLEDGMENTS

First and foremost I would like to thank my mother, Jannette Rodríguez Nieves, for being my best friend and biggest supporter. To her, I dedicate this work as it will be a testament of mine and your success. Along with this, I want to thank my family and friends for the support, encouragement, and company in this long journey.

The University of Chicago has been a place of growth and development for me. I am grateful and proud to be part of the community at this University. More specifically thank you to my home Department of Organismal Biology and Anatomy and to my second home in the Department of Ecology and Evolution. I am grateful for all the interactions with faculty, admins, and fellow students along with this entire endeavor. Such growth and development could not have been especially possible without the support and guidance of my amazing thesis committee. I am grateful to Urs Schmidt-Ott, Victoria Prince, and Stephanie Palmer for always keeping me on the right track and guiding my work into its successful completion. Their advice and encouragement have pushed me and my work helping me excel at both my research and professional development.

Finally, I would like to thank the person without whom this thesis could not have been possible, my thesis advisor, Marcus Kronforst. I am really thankful to you for making my work and education possible. You believed in me since day one and even when it was hard for me to believe in myself. This faith in my ability to do the work in this dissertation was always present and kept me going during the most difficult parts. Thank you for your help, constant support, advice, and overall guidance within my education, research, and professional growth. You have developed an amazing space within your lab where each person can excel and grow while always collaborating. For this and many other reasons, I thank you for making this possible.

Along this line, I want to acknowledge the past and present members of the Kronforst lab. My thesis was possible due to your input and collaboration across many of the projects presented in this thesis. Everyone has provided important guidance, help, company, and support across this journal. I especially have to thank two postdocs who made my entire research a possibility. Thank you Darli Massardo and Nicholas VanKuren for the mentorship, collaboration, and friendship across my entire thesis. I would also like to thank the programs and funding sources that both made my research a possibility and provided mentorship along the way. Thank you to the IMSD for the support and training during the early stages of my Ph.D. I also want to thank the Developmental Biology Training Grant for its support and guidance. Thank you to the Art and Science Collaboration Grant and to the National Science Foundation for helping me complete my Dissertation.

Finally, I would also like to thank my support groups. One can find friends in many places and such friends can be there for you in many ways. Gaming has been that realm where friendships were born and developed for me. From my League community to my Final Fantasy Free Company and Static, you all help me stay sane when the pressure was on. Especially Ean James Losselyoung and Manuel Mangual. I can't thank you both enough. You both believe me and support me along the entire way in both my biggest success and most difficult steps and for that and many other reasons thank you.

DISSERTATION ABSTRACT

Butterfly coloration has motivated the curiosity of research across many biological disciplines. It has especially been relevant in trying to address the basis of phenotypic variation. Research in this area has mainly focused on uncovering the genetic basis of such color patterning schemes, leaving the precise developmental pathways linking genotype to phenotype shrouded in mystery. The gene *aristaless*, which plays a role in appendage patterning and extension, has been duplicated in Lepidoptera. One copy, *aristaless1* (*al1*), has been shown to control a white/yellow color switch in the butterfly *Heliconius cydno*, which suggests a novel function associated with color patterning and pigmentation. The second copy, *aristaless2* (*al2*), has had some limited evidence showcasing a color patterning role. However, both copies lack previous research showing whether they still carry out the ancestral role related to appendage development. This highlights the need for the characterization of both ancestral and novel roles with the hope of better understanding how developmental mechanisms are able to bridge the gap between genotype and phenotype. In summary, across this dissertation, I analyzed novel and ancestral roles of *al1* and *al2* across multiple developmental stages and tissues of *Heliconius cydno*.

First I investigated in **Chapter 2** the developmental roles of *al1* in embryos, larvae, and pupae using new antibodies, CRISPR/Cas9, RNAi, qPCR assays of downstream targets, and pharmacological manipulation of an upstream activator. Here I found that Al1 was expressed at the distal tips of developing embryonic appendages consistent with its ancestral role. In developing wings, I observed Al1 accumulation within developing scale cells of white *H. cydno* during early pupation while yellow scale cells exhibited little Al1 at this timepoint. Reduced Al1 expression was also associated with yellow scale development in *al1* knockouts and knockdowns. I also found

that Al1 expression appeared to downregulate the enzyme Cinnabar and other genes that synthesize and transport the yellow pigment, 3–Hydroxykynurenine (3-OHK). Finally, I provided evidence that Al1 activation was under the control of Wnt signaling. I proposed a model for Al1 new color patterning function in which high levels of Al1 during early pupation, which are mediated by Wnt, are important for melanic pigmentation and specifying white portions of the wing while reduced levels of Al1 during early pupation promote upregulation of proteins needed to move and synthesize 3-OHK, promoting yellow pigmentation. In addition, I discussed how the ancestral role of *aristaless* in appendage extension may be relevant in understanding the cellular mechanism behind color patterning in the context of the heterochrony hypothesis.

In **Chapter 3** I investigated the developmental basis of *al2* and expanded on the expression and cellular characteristics of *al1*. Armed with our knowledge and tools from *al1*, I used newly developed antibodies targeting Al2 to analyze its expression profile within embryos. This analysis was done in a comparative framework taking advantage of our previous knowledge from *al1* by doing co-staining of the organisms and tissues. Similar to *al1*, *al2* expression was observed in embryonic appendages showcasing again its expected ancestral role. However, a more careful analysis revealed a few distinct features between Al1 and Al2 subcellular and temporal characteristics. Similar to what has been described in the previous chapter, Al1 was always found to be cytoplasmic or extracellular. Al1 subcellular localization did not co-localize with nuclei. Furthermore, its expression was higher earlier in embryonic development (first 36 hours) and faded as development continued. Al2, on the other hand, had lower expression earlier in embryonic development but did co-localize with nuclei. Al2 expression increased as embryonic development continued. Later in development, Al2 exhibited extranuclear expression but still retained its nuclear localization. Some of the appendages that exhibited this tendency were the mouthparts,

spine, antennae, and legs. I observed the same pattern as well within the eyes. In summary, I found that both Al1 and Al2 still conserve some function with respect to appendage extension but have diverged with respect to subcellular localization and temporal expression.

I closed my dissertation with a discussion section focused on future experiments needed to address some of the questions that still remains. My work has validated the expression and function of Al1 by using knockouts. That work still remains to be done for the observed expression patterns in Al2. Furthermore, when knockouts of both Al1 and Al2 are available we can then ask questions with respect to the level of interaction and compensation between these two versions of the gene. The tight association in terms of localization suggests some interaction should be happening between them. When such experiments are done, we can then get a better understanding of any level of sub-functionalization, as is often seen in examples of duplicated genes. Finally, as part of my dissertation, I built several tools that will improve scientific research done in butterflies. These tools are discussed in the Appendices. **Appendix 1** presents a protocol I adapted from multiple systems to study color patterning processes in living pupae. It allows for *in vivo* imaging during terminal coloration of *Heliconius* wings across multiple days of pupation. **Appendix 2** showcases my work on building a morphological measurements dataset of butterfly scale ultrastructure. With it, I hope to answer whether scale morphology is associated with scale color fate or if it is just a proxy of phylogeny.

CHAPTER 1

GENERAL INTRODUCTION AND BACKGROUND

Animal color patterns have sparked the interest of humanity across many disciplines. From science to art, such marvelous patterns have inspired both curiosity and inquiry. Biology is not the exception to this, from the hypnotic stripes of mammal's fur, to the vibrant colors seen in bird feathers, and the dramatic color shapes seen in butterfly wings, animals have captivated and driven many questions across many disciplines within biological research. Such work has helped us understand the multiple levels of functional relevance that color patterns have for the life history of animals across the world. From predator avoidance by employing color patterns in camouflage, warning coloration, and mimicry, to using them to find a mate and communicate, animal coloration has been a key component for explaining the evolution, ecology, and behaviors of animals (Kronforst et al., 2012). Despite this widespread interest in color patterns, there has been relatively little attention placed on understanding how these patterns are created in the first place.

Within the field of developmental biology, this raises the fundamental question of how color patterns are created and shaped during an organism's development. Furthermore, how alteration to such developmental mechanisms leads to differences in coloration schemes and patterning remains shrouded in mystery greatly diminishing our ability to understand the evolutionary basis of color patterns. To tackle these questions, my dissertation uses *Heliconius* butterflies as a model system to first understand how developmental decisions are achieved and organized to create a pattern and then how alteration to such decisions leads to changes in the coloration scheme.

1.1 *Heliconius* butterflies as a model system for understanding the developmental basis of color patterning

The diversity and complexity of *Heliconius* color patterns is striking. What is even more exceptional, is that in this genus such magnificent diversity is only controlled by a handful of genes (Kronforst & Papa, 2015; Van Belleghem, et al., 2017). The simple genetic basis of such complex and diverse color patterns makes *Heliconius* butterflies ideal to approach questions targeting the developmental principles behind such coloration schemes. Another interesting quality of butterfly color patterning is that the developmental control of coloration happens across multiple early stages of butterfly development, even before the butterfly body plan is visible (Nijhout, 1991). *Heliconius* development starts after egg deposition (**Figure 1,** top panel). At that moment, development proceeds within the egg where the embryo develops for about 48 to 72 hours after deposition. Around 72 hours the caterpillar emerges and starts the first of five larval instar stages (**Figure 1**, middle panel). During larval growth, the wings start their development process within the caterpillar body as imaginal discs (**Figure 2,** top panel, Dinwiddie, et al., 2014, McMillan et al., 2020). The imaginal discs will grow further during pupation as pupal wings (**Figure 2,** top panel) across the seven days of pupation leading to the eclosion of the fully pigmented adult butterfly (**Figure 1**, bottom panel).

The activity of the small set of genes controlling coloration is scattered across multiple stages of this development process and starts as early as larval growth. Such genetic control is temporally distinct and spatially restricted specifying areas of the wings to distinct color fates (Kronforst et al., 2015). A color fate results from a combination of pigments and the optical properties of scales (Nijhout, 1991, McMillan et al., 2020). This color specification process happens within cells called scale cells, which are the pigmented functional units within a butterfly

wing (**Figure 2, middle panel**). These cells are specified to single color fates by the activity of patterning genes in a spatially distinct pattern (Kronforst & Papa, 2015; Van Belleghem, et al., 2017, McMillan et al., 2020). These patterning genes can then recruit specific pigmentation machinery (**Figure 2, bottom panel**; Hines, et al., 2012) and cytoskeletal components to achieve the designated color fate (Dinwiddie, et al., 2014). For example, black coloration was identified to be under the control of the genes *wntA* (Martin, et al., 2012) and *cortex* (Nadeau, et al., 2016), which are both active during larval development and spatially prefigure future melanic patterns during imaginal disc growth. Similarly, red coloration is under the control of the gene *optix* (Reed, et al., 2011; Martin, et al., 2014). However, in contrast to *wntA* and *cortex*, *optix* expression patterns establishe the red elements of the wing during pupation (Reed, et al., 2011; Martin, et al., 2014). Interestingly, such prefiguring observations are not universal for every color patterning gene across development. In the case of *cortex,* the expression domain appears to be less temporally restricted and more fluid across development. Despite also prefiguring the future pigmented pattern during specific timepoints (Nadeau, et al., 2016), recently its subcellular localization has been shown to affect the entire wing (Livraghi, et al., 2021) during pupation. This highlights that different patterning genes expression is temporally complex and to a certain extent very fluid, which enhances the need for careful characterizations that span multiple time points.

In addition to this temporal complexity, these genes also exhibit differences in their modes of action in order to achieve their respective patterning processes. The functional aspects of many of these color patterning genes have not been elucidated. However, based on gene and protein structure I can infer that this set of genes seems to be carrying out their function by employing different cellular mechanisms. For example, *wntA* is known to be a ligand for activating canonical *wnt* signaling (Martin, et al., 2012). On the other hand, *cortex*, which is also responsible for black

pigmentation, is categorized as a cell cycle regulator (Nadeau, et al., 2016). Additionally, and maybe more in line with expectations, *optix* is described as a transcription factor (Reed, et al., 2011; Martin, et al., 2014). By just comparing these examples, it can be observed already how genes involved with color patterning and pigmentation in *Heliconius* appear to have drastically different underlying mechanisms of actions. This further enhances the need to understand not only the patterning/temporal complexity associated with these genes but also the functional aspects associated with their developmental and cellular modes of action.

1.2 Developmental basis of white and yellow variation in *Heliconius* butterflies

In addition to black and red color patterns, *Heliconius* butterflies exhibit variation in white (unpigmented) and yellow (presence of the 3-hydroxykynurenine [3-OHK] pigment; Gilbert, et al., 1988) coloration. White and yellow variation has been biologically crucial for speciation events via mate preference differences and also to the mimicry of other non-palatable butterfly models (Chamberlain, et al., 2009). These color patterns have not been previously analyzed from a developmental point of view, highlighting their value when trying to understand the overall principles governing *Heliconius* coloration. Previous research has identified that white and yellow patterns and the switch among them are controlled by the gene *aristaless1* (*al1*; Westerman, et al., 2018). The gene *al1* stems from a gene duplication event at the base of Lepidoptera (Martin and Reed, 2010). Both the ancestral version *aristaless* (*al*) and the duplicated paralogs *al1* and *aristaless2* (*al2)* had not much information relating them to a color patterning function. However, the ancestral version has been characterized as a key regulator of appendage formation and patterning in flies (Campbell & Tomlinson; 1988, Schneitz, et al., 1993) and across insects like crickets (Beermann and Schroder, 2004; Miyawaki, et al., 2002) and beetles (Moczek, 2005). Such an appendage specification role extends even outside of insects as shown in work from velvet

worms (Oliveira, et al. 2014). There is limited evidence that this appendage development role has been maintained within Lepidoptera where the gene duplication event happened. Research in moths has shown that (*al1*) still carries out such a role with respect to appendage formation by guiding the extension of moth branched antennae (Ando, et al 2018). This background knowledge highlights the question of whether this ancestral appendage role is related in any way with the new color patterning function observed in *al1*.

The question proposed above is a complex one. First, it is not known within *Heliconius* or even butterflies if Al1 still carries out any role with respect to appendage formation during embryogenesis. Secondly, there is no expression data or developmental analysis that provides information on when and how *al1* controls white and yellow color patterns and the switch among such colors. Furthermore, the mechanistic link between the ancestral Al role and the novel Al1 function with respect to color patterning does not exist. Finally how Al2 relates to both of these functions remains a complete mystery.

1.3 Outline for the Dissertation and Experimental Highlights

Across this dissertation, I tackled these questions in a stepwise manner. Furthermore, I built the needed skills to further analyze more mechanistic questions in the future, not just involving *Heliconius* white and yellow pigmentation but butterfly coloration as a whole. This dissertation carefully characterizes the developmental events controlling white and yellow pigmentation in *Heliconius cydno* butterflies. It digs deeper into the developmental events controlling color patterning decisions and compares them to what we know from other genes within the *Heliconius* system. In the process, Al1 and Al2 were characterized with respect to both their ancestral role in appendage formation and in their role related to pigmentation. Furthermore, details about possible links between these two roles are carefully discussed in this work. Finally, and together with new

techniques described in the appendices, this work provides the basis for future research trying to analyze such developmental events in real-time and their implications for scale morphology and coloration overall.

1.4 Result Highlights

In summary, this dissertation proposes that both Al1 and Al2 in *Heliconius* butterflies are still associated with their ancestral appendage role. In contrast, several unique differences are described among them within this function highlighting possible sub-functionalization following the duplication. With respect to their relationship with pigmentation, my work proposes a model in which Al1 activity is needed for achieving the white fate and it is through downregulation of Al1 in the middle of the wing earlier in pupation that the switch from white to yellow can happen in *Heliconius* butterflies. Furthermore, as a result of this characterization, *al1* was found to have wider implications to other aspects of wing coloration. Al1 was found to be active across the entire wing and when this activity was removed, coloration shifts were also seen in the melanic parts of the wing suggesting a wider role than just white/yellow decisions. My work also provides the first description in *Heliconius* pigmentation of both upstream and downstream developmental signals associated with Al1 within its color patterning role. Finally, as part of my Appendices, I produced a database for scale ultrastructure addressing the relationship between color fate and ultrastructure and I describe how live imaging techniques can be applied in the study of terminal pigmentation.

1.5 Figures

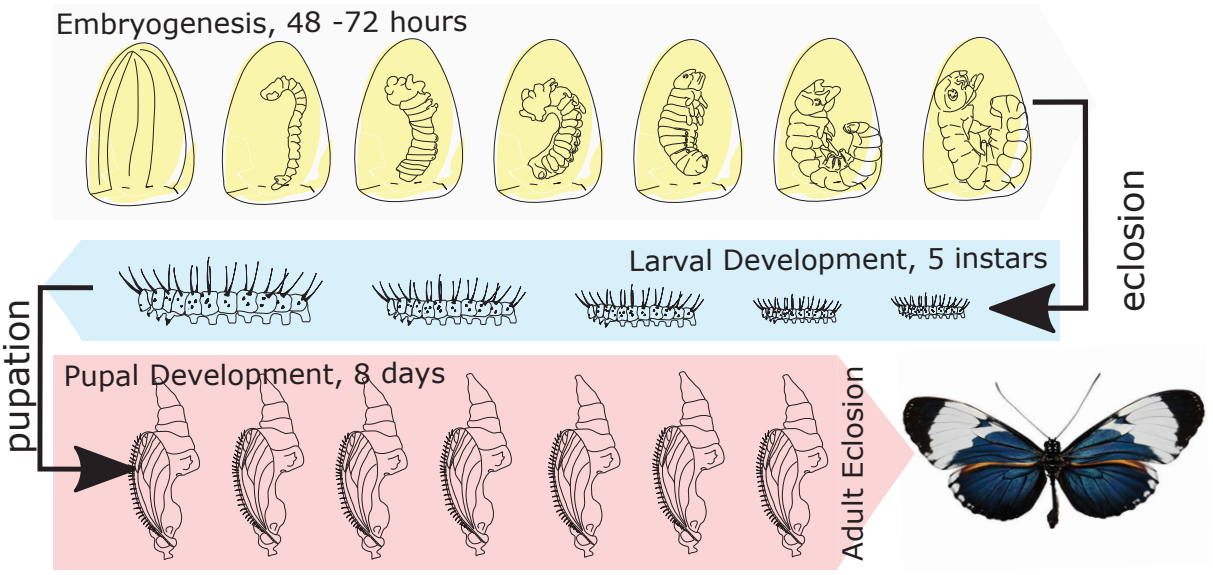

Figure 1: *Heliconius* butterfly development outline. The top panel (gray) of the image shows multiple stages of the embryonic development of *Heliconius* caterpillars following the depositio n of the egg leading to eclosion (around 48 to 72 hours after egg deposition, schemes based on embryology images done by the author of this dissertation). The middle panel (blue) highlights the 5 instars larval stages associated with the caterpillar growth leading to pupation. The bottom panel (red) shows the 8 days of pupal growth leading to the eclosion of the adult.

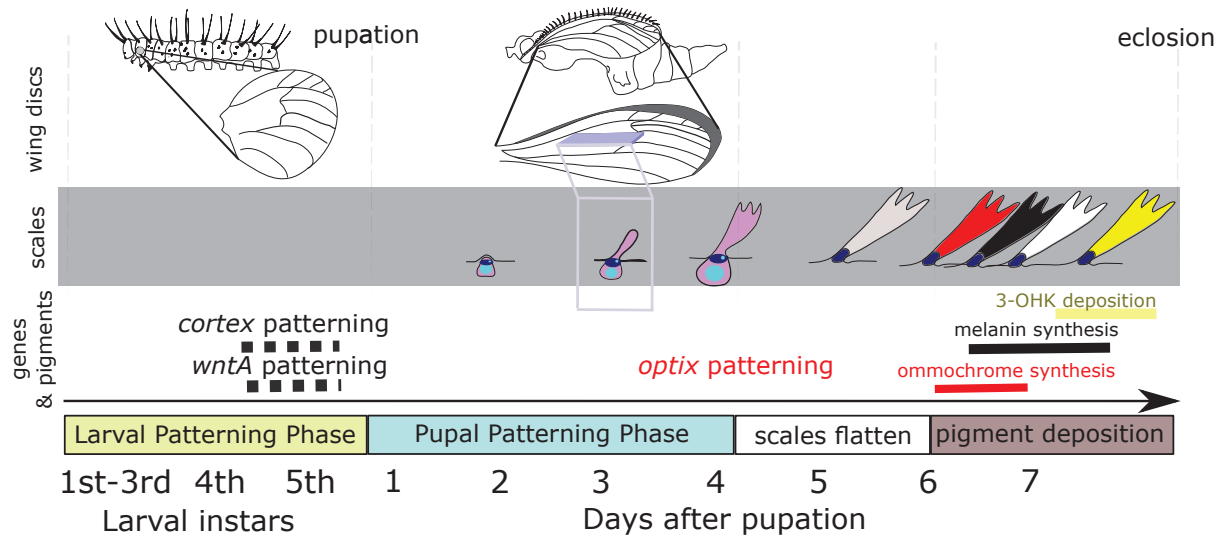

Figure 2: Summary of *Heliconius* wing pattern development. The top panel highlights the wing imaginal discs across the multiple phases of wing development at the organismal level. The middle panel describes developmental changes observed in the functional cells (scale cell in magenta and socket cell in dark blue) that will eventually become the pigmented scales (stages of scale development adapted from *Dinwiddie, et al., 2014*). The bottom panel of the image consolidates our knowledge about when the known patterning genes *wntA*, cortex and *optix* are expressed and when the expression results in terminal color synthesis of melanin and ommochromes, respectively. The yellow pigment (3-OHK) deposition window is also shown. Dashed gray lines separate the different phases.

CHAPTER 2

FROM THE FORMATION OF EMBRYONIC APPENDAGES TO THE COLOR OF WINGS: CONSERVED AND NOVEL ROLES OF ARISTALESS1 IN BUTTERFLY DEVELOPMENT

2.1 Abstract

Highly diverse butterfly wing patterns have emerged as a powerful system for understanding the genetic basis of phenotypic variation. While the genetic basis of this pattern variation is being clarified, the precise developmental pathways linking genotype to phenotype are not well understood. The gene *aristaless*, which plays a role in appendage patterning and extension, has been duplicated in Lepidoptera. One copy, *aristaless1*, has been shown to control a white/yellow color switch in the butterfly *Heliconius cydno*, suggesting a novel function associated with color patterning and pigmentation. Here I investigate the developmental basis of *al1* in embryos, larvae and pupae using new antibodies, CRISPR/Cas9, RNAi, qPCR assays of downstream targets and pharmacological manipulation of an upstream activator. I find that Al1 is expressed at the distal tips of developing embryonic appendages consistent with its ancestral role. In developing wings, I observe Al1 accumulation within developing scale cells of white *H. cydno* during early pupation while yellow scale cells exhibit little Al1 at this timepoint. Reduced Al1 expression is also associated with yellow scale development in *al1* knockouts and knockdowns. I also find that Al1 expression appears to downregulate the enzyme Cinnabar and other genes that synthesize and transport the yellow pigment, 3–Hydroxykynurenine (3-OHK). Finally, I provide evidence that Al1 activation is under the control of Wnt signaling. I propose a model in which high levels of Al1 during early pupation, which are mediated by Wnt, are important

for melanic pigmentation and specifying white portions of the wing while reduced levels of Al1 during early pupation promote upregulation of proteins needed to move and synthesize 3-OHK, promoting yellow pigmentation. In addition, I discuss how the ancestral role of *aristaless* in appendage extension may be relevant in understanding the cellular mechanism behind color patterning in the context of the heterochrony hypothesis.

Specific Acknowledgments:

This work was done in collaboration with **Nicholas VanKuren** (designed and ordered the Al1 antibody, performed the specificity tests for the antibody and guided me on performing the qPCR experiments) and **Darli Massardo** (ordered and synthesize guide RNAs for CRISPR knockouts in addition to performing the CRISPR injections and associated pinning of mutant adults).

I also thank Michael Hennessy and Carlos Sahagun for butterfly care and Steven Lane for assistance with dissections and staining. I also want to say thanks to Urs Schmidt-Ott, Victoria Prince, Stephanie Palmer, and reviewers for discussion and/or comments on the manuscript made about this work.

2.2 Introduction

The diversity and complexity of butterfly color patterns is striking. What is even more impressive is that this color pattern diversity within butterflies is often controlled by a small number of genes (Deshmukh, et al., 2017). Despite the importance of these color patterning genes for the life history and ecology of butterflies, we know very little about how similar or different these genes function during wing color pattern development. *Heliconius* butterflies are a great system to address this issue. In this genus, a handful of genes control the evolution and diversity

of multiple color patterns (Kronforst & Papa, 2015; Van Belleghem, et al., 2017). One example is the signaling ligand *wntA*, which is expressed early within the larval wing imaginal discs and specifies future black patterns on the adult wing (Martin, et al., 2012, **Figure 2**). Another example is the transcription factor *optix*, which controls red color patterns across *Heliconius* by localizing within the nucleus of scale building cells during mid pupation (Reed, et al., 2011; Martin, et al., 2014, **Figure 2**). One last example is the gene *cortex,* which is a cell cycle regulator involved in the specification of melanic elements of the wing (Nadeau, et al., 2016). Despite major developmental differences and although cortex knock-outs may have more widespread effects on scale development (Livraghi, et al., 2021), all three of these genes have expression patterns that spatially prefigure future adult black and red color pattern elements at different stages of wing development. In addition to black and red patterns, multiple *Heliconius* species vary in color on light portions of their wings, specifically whether these scales are white (unpigmented) or yellow (containing the hemolymph derived pigment 3-hydroxykynurenine [3-OHK]; Gilbert, et al., 1988). Recently, the genetic switch between white and yellow scale fates in *Heliconius cydno*, which has historically been referred to as the *K* locus (Kronforst, et al., 2006; Chamberlain, et al., 2009), was traced back to the gene *aristaless1* (*al1*) in *Heliconius cydno* (Westerman, et al., 2018). However, we know little about the developmental basis of *al1* color switching, including how and when during development this gene controls the decision between white and yellow color phenotypes. Furthermore, we have no information about how the developmental biology of *al1* compares to *optix*, *wntA,* and *cortex* and if any general developmental trends, like the spatial prefiguring often described for these other genes, will emerge in the context of *Heliconius* color patterning.

Here I investigate how *al1* specifies white and yellow wing coloration by studying the timing of *al1* transcription and protein localization in developing wings of the butterfly *Heliconius*

cydno, a species with polymorphic wing coloration. The homeobox transcription factor *aristaless1* is one of two paralogs stemming from a gene duplication event that occurred at the base of Lepidoptera (Martin and Reed, 2010). Much of what we know about the single-copy ancestral *aristaless* (*al*) comes from work in *Drosophila* and shows that it is often associated with the extension and patterning of appendages. (Schneitz, et al., 1993). Gene expression studies in flies (Campbell & Tomlinson, 1988; Schneitz, et al., 1993) have shown that *al* accumulates along the distal edges of extending structures such as leg, wing, and antennae during different developmental stages. Furthermore, knockouts of *al* in flies (Schneitz, et al., 1993) often result in malformed or missing distal elements of appendages. These observations in *Drosophila* have been reinforced in other insects like beetles (Moczek, 2005) and crickets (Beermann and Schroder, 2004; Miyawaki, et al., 2002). There is also some information on the developmental role of *al1* in Lepidoptera. For instance, in the moth *Bombyx mori, al1* has been shown to be crucial for the extension and branching patterns of antennae (Ando, et al., 2018). In this example, *al1* expression and protein localization were observed within all of the extending branches of the antennae (Ando, et al 2018). In addition, in some nymphalid butterflies *al2* has been shown to play a role in specifying melanic discal (black patches in the middle of the wing) color pattern elements on the wing (Martin and Reed, 2010). In summary, *al* has been described on multiple occasions and across several organisms as a key regulator of developmental processes. Previous descriptions of *al1*'s role in the extension of appendages and perhaps wing patterning beg the question of how this gene mediates the developmental decision between white and yellow wing patterns in *Heliconius* butterflies.

Here I analyze CRISPR/Cas9 knockouts in adult wings to describe the multiple effects that *al1* has on color patterning in *Heliconius*. I also use a combination of staining techniques to describe Al1 subcellular localization first in embryos appendages, and then across the development of the wing

in order to determine when and where Al1 may be controlling the decision between white and yellow color patterns. Then, I combine knockout and knockdown approaches with our Al1 staining to provide functional evidence for how Al1 subcellular localization relates to the final specification of color pattern. Finally, I perform quantitative PCR (qPCR) analyses to determine possible downstream genes under the control of Al1 and employ a pharmacological agent to dissect the role of an upstream pathway in the regulation of Al1. Our results reveal how *al1* controls white and yellow color patterns formation (specification to pigmentation) in *Heliconius* and help explain the developmental mechanisms leading to a fully pigmented *Heliconius* wing.

2.3 Results

2.3.1 *al1* knockouts switch white scales to yellow and black scales to brown but have no effect on yellow scales

Previous work used CRISPR/Cas9 knockouts to functionally test the involvement of *al1* in the switch between white and yellow wing color in *Heliconius cydno* (Westerman, et al., 2018). In these experiments, genetically white *H. cydno* with an *al1* knockout exhibited a switch of white scales to yellow scales (Westerman, et al., 2018). To study the developmental role of *al1* we generated new CRISPR/Cas9 knockouts and recovered both the previously described as well as novel effects. As previously described, *al1* knockout clones within the white band of a genetically white *H. cydno* switched white scales to yellow (**Figure 3A**). However, careful observation of these yellow clones in white *H. cydno* revealed that when these clones expanded over the melanic regions of the wing, black scales became brown (**Figure 3B**). Previous work reported that Al1 seemed to be acting as a repressor of the yellow fate (Westerman, et al., 2018). Based on this repressor activity I hypothesized that *al1* knockout clones in genetically yellow *H. cydno* would

have no effect on the yellow portions of the wing. In support of this hypothesis I did not see any effects on the yellow parts of the wing, yet interestingly, similar to white butterflies, clones within the melanic regions of yellow butterflies also exhibited a switch from black to brown scales (**Figure 3B**).

These results confirm the importance of *al1* for the development of white wing coloration. If *al1* is knocked out, scales then switch to the yellow fate. However, the newly described *al1* knockout effects in melanic regions suggest a general role of *al1* in scale development across the entire wing, not just in the white/yellow band. Based on the widespread effect observed in white *H. cydno,* I hypothesized that *al1* expression may be important for scale development across the entire wing except for the yellow band of yellow *H. cydno*. I tested this hypothesis by analyzing *al1* expression and protein localization across multiple developmental stages for both yellow and white *H. cydno* butterflies.

2.3.2 Al1 staining in embryos recapitulates the previous known role of Al with respect to proper appendage extension

Most of the previous Al1 work in nymphalid butterflies was done using the DP311 antibody, which is known to label homeodomain transcription factors like Al1. However, this reagent is known to cross-react with similar proteins like the paralog Aristaless2 (Martin and Reed, 2010). In order to avoid this, we developed specific antibodies against *H. cydno* Al1 epitopes to determine the protein subcellular localization and pattern of expression in wings (**Figure 12**).

Before looking into Al1 expression pattern in wings, I tested our antibody specificity in *Heliconius cydno* embryos where I analyzed its relationship relative to the ancestral Al function in appendages. I also aimed to provide expectations of its subcellular localization within appendages

as a point of comparison for wings. Similar to what has been reported in other insect systems (Campbell & Tomlinson, 1988; Schneitz, et al., 1993; Miyawaki, et al., 2002; Beermann and Schroder, 2004) for Al, I observed Al1 localized on the distal tip of appendages extending out of the primary body plan (**Figure 4A**). I observed accumulation within the cellular buds giving rise to the mouthparts within the head region (**Figure 4B**). In addition, I observed a clear accumulation of Al1 within the distal tips of the thoracic (**Figure 4C)**, abdominal (**Figure 4D**), and anal prolegs. I also observed accumulation on the dorsal side of the embryo which has not previously been described in other systems. Surprisingly higher magnification revealed no apparent co-localization with the nucleus of cells at the distal tips (**Figure 4B-D**). To further elucidate our antibody specificity and determine if Al1 expression was causally related to appendage extension, I stained CRISPR Al1 knockout embryos. I observed sections of the embryos depleted for Al1, as expected from a CRISPR knockout (**Figure 4E-G**). In addition, areas depleted of Al1 exhibited elongation defects when compared to the same appendages within the embryos that had normal levels of Al1. In addition to confirming a role for Al1 in appendage extension in *Heliconius* embryos, these data also provide evidence for the specificity of our newly developed antibodies, allowing us to further probe the role of Al1 in wing color patterning

2.3.3 Al1 accumulates in future white and black scale cell precursors, but not yellow scale cell precursors

Previous work with other nymphalid butterflies has shown that *al1* expression on larval wing discs resembles a modified pattern of the *aristaless* gene in flies (Martin & Reed, 2010). Using *in situ* hybridization and antibody staining, I found a similar pattern of expression of *al1* during larval wing disc development in white and yellow *H. cydno* (**Figure 11**). This expression

pattern appears to be unrelated to the white vs. yellow color decision, hence I switched our attention to pupal stages.

Based on our CRISPR/Cas9 results, I hypothesized that Al1 would be present more widely across the wing, including the forewing band, of white *H. cydno* but would be absent from the band in yellow *H. cydno.* Furthermore, quantitative real-time PCR suggested that *al1* is expressed at all pupal stages but generally increases over time (Westerman et al., 2018). I therefore analyzed wings ranging from 2 days to 4 days (before scales harden and become impermeable to antibodies, **Figure 2**) after pupal formation (APF). I aimed my dissections to the 3 days APF mark because it allowed an efficient dissection without compromising the integrity of the wing and staining before any impermeability happens. In white *H. cydno* imaginal discs (Day 3 APF), Al1 was localized in developing scale cells for both future white and black scales (**Figure 5A-D**). This localization of Al1 was observed everywhere across the pupal wing on both the dorsal and ventral sides. Al1 did not appear to co-localize with the scale cell nucleus when analyzing multiple vertical planes (**Figure 5A-D**) similar to what I observed in embryo appendages (**Figure 4)**. Careful observation of a side reconstruction from Z-stacks highlights that Al1 was concentrated within the cytoplasm of scale cells and absent, at least during these time-points, within the nucleus (**Figure 5E**). In contrast, Al1 was reduced or absent inside developing yellow scales (**Figure 5F-K**). This lack or lower levels of Al1 was more apparent during younger time points (day 2 to early day 3) and restricted to the dorsal side of the wing (**Figure 13**). Furthermore, as development continued, the overall level of Al1 on the dorsal side of yellow wings faded relative to that on the ventral side and this was not observed on white *H. cydno* wings (**Figure 13**). Using the vein patterns I inferred boundaries between future yellow and melanic parts of the wing and found a decrease in

fluorescence associated with the transition from the melanic part of the wing to the yellow band (**Figure 6**).

Al1 is a homeodomain transcription factor and so I tested if it co-localized with the nucleus of scale cells at a later time point. Specifically, I examined wings at 4 days APF. In contrast, I found that white and black scales in white *H. cydno* again showed high levels Al1 in the cytoplasm of scale cells but not in the nucleus (**Figure 14**). Similarly, yellow *H. cydno* wings did not show nuclear localization of Al1 in the future melanic regions either (**Figure 14)**. I found no evidence that Al1 ever localized to the nucleus at 2 to 4 days APF, yet it is still possible that nuclear localization does occur at a time point that I did not observe or was not able to analyze. I verified antibody specificity by performing several negative controls and repeating staining in white *H. cydno* butterflies with antibodies against two different Al1 epitopes (**Figure 15A-D**).

These results suggest that the presence of Al1 in scale cells may be relevant for scale development and pigmentation across the entire wing. Presence of Al1 in the non-melanic band (which has already been specified by other genes like *wntA* [Martin, et al., 2012]) inhibits pigmentation resulting in white scales while absence or lower levels of Al1 in these developing scales during a short window early in pupation results in the switch of white scales to yellow scales. To test this hypothesis, I examined Al1 expression in CRISPR/Cas9 knockouts and RNA interference (RNAi) knockdowns, which allowed me to directly correlate changes in protein localization with adult phenotype.

2.3.4 Al1 CRISPR knockouts and RNA interference knockdowns reduce levels of Al1 and recapitulate the white to yellow color switch

To test our hypothesis that reduced or absent Al1 promote the switch from white to yellow, I determined Al1 levels by antibody staining in white *H. cydno* pupal wings with *al1* CRISPR/Cas9 knockouts (70% of the adult wings showed some level of mosaic color switch phenotype). Pupal wings analyzed at 3 days APF exhibited a depletion of Al1 in patches across the wing (**Figure 7**). Our observations with adult butterflies suggest that these clones lacking Al1 result in the switch of white and black scales to yellow and brown, respectively. I also characterized the range of CRISPR clone size and shape by observing a large number of CRISPR clones across the wings of white H. cydno, both in adults (**Figure 16**) and by antibody staining pupal wings (**Figure 17**).

As a complementary approach to test this hypothesis, I used electroporation mediated RNAi (Fujiwara and Nishikawa, 2016) to knockdown locally *al1* in a specific area of the wing. RNAi injections performed hours after pupation recapitulated the white to yellow color switch observed on adult wings observed previously with CRISPR/Cas9 (**Figure 18A-B**). Pupal wing discs were also analyzed by immunostaining at 3 days APF to determine if there was any effect on the protein localization of Al1 after RNAi knockdown. As expected, I found that clones with scales lacking Al1 (**Figure 18C-D**) were concentrated near the injection site. Water injection controls showed no effect on developing scale cells from the injection or electroporation process (**Figure 15E-F**). Both of these results further support our hypothesis that the white scale fate is associated with high levels of Al1 and by contrast lower levels or absent Al1 is associated with the yellow scale fate.

2.3.5 Ommochrome pathway genes are differentially expressed between white and yellow wings

To infer the potential downstream consequences of differential *al1* expression, I compared expression of a number of putative pigmentation genes between white and yellow *H. cydno* wings.

The difference between yellow and white wings is ultimately due to the presence or absence of the yellow pigment 3-OHK. Based on this, I focused on two enzymes involved in the production of 3-OHK, Kynurenine formamidase (Kf) and Cinnabar (Hines, et al., 2012). In addition, there is experimental evidence that 3-OHK or its precursors can be transported directly into the cell from the hemolymph (Gilbert, et al., 1988; Reed, et al., 2008). Therefore, I also analyzed the transporters White, Scarlet, Karmoisin and three members of the ATP-binding cassette (ABC) family, all of which have been implicated in 3-OHK transport or pigment movement in other *Heliconus* species (Hines, et al., 2012; **Figure 8A)**. I found that the enzyme Cinnabar, as well as the transporters White, Scarlet, and Karmoisin, showed increased relative expression in yellow wings compared to white wings (**Figure 8B)**. The increase in relative expression peaked at 6 days APF and exhibited the highest levels in the medial part of the wing (future yellow band). Similar differences were also observed in proximal and distal portions of the wing but to a lesser extent. Kynurenine formamidase (**Figure 8B)** and the ABC transporters (**Figure 19)** showed different trends and did not differ between white and yellow individuals. The results suggest that the white fate is achieved by reducing the expression of enzymes and transporters needed to make and move 3-OHK. This, in turn, suggests that such reduction in activity of genes needed for yellow pigmentation may be a result of Al1's presence. I hypothesize that the reduction in Al1 expression observed earlier during pupation in yellow butterflies leads to the upregulation observed later in the enzyme Cinnabar and the transporters White, Scarlet, and Karmoisin.

2.3.6 Wnt signaling acts as an upstream positive regulator of Al1

Previous work on the role of Al1 in the development of moth antennae has shown that its expression is upregulated by Wnt signaling (Ando, et al., 2018). Therefore, I sought to test the potential role of Wnt signaling in the regulation of Al1 on developing *Heliconius* wings. Given

that the presence of Al1 results in white scale development, I hypothesized that inhibiting Wnt-mediated transcription should lead to reduced or absent Al1 and a white to yellow switch. (**Figure 9A**). In addition, I validated our manipulations on Wnt signaling in yellow butterflies by using an inhibitor against GSK3 which should activate Wnt signaling. Because Al1 is naturally downregulated in yellow butterflies, I hypothesized that activation of Wnt signaling should enhance Al1 expression and promote a yellow to white color pattern switch (**Figure 9A**). Finally, as proof of concept that my pharmacological agents were affecting Wnt signaling, I also assayed the effects of inhibiting and activating Wnt signalizing on the development of melanic scales, which is known to be under the control of WntA activity (Martin, et al., 2014). It has been shown that scales lacking WntA activity become paler or completely revert to a different color fate from the wing (Mazo-Vargas, et al., 2017). Furthermore, previous work has shown that increasing Wnt responsive activity in non-melanic parts of the wing by using the pharmacological agent Heparin switches non-melanic scales into melanic ones (Martin, et al., 2012**)**. Therefore, I hypothesized that reduced Wnt activity in melanic portions of the wing should result in paler or non-melanic scales while activating Wnt in non-melanic parts of the wing should promote melanization (**Figure 9A).**

Our data showed that exposing the pupal wing to the Wnt signaling inhibitor iCRT3 did produce a white to yellow switch as predicted (**Figure 9B-C**). In parallel, when the Wnt inhibitor was used on melanic parts I observed the change from black to a paler color as expected from a WntA knockdown (**Figure 9D-E**). Furthermore, wings exposed to the inhibitor also showed depleted levels of Al1 when comparing the dorsal (in closer contact to iCRT3) and ventral sections on the wing (**Figure 9E-G**). DMSO/PBS controls showed normal Al1 levels, highlighting that the procedure itself did not cause the observed effect (**Figure 9F**). Furthermore, the untreated wing of

the same butterfly showed normal levels of Al1 as well. Yellow wings that were treated with the GSK3 inhibitor CHIR99021, which promotes Wnt signaling, developed white scales as hypothesized (**Figure 9J-K**). Finally, I also observe several melanic scales within yellow band region as expected by a Wnt gain of function (**Figure 9L-M**).

Following exposure to iCRT3, some wings exhibited zones with peculiar scale phenotypes (**Figure 9H**). Examination of these zones showed that some of the scales were normal size and had normal Al1 levels but others were smaller and exhibited lower Al1 levels (**Figure 9H'**). To our knowledge, there have not been any reports of scales showing differential growth rates within the same scale fate. This may be a secondary effect from other gene targets affected by inhibited Wnt signaling and then the lower Al1 levels are just a result of a smaller scale. An alternative explanation could be that Al1 also influences processes related to scale growth and elongation (as shown in other systems; Campbell and Tomlinson, 1988; Schneitz, et al., 1993; Ando, et al., 2018) and by partially depleting its levels with iCRT3 I am altering those functions.

2.4 Discussion

Our results suggest a model for how the decision between white and yellow scale fate is achieved under the control of *al1* during wing development in *Heliconius* butterflies (**Figure 10**). Overall, our data show that Al1 accumulates within the cytoplasm of future white and melanic scales but is depleted from future yellow scales during the early stages of pupation (2 days APF). These results suggest that the presence of Al1 within the cytoplasm is relevant for the specification and/or pigmentation of both white and black scales but not yellow scales. Evidence in favor of this model includes *al1* CRISPR/Cas9 knockout clones that span both white and black portions of the wing. Scales within these clones show a switch to yellow and brown respectively. However, *al1*

knockouts have no observed effects within the yellow band. Knockouts by CRISPR/Cas9 and knockdowns by RNAi result in depleted levels of *al1* in developing scales during early pupation as well as an associated switch from white to yellow scales. Our model is further informed by the preliminary observation that Al1 seems to promote the white color fate by negatively regulating genes important for the synthesis and transport of 3-OHK. In addition, I also validated the role of Wnt as an important upstream signal for Al1 activation providing a more complete developmental context. These functional data highlight how Al1 specifies the development of black and white scales and inhibits yellow pigmentation.

Our results for *aristaless1*'s role in the control of white and yellow wing coloration provide a different patterning scheme for the specification of wing color patterns. Previous work with other *Heliconius* color patterning genes has shown how the expression of these genes during earlier developmental stages (larval or pupal) resembles the future adult color pattern (Reed, et al., 2011; Martin, et al., 2012; Martin, et al., 2014; Nadeau, et al., 2016). This spatial prefiguring is very clear with all three of the previously described *Heliconius* color patterning genes: *optix* (Martin, et al., 2014), *wntA* (Martin, et al., 2012) and, *cortex* (Nadeau, et al., 2016). Furthermore, CRISPR/Cas9 knockouts of both *optix* (Zhang, et al., 2017) and *wntA* (Mazo-Vargas, et al., 2017) result in the lack of their respective color patterns. All of these genes, acting as activators, organize and promote their respective color patterns. On the other hand, I observe that Al1 is present in the entire wing and represses the yellow scale fate. It is the absence of that repression which ultimately results in the color switch and pattern establishment I observe in the adult. While repression is a well-described developmental phenomenon, the color pattern variation achieved via repression of *al1* makes this a unique mechanism relative to other *Heliconius* color patterning genes.

Considering *al1* along with *wntA*, *optix*, and *cortex* it becomes clear that even though all of these genes control wing color patterning, they do so by very different mechanisms. For example, WntA is a signaling ligand that has its effect early within the larval imaginal discs (Martin, et al., 2012). As a signaling molecule WntA is restricted in its ability to diffuse to other nearby cells (Martin, et al., 2012) and therefore it may function primarily during larval development as opposed to pupal development where scale cells are more discrete and distantly distributed. Optix is a transcription factor that is directly localized to the nucleus of red scale precursors during mid-pupation (Martin, et al., 2014), possibly activating downstream targets needed to eventually produce red scales. Cortex is another unique scenario; as a cell cycle regulator in other systems, it is currently unknown how such a protein controls the melanic color patterns it resembles during its pupal expression (Nadeau, et al., 2016). Finally, Al1 is a homeodomain protein involved in appendage extension (Campbell and Tomlinson, 1988; Schneitz, et al., 1993; Beermann and Schroder, 2004, Ando, et al., 2018) which I have found to control multiple aspects of wing pigmentation. Al1 does this by localizing within scale cell precursors during early pupation yet it is specifically depleted from future yellow scales. This information highlights that very different types of genes can be major regulators of color patterning by employing various mechanisms associated with their identity. This developmental description of *al1* serves as the foundation for trying to answer the question of how differences in the levels of *al1* result in the white and yellow color switch. Here I have provided evidence in favor of a model whereby *al1* is, by some direct or indirect mechanism, acting as a repressor of genes involved in yellow pigmentation.

In terms of a direct mechanism, the most straightforward scenario involves Al1 repressing genes involved in yellow pigmentation (*cinnabar*, *white*, *scarlet,* and *karmoisin*) in the nucleus, as

expected of a transcription factor. However, I am particularly intrigued by the observation that Al1 was never found localized in the nucleus during the analyzed time points. It is important to acknowledge that there could still be a specific time point in which Al1 translocation happens leading to the transcriptional control of downstream proteins needed for proper yellow pigmentation. In addition, there is a possibility that a post-translational modification—for example a cleavage event like the ones observed in BMP proteins (Künnapuu, et al. 2009) or in another Paired-like homeodomain protein ESXR1 (N-terminus translocate to the nucleus and C terminus stays cytoplasmic, Ozawa, et al., 2004)—occurs with Al1 which affects our ability to observe nuclear co-localization. However, regardless of the possibility of our inability to observe a possible nuclear localization of Al1, there is still experimental evidence showcasing that some transcription factors can regulate other downstream processes and showcase dynamic states between cytoplasmic and nuclear localizations. For example, the protein Extradentricle (Exd) which is exported to the cytoplasm when Homothorax is not present (Abu-Shaar, et al., 1999) can exhibit different patterns of cytoplasmic or nuclear localization depending on what part of the leg imaginal disc is being patterned (Abu-Shaar, et al., 1999). Furthermore, in such a system an increase in the accumulation from cytoplasmic Exd can lead to an overcoming of the signals keeping the protein cytoplasmic, allowing a portion of them to go into the nucleus even when Homothorax is not present (Abu-Shaar, et al., 1999). This is an interesting case considering that both Exd and Al1 are homeodomain proteins and similar accumulation is visible in our data. Therefore, it is possible that Al1 could act as a direct regulator (by an un-observed nuclear translocation or a cleavage event) of the differentially expressed genes needed for yellow pigmentation.

An alternative possibility is that Al1 regulates wing pigmentation indirectly via a process known as the Heterochrony hypothesis (Koch, et al. 2000). This is an interesting possibility based

on what we know about the role of Aristaless in appendage extension (Campbell and Tomlinson, 1988; Schneitz, et al., 1993; Ando, et al., 2018) and based on our data showing dIfficiency of appendage extension following Al1 knockouts. Although, Aristaless is described as a homeodomain transcription factor, most of the literature describing its expression and subcellular localization is related to its role during the extension of body appendages at both the single-cell and multicellular level (Campbell and Tomlinson, 1988; Schneitz, et al., 1993; Ando, et al., 2018). In *Drosophila*, Aristaless is well characterized for its role in the extension and proper patterning of the arista (a highly modifiable bristle that extends out of the antennae). Previous work has shown that if Aristaless is not present, pronounced size reductions and malformations of the arista occur (Schneitz, et al., 1993). Similar elongation defects to the ones I observed in our embryos are seen when Al1 expression is reduced in the multicellular antennae of moths. In this system, Al1 is needed for the proper patterning and the directional elongation of the cells that form part of the antennae. Furthermore, outside of insects the Aristaless-like Homeobox (ALX) protein is a key regulator of rodent pigmentation (Mallarino, et al., 2016). Such regulation in principle is controlled by adjusting the rate of maturation of melanocytes, which are the pigmented cells that ultimately carry out the pigment synthesis of the hairs on the rodent body (Mallarino, et al., 2016). These observations support the idea that Al1 could be controlling pigmentation outcomes by altering rate of scale development. Another, piece of evidence that further promotes Al1 as a candidate capable of regulating the cell cycle and affecting scale maturation time, is again the Paired-like homeodomain protein ESXR1. The C-terminal region of ESXRI stays in the cytoplasm after proteolytic cleavage and inhibits cyclin degradation which regulates the cell cycle and even produces cellular arrest (Ozawa, et al., 2004). This effect on the cell cycle produced by a cleaved component of a paired-like homeodomain protein makes it an appealing mechanism for the

heterochronic shift I am hypothesizing. These examples raise the possibility that Al1 may be altering the developmental rate of scales which, in turn, influences color by indirectly altering expression windows of transporters and enzymes necessary for pigmentation. Yellow pigmentation in *Heliconius* happens just a few hours before eclosion, and therefore small alterations to the developmental timing of scales could result in the presence or absence of 3-OHK.

Future work will determine whether Al1 directly affects downstream target genes by regulating their transcription or indirectly as a secondary effect from altering scale maturation time. Our work serves as the first developmental description of Al1 and helps us understand butterfly color patterning as a stepwise process involving multiple layers of gene regulation terminating in pigmentation. Our work also highlights the diversity of genes and developmental mechanisms responsible for butterfly wing patterning.

2.5 Methods

Butterflies rearing

Butterflies were reared in greenhouses at the University of Chicago with a 16h:8h light:dark cycle at ~27ºC and 60% – 80% humidity. Adults were fed Bird's Choice artificial butterfly nectar. Larvae were raised on *Passiflora biflora* and *Passiflora oerstedii*.

CRISPR/Cas9 injections

CRISPR/Cas9 experiments were performed following Westerman et al. (2018). We used HC_gRNA_02_Al1 (GTTCTAGGAGAATCGTCCTTTGG) and HC_gRNA_03_Al1 (GGAGGAGGTCTCTCGGAGGCTGG) gRNAs to generate deletions in *Al1* in *Heliconius cydno galanthus* and *Heliconius cydno alithea* (**Figure 3).** The concentration of Cas9 (PNA Bio) and sgRNAs varied between 125 ng/µl−250 ng/µl and 83 ng/µl−125 ng/µl, respectively. Mixes were

heated to 37ºC for 10 min immediately prior to injection and kept at room temperature while injecting. To collect eggs for injections, we offered adults fresh *Passiflora oerstedii* and allowed ~2 hours for oviposition. Eggs were washed for 2 min in 7.5% benzalkonium chloride (Sigma Aldrich), rinsed thoroughly with water, and then arrayed on double-sided tape on a glass slide for injection. The eggs were injected using a 0.5-mm borosilicate needle (Sutter Instruments, Novato, CA, USA) and then kept in a humid petri dish until hatching, then transferred to a fresh host plant and allowed to develop. Adults were frozen and pinned before imaging. Following injection, 69 white and 4 yellow individuals reached adulthood. From them, 40 white, and 3 yellow individuals had a phenotype.

Imaging of wild type and CRISPR adult wings

Butterflies were pinned to flatten the wings and dry the tissue allowing for better imaging and then photographed. Details of wild type and adult wings were imaged using a Zeiss stereomicroscope Discovery.V20 with AxioCam adapter. Z-stacks and maximum intensity projections were produced using the Axiovision software. All Images had their intensity and scale bars edited with ImageJ Software.

Butterfly wing dissections

Butterflies were dissected at both larval and pupal stages following Martin et al. (2014). The protocol and adaptations to it were carried out as follows. Larvae and pupae were anesthetized in ice for 20 mins before dissection. To obtain the larval wing discs the larvae were pinned on the first and last segment. A small cut was performed using micro-dissection scissors on the second (forewing) and third segment (hindwing) to remove the imaginal discs. The discs were then pipetted out to a 16 well tissue culture plate with 1 ml per well of a 4% Paraformaldehyde solution

for fixing. Larval imaginal discs were then fixed between 20 to 30 mins. To obtain the pupal wing discs the pupae were pinned on the head and most posterior section of the body. The denticle belt was then removed using dissection forceps to allow for easier access to the wing. Then micro-dissection scissors were used to carefully cut around the wing margin using the pupal cuticle as a guide. The piece of cuticle together with the forewing imaginal disc was removed and placed directly in a 16 well tissue culture plate with 1 ml per well of a 4% Paraformaldehyde solution for fixing. Pupal wings were fixed for 30 to 45 mins and then cleaned of any peripodial membrane by using fine forceps. After fixation, the tissue was then washed with PBST (PBS + 0.5% Triton-X100 for antibody staining or with PBS, + 0.01% Tween20 for *in situ* hybridization) five times to then be stored at 4ºC until stained (not more than 30 days).

Embryos fixation and dissection.

Eggs were collected from plants between 24 to 36 hours after deposition. I adapted the fixation scheme from Brakefield et al. (2009). Eggs were first transferred to 1.5 ml tubes and washed on PBS to remove any dirt. Eggs were then permeabilized and had their chorion removed with 5% Bleach (PBS) for 6 minutes. Eggs were then washed 5 times for 5 minutes in PBS to remove the excess bleach. I added 1 ml per tube of a 4% Paraformaldehyde solution (PBS) for fixing for 30 to 60 minutes. Eggs were then washed in PBST (PBS + 0.5% Triton-X100) 2 times for 5 minutes and then taken into a methanol series (25%, 50%, 75% methanol solutions in PBS at 4◦C). Eggs were then transferred to 100% methanol and stored at -20◦C for 5 days. Eggs were then transferred using plastic pipettes to a glass dissection plate with pre-chilled 100% methanol for dissection with fine forceps and dissection needles. Dissected embryos were then pipetted carefully into a 16 well tissue culture plate with 1 ml per well of chill methanol. These embryos were taken back through a 1 ml per well methanol series (75%, 50%, 25% methanol solutions in

PBS at 4◦C) for rehydration. Then embryos were washed twice with 1 ml of PBST per well and stored in PBST at 4◦C for antibody staining.

al1 in situ hybridization of larval wings

I designed and synthesized *al1*-specific probes using the *H. cydno al1* transcript model (selected region shows 100% identity with *aristaless1* and 60% identity with *aristaless*2 transcript model). A 250 base-pair region from *al1* was amplified using primers (forward GTTCCCTCGCAGCCATTCTT; reverse TACGGCACTTCACCAGTTCT) by PCR, cloned into a TOPO vector (Invitrogen), and transformed into competent *E. coli* DH5a cells. I grew 3 replicates of 2 positive colonies and extracted DNA using a miniprep DNA extraction kit. I confirmed insert sequences via Sanger sequencing, linearized plasmids using Not1 and Sac1 restriction enzymes (New England Biolabs), and synthesized probes using a reverse transcription kit (Qiagen) with added DIG labeled nucleotides. The synthesized probes were purified using Qiagen RNAeasy columns.

In situs were performed following Ramos and Monteiro (2007). The entire process was carried out in 16 well tissue culture plates. Tissues stored in PBST (PBS, Tween20) were subjected to a mild digestion for 5 minutes in Proteinase K (0.025mg/ml). Digestion was stopped using a stop buffer (2mg/ml glycine in PBS 0.01% tween20). Tissue was washed 5 times for 5 min with PBST, then incubated in a pre-hybridization buffer (50%formamide, 5XSSC, 0.1% Tween20, and 1mg/ml Salmon Sperm DNA) for 1 hour at 55°C. 1 ml of Hybridization buffer (50%formamide, 0.01g/ml glycine, 5XSSC, 0.1% Tween20, and 1mg/ml Salmon Sperm DNA) with approximately 50 ng of the used probe against *al1* was added to each well and left to incubate at 55°C for at least 48 hours. The tissue was then washed 5 times for 5 min in pre-hybridization buffer and then left washing in pre-hybridization buffer for 24 hours at 55°C. Wings were then blocked in 1% bovine

serum albumin (BSA) in pre-hybridization buffer for 1 hr at 4ºC. Anti-DIG antibody was added (1:2000) to each of the wells and incubated overnight at 4°C. The tissue was then washed with PBST extensively (10 times or more for 5 minutes) before development with BM-purple (1ml peer well, Roche Diagnostics). Time of development was approximately 24 hours at 4°C. Stained tissue was imaged using Zeiss stereomicroscope Discovery.V20 with AxioCam adapter. Scale bars were added using ImageJ software. I analyzed wing imaginal discs of white butterflies at both fourth and fifth instar stages (3 individuals, wings split between sense and antisense probes).

Al1 antibody staining of embryos, larval, and pupal wings

We raised polyclonal antibodies against two Al1 peptides in the company GenScript (New Jersey, USA). Peptide antigens (Al1-1: QSPASERPPPGSADC, Al1-2: DDSPRTTPELSHA) are located in the N-terminal 40 amino acids of Al1 and share 25% and 30% identity with Al2. Polyclonal antibodies were affinity purified after harvesting and tested for specificity by performing Dot blot tests as described in **Figure 12.**.

I performed antibody staining in larval and pupal wings following Martin et al. (2014). I also applied this staining protocol to embryos. Tissue stored in PBST (PBS, Tritonx) was blocked in 1% BSA in PBST for two hours, then incubated overnight in 1 mL blocking buffer and Al1 specific antibody (1:1000 for pupal wings and embryos, 1:300 for larval wings). Tissue was washed twice quickly, then 5 times for 5 mins in ~0.5 mL PBST, then incubated in 1 mL the secondary staining solution (goat anti-rabbit-AlexaFluor 488 [Thermofisher] at 1:1000, Hoechst 33342 at 1:1000 [Thermofisher] and Phalloidin-AlexaFluor555 at 1:200 [Thermofisher] in blocking buffer). The tissue was washed extensively and then mounted on glass slides using VectaShield (Vector Labs) on glass slides. Images were collected using a Zeiss LSM 710 Confocal Microscope and processed using Zen 2012 (Zeiss) and ImageJ. For wild type antibody stainings I

used pupal wings between 2-4 days APF of both white and yellow butterflies (20 individuals for white and 6 individuals for yellow). For white CRISPR knockout butterflies I used wings 2 days APF, (3 individuals, 2 of which showed a phenotype), 3 days APF (4 individuals, 3 of which showed a phenotypes), and 4 days APF (3 individuals, 2 of which showed a phenotype). For embryos I used 5 wild type and 4 CRISPR embryos (3 of which had a phenotype).

Electroporation of pupal wings for RNA interference

Electroporation-mediated RNA interference experiments were performed following Ando and Fujiwara (2013) and Fujiwara and Nishikawa (2016). We designed and synthesized Dicer substrate short interfering RNAs (DsiRNAs) targeting the first exon of *Al1* using Integrated DNA Technologies (USA). Al1.DsiRNA-1 targets 5'-ATGAATTTACTCCAAAAAGAAAG.

Fresh pupae, within the first hour of pupation, were used to perform the injections. For each experiment, the pupa was placed on a petri dish under a stereoscope and had its forewing displaced over a 1% agar (1xPBS) pad. One microliter of 250 μM DsiRNA in water was injected into one of the pupal wings using borosilicate glass needles (with filament; GDC-1 from Narishige, USA) pulled on a Narishige PC-10 with 1 step at setting 67. A 1xPBS bubble was placed on top of the injection site to perform electroporation using 5 x 280 ms pulses of 10 V over 5 sec. The wing was then placed back in its original position and the insect was allowed to recover for 24 hours before being hung again vertically. Some electroporated pupae were allowed to develop to ad ulthood and others were dissected 3 days APF for staining following the methods described above. Approximately 45 pupae were treated. I used wings at 3 days APF from 5 individuals for Al1 stainings (3 of which showed a phenotype). From the remaining 40 pupae, 14 survived to at least pre-eclosion stages (5 showed an adult phenotype).

qPCR gene expression analysis of downstream target genes

I collected pupal forewings 4, 6, and 7 days APF of both white and yellow *Heliconius cydno* butterflies (three biological replicates of each color at each time point). The collected wings were cut into 3 sections (proximal, medial, and distal) using the venation pattern as a guide for consistent cuts (**Figure 8A**). Following dissection, the tissue was stored in RNA later (Ambion, USA) at -80ºC until RNA extraction. The same sections from the two wings in each individual were grouped. Samples were thawed on ice, then washed twice with ice cold PBS before total RNA extraction using TRIzol (Invitrogen, USA) and the manufacturer's protocol. Extracted RNA was re-suspended in 50 µL of RNAse free water. Purified RNA (2 µg) was used to perform cDNA synthesis using the ABI High Capacity cDNA Reverse Transcription Kit (Thermo Fisher 4368814) following the manufacturer's instructions. cDNA pools were diluted 10X in TE and stored at 4ºC until qPCR.

All qPCRs were performed in 10 uL reactions with the BioRad iTaq Universal SYBR Green Supermix (Bio-Rad, USA) on a Bio-Rad CFX96 thermal cycler. I tested primer efficiencies using a 2-fold dilution series of one cDNA pool and only used those with efficiencies between 90% and 106% when possible (**Table 1**). I used *ef1a* as the ubiquitously expressed control gene to standardize our values during the qPCR assays. A single experimental gene and the control gene were tested for all samples in a single plate, and all reactions were technically replicated twice. Relative expression levels were calculated using the ΔC_T method. I then scaled ΔC_T values for a particular gene to 1 by dividing sample ΔC_T values by the highest ΔC_T value for that gene. Calculations were performed in R (version 3.5.2).

ICRT3 and CHIR99021 test on Wnt signaling

The inhibitor of β-catenin responsive transcription (iCRT3, MedChemExpress Cat. No.: HY-103705, stock concentration; 10 μg/μL in DMSO) and the inhibitor of the repressor GSK3 α/β, (CHIR99021, Sigma-Aldrich Cat. No.: 252917-06-9 stock concentration; 5 μg/μL in DMSO) were used on pupal wings 2 to 4 days APF. The pupae were cold anesthetized for 5 minutes before making a small opening on the cutical covering of the pupal wing. Then the piece of cuticle covering the opening was lifted in order to add 3μL of the inhibitor solution (400ng/μL iCRT3/ CHIR99021 in PBS1x or in 1xPBS/DMSO). For controls, pupae with just the opening as well as pupae with 3 μL of 1XPBS/DMSO were used. After the addition of the solutions, the piece of the cuticle was placed back and the pupa was left resting without hanging for 24 hours to allow for healing and recovery. If the wing was going to be imaged the dissection and staining was carried out as described above. In the case where the butterfly was going to be allowed to develop to adulthood it was hung again between 24 to 48 hours after exposure and taken back to the greenhouse. Approximately 60 pupae of white *H. cydno* were treated with ICRT3. I used wings between 2 to 4 days APF from 10 individuals for Al1 antibody stainings (6 of which showed a phenotype [2 of them had scale size phenotypes]). Of the remaining 50 treated butterflies, 15 survived to at least pre-eclosion stages (7 showed an adult phenotype). Three yellow H. cydno pupae were treated with CHIR99021, of which all 3 showed one or both phenotypes of yellow scales switching to white or black.

2.6 Figures

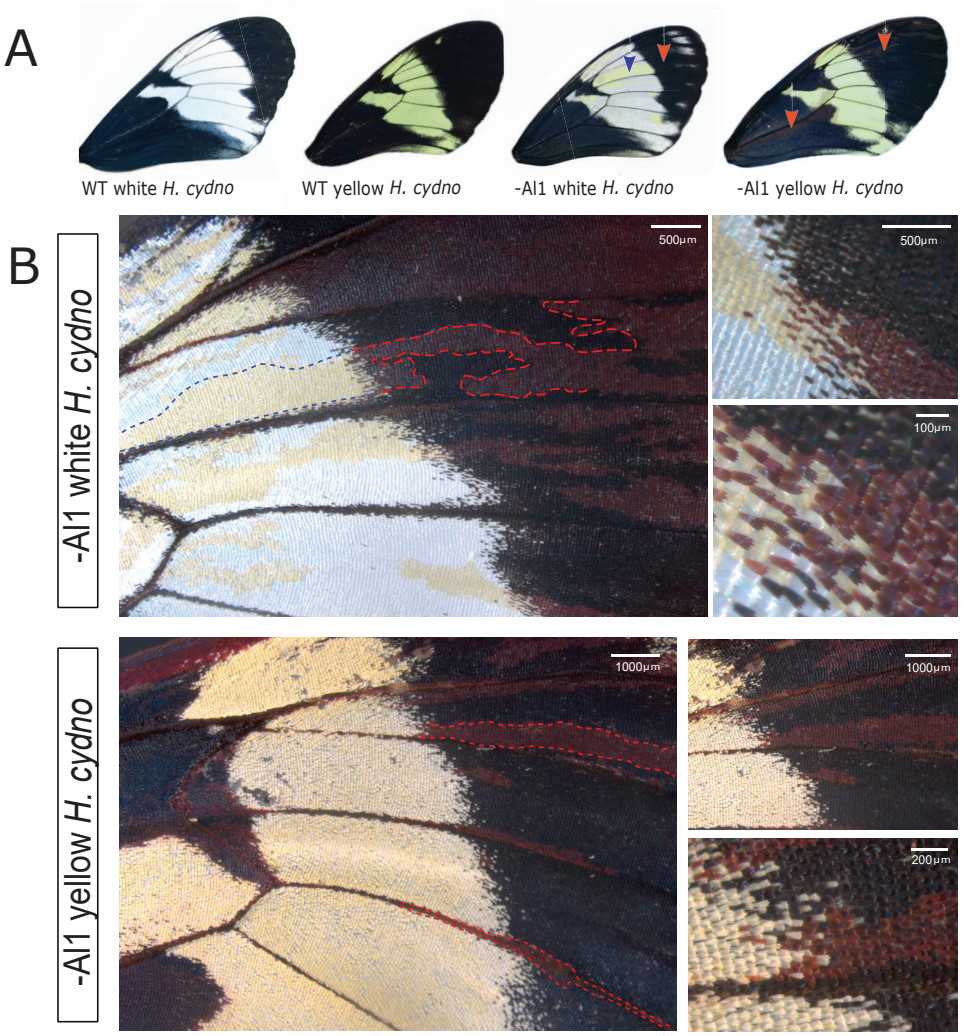

Figure 3: Wild type and al1 CRISPR/Cas9 knockout forewings of white and yellow *H. cydno*. (**A**) Full adult forewing view of wild type and al1 knockouts of both white and yellow *H. cydno*. Blue arrowheads highlight mutant yellow clones inside the white regions and red arrowheads highlight mutant brown clones inside the melanic regions of wing. (**B**) Higher magnification view of the mutant parts of the wing for both white (top panel) and yellow (bottom panel) *H. cydno* butterflies. Dashed blue lines highlight the parts of the clone that switched from white to yellow and dashed red lines highlight the parts of a clone that switched from black to brown.

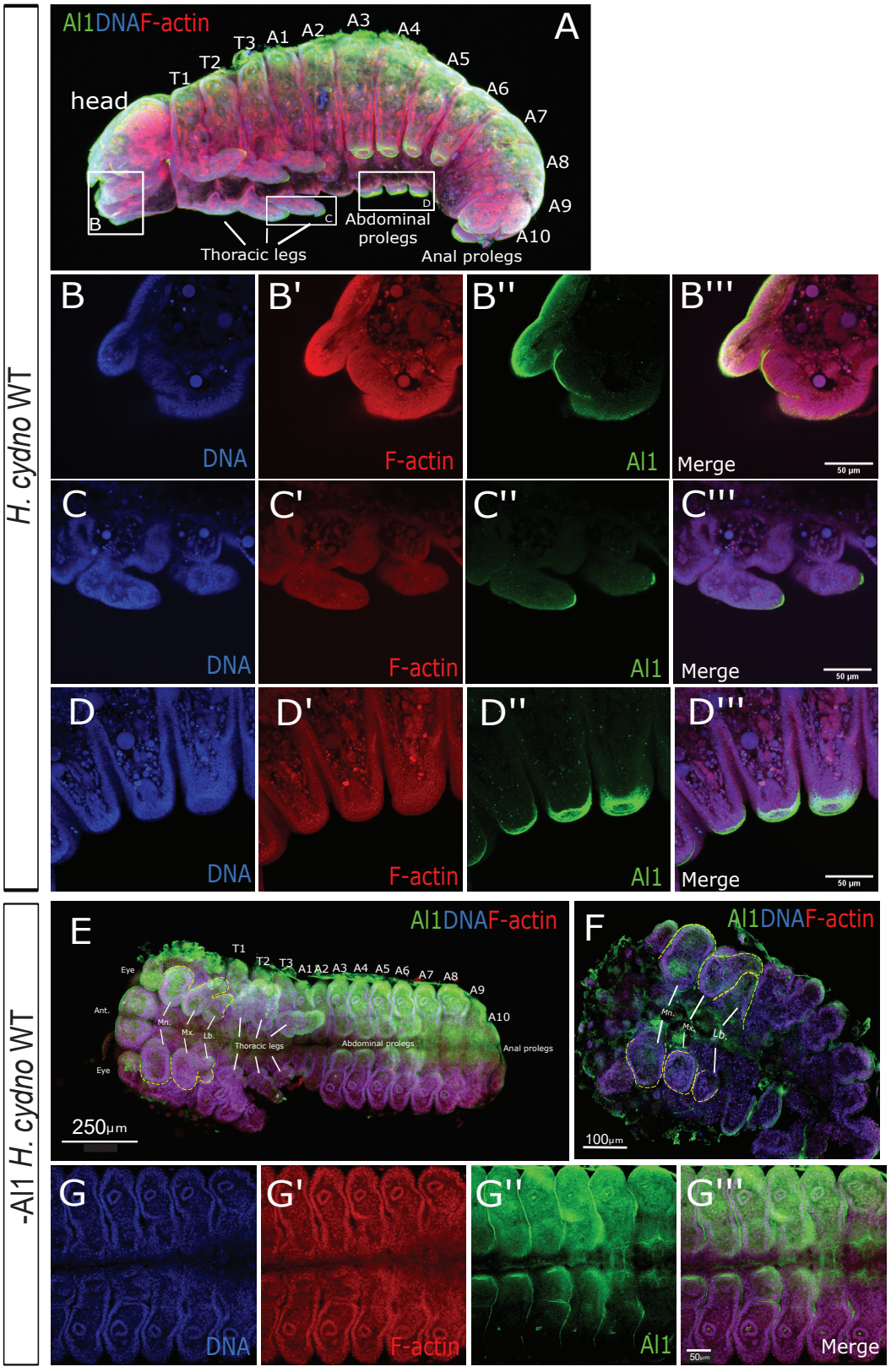
H. cydno WT
-Al1 H. cydno WT
Al1DNAF-actin
A
head
T1
T2
T3
A1
A2
A3
A4
A5
A6
A7
A8
A9
A10
B
C
D
Abdominal prolegs
Thoracic legs
Anal prolegs
B
B'
B''
B'''
DNA
F-actin
Al1
Merge
50 µm
C
C'
C''
C'''
D
D'
D''
D'''
E
F
Eye
Ant.
Mn.
Mx.
Lb.
250µm
100µm
G
G'
G''
G'''
50µm

Figure 4: Immunodetection of Aristaless1 in wild-type and -Al1 CRISPR *Heliconius cydno* embryos. (**A**) Immunodetection of Al1 in wild-type embryos. White boxes highlight the mandibula (**B**), thoracic legs (**C**), and abdominal legs (**D**) zones shown at a higher magnification in the next panels. (**E-F**) Immunodetection of Al1 in injected -Al1 CRISPR embryos. (**G**) Higher magnification of the abdominal prolegs showcasing a zone lacking Al1. The segments and appendages are labeled for the full view embryos (**A, E-F**). Full embryo views highlight Antennal (Ant.), eyes, Mandibular (Mn), Maxillar (Mx), and Labial (Lb) head appendage precursors. The 3 pairs of thoracic legs, 4 pairs of abdominal prolegs, and the pair of anal prolegs buds are also marked. Panels show detection of DNA (**B,C,D,G**), F-actin (**B',C',D',G'**), Al1 (**B",C", D', G"**), and a merge (**A, B'",C",D",E-F,G"'**).

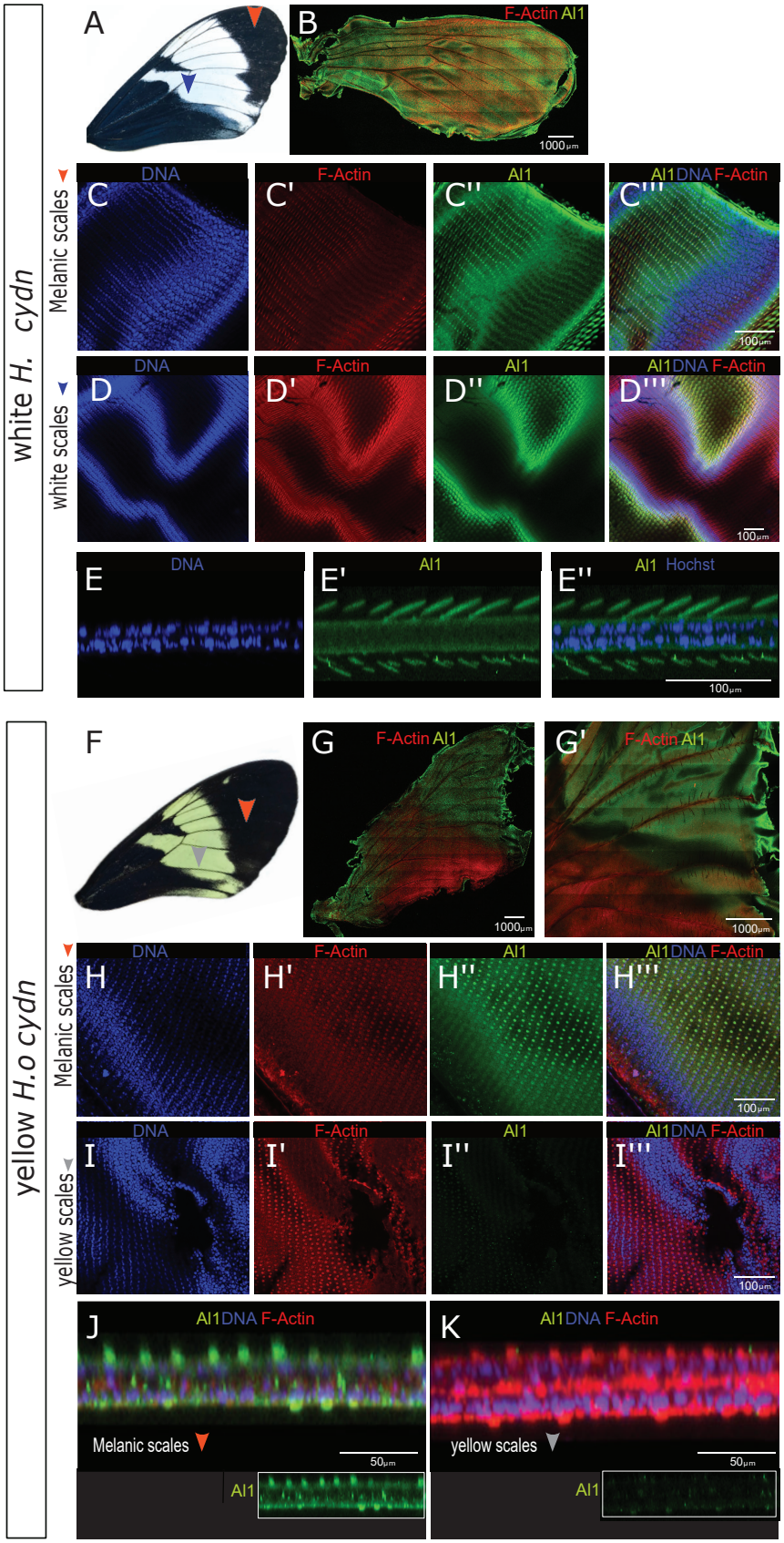
white H. cydn
A
B
F-Actin Al1
Melanic scales
DNA
C
F-Actin
C'
Al1
C''
Al1 DNA F-Actin
C'''
100µm
white scales
D
D'
D''
D'''
E
E'
Al1 Hochst
E''
1000µm
yellow H.o cydn
F
G
G'
yellow scales
H
H'
H''
H'''
I
I'
I''
I'''
J
K
Melanic scales
yellow scales
50µm
Al1

Figure 5: Immunodetection of Aristaless1 in white and yellow *Heliconius cydno* pupal forewings. (**A**) Adult forewing of a white *Heliconius cydno*. (**B**) Al1 detection in a full pupal wing of a white *Heliconius cydno* (3 days APF). (**C**) Details of Al1, DNA and actin detection in precursor scale cells of future melanic scales from a white *Heliconius cydno*. (**D**) Al1 detection in precursor scale cells of future white scales. (**E**) Side digital reconstruction from z-stack showing Al1 within precursor scale cells from the white part of the wing. (**F**) Adult forewing of a yellow *Heliconius cydno*. (**G**) Al1 detection in a full pupal wing of a yellow *Heliconius cydno*. **H**) Details of Al1 detection in precursor scale cells of future melanic scales from a yellow Heliconius cydno. (**I**) Al1 detection in precursor scale cells of future yellows scales. (**J-K**) Side digital reconstruction from z-stack showing differences in Al1 detection within precursor scale cells from yellow and melanic portions of a yellow *Heliconius cydno* wing. Panels show detection of DNA (**C,D,E,H,I**), F-actin (**C',D',H',I'**), Al1 (**C",D", E', H",I"**), F-actin/DNA (**B, G**) and a merge (**C"', D"',E",H",I"',J-K**) view. Scale bars: B, G are 1000 μm; **C-E and** H-I are 100 μm; **J-K** are 50 μm.

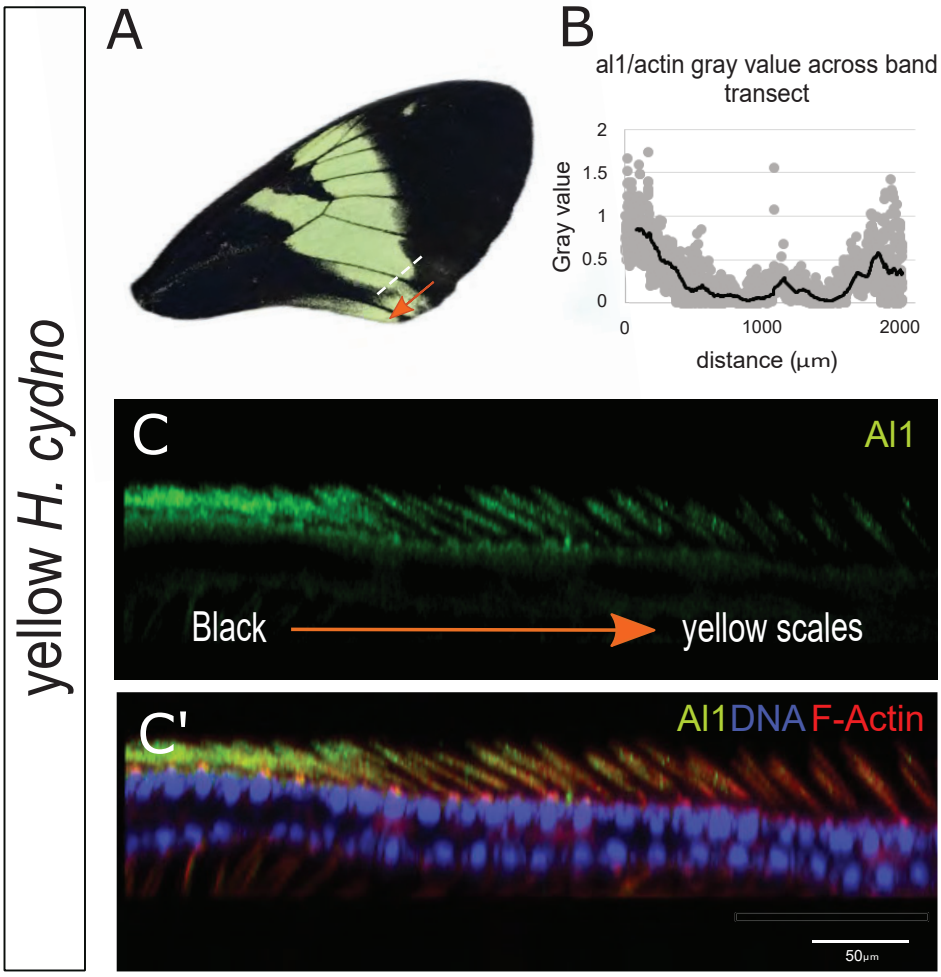

Figure 6: Immunodetection of Aristaless1 at the boundary between black and yellow scales in *Heliconius cydno* pupal forewing imaginal discs (3 Days APF). (**A**) Dorsal view of an adult yellow *H. cydno* forewing. (**B**) Quantification of the pixel gray value of a transect spanning across the presumptive yellow patch flanked by melanic regions at the stage of 3 Days APF. (**C**) Side view digital reconstruction from z-stack to observe the Al1 detection at the boundary between future melanic and yellow scales. Panel show detection Al1 (**C**) and a merged version (**C'**) with DNA and F-Actin detection. The orange arrow indicates the adult corresponding orientation for both the transect (white dashed line) for the B panel and the Z-stack of the side reconstruction of **C**. Scale bars: **C**, 50 µm.

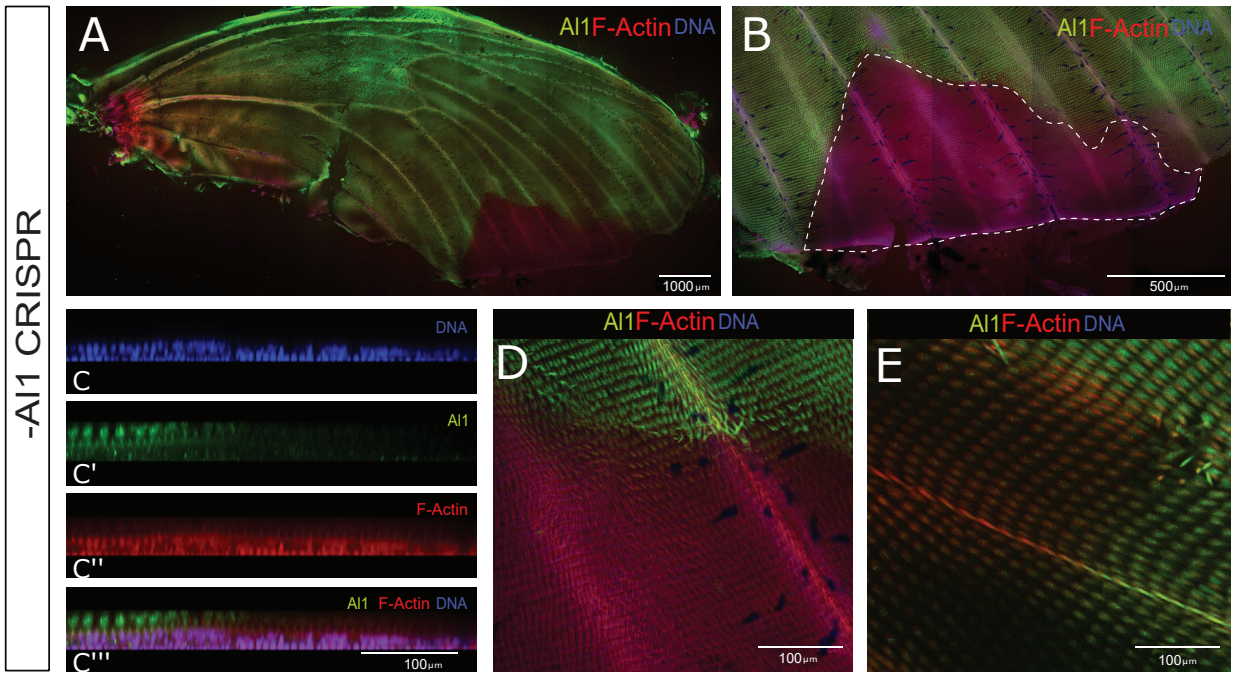

Figure 7: Immunodetection of Aristaless1 in *al1* CRISPR knockout pupal wings of white *Heliconius cydno* forewings (3 Days APF). (**A**) Immunodetection of Al1 in an *al1* CRISPR knockout forewing shows Al1 depleted clones. (B) Closer view of an extensive clone (white dashed line) within the distal edge of the wing. (**C**) Side digital reconstruction from a z stack showing the transition from high Al1 (left, outside the clone) to absent Al1 (right, within the clone). Panels show detection of DNA (**C**), Al1 (**C'**), F-actin (**C''**), and a merge (**C'''**) view. (**D-E**) Views of the scale precursors inside and outside of different CRISPR clones. Panel **A, B, D**, and E show both Al1 and F-actin.

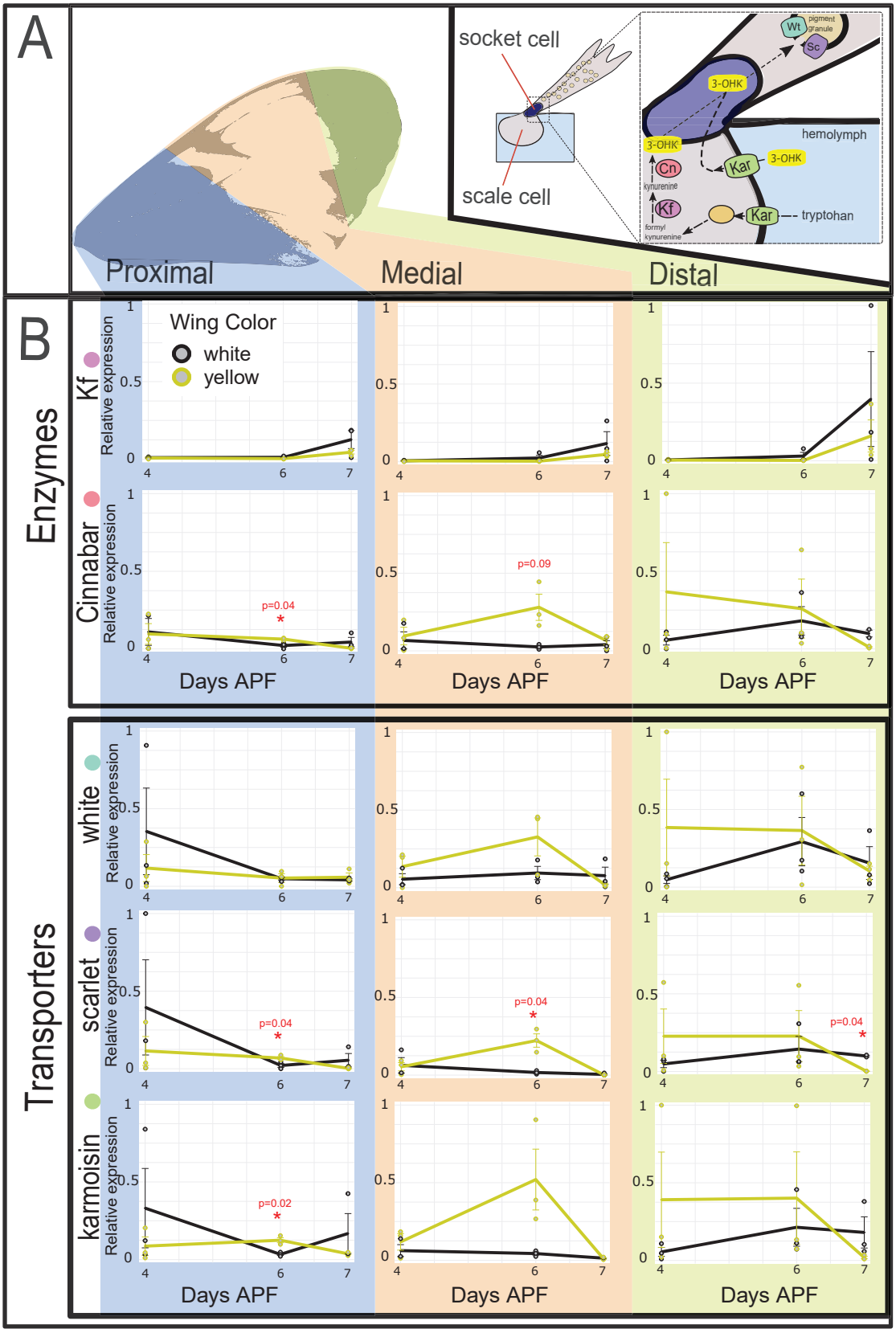
A
socket cell
scale cell
Wt
pigment granule
Sc
3-OHK
hemolymph
3-OHK
Cn
kynurenine
Kar
3-OHK
Kf
formyl kynurenine
Kar
tryptohan
Proximal
Medial
Distal
B
Enzymes
Transporters
Wing Color
white
yellow
Kf
Cinnabar
white
scarlet
karmoisin
Relative expression
Days APF
p=0.04
p=0.09
p=0.04
p=0.04
p=0.02

Figure 8: Analysis of candidate pigmentation genes that may act downstream of Aristaless1. (**A**) The top panel highlights distinct sections of the adult wing analyzed (left) and a pathway model (right) for the candidate genes of interest. The model showcases a view of the scale and socket cells and highlights the genes involved in the synthesis and transport (direct or after synthesis) of 3-hydroxykynurenine (3-OHK) yellow pigment. Enzymes: Kynurenine formamidase (Kf), Cinnabar (Cb); Transporters: White (Wt), Scarlet (Sc), Karmoisin (Kar). (**B**) Relative expression levels of each candidate gene in white and yellow pupal forewings sections (proximal, media, distal) across 3 different time points (4, 6, 7 days APF). The relative expression values are scaled to the highest value across the wing sections for each of the genes. Enzymes are shown in the middle panel and transporters on the bottom panel. Statistical significance was assessed using t-test and *p* values are shown for significant (asterisk) and nearly significant comparisons.

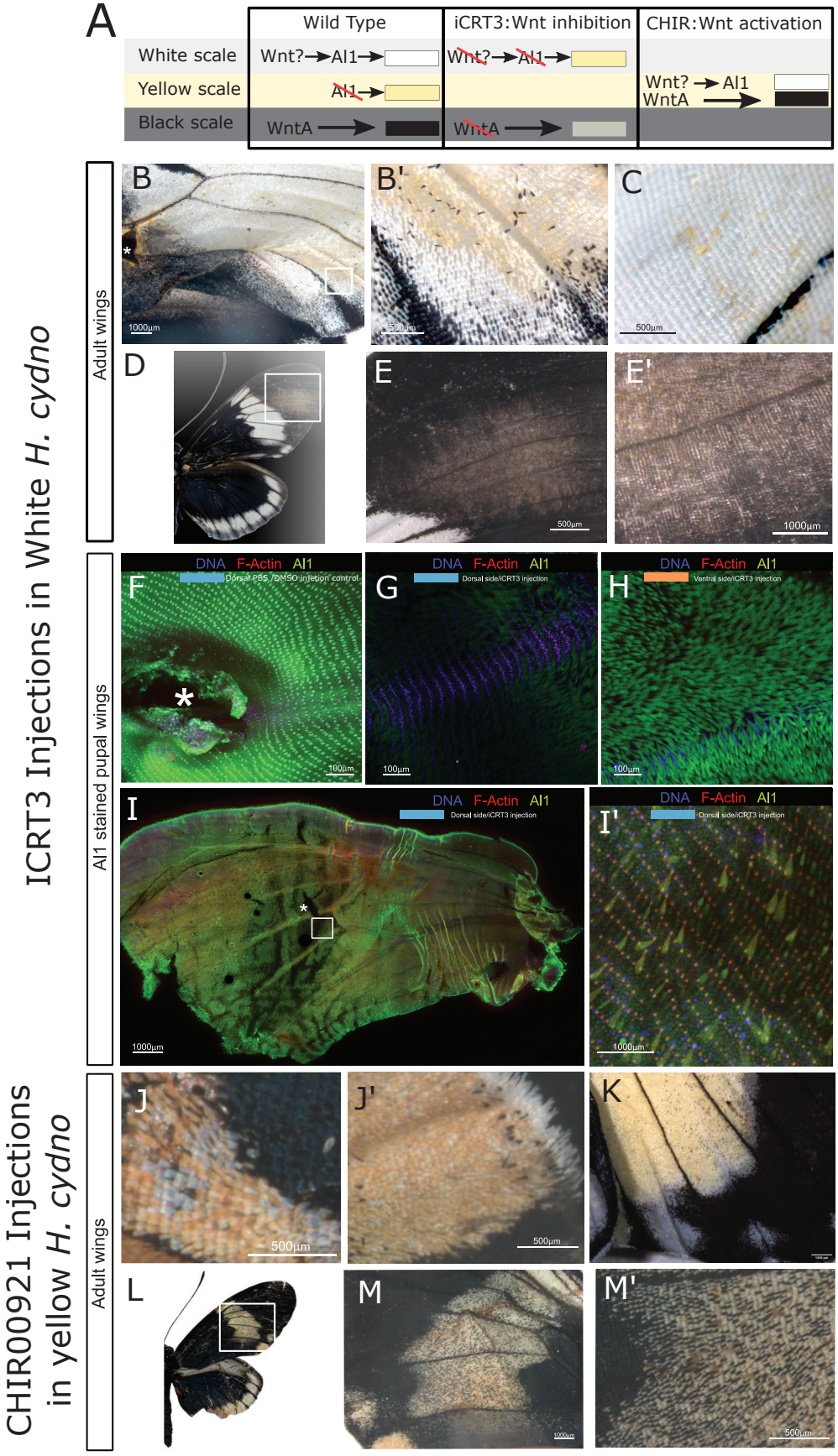
A
Wild Type
iCRT3:Wnt inhibition
CHIR:Wnt activation
White scale
Yellow scale
Black scale
Wnt?
Al1
WntA
ICRT3 Injections in White H. cydno
Adult wings
Al1 stained pupal wings
CHR00921 Injections in yellow H. cydno
Adult wings
B
B'
C
D
E
E'
F
G
H
I
I'
J
J'
K
L
M
M'
DNA F-Actin Al1
Dorsal PBS /DMSO injection control
Dorsal side/iCRT3 injection
Ventral side/iCRT3 injection
1000µm
500µm
100µm

Figure 9: Aristaless1 is regulated by Wnt signaling. (**A**) Scheme for the phenotypic color outcome for both wild type white and yellow butterflies. The hypothesized scenarios caused after exposure to the iCRT3 and CHIR00921 inhibitors affecting Wnt signaling is presented for both the white and yellow background. In it, we expect the white to yellow color switch following the reduction in Al1 levels caused by diminished Wnt signaling and the yellow to white switch following increase Al1 as a cause from enhancing Wnt signaling. Outcomes with respect to melanic scales are also shown as a read out from WntA activity. (**B**) Adult white wing injected at 3 days APF with iCRT3 and observed after eclosion. White square is shown as a detail view in C'. (**C**) Adult wing on the opposite side to the injection. (**D-E**) Adult right wing showing the effects of iCRT3 on melanic scales. Detailed view of the affected side (**E**) and scales are shown (**E'**). (**F-I**) Developmental validation of the iCRT3 effects on Al1 protein levels. The injection control (**F**) with 1Xpbs/DMSO is show as well as the dorsal (**G**) and ventral (**H**) sides of a pupal wing exposed to the drug around 3 days APF and dissected 24 hours after exposure to the agent. A different full wing with the same treatment is shown (**I**) with a wider area of effect. Severe scale size defects are visible in an amplified view from the white square (**I'**). (**J**) Different parts of an Adult yellow wing injected at 3 days APF with CHIR00921 and overserved after eclosion. (**K**) Ventral side of a different individual treated in the same way. (**L-M**) Adult right wing showing the effects of CHIR00921 with respect to the formartion of melanic scales. Details are shown (**M**). Asterisk showcases injection sites. In **F-G** the injection site is on the left outside the field of view.

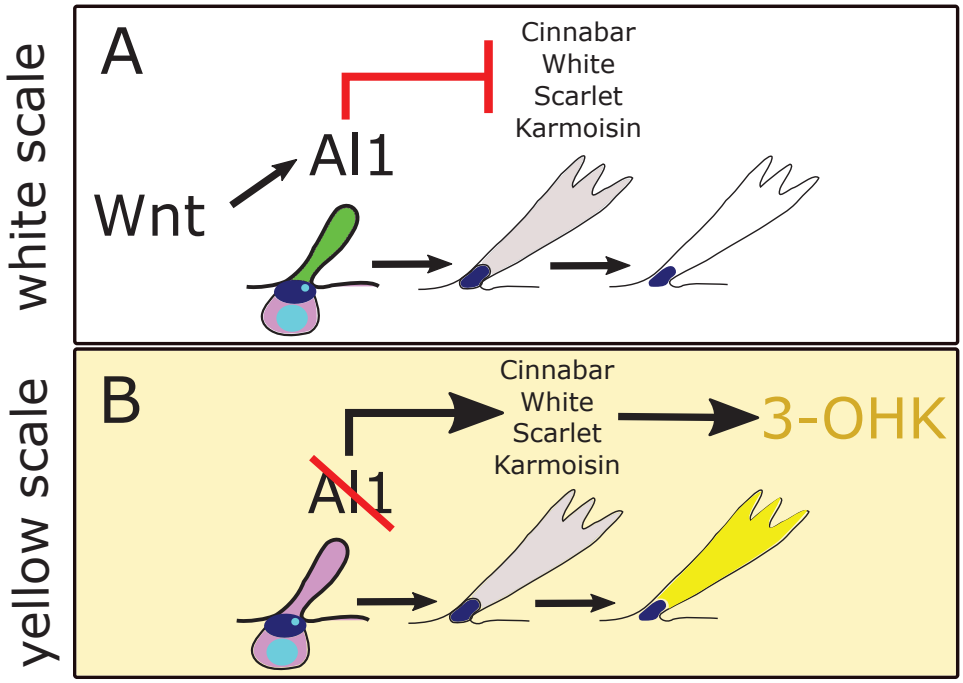

Figure 10: Graphical model for the role of Al1 in the specification H. cydno wing color. (**A**) White scale fate in which Al1 presence in developing scale cells lead to the inhibition of genes needed for yellow pigment uptake and production. (**B**) Yellow scale fate in which, reduced or absent Al1 results in the activation of genes involved with the production and movement of the yellow pigment 3-OHK.

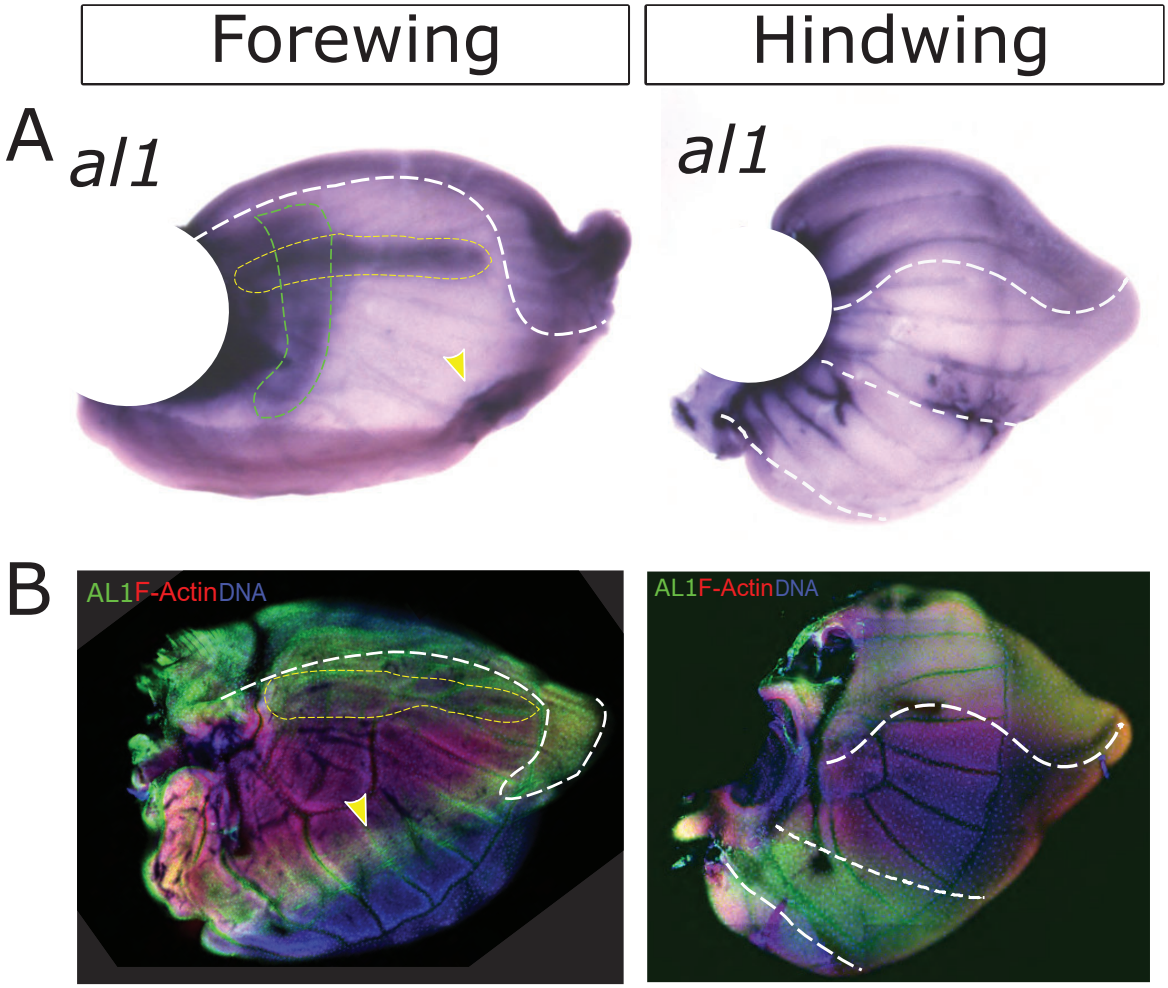

Figure 11: Detection of aristaless1 by mRNA in situ hybridization and Al1 specific antibodies in white *H. cydno*. (**A**) mRNA in situ hybridization of 5th instar larval forewing and hindwing. (**B**) Al1 antibody staining of 5th instar larval forewing and hindwing. Dotted lines are used to highlight previously described domains of expression from *Martin and Reed (2010)*. White dotted lines showcase the anterior curved domain (both forewings and hindwings) and posterior narrow band (hindwings). The yellow dotted lines highlight the horizontal expression domain along the anterior veins of forewings. The green dotted line highlights a vertical expression domain observed only in our in situ hybridization forewing. This domain has previously been reported as an Al2 expression pattern, suggesting some cross-reaction from the used probe. The yellow arrowhead highlights a posterior expression domain not previously described before and observed in both in situ and antibody-stained forewings.

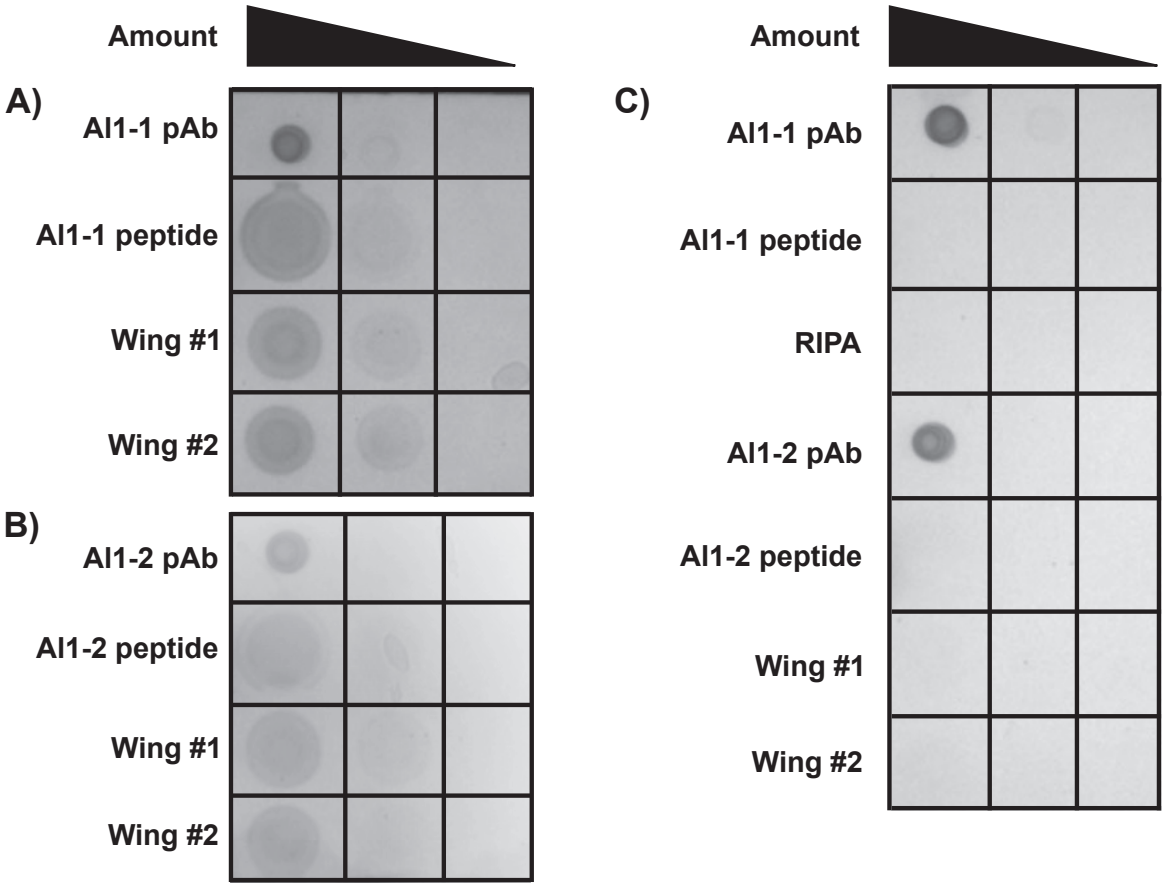

Figure 12: Dot blot test to determine the specificity of the Al1 antibodies. We spotted 2 uL each of three amounts of each antibody, peptide antigen, or protein prep (Wing #1, Wing #2), then probed blots using 5 ug/mL Al1-1 (**A**), 5 ug/mL Al1-2 (**B**), or no primary antibody (**C**). All blots were then probed with goat anti-rabbit secondary antibody conjugated to alkaline phosphatase (Invitrogen 65-6122). All three blots were developed for 15 min in the same container using Roche BM Purple AP substrate (11442074001) before imaging on a BioRad GelDoc XR+. Dot amounts: antibodies and peptides = 200 ng, 20 ng, 2 ng; protein preps: 1X, 0.2X, 0.05X.

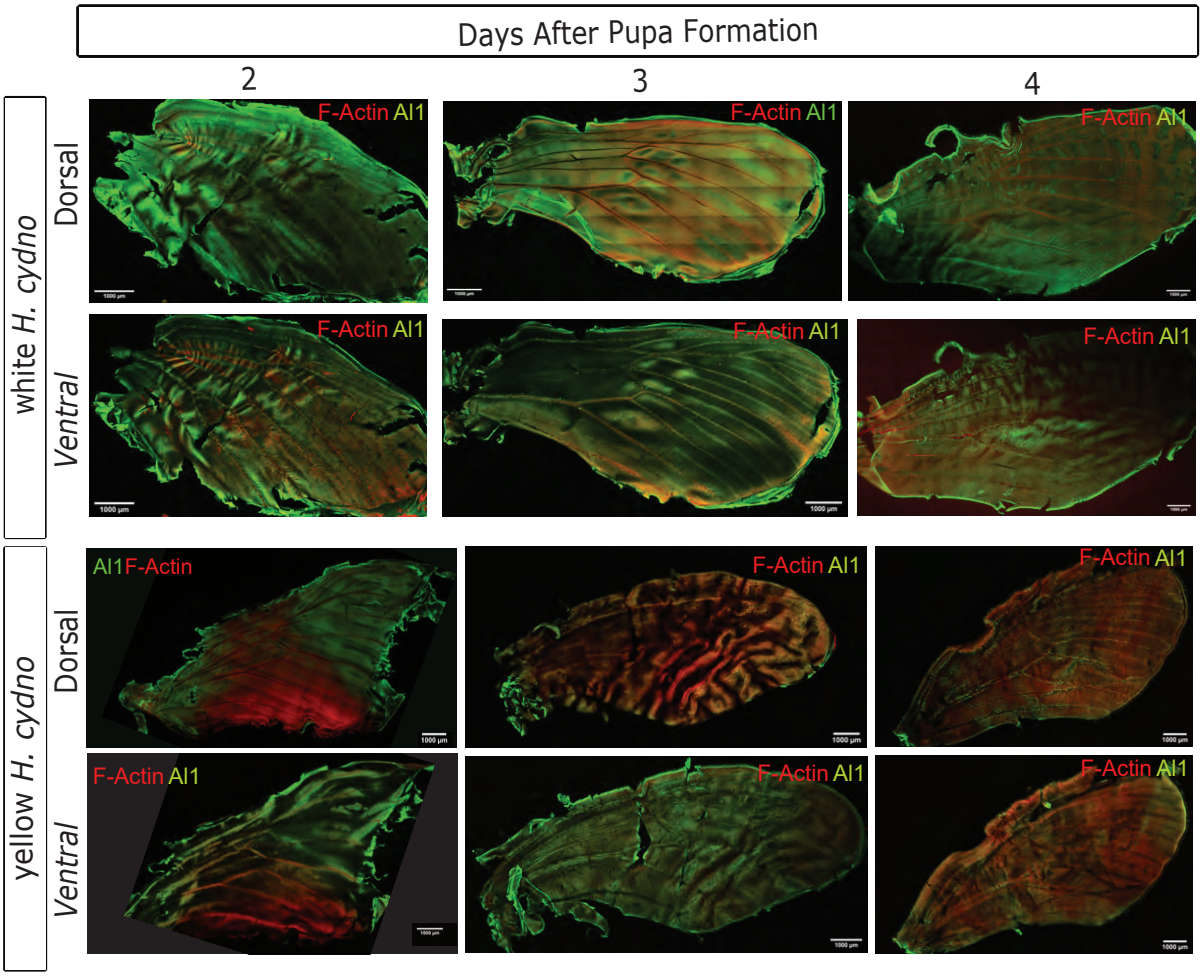

Figure 13: Temporal and spatial differences in Al1 protein localization between white and yellow *Heliconius cydno* wings. (A) Immunodetection of Al1 in white *H. cydno* forewings at different stages of early pupation (2 to 4 days APF) for both the ventral and dorsal side of the wing. (B) Immunodetection of Al1 in yellow *H. cydno* forewings at comparable stages to the white wings in panel A. Both ventral and dorsal parts of the wing are shown as well. Both panels show detection of Al1 and actin.

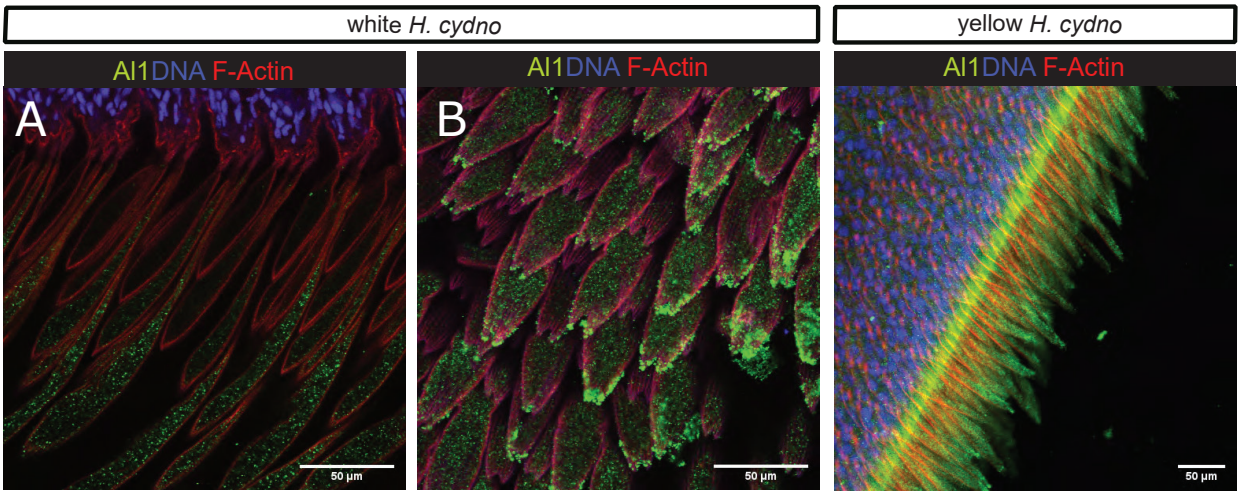

Figure 14: Immunodetection of Aristaless1 in melanic scales for both white and yellow *Heliconius cydno* pupal forewings (late 4 Days APF). (**A**) Imaging of longer border scales to appreciate details on the protein subcellular localization. View of bi-forked (**B**) and tri-forked (**C**) scales with accumulating Al1 in the scale cell body of a yellow *H. cydno* highlighting lack of co-localization with the nucleus.

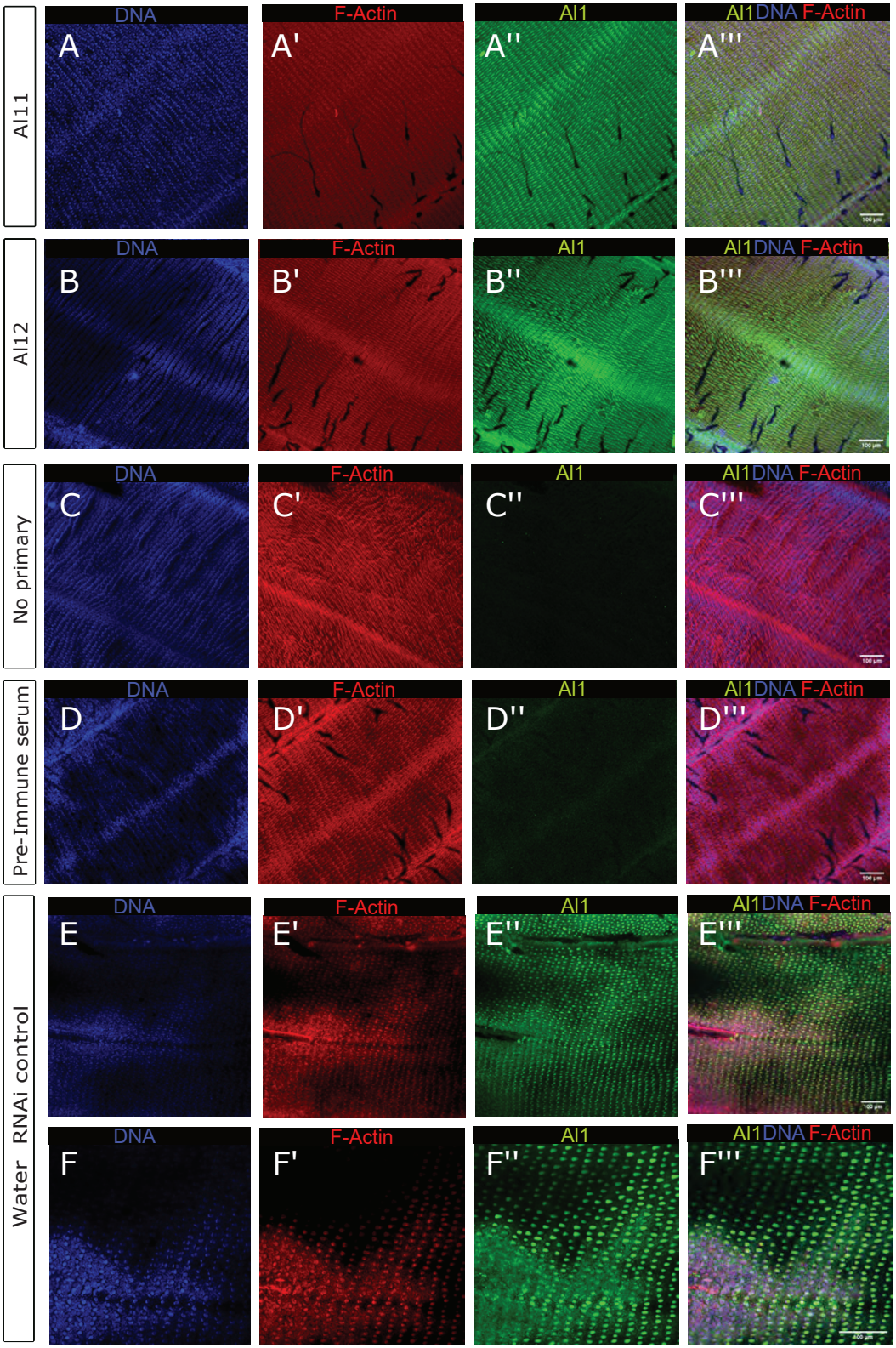
Al11
Al12
No primary
Pre-Immune serum
Water RNAi control
DNA
F-Actin
Al1
Al1DNA F-Actin
A
A'
A''
A'''
B
B'
B''
B'''
C
C'
C''
C'''
D
D'
D''
D'''
E
E'
E''
E'''
F
F'
F''
F'''

Figure 15: Immunodetection of Aristaless1 in white *Heliconius cydno* pupal forewings (between 2-3 days APF) across several control setups. (**A**) View of Al1 detection in scales by using the Al11 specific antibody (antibody used for all the immunodetections assays shown in the manuscript). (**B**) Al1 detection in scales by using the Al12, a different Al1 specific antibody targeting another part of the protein. (**C**) Negative control wing without any primary antibody. (**D**) Negative control wing in which the primary antibody was substituted by the pre-immune serum. (**E-F**) Al1 Immunodetection after a control water injection and electroporation. (**E**) View of an extended portion of the wing. (**F**) Closer view of scale cells to highlight details of Al1 protein detection following the manipulation. Panel show detection of DNA (**A-F**), F-actin (**A'-F'**), Al1 (**A''-F''**), and merge (**A'''-F'''**). The water injection site is located on the right corner outside of the field of view of the image.

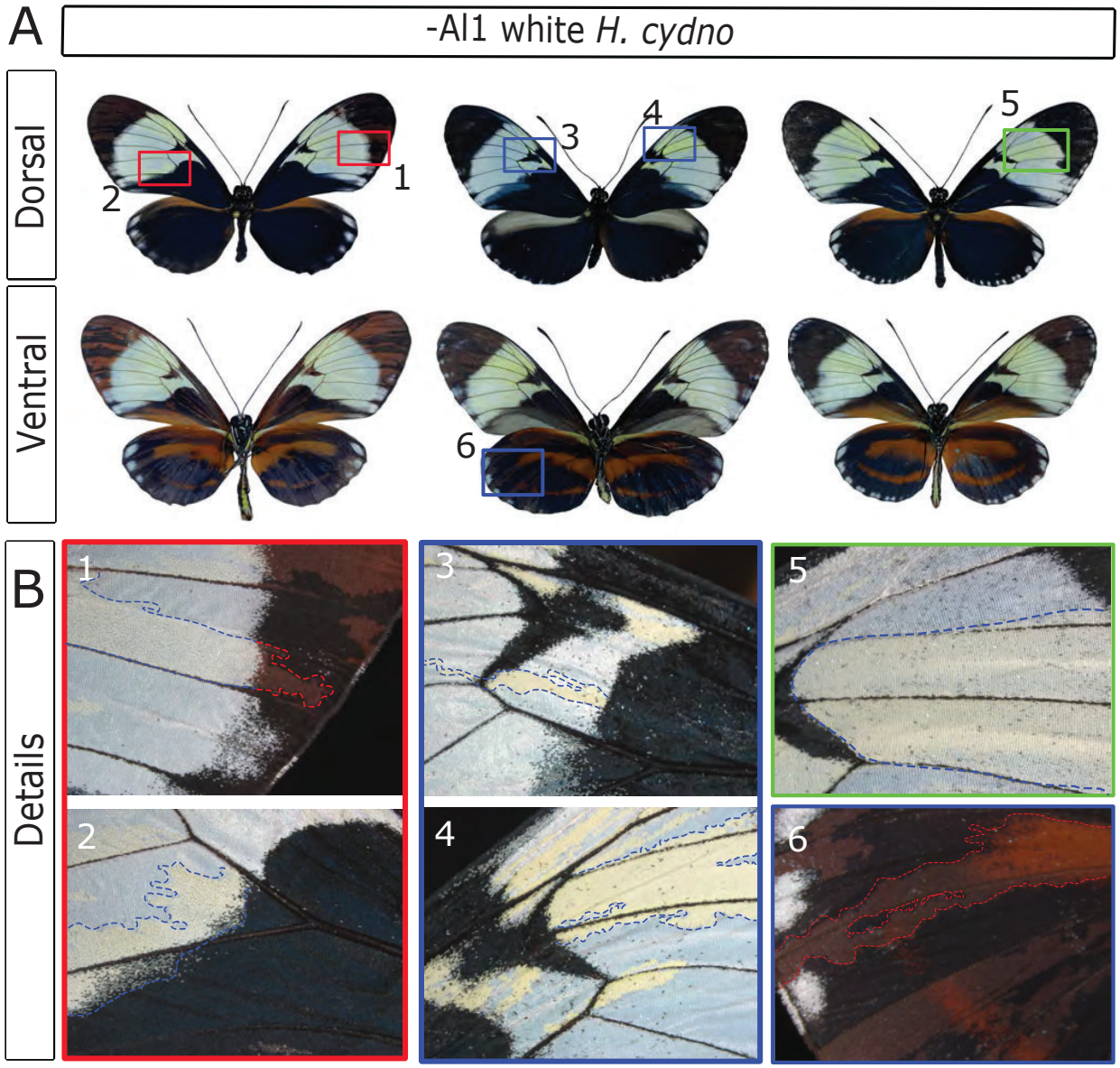

Figure 16: Showcase of the clones variation in Al1 CRISPR adults. (**A**) Whole butterfly views (both dorsal and ventral sides) of adults with Al1 CRISPR clones. The numbered squares are highlighted as closer views of the clones (B). Some of the clones in which scales shift from white to yellow are highlighted by the blue dotted line and the clones in which scales shift from black to brown are highlighted by the red dotted line.

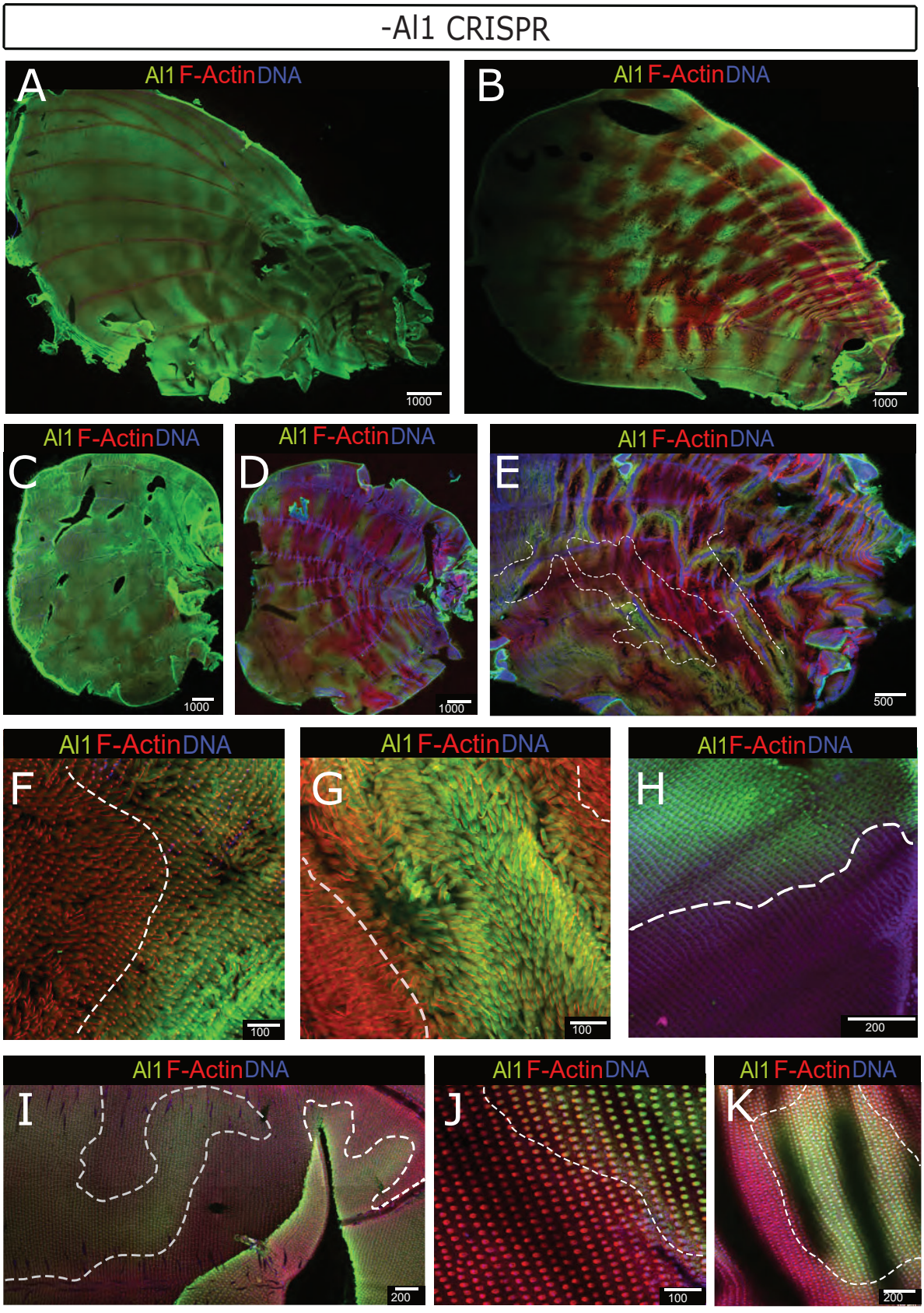
-Al1 CRISPR
A
Al1 F-Actin DNA
1000
B
Al1 F-Actin DNA
1000
C
Al1 F-Actin DNA
1000
D
Al1 F-Actin DNA
1000
E
Al1 F-Actin DNA
500
F
Al1 F-Actin DNA
100
G
Al1 F-Actin DNA
100
H
Al1 F-Actin DNA
200
I
Al1 F-Actin DNA
200
J
Al1 F-Actin DNA
100
K
Al1 F-Actin DNA
200

Figure 17: Showcase of the clones variation by immunodetection in Al1 CRISPR pupal wings (48 to 72 APF). (**A**) Low density to no clone forewing. (**B**) High clone density forewing highlighting scales lacking Al1. (**C**) Low density to no clone forewing. (**D**) High clone density hindwing highlighting scales lacking Al1. (E) Another High clone density forewing in which the clones have been highlighted with a white dotted line. (**I-K**) Details across multiple wings of different stages (48 to 72 APF) are shown to highlight the lack of Al1 within the clones. In all the detail views the boundaries are shown with a white dotted line.

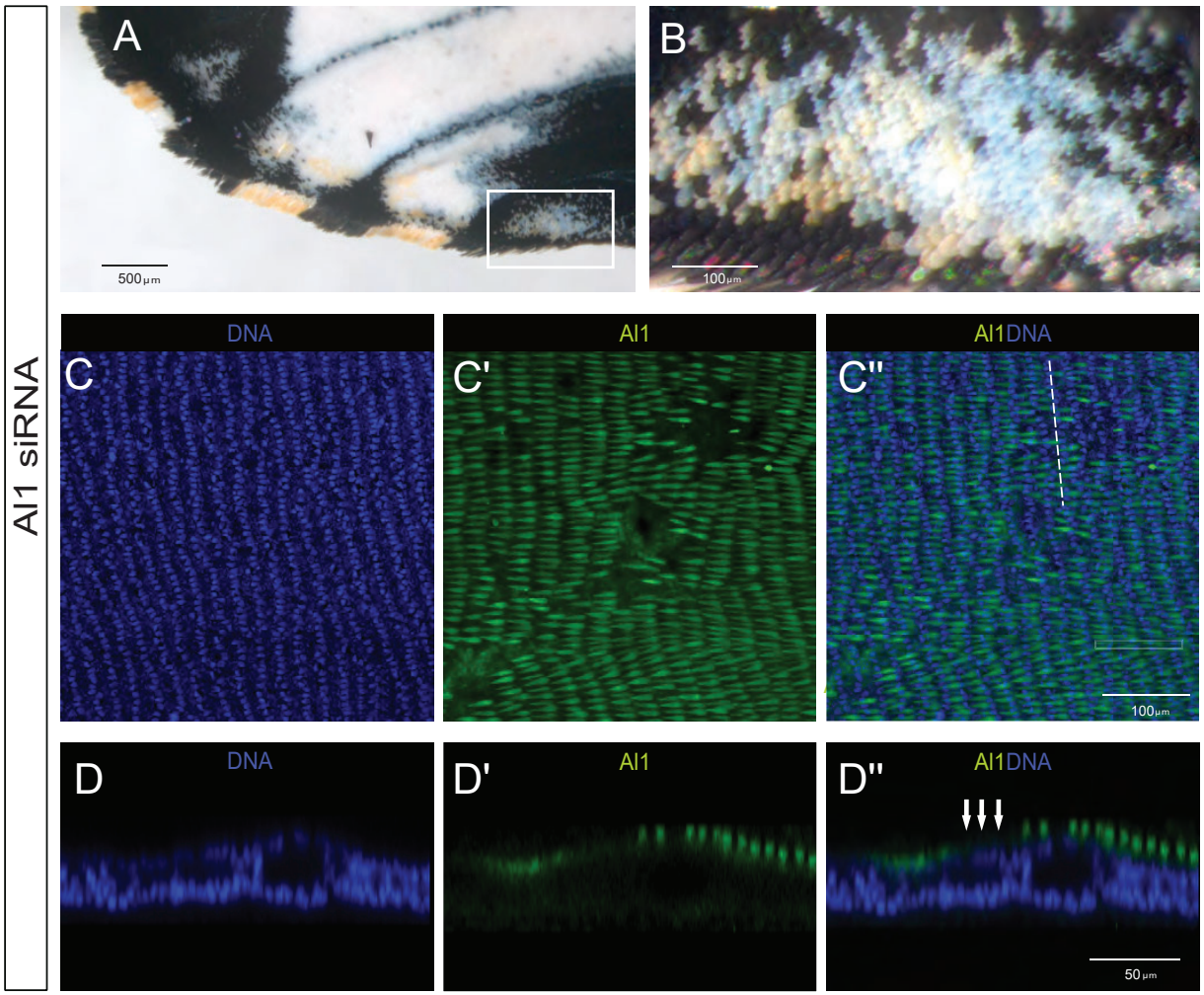

Figure 18: Immunodetection of Aristaless1 in *al1* RNAi knockdown pupal forewings of white *Heliconius cydno* (3 Days APF). (**A**) al1 knockdown adult wings showing areas of the wing switching from white scales to yellow scales. (**B**) Higher magnification of the white square shown in A. (**C**) Immunodetection of Al1 in an al1 knockdown pupal imaginal disc (3 days APF) showing patches of reduced or absent Al1 localization. (**D**) Side digital reconstruction (white dashed line indicate cross section in C'') from a z-stack of one of the patches in panel C to observe scale morphology and the absence of al1 in presumptive affected scales. Panel show detection of DNA (**C,D**), Al1 (**C',D'**) and a merge (**C'', D''**) view. Scale bars: **A**, 500 µm; **B-C**, 100 µm; **D**, 50 µm.

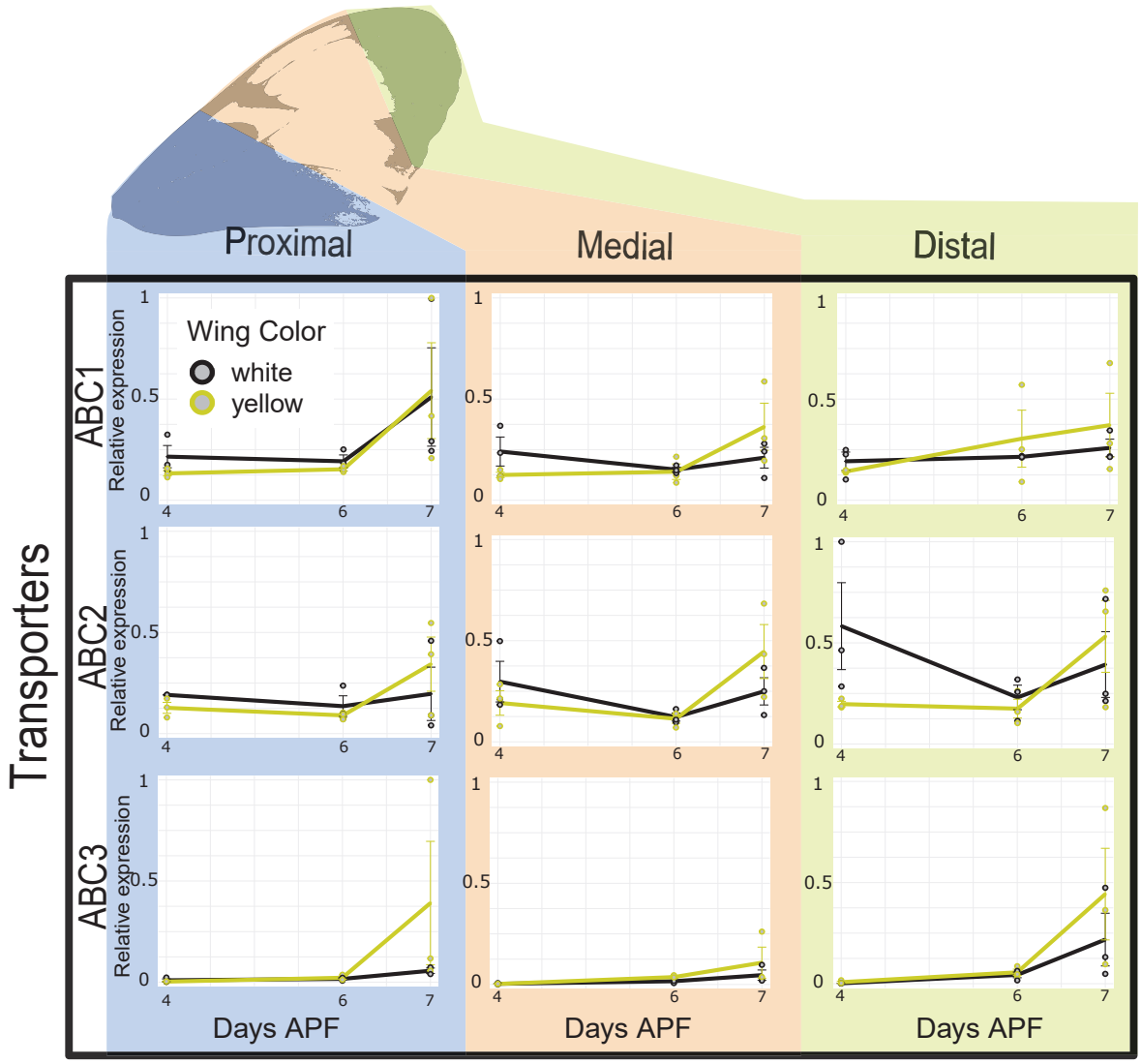

Figure 19: Downstream ABC transporters qPCR expression analysis between white and yellow *H. cydno* butterflies. Relative expression levels of each of the analyzed ABC transporters in white and yellow pupal forewings sections (proximal, media, distal) across 3 different time points (4, 6, 7 days APF). The relative expression values are scaled to the highest value across the wing sections for each one of the genes. The significance in the observed differences was tested using t-test. None of tested differences showed significance.

Gene	Fwd primer seq	Rvs primer seq	Product Length	Efficiency (%)
***ef1a* (control)**	GCTGACGGTAAATGCCTCAT	CAGGAGCGAACACAACAATG	180	96
Kf	CACCGCTACGCTACCAGAAA	CCCTGAAGCCGGTATGATCC	189	106
Cinnabar	ATGGACAGGGTATGAACGCC	CATCTATCGCCTTCCGGGTG	213	101
White	CAGGAGTTGAAAGCATCGCG	GTCGTGTGCGCCATAGTAGT	180	99
Scarlet	AATTTTGGGTCGACATCGCG	ACGACACATTAAATAACAGCAACA	156	103
Karmoisin	TGGCCGGGTTAATTCATGCT	TTCGAGTTCGTCTGCTAGTTT	171	90
ABC1	CCGCGTCATCGTCATGGATA	AGCACCACTGTCGCTTACTT	250	55
ABC2	GTGGAGCTAAAAGAGGCGGT	TTCTGTAATAGGACGTGCGG	215	94
ABC3	ATTCCGCCTCGCAATTGTTG	GCCGGTATTGCAGCTTTCAA	219	92

Table 1: qPCR gene primers and efficiency tests

CHAPTER 3

COMPARATIVE VIEWS OF ARISTALESS1 AND ARISTALESS2: EXPRESSION AND FUNCTION ACROSS BUTTERFLY EMBRYOLOGY AND WING DEVELOPMENT

3.1 Abstract

Aristaless is a major regulator of developmental processes. It is well known for its role within appendages specification and extension across insects. Butterflies have two copies of *aristaless* as a result of a gene duplication event, *aristaless1* (*al1*) and *aristaless2* (*al2*). Previous work in *Heliconius* has shown that both copies seem to have novel functions related to wing color patterning. Here I expand our knowledge on the expression profiles associated with both ancestral and novel functions of Al1 across embryogenesis and wing pigmentation. Furthermore, I characterize for the first time Al2 expression providing a comparative framework for the role of duplicates of the gene within novel and ancestral roles. Our work shows that both Al1 and Al2 expression is associated with developing appendages (leg, mouth, spines, and eyes) in embryos. Interestingly, Al1 appears to show higher expression earlier in embryogenesis while Al2 highest levels are shifted to later stages of embryonic development. Furthermore, Al1 localization appeared more extranuclear/extracellular while Al2 co-localized tightly with nuclei early when its expression was low and then diffused more extranuclearly later in development. These observations appeared to be maintained in pupal wings as well. Overall, these data suggest similar novel and ancestral roles that might exhibit shifts in temporal and spatial expression. This work expands our knowledge of Aristaless function and expression across multiple events in butterfly development. In addition, and more fundamentally, our study helps us understand the principles

behind gene duplication and sub-functionalization associated with carrying both ancestral and novel developmental functions.

Specific Acknowledgments:

This work was done in collaboration with **Nicholas VanKuren** (designed and ordered the Al1 and Al2 antibody), **Darli Massardo** (ordered and synthesize guide RNAs for CRISPR knockouts in addition to performing the CRISPR injections and associated pinning of mutant adults), and **Isabella Cisneros** (performed Al2 stainings for both pupal and embryonic tissue).

3.2 Introduction

Across invertebrates, Aristaless has been show to function as a key regulator of proper patterning and appendages extension (Campbell & Tomlinson, 1988; Schneitz, et al., 1993, Beermann and Schroder, 2004; Moczek, 2005,). In flies, Aristaless was first described based on its role in the formation of a hair-like structure called the arista which extends from the antennae (Schneitz, et al., 1993). Since then *aristaless* expression in flies has been shown to be relevant for the patterning of imaginal discs (both leg and wings) and their eventual extension into future adult structures (Campbell & Tomlinson, 1988; Schneitz, et al., 1993). Outside of flies, Aristaless maintains such a role with respect to appendages extension and specification. In *Gryllus*, early embryology work has shown how the expression of *aristaless* is associated with the tips of appendage buds growing out of the primary body plan (Miyawaki et al., 2002; Beermann and Schroder, 2004). Similarly, research in beetles has shown that the extension and branching patterns associated with their horns are also related to Aristaless activity (Moczek, 2005). Furthermore, outside of insects, recent evidence has shown that velvet worms also exhibit *aristaless* expression early in embryogenesis within the cells forming the leg buds. In summary, *aristaless* has become

a key gene for the regulation of patterning, extension, and formation of appendages across several invertebrate species.

In Lepidoptera, the *aristaless* gene has gone through a duplication event (Martin and Reed, 2010). Research of this gene in butterflies and moths has mainly used a non-specific antibody that targets products of both copies of the gene (in addition to other homeodomain proteins; Martin and Reed, 2010). In moths, previous work has shown that one or both *aristaless* copies have important roles when it comes to the formation and proper patterning of the antennae (Ando, et al., 2018). Similarly, Aristaless activity in butterflies has been shown to be associated with color patterning processes happening in wings. Furthermore, more specific approaches have suggested that different expression profiles for the two copies of the gene, *aristaless1* (*al1*), and *aristaless2* (*al2*), might be related to the patterning of specific color elements (Martin and Reed, 2010). Related to this novel color patterning function, I recently studied *al1* in detail as the key regulator of the white and yellow color pattern switch between *Heliconius* butterflies (**Chapter 2**). Furthermore, I also showed that *al1* expression and activity are needed for the proper formation of embryonic appendages in *Heliconius* (**Chapter 2**). My developmental characterization suggests that the Al1's role in color patterningis achieved by possibly altering scale maturation or elongation rate, which would connect both ancestral and novel roles for the gene. This newly described function underscores the need for a deeper characterization of Al1 within this appendage extension role. Furthermore, no data are available related to Al2 expression or activity in the context of appendage formation or color patterning, making any comparative work or assessments of sub-functionalization difficult.

As part of this work, I aim to answer these questions in more detail by applying new tools developed in *Heliconius* butterflies. I used newly developed antibodies that specifically target both

gene products in order to tease apart expression differences between them. Furthermore, I applied these antibodies to adapted protocols that allow us to analyze early embryology for the first time in *Heliconius* butterflies. Embryos prior to eclosion were used in order to analyze expression differences between Al1 and Al2 within appendage precursors. I coupled our early embryology analysis with pupal tissue staining to provide a complete view of the differences associated with Al1 and Al2 activity across development.

Our work provides evidence that Al1 expression is associated with both appendages and pupal wing cells during pupation. In addition, I show that Al1 activity in embryos is shifted earlier in embryological development and fades as development continues. Al1 is present within the mouthparts and legs, as previously described, but it is also shown to accumulate within eyes, spine cells, and along the dorsal side of the embryo. Al2, on the other hand, is shifted toward later stages of embryological development. Al2 expression was also observed within the same structures as Al1. The biggest difference between Al1 and Al2 was observed at the subcellular localization and temporal level. There I noticed that Al1 often appeared more diffuse and extranuclear (later stages) while Al2 appeared to co-localize with the nucleus earlier in embryogenesis where its expression was low and then appeared also extranuclear later in embryonic development. These observations suggest that both genes might be still involved with the same developmental roles but might be carrying the function in temporally distinct domains. Whether there is any interaction or compensation still remains as an interesting question. This research provides the first description of the role of Al2 with respect to appendage extension in butterflies and compares it with a more careful characterization of Al1. Finally, this work helps us understand how developmental profiles can shift following duplication events, possibly leading to different levels of sub-functionalization.

3.3 Results

3.3.1 Al1 and Al2 expression patterns are temporally distinct but still associated with embryonic appendages

I detected Al1 and Al2 presence by using specific antibodies across embryos early (around the first 24 hours post deposition) and late (around 28 hours post-deposition) stages of development. As previously shown (**Chapter 2**), Al1 was observed early in embryological development at the tip of appendages (**Figure 20A**) like the mouth part precursors (**Figure 20B**), and legs (**Figure 20D**). I also noticed for the first time Al1 localization within the cells giving rise to the eye (**Figure 20C**). Al1 expression early in embryological development did not overlap with the nucleus and appeared extranuclear. At the same early stages, I observed very weak presence of Al2 perfectly overlapping with the nuclei of the cells forming these appendages (**Figure 20**).

As development continued, this pattern of expression drastically shifted. Later embryos exhibited very little to no Al1, but Al2 expression increased (**Figure 21A**). When specific parts of the embryos were analyzed, I observed Al2 co-localization with the nucleus but also an extra nuclear domain associated with extending appendages. This was visible across the mouthparts (**Figure 21B**) and hook structures at the tip of the legs (**Figure 21D**). Similarly, the eyes also exhibited an accumulation on a tetrad-like structure associated with cells that form part of the eye (**Figure 21C**).

3.3.2 Al1 also accumulates dorsally in developing embryos.

In addition to the described patterns of localization for Al1, I also noticed that starting early in development, Al1 was strongly accumulated dorsally (**Figure 22A**). Interestingly, this accumulation also appeared to shift more posteriorly as the embryo extended in the

anterior/posterior axis during development (**Figure 22B**). As the embryo reached the maximum size around 48 hours post egg deposition, the expression of Al1 across the dorsal side of the embryo disappeared (**Figure 22C**). Again the observed accumulation appeared more diffuse and did not coincide with nuclei.

3.3.3 Al1 and Al2 localization is tightly linked with spine growth and development

Al1 and Al2 were detected tightly associated with spines across embryonic development (**Figure 23**). Early in development, Al1 was associated with the dorsal side, as explained above. In addition, the spine cell precursors exhibited Al1 accumulation along the extending actin filament (**Figure 23A**). Later in development, spines exhibited accumulation of Al2 along the entire spine and within the nuclei around the extending area (**Figure 23B)**. Al2 was especially accumulated within the nuclei closest to the actin projection (most exterior nuclei) within the spine (**Figure 23C,** red arrowhead**)** when compared with the other nuclei. In addition, later in embryonic development, Al1 appeared to surround some developing spines very tightly (**Figure 23D-F**). This was even more noticeable across spines on the last segment of the embryo.

3.3.4 Al1 localization is associated with pupal wings scale cell precursors but does not co-localize with nuclei

The observed pattern of Al2 expression, transitioning from nuclear to extranuclear, makes us consider whether Al1 activity previously described in pupal wings or across early embryology also follows this trend. Due to the difficulty of working with embryos earlier than 24 hours I used day 1 white pupal wings (24 hours following pupation) to get information on Al1 and also included, for the first time, data on Al2 with respect to developing scales. Firstly, I observed very little Al2 (**Figure 24**) and, as expected, it clearly coincided with the nucleus. Al1 expression was

higher but did not completely overlap with nuclei boundaries (**Figure 24**). Wing scale elongation is just starting at this stage. Therefore, this partial overlap was probably an effect of the scale cell cytoplasm extending from the wing upward. Side reconstruction and further time points may be needed to accurately determine if Al1 ever has a specific stage in which its localization overlap with nuclei.

3.4 Discussion

Our work here presents the first characterization of Al2 expression and its relationship with the ancestral role of appendage development. I performed this characterization in a comparative framework by further describing the Al1 pattern of expression across multiple stages of embryonic development and including analysis of Al2 across the same stages. I first described how Al1 expression is higher earlier in development while Al2 expression increases later. Even when this temporal shift is clear between the two versions of the gene, they both seem to still be associated with appendages. In addition to the previously described localization of Al1 (**Chapter 2**) with legs and mouth appendages, I also expanded such characterization of Al2 to the same structures which also shows a similar trend. I also reported that Al1 and Al2 localization is associated with the eyes and spines across embryonic development. In addition, Al1 was described to be localized dorsally during embryonic development. Such dorsal localization appears to follow along with the anterior/posterior extension of the embryo (**Figure 25**).

Finally, I made note that Al2 exhibits co-localization with nuclei during early and late stages of development and it exhibits a shift to extranuclear domains later in development. On the other hand, Al1 was always seen localized extranuclearly or even extracellularly. This seems to be maintained even when looking at developing scale cell precursors on pupal wings. Overall our

work describes some similarities between Al1 and Al2 with respect to their association with appendages. However, I also clearly describe differences in terms of the spatial and temporal control of their expression when it comes to their role in appendage formation and extension. More mechanistic work is needed to further elucidate the functional basis of these spatial and temporal differences.

Our work here addressing the characterization of Al1 and Al2 within ancestral (appendage extension) and novel roles (pigmentation) also expands on our views related to gene duplication and sub-functionalization. It is well known how gene duplication can often lead to sub-functionalization. This sub-functionalization can be associated with shifts in spatial and temporal patterns of expression and can lead to a division of functions. Here I do not observe one copy of the gene only expressed in specific appendages but instead, I see a tight relationship between both copies when it comes to expression across all appendages. Based on immunodetection alone, it seems that both copies are associated with appendage growth or extension. This highlights a set of interesting questions. First, if both Al1 and Al2 are needed for appendage formation or elongation, why are they shifted temporally? Along this same line, why does Al1 appear to be more extracellular while Al2 appears to be more nuclear?

One possible explanation is that there is some level of cooperation needed for the formation of appendages. In this scenario, the ancestral *aristaless* function has been now split between these two versions of the gene. I previously discussed how surprising it is that Al1 does not appear to be nuclear (**Chapter 2**). Although there could still be other time points in which nuclear localization happens, another alternative could be that Al2 might be the one driving regulatory activity. This could be achieved by a possible interaction between Al1 and Al2 or maybe by both of them being regulated by the same components. Due to the deficiencies in appendage extension and coloration

observed when Al1 is knocked-out (**Chapter 2**), I believe that knockouts of Al1 alone are sufficient to produce an effect. This highlights the need for other experiments addressing any relationship among the expression of both genes by doing knockouts against one and then observing the adult phenotypes and expression pattern of the other. These kinds of experiments will inform us about any relationship or compensation happening between both copies of the gene.

3.5 Methods

Butterflies rearing

Butterflies were reared in greenhouses at the University of Chicago with a 16h:8h light:dark cycle at ~27ºC and 60% – 80% humidity. Adults were fed Bird's Choice artificial butterfly nectar. Larvae were raised on *Passiflora oerstedii*.

Embryos fixation and dissection

Eggs were collected from plants between 24 to 36 hours after deposition. I adapted the fixation scheme from Brakefield et al. (2009). Eggs were first transferred to 1.5 ml tubes and washed on PBS to remove any dirt. Eggs were then permeabilized and had their chorion removed with 5% Bleach (PBS) for 6 minutes. Eggs were then washed 5 times for 5 minutes in PBS to remove the excess bleach. I added 1 ml per tube of a 4% Paraformaldehyde solution (PBS) for fixing for 30 to 60 minutes. Eggs were then washed in PBST (PBS + 0.5% Triton-X100) 2 times for 5 minutes and then taken into a methanol series (25%, 50%, 75% methanol solutions in PBS at 4◦C). Eggs were then transferred to 100% methanol and stored at -20◦C for 5 days. Eggs were then transferred using plastic pipettes to a glass dissection plate with pre-chilled 100% methanol for dissection with fine forceps and dissection needles. Dissected embryos were then pipetted carefully into a 16 well tissue culture plate with 1 ml per well of chill methanol. These embryos were taken back through

a 1 ml per well methanol series (75%, 50%, 25% methanol solutions in PBS at 4◦C) for rehydration. Then embryos were washed twice with 1 ml of PBST per well and stored in PBST at 4◦C for antibody staining.

Butterfly wing dissections

Butterflies were dissected at early pupal stages following Martin et al. (2014). The protocol and adaptations to it were carried out as follows. The pupae were anesthetized in ice for 20 mins before dissection. To obtain the pupal wings the pupae were pinned on the head and most posterior section of the body. The denticle belt was then removed using dissection forceps to allow for easier access to the wing. Then micro-dissection scissors were used to carefully cut around the wing margin using the pupal cuticle as a guide. The piece of cuticle together with the pupal forewing was removed and placed directly in a 16 well tissue culture plate with 1 ml per well of a 4% Paraformaldehyde solution for fixing. Pupal wings were fixed for 30 to 45 mins and then cleaned of any peripodial membrane by using fine forceps. After fixation, the tissue was then washed with PBST (PBS + 0.5% Triton-X100 for antibody staining five times to then be stored at 4ºC until stained (not more than 30 days).

Al1 antibody staining of embryos, larval, and pupal wings

We raised polyclonal antibodies against two Al1 peptides and 1 Al2 peptide using the company GenScript (New Jersey, USA). Peptide antigens (Al1-1: QSPASERPPPGSADC, Al1-2: DDSPRTTPELSHA, Al2: CGSGSGMDDEDIPRR) are located in the N-terminal 40 amino acids and share 25% and 30% identity between Al1 and Al2. Polyclonal antibodies were affinity purified after harvesting and tested for specificity by performing Dot blot tests as described (**Chapter1: Figure 12**).

I performed antibody staining in larval and pupal wings following Martin et al. (2014). I also applied this staining protocol to embryos. Tissue stored in PBST (PBS, Tritonx) was blocked in 1% BSA in PBST for two hours, then incubated overnight in 1 mL blocking buffer and Al1 and/or Al2 specific antibodies (1:1000 for pupal wings and embryos). Tissue was washed twice quickly, then 5 times for 5 mins in ~0.5 mL PBST, then incubated in 1 mL the secondary staining solution (goat anti-rabbit-AlexaFluor 488 [Thermofisher] at 1:1000 for Al1, Donkey anti-rat-AlexaFlour 555 [Thermofisher] at 1:1000 for Al2, Hoechst 33342 at 1:1000 [Thermofisher] and Phalloidin-AlexaFluor555 or Phalloidin-AlexaFluor647 at 1:200 [Thermofisher] in blocking buffer). The tissue was washed extensively and then mounted on glass slides using VectaShield (Vector Labs) on glass slides. Images were collected using a Zeiss LSM 710 Confocal Microscope and processed using Zen 2012 (Zeiss) and ImageJ. For wild-type Al1 and Al2 double antibody staining's of embryos I used and imaged about 5 individuals for both early and late time points. For wild-type pupal wings in quadruple staining's, I used forewings from 2 individuals. For Al1 and actin imaging across embryological development used a total of 5 embryos across different stages of development between 24 to 36 hours after egg deposition.

3.6 Figures

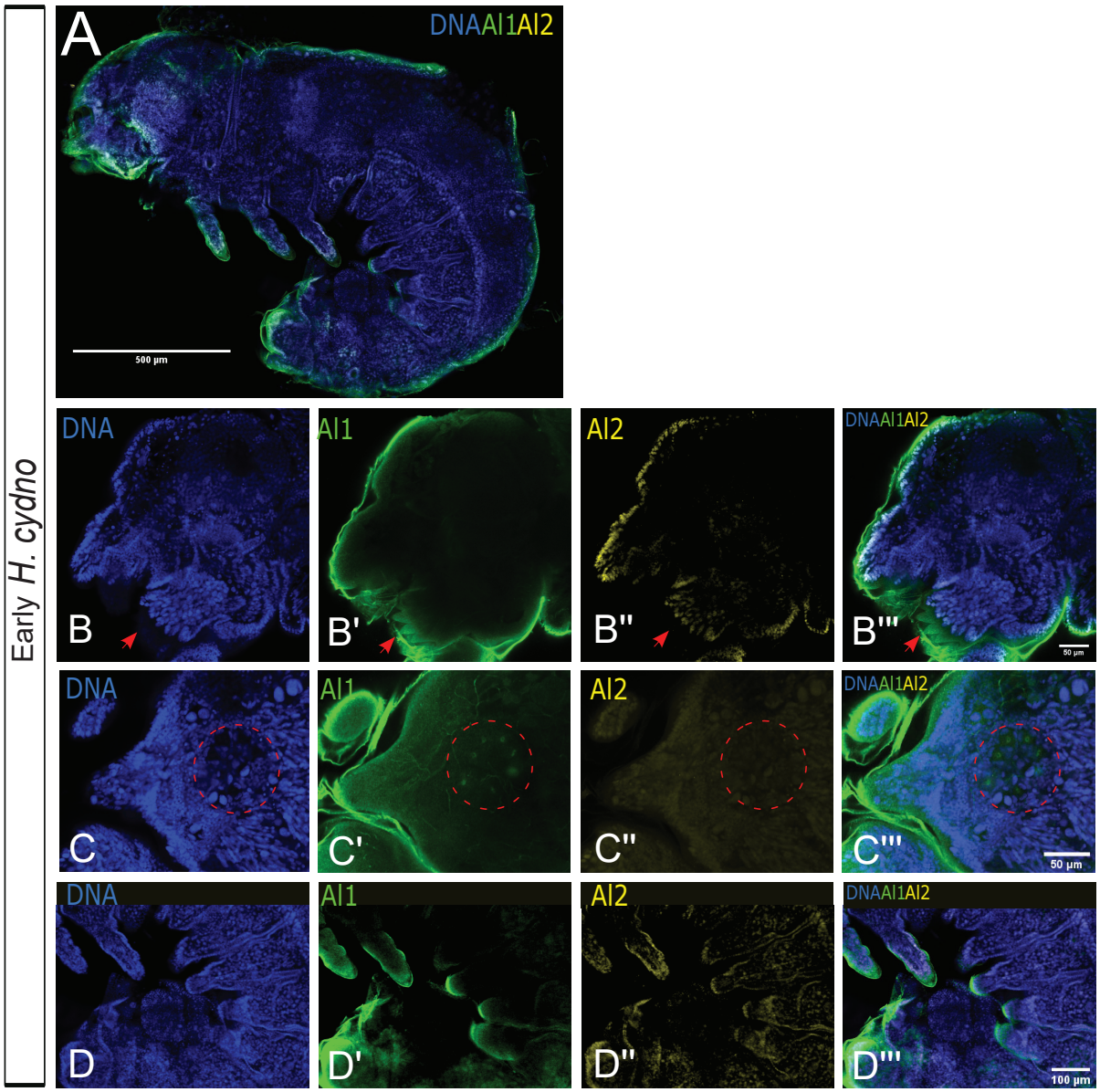

Figure 20: Immunodetection of Aristaless1 and Aristaless2 in wild-type *Heliconius cydno* embryos early in development. (**A**) Immunodetection of Al1 and Al2 in a full embryo. Highlights of the mouthparts (**B**), eye (**C**), and legs (**D**) are shown. Red arrowheads highlight the serrated structure from the mandibula. The red circle highlight the eye region on the C panel. Panels show detection of DNA (**B, C, D**), Al1 (**B', C', D'**), Al2 (**B'', C'', D''**), and a merge (**A, B''', C''', D''').**

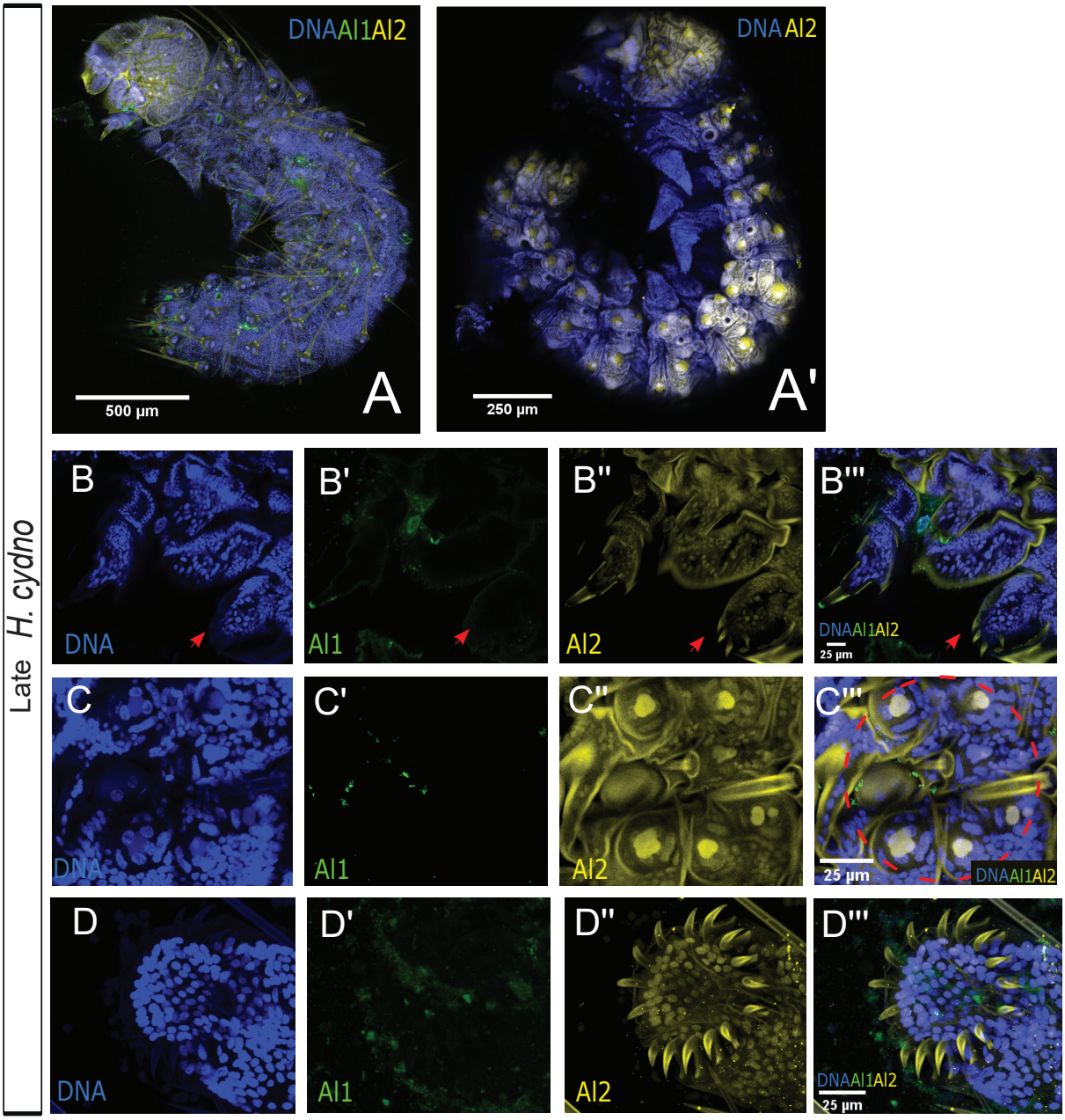

Figure 21: Immunodetection of Aristaless1 and Aristaless2 in wild-type *Heliconius cydno* embryos late in development. (**A**) Immunodetection of Al1 and Al2 in a full embryo. (**A'**) A view of the superficial spine cells is also shown. Highlights of the mouthparts (**B**), eye (**C**), and leg tip (**D**) are shown. Red arrowheads highlight the serrated structure from the mandibula. The red circle highlight the eye region on the **C** panel. Panels show detection of DNA (**B, C, D**), Al1 (**B', C', D'**), Al2 (**B'', C'', D''**), and a merge (**A, A', B''', C''', D'''**).

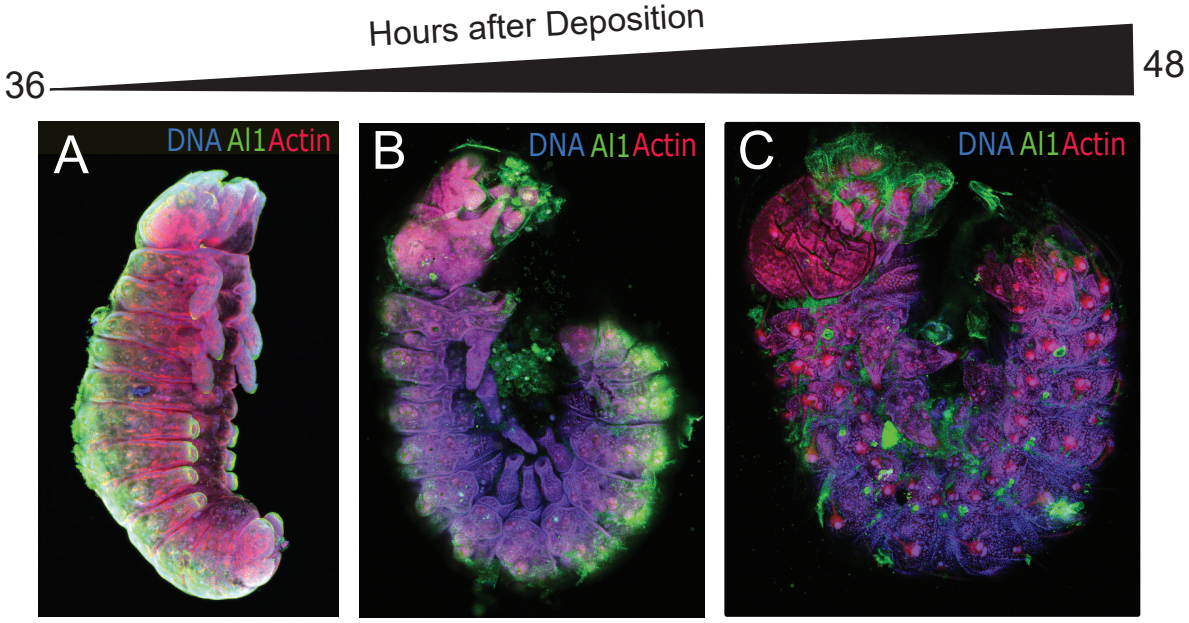

Figure 22: Immunodetection of Aristaless1 highlighting the dorsal domain of expression in wild-type *Heliconius cydno* embryos across development. (**A-C**) Immunodetection of Al1 across development. Hours after deposition are described at the top of the image. All merged panels show detection of DNA, F-actin and Al1.

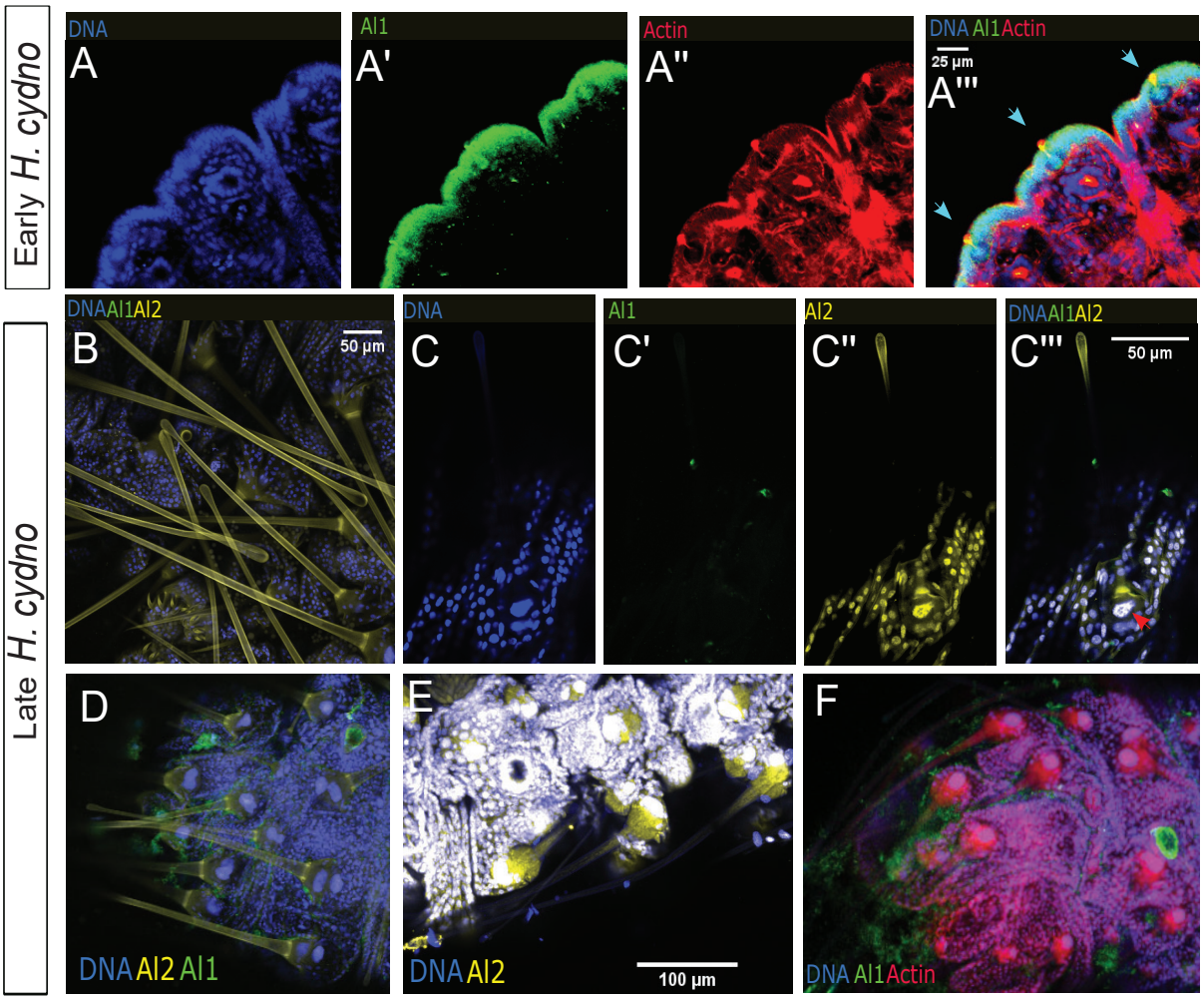

Figure 23: Immunodetection of Aristaless1 and Aristaless2 in *Heliconius cydno* spines across embryonic development. (**A**) Al1 and Al2 detection in early spine cells. (**B-F**) Al1 and Al2 detection in late spine cells closer to eclosion. The **B** panel showcases a view of multiple spines extending from the body. Details of one of the late spine cells are shown in panel C. The spines across the posterior tip are shown in panels **D-F**. Panels show detection of DNA (**A,C**), F-actin (**A''**), Al1 (**A', C'**), Al2 (**C''**), and a merge (**A''', B, C''', D-F**).

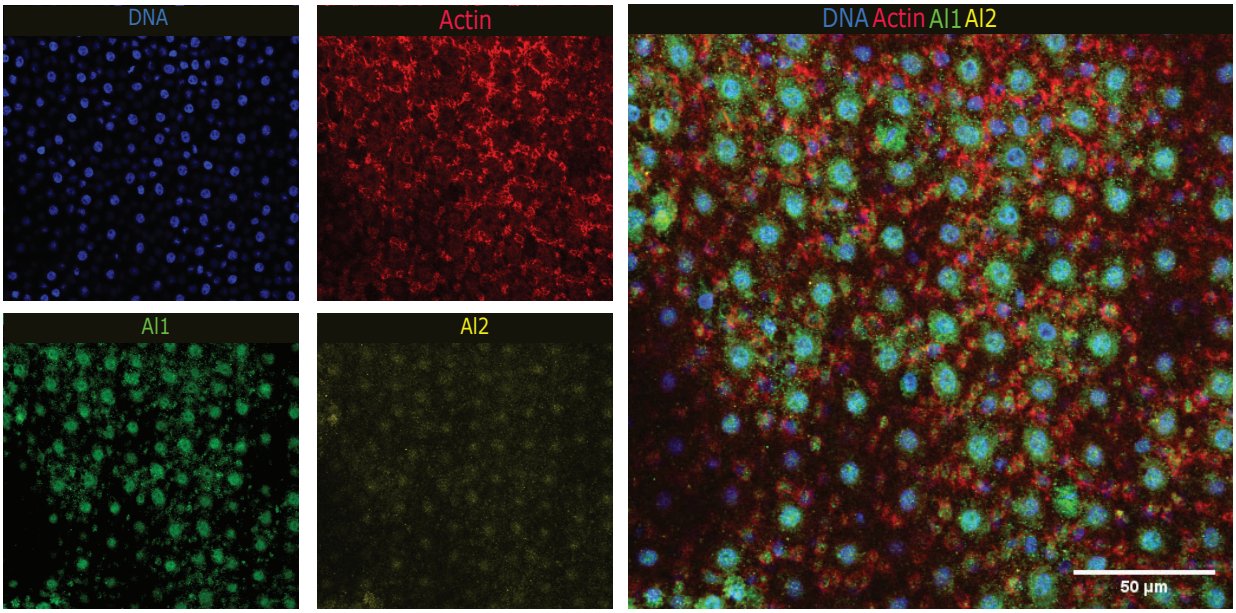

Figure 24: Immunodetection of Aristaless1 and Aristaless2 in *Heliconius cydno* day 1 white pupal wings. The panels show a close view of wing scale cells stained in a quadruple staining set up for DNA, F-actin, Al1, and Al2. The merge is shown on the right.

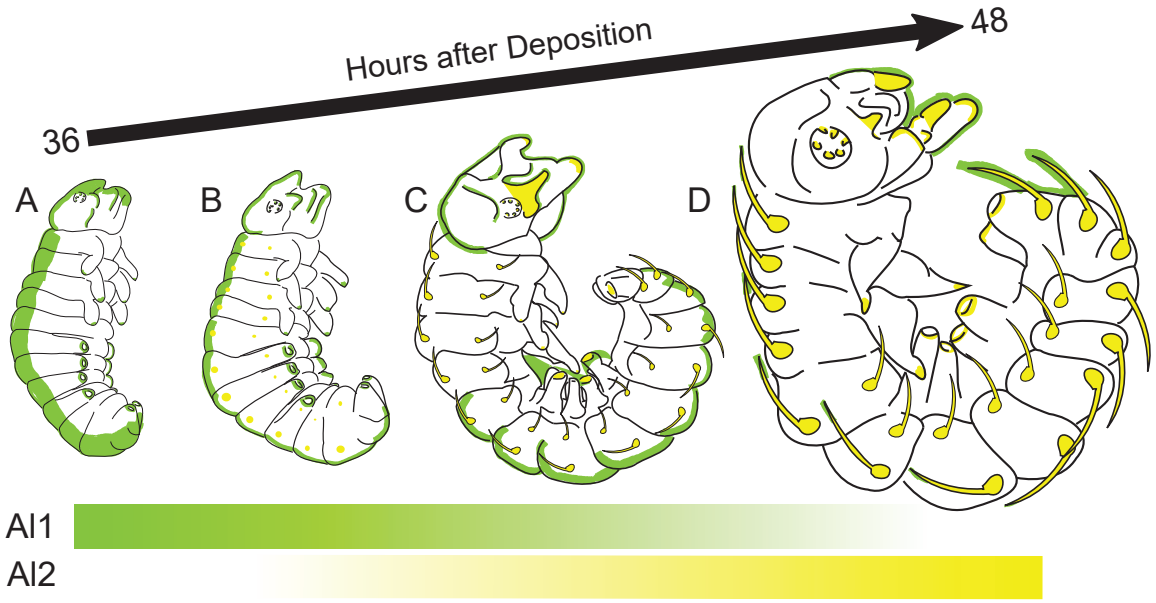

Figure 25: Schematic representation of Al1 and Al2 Immunodetection across embryonic development. The schematic showcases how Al1 activity appears to be shifted earlier in development while Al2 appears to be shifted late in development.

CHAPTER 4

GENERAL DISCUSSION

White and yellow wing pattern variation is crucial for the biology and life history of *Heliconius* butterflies (Kronforst, et al., 2006; Chamberlain, et al., 2009). Recently, research has mapped the white and yellow wing color switch to the gene *al1* (Westerman et al., 2018). The ancestral, pre-duplication version of Al has been implicated in the regulation of appendage formation (Campbell & Tomlinson; 1988, Schneitz, et al., 1993; Beermann and Schroder, 2004; Miyawaki, et al., 2002), highlighting a very different function than color patterning. The work presented in this dissertation focused on characterizing the developmental function of *al1* with respect to both its ancestral role in appendage formation and its new function as a color patterning gene (**Chapter 2**), allowing us to further understand color patterning and its evolutionary principles in nature. Furthermore it provides a comparative framework by investigating, for the first time, Al2 function in both ancestral and novel roles, further increasing our knowledge about the functional basis of both copies of the gene but also providing details on differences among them following the gene duplication event (**Chapter 3**).

More specifically, as part of **Chapter 2**, I analyzed first whether *al1* still carries the ancestral role with respect to appendage extension by first checking if it is expressed within extending appendages during embryological development. I validated this role using CRISPR knockouts. With such experiments, I was able to first observe that Al1 does, in fact, accumulate at the distal tips of appendages during early embryological development consistent with Al function observed in other insects (Campbell & Tomlinson; 1988, Schneitz, et al., 1993; Beermann and Schroder, 2004; Miyawaki, et al., 2002). Furthermore, Al1 knockouts exhibited depleted levels of

Al1 and furthermore showcased malformations associated with the extension and formation of appendages further providing evidence that Al1 still carries out this ancestral function.

After characterizing Al1 with respect to its ancestral function, I moved ahead and explored its novel function with respect to color patterning. I first analyzed Al1 expression during wing development between white and yellow to elucidate what differences might be responsible for the color pattern switch between individuals. Previous work has shown that CRISPR knockouts result in the switch of genetically white scales to yellow, suggesting that Al1 is important for specifying white scales or inhibiting yellow scales (Westerman, et al., 2018). By analyzing CRISPR wings, I was able to provide the new observation that CRISPR wings also exhibit effects on the black portion of the wing. These scales within CRISPR negative clones switch from black to brown color. This observation suggests that Al1 has an effect that is wider than the white and yellow parts of the wing. When I analyzed the pattern of expression of Al1 in white butterflies I observed this wing-wide role reflected, as it seems that every scale precursor cell exhibited expression of Al1 within a white wing. However, when I analyzed wings from future yellow individuals I observed that during a narrow window early in pupal development, Al1 is downregulated in the middle part of the wing (future yellow region). These observations suggest that Al1 presence is needed across the entire wing to inhibit yellow pigmentation. Then it is by downregulating Al1 activity in the future yellow parts of the wing that such a yellow fate is achieved. This observation was again validated by using CRISPR knockouts and RNAi.

Finally, as part of this chapter, I explored the developmental components around Al1 by looking at an upstream regulator and downstream effector genes responsible for carrying out terminal pigmentation. To do this, I used pharmacological agents to test whether Wnt signaling is upstream of Al1 as has been shown in a moth (Ando et al. 2018). First, by using pharmacological

agents I showed the white to yellow switch by inhibiting Wnt activity. Furthermore, when Wnt activity was enhanced, I was able to observe some yellow scales switch to white. This suggests that Wnt appears to be upstream of Al1 activity with respect to color patterning. I validated this observation by showing that when Wnt activity is reduced, Al1 subcellular localization is also depleted. Furthermore, some malformations are also observed within developing scales associated with their size when Wnt signaling is disrupted, suggesting some interesting future questions with respect to the role of Al1 with appendage extension and its relationship with Wnt signaling. I also analyzed downstream effectors genes under the control of Al1 to try to elucidate how this difference in Al1 expression is transferred into distinct terminal pigmentation outcomes. To do that I analyzed wings across the last days of pupation by qPCR to check for the expression level of different candidate genes related to yellow pigmentation. With this approach, I observed that following the window in which Al1 is downregulated in yellow, there is an activation of an enzyme and transporters needed to synthesize and move the yellow pigment or its precursors into the scales. This suggests that Al1 activity across the wing downregulates specific biochemical components needed for yellow pigmentation and it is not until Al1 is downregulated that yellow pigmentation can occur.

The second chapter of this dissertation addressed both Al1 expression and function within its ancestral (appendages) and novel (wing color) roles. As part of **Chapter 3,** I expanded on the cellular and temporal characteristics of Al1, but now comparing it with Al2 in order to have a full picture of the relationship between these paralogs and their relevance for both appendages and wing pigmentation. First, as part of this section, I analyzed Al2 expression during early embryogenesis to compare to Al1. The first thing I noticed by doing this was that Al2's highest expression is shifted later in development when compared to Al1. Furthermore, I described how

Al1 in embryos looked more diffuse and extranuclear with respect to its cellular localization. This was not consistent with Al2. During the analyzed timepoints, Al2 appeared to be localized with the nucleus earlier in development, but as time progressed, I noticed that its expression extended across extending appendages. Al1 subcellular localization in all extending appendages appears to precede Al2 activity. This observation suggests that both Al1 and Al2 are temporally shifted in expression but are still associated with appendages. Analysis of Al2 expression at pupal stages does showcase this same trend of Al1 being more diffuse while Al2 seemed more localized with the nucleus. Future analyses are needed to determine if this difference between white and yellow individuals is maintained for Al2 and further analyze if this temporal shift is also present during wing development.

The experimental chapters have addressed Al1 and Al2 patterns of expression at both ancestral and, to a certain extent, novel color patterning roles. Al1 activity has been validated using knockouts but Al2 expression remains to be validated. Despite our progress in understanding how these duplicated versions of the gene relate to their ancestral and novel functions a lot still remains to be understood. Although much of the presented evidence linking both ancestral and novel roles is by association, as part of **Chapter 2**, I discuss how Al1 role in appendage extension may relate to its color patterning function via effects on scale development rate. Heterochronic shifts have been shown to be relevant in scale color identity specification (Koch, et al. 2000). Being that scales are structures that also extend out of the primary body plan, the Al1 appendage formation role might be more relevant for the color identity decision than originally expected. As mentioned above the work of this dissertation has been focused on validating Al1 expression. Now that I have some information on Al2 suggesting a possible relationship with Al1 expression more work is needed to analyze whether the expression of these two paralogs is synergistic or related in any

way. For this, stainings are needed where one or both of the genes has been knocked out. This, together with several reciprocal experiments, are carefully described below.

Finally, this dissertation includes two appendices focused on work done to build resources and analyze certain aspects associated with terminal pigmentation and scale ultrastructural qualities. **Appendix 1** includes novel work focused on developing and adapting live imaging techniques for the study of *Heliconius* pigmentation. For it, I applied a baseline of techniques used on other butterfly species and adapted the protocols to analyze the events across late pupation before and during terminal pigmentation. With this approach, I was able to record, for the first time, the terminal pigmentation of white and yellow *Heliconius cydno* in real-time. This allows us to make several observations about the differences between black pigmentation and yellow pigmentation. In general, black pigmentation happened earlier, consistent with previous observations (Gilbert, et al., 1988; Hines et al. 2012). It was also more uniform, stereotypical, and happened across a wider window of time. Yellow pigmentation happened very late in pupation (just a few hours before eclosion, again consistent with previous work; Gilbert, et al., 1988). The yellow pigments appeared on the wing less uniformly, often starting very localized and then diffusing from that center. I was also able to observe scale shifts in ultrastructural qualities (shifts in UV reflectance) after black pigmentation but before yellow deposition by doing live recordings under UV light. Finally, by applying confocal microscopy I recorded the presence of the yellow pigment 3-OHK which is fluorescent under UV light (Finkbeiner and Briscoe, 2021). This information could be applied together with our live imaging approaches to eventually analyze yellow pigmentation coming into scales by using confocal microscopy in a living specimen.

As part of **Appendix 2**, I went deeper into scale ultrastructural morphology. Wings in butterflies are covered by scales which are the functional units adopting specific color fates. Scale coloration is created from the combination of pigments and ultrastructural coloration created from the optical properties of scales. Such ultrastructural qualities are very morphologically diverse (Ghiradella, 1991; Prum et al. 2006). Recently, a link between scale pigmentation identity and specific ultrastructural morphology has been proposed (Davis et al. 2020). Such a link has never been carefully explored due to the lack of centralized data sets with consistent measurements across species and scale color types. As part of this appendix, I was able to produce such a dataset that spans 35 species across 5 different families and 15 distinct scale color types for a total of over 6000 individual measurements from 7 morphological features and several other structural descriptors. Furthermore, I was able to perform some basic analysis to first investigate some general properties of scale ultrastructural morphology. Currently, these data are being used in collaboration with other researchers to further elucidate the question of whether there is, in fact, a link between scale color fate and its ultrastructural morphology.

Even, when a lot of progress has been made, in our understanding of the developmental role of Al1 in white and yellow pigmentation and the implications of Al1 and Al2 concerning appendage development, there still remain many questions to answer. As part of this final discussion, I go over some of these unanswered questions and describe some experimental approaches to tackle them.

4.1 Functional differences between Al and Al2 within their role in appendage extension

Al1 and Al2 were both seen to be associated with appendages (**Chapter 2-3**). However, only some evidence exists that showcases appendage malformations when Al1 is knocked out

(**Chapter 2**). These experiments addressing their functional characterization have not been expanded to Al2. Furthermore, the tight association between Al1 and Al2 domains remains interesting and suggestive of possible interaction due to the observed spatial and temporal differences observed (**Chapter 3**). Moving forward, in order to completely elucidate the Al1/Al2 relationship and the relevance of such interactions with respect to their function, I will need to dissect each component within a comparative analysis. I am proposing a set of knockout experiments to address the level of interaction and functional basis of Al2 activity to match our knowledge from Al1. **Chapter 2** already showed that Al1 knockouts do, in fact, deplete Al1 levels in embryos and wings and cause morphological changes in butterfly wings (white to yellow) and embryo appendages (extension deficiencies). In order to follow up on these results and to expand them to Al2, I would first take the same knockout approaches against Al1 and now include immunodetection against Al2. This will help determine if there is any effect of Al1 activity on Al2 expression. This will further inform me of any possible interactions or division of roles between the genes.

To do this, I already have in the lab guide RNA constructs targeting Al2. This coupled with our protocols and reagents against Al1 would allow us to do individual Al1 and Al2 knockouts as well as double knockouts. For Al2 I would look for similar effects to Al1. However, moving forward I would like to more carefully observe appendages and spines as these are structures that show constant expression of one or both Al genes across embryogenesis. Furthermore, the double knockouts would allow us to analyze any possible compensation between the genes by looking at more severe phenotypes on both the caterpillar appendages and adult wings/scales. Such scale morphology analysis could be coupled with SEM microscopy to determine the effects of each gene on the final ultrastructure of scales. I would then complement all our phenotypic characterization

with staining of knockout tissue to determine if there is first any depletion on Al2/Al1 as expected, and any possible effects on the expression of one of the genes when the other one is knocked out. In summary, I would have Al1/Al2 individual knockout tissue stained for both copies of the gene. And double knockout tissue as well stained for both copies of the gene. Once both of these experiments are completed, I should have information on the functional basis of Al2 and the level of interaction between the two copies of the gene when it comes to appendage development and pupal scale growth and coloration.

To further elucidate the relationship between both copies of the gene, I would also analyze if the interaction previously described for Al1 with other pathways like Wnt signaling (**Chapter 2**) also exist with respect to Al2. As part of Chapter 2, I described how Wnt signaling appears to be upstream of Al1 by employing pharmacological agents enhancing or reducing Wnt activity (**Chapter 2**). This is very interesting considering that the same relationship has been shown for antennal development in moths (Ando et al., 2018). The same pharmacological agents can be used to then address their effect in Al2 to further analyze if both Al1 and Al2 are responding in the same way or whether there appears to be differences in their regulation. In the case no visible phenotypes are present following Al2 knockouts, I would use antibody staining to analyze the effects on the protein levels following the application of the pharmacological agent. Other developmental pathways have also been shown to be implicated with the regulation of Al1/Al2 in moths. For example, Notch and Dll have also been shown as regulators of Al1/Al2 activity (Ando et al., 2018). This opens future work that could be done using other pharmacological agents to further map out the effect of these pathways on Al1 and Al2 expression or activity during embryogenesis and pupation. Furthermore, and more interestingly, all research in Lepidoptera up to this point has attributed the role or effects of Al to both copies of the genes due to the use of tools that cannot

distinguish between the two copies. The experimental approaches described here would allow me to first uncover the functional basis of both copies of the gene and take it a step further by analyzing how their duplication has led to changes in developmental pathway connectivity. This work has major relevance in the study of gene duplication, sub-functionalization, and the evolutionary basis of developmental pathways.

4.2 Regulatory qualities of Al and Al2 and possible protein interactions

Being that Al is described as a homeodomain transcription factor based on structure, the question remains if Al1 and Al2 do also carry out any downstream gene regulation. One way to get at this is using our antibodies in pull-down approaches like CUT&RUN (Cleavage Under Targets & Release Using Nuclease) or CHIP-seq to specifically sequence the areas in the genome bound to Al1 and Al2. Once this is done, I would prepare libraries of these sequences in order to identify what genes might be under the regulation of Al1, Al2, or both. This would provide a list of possible candidates under the direct regulation of Al1 or Al2. There are a couple of limitations associated with this approach. The areas sequenced could be hard to interpret due to limited information on the regulatory qualities of cis-elements in butterflies. However, even when such limitations exists this approach would still provide gene candidates closest to the presumptive cis-regulatory elements at least working in unison with the qPCR data shown in **Chapter 2**. Another limitation could be associated with a possible lack of regulatory roles for one or both versions of the gene. If that is the case, this approach could still inform us that such downstream transcriptional regulation may not be happening directly, which on its own is still a relevant result.

Similarly, possible dimerization events implicated in transcriptional regulation have been described between Al and other proteins (also associated with appendage formation, Tajiri et al., 2007). Such protein-protein complexes are believed to have regulatory roles. In order to determine,

if these kinds of interactions are happening between the two versions of the gene or with other proteins, some biochemical approaches could be used. Yeast-2-hybrids could be a simple way to analyze possible interactions in a candidate-based approach. However, it is a candidate-based approach that would only let us target possible interactions between proteins hypothesized to be interacting. Both versions of the gene as well as *clawless* or *Barh1* could be a good starting point based on previous data (Tajiri et al., 2007). However, the list of possible dimerization targets is only informed from a small amount of data from other systems making this candidate approach very challenging. A more challenging approach that requires a level of biochemistry expertise would be to perform pull-down approaches similar to the ones described above but now targeting the protein complexes. Such complexes can be dissociated by employing mass spectrometry with both the original interacting complexes and following dissociation. These mass spectrometry data could be used to complement crystallography approaches to determine what proteins could be interacting with Al1 and Al2. This set of approaches, although unbiased, would require a high level of expertise and a longer window of time to properly carry out.

4.3 Extranuclear localization of Al1

Another interesting result that is worth following up is the observation from Chapter 3 showing how Al1 appears always to be extranuclear while Al2 shows a shift from nuclear to extranuclear. This observation is one of the most puzzling results of my entire dissertation. Al1 was never seen to co-localize with the nucleus, which is interesting given that Al1 is categorized as a homeodomain transcription factor. Chapter 2 does include several scenarios and examples of other homeodomain proteins that do carry out regulatory activity outside the nucleus. I propose that one way to address this possible lack of nuclear translocation is to analyze even earlier in development to see if this shift from nuclear to cytoplasm seen with Al2 ever happens with respect

to Al1. Although this is not an easy task due to the difficulty in dissection and manipulation of the tissue, some options do exist that may allow us to observe some of these earlier time points. One easier time point I have not looked that carefully is larval wings. In terms of Al1, our limited amount of stains (limited due to the difficulty of the removal of the peripodial membrane) do suggest that no nuclear co-localization is happening on larval wings. However, more time points from larval wings closer to pupation may provide a wider sample size to analyze whether Al1 appears to co-localize with the nucleus. Along the same line, earlier time points in embryonic development may provide a similar answer. The only limitation of targeting embryos before the 24-hour mark is the difficulty associated with their dissection. I have developed protocols for staining embryos within the egg for DNA and actin markers. However, those eggs are impermeable to the big antibodies used in this work. However, employing more aggressive detergents or pore-inducing chemical reagents like glycolic acid (used on wings for opening membranes) could allow staining without dissecting the embryos out of the eggs.

4.4 Finding the functional link between appendages and wing coloration

Finally, one of the biggest mysteries that remain about Al1 and Al2, to some extent, is how they functionally control appendage extension. Furthermore, how such appendage functions relate to their role in pigmentation. Chapter 2 does go into detail about possible links between the two functions. It does this primarily by referencing the heterochrony hypothesis (states scale color fate is linked to its maturation time; Koch et al., 2020) as a principle of scale determination. Under such circumstances, if we think of scales as single-cell appendages extending we could see a link to other single-cell appendages under the control of *aristaless*. Some of these include the arista bristles in flies (Campbell and Tomlinson, 1988; Schneitz, et al., 1993), the horns adornments of beetles (Moczek, 2005), and the antennae branches in moths (Ando et al., 2018). If these principles

are the same as multicellular appendages like legs and the antennae then the question remains of what are *aristaless*, *al1*, and *al2* doing to control or organize such growth processes. Appendage elongation is guided by both extending cytoskeletal components and vesicle transports carrying cytoplasmic components. This process requires stabilization and control of multiple elements like polymerization of cytoskeletal components like actin and microtubules, regulation of cell growth and cell shape, cell-to-cell communication, and complex trafficking systems. Moving forward, and based on our observations for the differences in the subcellular localization of Al1 and Al2, it would be interesting to further analyze their involvement in such cellular processes.

I believe spine growth could be a great system to further explore this. Both Al1 and Al2 are expressed very distinctively during spine development as shown in Chapter 3. Furthermore, spine cells seem to be simpler cellular systems seemingly composed of only 2 cells (probably one neuronal and one structural similar to what is reported in scales and bristles in flies [Nijhout, 1991]). Spine cells also come with the advantage of big and superficial cellular bodies making observations about their growth easier. I believe a good first approach would be to do a careful time series analysis of both Al1 and Al2 staining coupled with staining of several markers against multiple cellular components like actin, tubulin, and membrane markers. This coupled with high magnification confocal microscopy might first inform us of changes within the organization of the cell correlated with Al1 and Al2 activity. Furthermore, having CRISPR Knockout embryos for both Al1 and Al2 may allow dissecting this even further by looking at spines within and outside of CRISPR clones. This would provide an interesting comparison of shifts in cellular events or structure associated with the presence or absence of Al1 and Al2 activity.

Another approach that could be used to learn more about the role of Al1 and Al2 within scale growth and cytoskeletal structure would be to look more closely at scale ultrastructure on

adult wings. It has been shown that scale ultrastructure is affected by both rates of development and the organization of cytoskeletal components like actin earlier in development, which serves as a blueprint for chitin in the adult structure (Dinwiddie et al., 2014). As part of our Appendix 2, I recorded data of wild-type and Al1 deficient white scales that give us some preliminary insight. It can be observed that Al1 deficient scales do show malformations in scale ultrastructure mainly causing the width of the ridges to shift caused by extra and uneven crossribs. This would suggest that Al1 may be important in some cellular processes needed for proper growth and organization of scales. More careful analyses with a bigger sample size are needed to further elucidate the importance of Al1 and Al2 for proper scale growth.

A third approach to this same question is to employ a qPCR strategy similar to **Chapter 2** but instead of using pigmentation effector genes, to look for differential expression of genes associated with actin, tubulin, or chitin polymerization. That, together with genes involved with cellular trafficking or elongation factors, could be a good first set to dissect differences. Along the same line and with a more unbiased approach, RNA-seq could also be used to find other targets that might be downstream of Al1 activity. Such target might be related to either pigmentation or appendage extension in both cases resulting in very interesting and informative outcomes. I already have RNA extractions for multiple yellow and white wings spanning sections of the wings with different color patterns. This RNA extracted from wings could be used for both qPCR approaches and RNA-seq.

In general, a few of the suggestions above tackle some of the possibilities that Al1 and Al2 might have important roles with respect to regulation of cellular processes needed for appendage specification and elongation, linking both ancestral and novel gene functions. Is Al1 regulating pigmentation as a result of its appendage extension role during scale development or is Al1 directly

regulating downstream genes involved in pigmentation, as suggested from our data in **Chapter 2**? I want to clarify again that these are not mutually exclusive and the actual function may reside somewhere in the middle of both functions. Regardless, the future directions mentioned above will provide more information about Al1 and Al2 function within cells and multicellular appendages, getting us closer to completely understanding the principles behind both butterfly embryology and coloration.

"Will extending the color pallet lead researchers to paint a different picture of the development and evolution of color patterns?"

Adapted from: Wittkopp & Beldade, 2009

APPENDICES

APPENDIX 1: APPLICATION OF NOVEL IN VIVO IMAGING TECHNIQUES FOR THE STUDY OF PIGMENTATION IN HELICONIUS BUTTERFLIES

5.1 Abstract

Butterfly pigmentation has been a powerful tool to study phenotypic diversity. Most of this research has focused on the genetic basis of pigmentation which has given rise to a lot of careful characterizations of the developmental mechanisms behind such color patterns. However, butterfly terminal pigmentation analyses have been restricted to specific species and to temporal snapshots. Here I adjust live imaging protocols for studying butterfly pigmentation to the *Heliconius* system to analyze *in vivo* their terminal pigmentation steps. I perform live imaging of previously reported stages for melanin pigmentation and characterize events during the shift from white to yellow pigmentation. Finally, I couple our live imaging approaches with UV light to analyze specific features of scale morphology and the yellow pigment acquisition in scales.

Specific Acknowledgments:

This work was done in collaboration with **Darli Massardo** (butterfly rearing and maintenance prior to the experimental set up) and **Lukas Elsrode** (performed sample preparation for live imaging runs of wild type white and yellow *Heliconius cydno* butterflies).

5.2 Introduction

Analysis of butterfly pigmentation within the field of developmental biology has focused on fixed tissue, mainly targeting earlier stages of the color patterning process (Kronforst and Papa, 2015). During the development of the wing patterning genes serve as the blueprint for the future pigmentation machinery which, by employing enzymes, carries out terminal pigmentation during the later stages of pupation (Reed at al., 2008). This terminal pigmentation process is well organized and temporally complex due to several factors like patterning genes controlling pigmentation elements (Reed at al., 2008; Hines et al., 2012) and scale developmental rate (Koch et al., 2018). Recently, this has highlighted the need for the development of *in vivo* techniques to analyze the process of terminal pigmentation and to complement fixed tissue approaches. Live imaging techniques give access to different questions by allowing us to see events in real-time. These approaches can help us understand when and where in the wing such processes start, the steps toward the final pigment, and any general rules or principles among different pigment synthesis pathways and their underlying genetic control.

Here I applied and adjusted limited unpublished *in vivo* imaging protocols (provided by Dr. Ryan Null) for analyzing the terminal pigmentation events in butterflies to the genus *Heliconius*. In this group, the genetic basis of color patterning has been well resolved (Kronforst and Papa; 2015). In addition, many developmental studies do exist that have provided expression data for specific color elements, like in the case of genes *wntA* and *optix* (Kronforst and Papa; 2015). Melanic patches under the control of *wntA* and red patterns under the control of *optix* have also been shown to develop by looking at snapshots of their terminal pigmentation process (Reed at al. 2008, Hines et al., 2012). However, these butterflies also exhibit diversity with respect to the presence or absence of the yellow pigment under the control of Al1. Here Al1 activity represses the yellow fate promoting a white wing while the lack of Al1 results in an upregulation of enzymes

needed for the formation of the yellow pigment 3-OHK (See data in Chapter 1). Yellow pigmentation has little to no *in vivo* description, not even by snapshots like the red and black color elements. This highlights the need to first apply and further develop live imaging techniques to observe the timing and formation of yellow color patterning. A live imaging approach allows more careful observations, which can complement previous work which only shows snapshots of specific pigments. In addition, by focusing on both white and yellow butterflies, I am able to fill the gap in knowledge for these color patterns and learn more about the temporal and spatial basis of 3-OHK pigmentation in wings. Finally, once I analyze the developmental features of the different components of the final pigmented wing, I can start to provide information about any commonalities among different pigmentation outcomes and provide insight about relationships between the patterning genes and terminal pigmentation events.

As part of this work, I first adapted and developed a protocol for studying live imaging events in white and yellow *Heliconius cydno* during terminal pigmentation. For this, I opened a window through the cuticle that would allow us to see the development of the wing *in vivo* while pigmentation was still happening. I then recorded the development of the wing in one minute intervals to provide a careful characterization of the events leading to the final pigmented wing. I performed this process with both white and yellow *Heliconius cydno*. Finally, I used UV light in some of our live recordings to analyze some of the features of the yellow pigment and the morphological qualities of scales.

5.3 Results

5.3.1 White *Heliconius cydno* pigmentation features

Our protocol was efficient in maintaining butterflies alive while imaging for 20 to 50 hours. Using this protocol I was able to record the terminal pigmentation stages of white *Heliconius cydno* butterflies (**Video 1**, **Figure 26**). Melanic pigmentation started between 6 to 7 days after pupa formation (APF) as shown from other studies (Reed at al., 2008; Hines et al., 2012). Our observed individuals exhibited a progressive, mostly proximo-distal, pigmentation trend. Similarly, the proximal part of the wing finished melanic pigmentation earlier than the distal side. The observed time between the start of melanic pigmentation (light brown) to finalized dark melanin was around 14 hours. The change from lighter brown to darker melanin was clearly visible and not affected by the techniques and reagents used.

5.3.2 Yellow *Heliconius cydno* pigmentation features

Both the time and the progressive trend of melanic pigmentation were also observed in yellow *H. cydno* (**Video 2**, **Figure 27 & 28**). Yellow pigmentation started after the melanic pigmentation was completed. Melanic pigmentation took around 15 hours. Interestingly, yellow pigmentation only took around 2-3 hours to complete and was very close to eclosion, as indicated by attempts by the butterfly to exit the chrysalis. Probably due to the experimental preparations, some of the yellow individuals did not have an even distribution of yellow pigment on the wing at the end of the pigmentation process. This was noticeable when the plastic wing cover was kept in place throughout the pigmentation process. (**Figure 27**). However, and more surprisingly from all the observed individuals and different from any other color component of the wing, the yellow pigment coming into the wing started very localized in a section and then spread to the rest of the wing band.

5.3.3 UV light and confocal microscopy can be used to study other features of terminal pigmentation

I took advantage of some of the optical properties of white scales (High UV reflectance) and the yellow pigment 3-OHK (fluorescent under UV light; Finkbeiner et al., 2017; Finkbeiner and Briscoe, 2021) to analyze some of the morphological events occurring during terminal pigmentation. Doing a time series under UV light of a yellow butterfly (during the last 24 hours of pupation) showcased morphological transformation of scales observed by differences in UV reflectance. White scales have been shown to have high UV reflectance (Westerman et al.,2018). As time progressed after black pigmentation was finished, more scales within the band region changed to this UV reflectance state (**Video 3**, **Figure 29A**). With this analysis, I could not observe the yellow pigmentation happening under the UV light, probably due to issues of survival under UV light or the optics of the system with the plastic covering. However, by employing the same cuticle removal technique now closer to the onset of yellow pigmentation, and in confocal microscopy, I was able to observe the yellow pigment within scales of the wing just minutes before the butterfly attempted to eclose (**Figure 29B**). These preliminary observations suggest that fluorescent microscopy and the UV properties of these scales could be used for a more detailed analysis of how yellow pigmentation and scale development occurs on *Heliconius* wings.

5.4 Discussion

As part of this work, I was successful in adapting live imaging protocols from other species (Brakefield, et al., 2009) to *Heliconius cydno* butterflies in order to study white and yellow terminal pigmentation. I was able to record in detail both white and yellow terminal pigmentation events which highlight several events observed by single snapshots in previously published work (Reed at al. 2008, Hines et al., 2012). Some of these observations included, firstly, the progression from lighter to darker melanin associated with the steps of melanin synthesis. Secondly, I observed how black color patterns are completely laid out before yellow pigmentation starts, which only happens

in a short two to three hours window just before eclosion. I also made note of several new observations like the uniform and proximo-distal progression observed in black pigmentation. Such progression was slower, extending over 24 hours. Yellow pigmentation, although less stereotypical, followed a more posterior to anterior progression. Finally, I showed that UV light and confocal microscopy have the potential for future studies of terminal pigmentation. Our recordings under UV light highlighted changes in the UV reflection properties for scales within the wing band. Furthermore, by using confocal microscopy, I was able to observe the yellow pigment on the wing of a pre-eclosion pupa.

I also encountered several limitations that prevented us from imaging certain events. Survival under UV light was very limited, which resulted in the death of any pupa imaged longer than 24 hours. Furthermore, because the time window of yellow pigmentation is very narrow, it was not trivial to start imaging just before it started. This issue was further exacerbated by doing these recording with confocal microscopy. Due to confocal regulations, the temperature in the room during imaging is colder than growing conditions, which severely slowed down the rate of development for the pupa making the time window of imaging larger and further affecting survival. All of this together made the imaging under UV light and confocal a bigger challenge. However, despite these limitations, I was still able to get recordings by both approaches. This implies that a bigger sample size and a more careful imaging regimen (probably keeping pupas closer to eclosion) will provide more details.

5.5 Methods

Butterfly rearing

Butterflies were reared in greenhouses at the University of Chicago with a 16h:8h light:dark cycle at ~27°C and 60% – 80% humidity. Adults were fed Bird's Choice artificial butterfly nectar. Larvae were raised on *Passiflora oerstedii*.

Sample preparation for live imaging:

I took pupae from the greenhouse into the lab 6 days APF. I then carefully removed the cuticle covering the forewing. The opening was started in the middle of the wing section. Then I peeled pieces of the cuticle carefully until a big enough window to see both inside and outside the middle portion of the wing (future white or yellow band) was achieved. The vein pattern was used to infer the band position in case pigmentation was not apparent. The removed cuticle would not reach too deep into the cuticle outside the wing cover as it would compromise the integrity of the pupa and lead to desiccation. The windows were mostly restricted to the middle section of the band using the Cu veins as reference. I employ PTU to inhibit the melanization that is triggered as a wound healing mechanism. I applied sets of PTU to the forewing until a bubble dome was visible. Then I cut a piece of saran plastic slightly bigger than the opening on the pupa. The plastic was placed over the opening and then tucked in the corners to go under the remaining cuticle to make sure it was properly sealed. I then placed the pupa on a wet piece of kimwipe (PBS) and positioned it under the scope next to a humidifier to avoid desiccation. I used a Zeiss stereomicroscope Discovery.V20 with AxioCam adapter. The live recordings were performed using the Zen 2020 software with the timelapse supplement under normal and UV light. All images were analyzed using the Zen and ImageJ Software. A total of three yellow (two of which completely showcased yellow pigmentation) and four white *Heliconius cydno* were imaged under normal light and one yellow was imaged under UV light.

Confocal Imaging of 3-OHK

The fluorescent signal of 3-OHK was analyzed using confocal microscopy on yellow scales. The parameters were adjusted based on the peak absorbance/excitation of 3-OHK (Finkbeiner 2017; 380 nm). Images were taken using Zeiss LSM 710 Confocal Microscope and processed using Zen 2012 (Zeiss) and ImageJ. Two yellow individuals were used for confocal imaging (only one made it to yellow pigmentation).

5.6 Figures

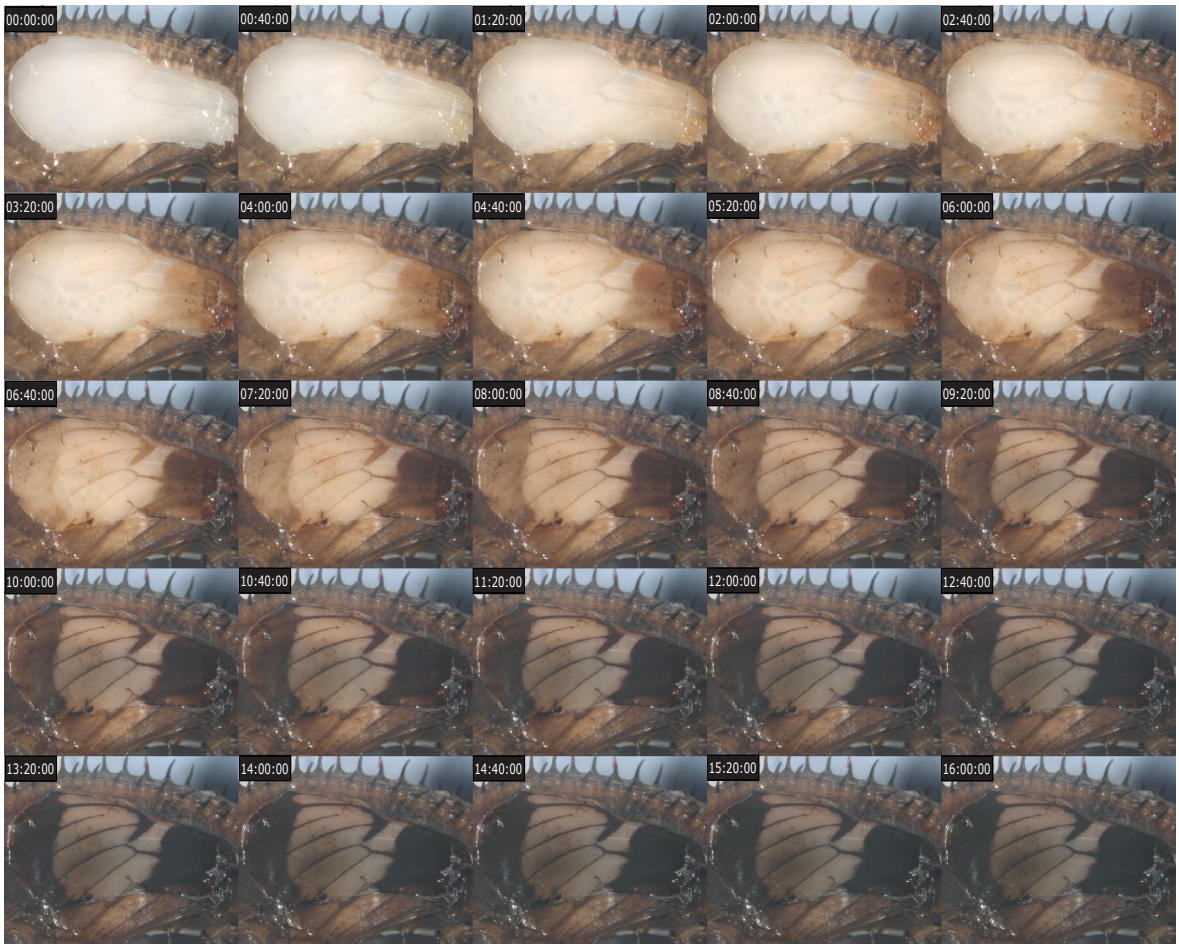

Figure 26: Developmental time series of the terminal pigmentation steps of White *Heliconius cydno* pupa. The recording started around 6 days APF. The time stamps are shown on the top left corner of each panel. Each panel corresponds to the slice at 40 minutes of imaging.

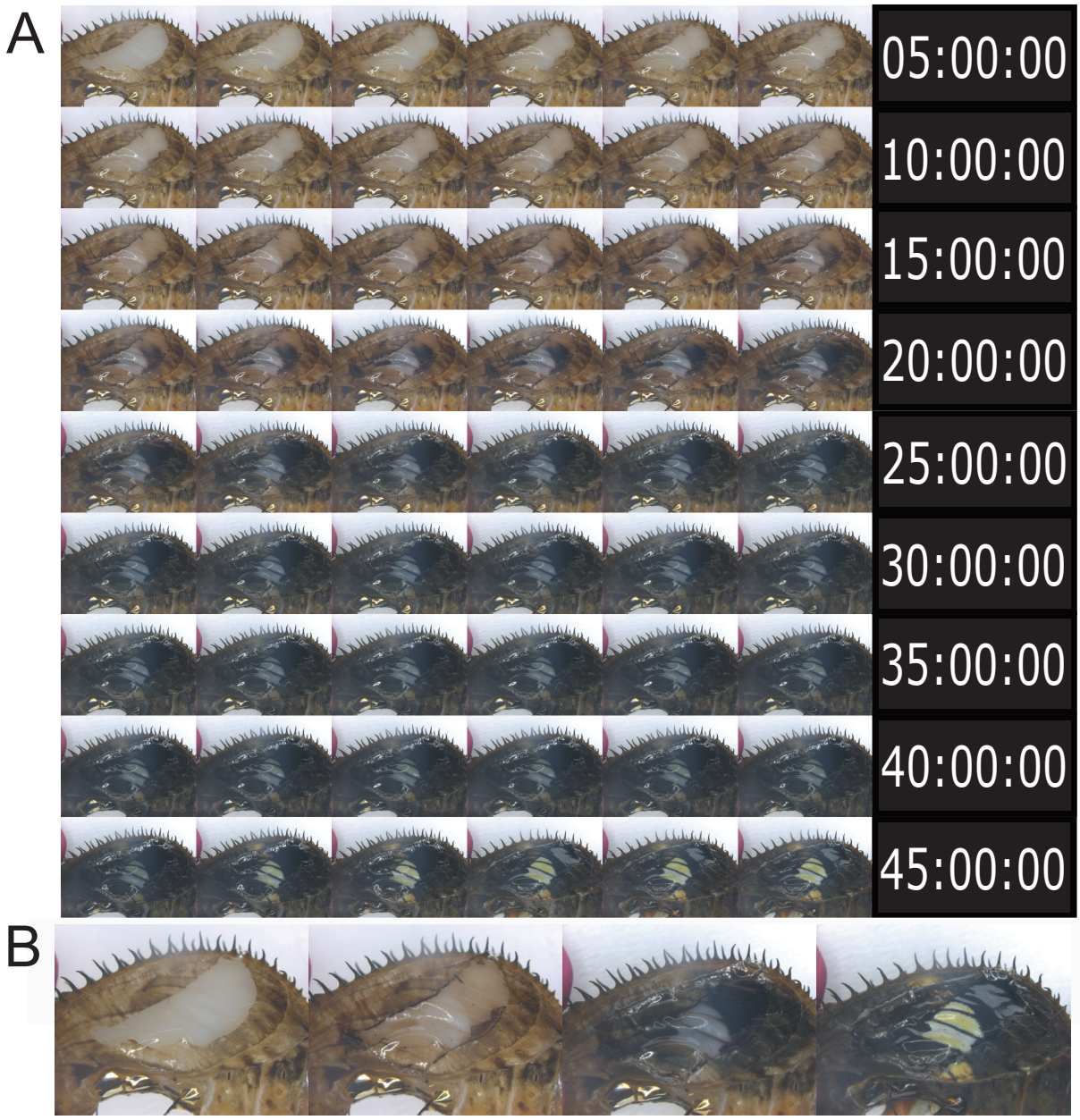

Figure 27: Developmental time series of the terminal pigmentation steps of yellow *Heliconius cydno* pupa. The recording started around 6 days APF. The time stamps are shown on the right side of each panel. Each panel corresponds to the slice at 50 minutes of imaging. Panel A showcases the full set of slices with the time details and panel B highlights the biggest transitions.

Figure 28: Yellow *Heliconius cydno* pupa on the last 3 hours of pupation. The plastic cover has been removed to be able to clearly see the yellow pigment. White arrow highlights an area of yellow pigment accumulation.

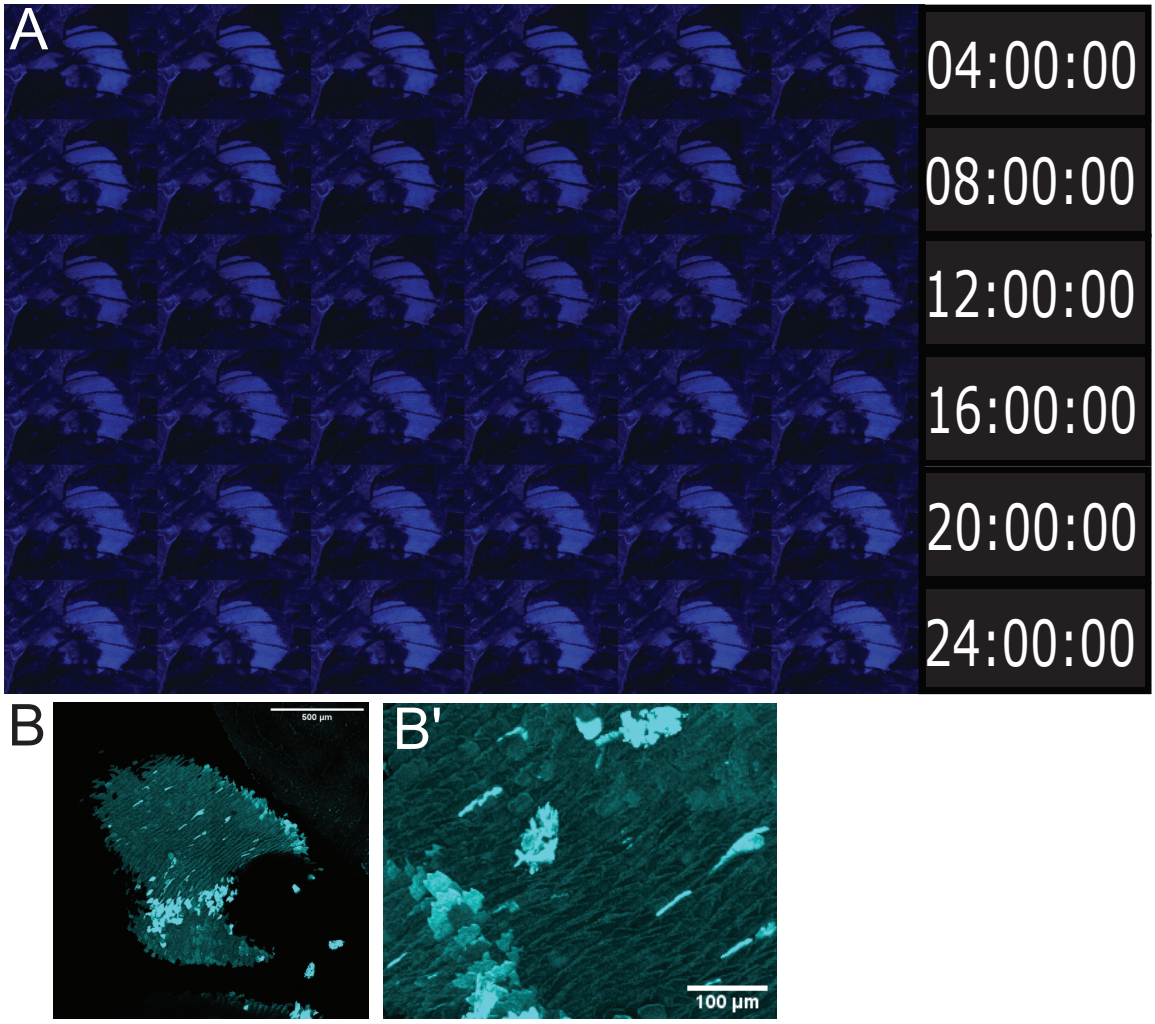

Figure 29: Time series analysis during terminal pigmentation of yellow *Heliconius cydno* pupa under UV light. (**A**) Time series of a yellow *Heliconius cydno* pupa under UV light. The recording started around 6.5 days APF. The time stamps are shown on the right of each panel (each panel corresponds to 40 minutes of imaging). (**B**) Confocal images of a yellow *Heliconius* pupa hours before eclosion showcasing the yellow pigment within the scale. B' highlights a detail of a yellow scale.

APPENDICES

APPENDIX 2: BUILDING A BUTTERFLY WIDE DATABASE FOR THE ANALYSIS OF SCALE ULTRASTRUCTURE MORPHOLOGY AND ITS RELATIONSHIP WITH COLOR IDENTITY

6.1 Abstract

Butterfly scales have complex and diverse ultrastructure. These ultrastructural qualities have often been studied for their implications on structural coloration. However, recent work has also shown a relationship between ultrastructure and the pigmented color fate. This may suggest that ultrastructure morphology might be tied to the same underlying processes determining pigmentation outcomes and the specification of color identity. While plenty of data exist showcasing the morphological qualities of specific colored scales, there is almost no work comparing scale ultrastructure among different butterflies groups. Furthermore, outside of very specific color scale types, there is almost no work comparing morphological traits across multiple groups and multiple colored scale fates. Such comparisons are even more challenging due to the lack of a centralized dataset that includes morphological data on scale ultrastructure across butterflies and with the representation of multiple color identities. Here I present our work in trying to build a rich data set on scale ultrastructural morphology that will eventually allow us to tackle questions about the relationship between pigmented color fate and scale morphology. Our dataset includes 38 species spanning 7 different families. I included over 15 distinct scale color types for a total of over 7000 individual measurements from 7 morphological features. I also included data on mutant or altered scales and even other morphological qualities associated with scale

ultrastructure. I also include preliminary analyses of several of our morphological features to start tackling several of the trends observed within our wide dataset.

Specific Acknowledgments:

This work was done in collaboration with **Darli Massardo** (literature search and contacting authors to acquire images to perform the measurements), **Roberto Marquéz** (guided me in the preliminary analysis and contributed to organization and interpretation of the data), and **Lukas Elsrode** (performed morphological measurements of both wild type and mutant scale ultrastructure, in addition he contributed to the preliminary analysis done).

6.2 Introduction

Butterfly colors have been a topic of fascination for many fields across several scientific disciplines (Kronforst et al. 2012). These color patterns are made up of morphologically complex structures called scales (Nijhout, 1991; Ghiradella, 2010; **Figure 30A**). Butterfly scales are the functional, individual units that across a developmental process adopt a single color fate (Nijhout, 1991; Janssen et al., 2001). These color fates are a combination of pigmented biochemical components and ultrastructural physical qualities (Nijhout, 1991; Janssen et al., 2001; Ghiradella, 2010). Previous research has provided evidence that such color identity associated with specific pigments can also be linked to specific ultrastructural morphological qualities (Janssen et al., 2001, Davis et al., 2020). For example, ultra-black scales, which are a kind of darker melanic scales, have evolved independently multiple times across the phylogeny of butterflies (Davis et al., 2020). Ultra-black scales have also been shown to converge to the same ultrastructural quality of extra-long trabeculae (Davis et al., 2020). This raises the question of whether scale ultrastructural morphology is linked to color identity or if it is just a proxy of phylogenetic relationship, making

the observation of ultra-black scale more of the exception rather than the rule. In order to answer this, a database is needed that spans multiple butterfly groups and multiple scale color types.

Although plenty of Scanning Electron Microscopy (SEM) data exist on scale ultrastructural qualities, we lack consistent measurements across a big sample size. Furthermore, no centralized and accessible dataset exists for scale ultrastructure. Here I present our work on producing a consistent dataset including several morphological measurements across multiple butterfly groups with the representation of several color identities. All of this together with the hope to produce one of the first datasets on scale morphology with consistent measurements across a big sample size. Such dataset would allow us to tackle the questions described above.

6.3 Results

6.3.1 Morphological measurements

As part of this work, I analyzed 38 species across 7 different families and 15 distinct scale color types for a total of over 7000 individual measurements from 7 morphological features and several other structural descriptors. For all the analyzed scales I included both the reported color and the RGB value based on the species images. Some of the measurements I took into consideration were the area and perimeter of the openings of scales in addition to circularity descriptors, the distance between ridges, and the thickness of crossribs (**Figure 30B**). All this measurements were done from top views of scales in which the visual openings created between crossribs and ridges were categorized as windows for area, perimeter and circularity measurements. I also included measurements on the height of the trabeculae when side views or cross-sections were available (**Figure 30C**). In addition, other morphological qualities were recorded like the presence of a membrane covering windows, beads, scutes, or other kinds of adornments. All of these measurements were put together to perform preliminary comparative

analyses with the hope to tackle the question of whether scale color identity is associated with particular morphological qualities. I also aim to analyze the alternative hypothesis of whether scale morphology is just a proxy of relatedness by including phylogenetic data in our future analyses.

6.3.2 Building a dataset of butterfly scale ultrastructure

After the initial selection process I focused on using images from 25 publications to collect data on scale ultrastructure morphology (**Table 2**). From this selection process I included measurements on 38 butterfly species and a handful of moth species (Full list of species in **Table 3**). For all species I measured five morphological traits from the top view of scales (crossrib thickness, ridge to ridge distance, and descriptors of their windows opening including perimeter area and circularity). When side reconstructions or cross-sections were available, I measured both the ridge elevation and the trabeculae length. Raw data for all the measurements of wild type butterflies are included in **Table 4**. Averages and other recorded descriptors of ultrastructure qualities of scales are summarized as well in **Table 3**. As part of this process, I included a smaller sample size of mutant or manipulated scales in which both the wild type color and the color after the manipulation was recorded (**Table 5**). For all our measurements I recorded and noted both the color described by the author and the color based on the RGB value to further remove some of the subjective perception or naming conventions.

6.3.3 Preliminary data analyses

I took advantage of the data and performed a number of preliminary analyses. For example, I noticed that the thickness of the cross ribs, despite very different ultrastructural morphologies, remained very constant among pigmented scales (**Figure 31A**). One scale, reported by the authors as glass scales, which exhibited one of the most drastically different ultrastructural morphologies, was one of the few cases in which the cross rib thickness was more variable. This observation is

probably tied to its iridescent qualities and out of the norm morphology. Window morphology is often one of the traits with the most morphological variation. Taking into account the area and the circularity of the scales windows from the top I uncover that most scales have a high circularity value (trending closer to the more rounded window) and a lower window area (**Figure 31B**). Furthermore, the observed trend highlights that as the area of the openings increased the circularity also increased. This observation is probably due to a combination of the overall geometry of the scales or by the developmental constraints associated with the process of creating the scales in the first place. One interesting observation is how scales with low circularity and low area don't appear in all our sampling suggesting that making a squared window becomes specially challenging when such window is smaller in area. Again this informs about possible developmental constraints associated with the formation of scales. This observation also highlighted that in order to obtain a better descriptor of similarities of scales from the same color among distantly related species I would need to include more metrics into the comparisons. For that I used Principal Components Analysis (PCA) including all of our measurements obtained from top views of the scales. I performed a PCA using the first 5 measurements done from the top views of scales for our entire dataset (**Figure 31C**). No clear separation of groups was apparent. Moving forward, restricting our PCA analyses to specific groups and removing scales with very different morphologies will probably yield a more clear result.

6.4 Future Directions

Our foundational work serves as a good starting point for analyzing the relationship between scale pigmentation and ultrastructure. As I move forward with analysis of my dataset I have to incorporate another complex consideration. As I compare scale color with scale

ultrastructure I have to also consider the relatedness among the compared species. This will help me determine if some of the observed trends are really due to the relationship between morphology and color identity or if any of the trends are just caused by their phylogenetic relationship. With that in mind and moving forward I will collaborate with other researchers to include the phylogenetic relationship into our future comparative analysis. This will help us disentangle phylogenetic signals from any trends relating pigmented scales with specific ultrastructural morphologies.

6.5 Methods

Selection of images for the analysis

Images were selected from a big search of butterfly scale ultrastructure in the literature. The main metric for the selection was the availability of a completely top view of the scale dorsal ultrastructure with a reported scale bar associated with it. Based on the interest on pigment fate relationship with scale ultrastructure I focused on scales with primary pigmented color instead of structural coloration. The selected publications and species represented for the images are described in **Table 3**.

Ultrastructural measurements and descriptors.

For each image of scale ultrastructure available, I selected a zone that had around 10 to 20 openings separated by crossribs when looking from the top of the scale. When the top view of the scale was available I recorded the crossrib thickness and the ridge to ridge distance (**Figure 30B, 1-2**). Then by using the lasso tool from ImageJ I manually recorded the area, perimeter, and circularity (0 to 1 value, 0 being a square and 1 being a perfect circle) of windows present in top

views of scales (**Figure 30B, 3-5**). Finally, when the side view or cross-section of the scale was available I recorded the ridge elevation and the length of the trabeculae (**Figure 30C, 6-7**). For the images, several morphological descriptors were recorded as well when present. Such descriptors include the presence of a membrane on top of the scale window, scutes running alongside ridges, the presence of beads associated with pigment granules, and the presence of other morphologically complex adornments sticking out of primary described structures. I included 20 biological replicates for all the measurements within the same scale. If the available image had less than 20 biological replicates I included the maximum number of measurements. I recorded the details as well of the color description provided by the authors as well as an RGB value obtained from the images provided within each publication. When mutants were available or analyzed, I also included information on the manipulation done to the individuals. All the data was recorded in a centralized data table in google drive. Averages and all the data manipulation were done using the R software and Python. **Table 4** includes all the raw measurements done across all the selected species and images. **Table 5** includes all the measurements with scales from genetically modified butterflies. **Table 3** also includes all the averages for all the measurements and details of other morphological descriptors.

6.6 Figures

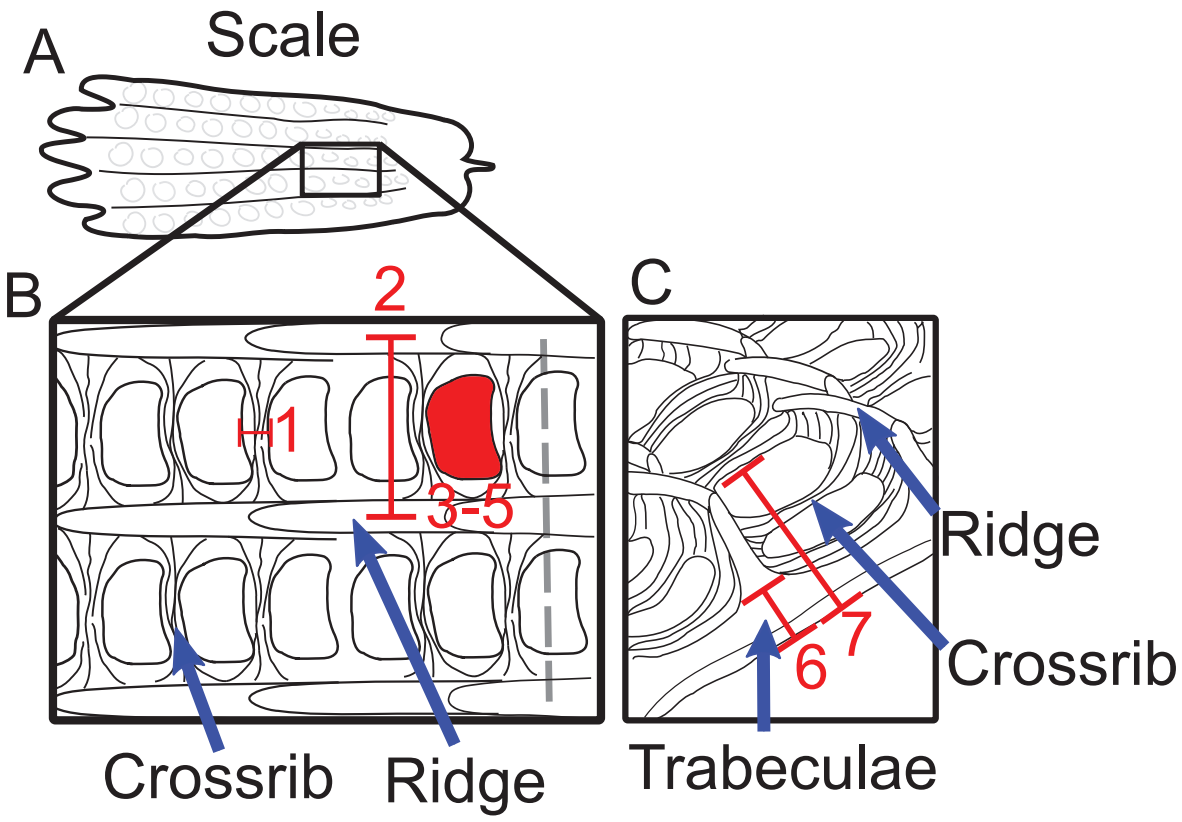

Figure 30: Scheme of scales ultrastructure components and details of measured morphological features. (**A**) View of a complete butterfly scale. (**B**) Top view magnified details of scale ultrastructure. (**C**) Cross-section view of panel **B** (dotted gray line) highlighting other ultrastructural features. Parts of the scale are labeled and highlighted with blue arrows. Measured morphological features are marked with red and numbered. 1 corresponds to crossrib thickness, 2 to ridge to ridge distance, 3-5 are descriptors of the windows or openings on the scale (3 is the area, 4 is the perimeter and 5 is the circularity), 6 is the ridge elevation, and 7 is the length of the trabeculae.

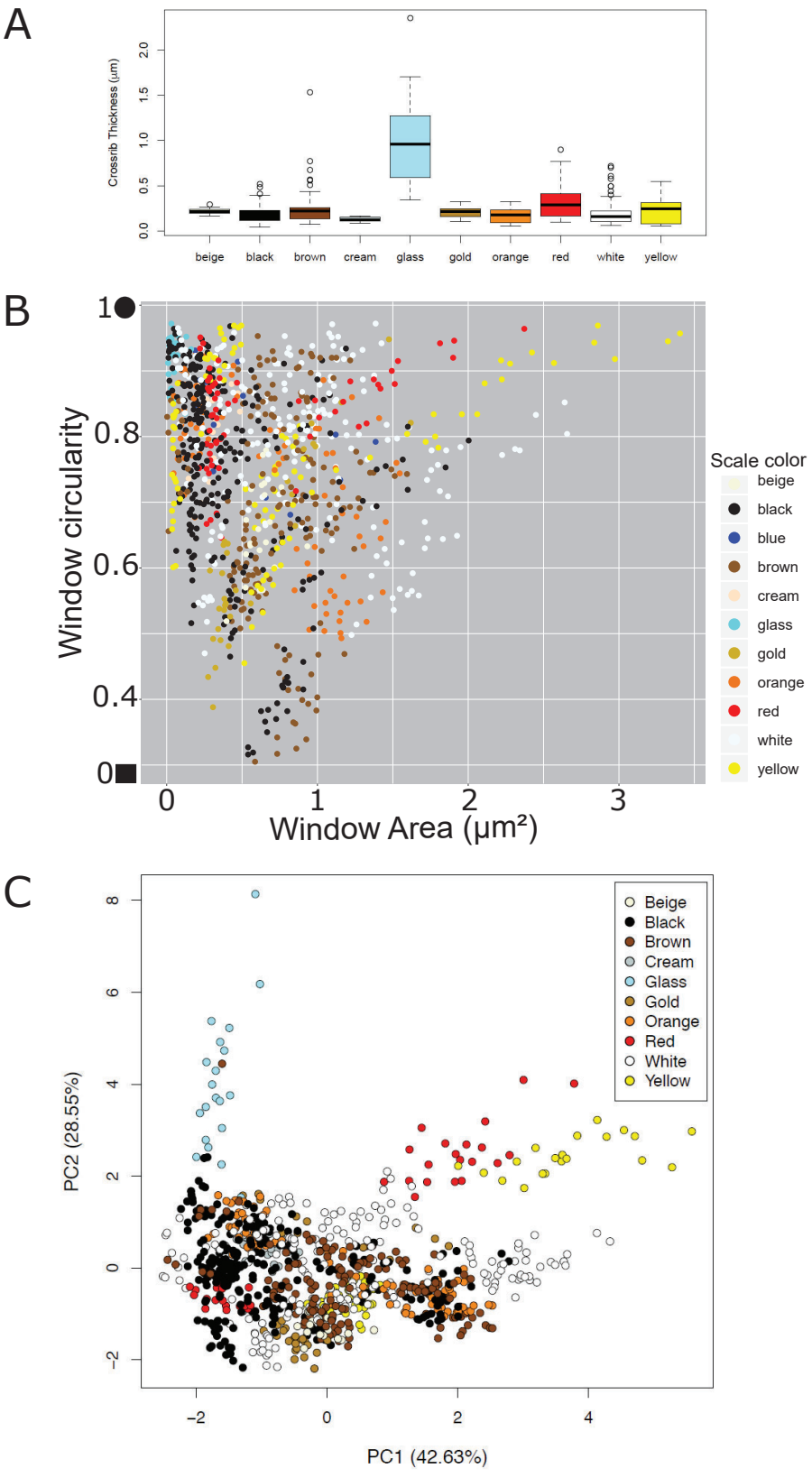
A
Crossrib Thickness (µm)
0.0
0.5
1.0
1.5
2.0
beige
black
brown
cream
glass
gold
orange
red
white
yellow
B
Window circularity
0
0.4
0.6
0.8
1
Window Area (µm²)
0
1
2
3
Scale color
beige
black
blue
brown
cream
glass
gold
orange
red
white
yellow
C
PC2 (28.55%)
−2
0
2
4
6
8
PC1 (42.63%)
−2
0
2
4
Beige
Black
Brown
Cream
Glass
Gold
Orange
Red
White
Yellow

Figure 31: Preliminary analysis of scale ultrastructure and their relationship with specific color fates. (**A**) Crossrib thickness values across several wildtype scales. (**B**). Window circularity (0 to 1 value were 0 is a perfect square and 1 is a perfect circle) against the area of the window across different color scales (**C**) PCA analysis including all 5 of the measurements (crossrib thickness, ridge to ridge distance, windows perimeter, window area, and window circularity) taken from top views of scales.

Tables:

Table 2: Meta-data details on measurements on scale ultrastructural morphology across butterflies

Table 3: Selected species, references, and average measurements done for both wildtype and mutant butterflies

Table 4: Raw data table of all the measurements across all our datasets for wild type butterfly scales

Table 5: Data on genetically modified or chemically altered butterfly scales

Species	38
Families	6
Scale colors (author reported)	15
Wild type scales messurments	over 7000
Modify Scales messurments	over 1000
Messured morphological traits	7
Referenced publications	25

Table 2: Meta-data details on measurements on scale ultrastructural morphology across butterflies

Family	Genus	Specie	Genotype	Labeled color	Irridiscent color	RGB value	wing location	Window area (µm^2)	Window perimeter (µm)	Window circularity	Crossrib thickness (µm)	Ridge to ridge distance (µm)	Trabeculae Length (µm)	Ridge elevation (µm)	Pigment granueles	Membrane	Other adorments	Scutes	Reference
Nymphalidae	Bicyclus	Bicyclus anynana	wt	black		rgb(6, 3, 0)	eyespots	0.4464	3.188	0.55125	0.23075	1.25885			no	no	no	no	Matsuoka & Monteiro 2018
Nymphalidae	Bicyclus	Bicyclus anynana	wt	brown		rgb(125, 98, 61)	eyespots	0.6325	3.5117	0.5905	0.2288	1.1509			no	no	no	no	Matsuoka & Monteiro 2018
Nymphalidae	Bicyclus	Bicyclus anynana	wt	beige		rgb(228, 189, 115)	eyespots	0.6213	3.46175	0.6569	0.2156	1.0461			no	no	no	no	Matsuoka & Monteiro 2018
Nymphalidae	Bicyclus	Bicyclus anynana	wt	white		rgb(255, 255, 255)	eyespots	0.2911	2.4431	0.63955	0.17475	0.89565			no	some	no	no	Matsuoka & Monteiro 2018
Nymphalidae	Bicyclus	Bicyclus anynana	wt	gold		rgb(249, 168, 13)	eyespots	0.3517	2.9587	0.5382	0.2396	0.9928			no	some	no	no	Matsuoka & Monteiro 2018
Nymphalidae	Bicyclus	Bicyclus anynana	mutant-yellow	brown		rgb(97, 61, 8)	eyespots	0.4067	3.240889	0.5025	0.152444444	1.410333333			no	yes	no	no	Matsuoka & Monteiro 2018
Nymphalidae	Bicyclus	Bicyclus anynana	mutant-yellow	yellow		rgb(202, 159, 104)	eyespots	0.9236	4.35525	0.57845	0.1666	1.6708			no	some	no	no	Matsuoka & Monteiro 2018
Nymphalidae	Bicyclus	Bicyclus anynana	mutant-yellow	yellow		rgb(249, 179, 11)	eyespots	0.5464	3.61985	0.52385	0.19815	1.60045			no	some	no	no	Matsuoka & Monteiro 2018
Nymphalidae	Bicyclus	Bicyclus anynana	mutant-yellow	yellow		rgb(245, 207, 129)	eyespots	0.831	4.21955	0.5989	0.19455	1.7721			no	no	no	no	Matsuoka & Monteiro 2018
Nymphalidae	Bicyclus	Bicyclus anynana	mutant-yellow	yellow		rgb(255, 255, 255)	eyespots	0.4467	2.8157	0.644	0.1709	1.45595			no	some	no	no	Matsuoka & Monteiro 2018
Nymphalidae	Bicyclus	Bicyclus anynana	mutant-DDC	grey		rgb(130, 136, 134)	eyespots	0.3699	2.9121	0.51235	0.16575	1.2415			no	yes	no	no	Matsuoka & Monteiro 2018
Nymphalidae	Bicyclus	Bicyclus anynana	mutant-DDC	white		rgb(163, 128, 89)	eyespots	1.1413	5.12365	0.51205	0.25195	2.17595			no	yes	no	no	Matsuoka & Monteiro 2018
Nymphalidae	Bicyclus	Bicyclus anynana	mutant-DDC	yellow		rgb(240, 225, 143)	eyespots	0.8246	4.345263	0.547526	0.200210526	1.882947368			no	yes	no	no	Matsuoka & Monteiro 2018
Nymphalidae	Bicyclus	Bicyclus anynana	mutant-DDC	white		rgb(167, 195, 246)	eyespots	1.143	5.00305	0.56705	0.1986	2.0415			no	yes	no	no	Matsuoka & Monteiro 2018
Nymphalidae	Heliconius	Heliconius telesiphe	wt	red		rgb(200, 55, 3)	forewing band	1.2798	4.41065	0.86855	0.43585	3.09185			no	some	no	yes	Wilts et al 2017
Nymphalidae	Heliconius	Heliconius sara	wt	yellow		rgb(247, 242, 159)	forewings band	1.9861	5.5969	0.86825	0.3564	3.27905			no	some	no	yes	Wilts et al 2017
Nymphalidae	Heliconius	Heliconius cydno	wt	black		rgb(44, 46, 58)		0.5194	2.7477	0.79595	0.09775	1.1481			no	some	no	yes	Kronforst unpublished data
Nymphalidae	Heliconius	Heliconius cydno	wt	white		rgb(249, 254, 254)		0.1	1.161583	0.913417	0.3534	0.920833333			no	yes	no	yes	Kronforst unpublished data
Nymphalidae	Heliconius	Heliconius cydno	mutant-al1	brown		rgb(65, 46, 57)		0.4221	2.75405	0.80725	0.251	2.0126			no	some	no	yes	Kronforst unpublished data
Nymphalidae	Heliconius	Heliconius erato	wt	yellow		rgb(209, 221, 70)	dorsal hindwing	0.3922	2.20285	0.92265	0.118631579	1.7214			no	some	no	yes	Aymone et al 2012
Nymphalidae	Heliconius	Heliconius erato	wt	black		rgb(20, 20, 19)	dorsal hindwing	0.1837	1.8311	0.6934	0.10405	0.81375			no	no	no		Aymone et al 2012
Nymphalidae	Heliconius	Heliconius erato	wt	red		rgb(148, 25, 21)	dorsal hindwing	0.3059	2.1506	0.87135	0.16845	0.88865			no	some	no		Aymone et al 2012
Nymphalidae	Hypolimnas	Hypolimnas salmacis	wt	brown		rgb(71, 42, 13)	dorsal forewing	0.6258	2.9612	0.8958	0.0934	1.1278	1.549556	2.23725	no	yes	no	yes	Siddique et al. 2016
Nymphalidae	Hypolimnas	Hypolimnas salmacis	wt	white		rgb(243, 230, 217)	dorsal forewing	0.9676	3.8242	0.8231	0.073	1.3798	1.335889	2.339777778	no	no	no	yes	Siddique et al. 2016
Nymphalidae	Morpho	Morpho peleides	wt	black		rgb(81, 67, 55)	ventral eyespots	0.3219	2.46735	0.73075	0.201666667	1.4288			no	no	no	yes	Aymone et al 2012
Nymphalidae	Morpho	Morpho peleides	wt	brown		rgb(85, 71, 55)	ventral wing	0.9597	3.89815	0.6969	0.2236	2.00495			no	no	no	no	Aymone et al 2012
Nymphalidae	Danaus	Danaus genutia	wt	yellow		rgb(243, 210, 142)	forewing	0.7218	3.7962	0.6176	0.24455	1.5978			no	no	no	yes	Zhang et al. 2018
Nymphalidae	Melanitis	Melanitis leda	wt	orange		rgb(140, 66, 36)	dorsal wing	1.2113	5.13765	0.56835	0.2547	1.81155			no	no	no	no	Sultan et al. 2016
Nymphalidae	Melanitis	Melanitis leda	wt	black		rgb(35, 30, 35)	dorsal wing	0.751	4.74845	0.41085	0.31125	2.07975			no	no	no	no	Sultan et al. 2016
Nymphalidae	Melanitis	Melanitis leda	wt	white		rgb(219, 212, 194)	eyespots	1.5492	5.6993	0.5976	0.26315	2.1864			no	yes	no	no	Sultan et al. 2016
Nymphalidae	Melanitis	Melanitis leda	wt	brown		rgb(199, 172, 129)	eyespots	0.866	5.26185	0.40065	0.2588	2.07045			no	no	no	no	Sultan et al. 2016
Nymphalidae	Penthema	Penthema adelma	wt	black		rgb(2, 2, 2)	dorsal hindwing	1.3207	4.80715	0.689	0.2702	1.7412			no	no	no		Sultan et al. 2016
Papilionidae	Papilio	Papilio xuthus	wt	cream		rgb(230, 229, 170)	dorsal hindwing	0.3322	2.1813	0.8645	0.1205	2.0459	3.11	4.006	no	some	no	yes	Stavanga et al. 2015
Papilionidae	Papilio	Papilio xuthus	wt	orange		rgb(199, 114, 29)	dorsal hindwing	0.3254	2.1013	0.84265	0.18475	1.9785	1.269667	2.186875	no	yes	no	yes	Stavanga et al. 2015
Papilionidae	Papilio	Papilio xuthus	wt	black		rgb(3, 3, 5)	dorsal hindwing	0.2049	1.66795	0.85535	0.1295	1.8439	0.936714	1.614666667	no	yes	no	yes	Stavanga et al. 2015
Papilionidae	Papilio	Papilio xuthus	wt	blue	blue	rgb(119, 132, 135)	dorsal hindwing	0.5782	2.873077	0.815846	0.186846154	2.445538462	0.944083	1.978285714	no	some	no	yes	Stavanga et al. 2015
Papilionidae	Papilio	Papilio polytes	wt	white		rgb(250, 250, 250)	dorsal hindwing	0.6132	2.95125	0.90665	0.18435	2.39105			no	some	no	yes	Kronforst unpublisedh data
Papilionidae	Graphium	Graphium sarpedon	wt	white		rgb(167, 173, 157)	ventral forewing	0.6779	2.80615	0.8387	0.1925	1.76835	17.0815	27.5664	no	some	no	yes	stevenga et al. 2010
Papilionidae	Graphium	Graphium sarpedon	wt	glass	glass	rgb(106, 135, 74)	ventral forewing	0.0515	0.7772	0.919	0.99085	2.52605	8.19425	14.131	no	some	no	yes	stevenga et al. 2010
Papilionidae	Battus	Battus philenor	wt	orange		rgb(159, 90, 39)	ventral hindwing	0.1245	1.36785	0.81705	0.21725	2.4903			no	no	no		Stevenga et al 2014
Papilionidae	Battus	Battus philenor	wt	black	blue	rgb(64, 139, 147)	ventral hindwing	0.0454	0.76355	0.9212	0.2641	2.23245			no	no	no		Stevenga et al 2015
Papilionidae	Papilio	Papilio maackii	wt	black		rgb(34, 34, 34)		0.2132	1.7594	0.83825	0.2015	2.0543			no	some	no		Kishimoto et al 2007
Papilionidae	Trogonoptera	Trogonoptera brookiana	wt	white		rgb(201, 199, 194)	ventral hindwing	0.3182	2.23665	0.86225	0.177	2.09355	1.731583	2.730142857	no	no	no		Wilts et al 2016
Papilionidae	Trogonoptera	Trogonoptera brookiana	wt	black		rgb(30, 35, 23)	dorsal forewing	0.2762	1.78105	0.869	0.1346	1.44635			no	no	no		Wilts et al 2016
Papilionidae	Papilio	Papilio nireus	wt	yellow	green	rgb(67, 170, 171)	dorsal forewing	0.0539	0.9249	0.7513	0.06555	3.1743	3.5601	4.2615	no	some	yes		Lou et al. 2012
Papilionidae	Pachliopta	Pachliopta aristolochiae	wt	black		rgb(29, 29, 29)	ventral forewing	0.1647	1.626	0.824684	0.081894737	1.744	1.3965	2.4865	no	no	no		Siddique et al. 2017
Papilionidae	Pachliopta	Pachliopta aristolochiae	wt	brown		rgb(60, 45, 30)	dorsal forewing	0.0786	1.008308	0.790769	0.5292	1.588769231			no	no	no		Siddique et al. 2017
Papilionidae	Papilio	Papilio helenus	wt	black		rgb(1, 1, 1)	ventral hindwing	0.2449	1.97445	0.7657	0.1676	2.44625			no	no	no		Lou et al. 2012
Papilionidae	Troides	Troides aeacus	wt	black		rgb(24, 24, 24)	ventral hindwing	0.1669	1.60605	0.80495	0.1486	1.37395			no	no	no		Lou et al. 2012
Pieridae	Catopsilia	Catopsilia pomona	wt	white	green	rgb(216, 224, 171)	ventral distal fore	2.1218	5.4342	0.76165	0.1048	2.3696			some	no	no		Mishra et al 2017
Pieridae	Catopsilia	Catopsilia pomona	wt	yellow	green	rgb(190, 196, 74)	ventral proximal f	0.7134	3.507263	0.741	0.071947368	1.632421053			yes	no	no		Mishra et al 2017
Pieridae	Pieris	Pieris rapae	wt	black		rgb(60, 55, 42)	dorsal forewing	0.796286	3.85	0.67	0.170875	1.831777778			no	no	no		Stavenga et al 2004
Pieridae	Pieris	Pieris rapae	wt	white		rgb(232, 234, 231)	dorsal forewing	1.1042	4.398	0.713	0.1189	1.802315789	1.132444	1.93	yes	no	no		Stavenga et al 2004
Pieridae	Pieris	Anthocharis cardamines	wt	orange		rgb(253, 143, 8)	dorsal wing	0.892111	3.720556	0.800778	0.072888889	1.535666667			yes	no	no		Giraldo Thesis 2004
Pieridae	Pieris	Delias nigrina	wt	white		rgb(213, 211, 179)	dorsal forewing	0.801833	3.685667	0.739667	0.1155	1.630333333			yes	no	no		Giraldo Thesis 2004
Pieridae	Colias	Colias crocea	wt	white		rgb(202, 204, 191)	ventral forewing	1.0176	4.049154	0.757308	0.099769231	1.614230769			some	no	no		Woronik et al. 2019
Pieridae	Colias	Colias crocea	wt	black		rgb(33, 24, 25)	ventral forewing	0.8632	3.558933	0.846533	0.202133333	1.673933333			no	no	no		Woronik et al. 2019
Pieridae	Colias	Colias crocea	mutant-BarH1	orange		rgb(242, 208, 108)	ventral forewing	0.9501	3.9594	0.7376	0.123733333	1.977733333			yes	no	no		Woronik et al. 2019
Pieridae	Colias	Colias crocea	mutant-BarH1	white		rgb(238, 231, 197)	ventral forewing	1.476444	4.995	0.741222	0.181888889	2.237			no	no	yes		Woronik et al. 2019
Pieridae	Colias	Colias crocea	mutant-orange	white		rgb(180, 179, 183)	ventral forewing	1.030125	3.933625	0.795875	0.2065	1.842375			no	no	no		Woronik et al. 2019
Pieridae	Colias	C. eurytheme	wt	orange		rgb(244, 152, 1)	ventral forewing	1.1021	4.431154	0.694308	0.092461538	1.866769231			yes	no	no		Woronik et al. 2019
Pieridae	Colias	C. eurytheme	wt	white		rgb(212, 225, 209)	ventral forewing	0.7318	3.40625	0.78925	0.0785	1.341			some	no	no		Woronik et al. 2019
Lycaenidae	Polymmatus	Polyommatus icarus	wt	brown	blue	rgb(127, 140, 190)	dorsal wing	0.926	3.600909	0.872636	0.110909091	1.556454545	0.810909	1.483833333	no	no	yes		Piszter et al 2014
Lycaenidae	Polymmatus	Polyommatus marcidus	wt	brown		rgb(124, 96, 38)		0.505	3.26255	0.59375	0.22835	1.46025			no	no	no		Balint et al. 2004

Lycaenidae	Thecla	Thecla opisena	wt	brown	green	rgb(67, 137, 44)	dorsal hindwing	1.1825	4.65285	0.69335	0.129	1.9186			no	no	yes		Wilts et al. 2017
Lycaenidae	Albulina	Albulina metallica	wt	gold	green	rgb(221, 248, 182)	ventral hindwing	1.0567	4.0664	0.7904	0.1031	1.7336	0.914	1.2774	no	some	yes		Kertész et al. 2018
Lycaenidae	Albulina	Albulina metallica	wt	brown	blue	rgb(114, 129, 180)	dorsal wing	0.9148	4.001	0.7158	0.1194	1.9652	1.0244	1.382	no	some	yes		Kertész et al. 2018
Lycaenidae	Cyanophrys	Cyanoprys remus	wt	blue		rgb(81, 106, 138)	dorsal wing	0.17645	1.62205	0.8197	0.10265	1.9363	1.43225	2.116333333	no	yes	no		Tamáska et al. 2013
Lycaenidae	Callophrys	Callophrys rubi	wt	brown	green	rgb(91, 187, 116)	dorsal wing	1.194438	4.722563	0.665125	0.1530625	2.0375625	2.3588	3.184416667	no	no	no		Tamáska et al. 2013
Lycaenidae	Polyommatus	Polyommatus daphnis	wt	brown	blue	rgb(152, 160, 184)	dorsal wing	1.2778	4.3747	0.8333	0.1101	1.945	0.6698	1.6105	no	no	no		Tamáska et al. 2013
Lycaenidae	Thecloxurina	atymna	wt	red		rgb(197, 64, 15)	dorsal wing	0.2947	2.2022	0.7714	0.0925	0.841			no	no	no		Tamáska et al. 2013
Hesperiidae	Carystoides	Carystoides escalantei	wt	white		rgb(217, 216, 204)	dorsal forewing ti	1.1321	3.91675	0.90935	0.34475	1.8141			no	some	no		Ge et al. 2017
Saturniidae	Bunaea	Bunaea alcinoe	wt	brown		rgb(51, 28, 14)	dorsal forewing	0.8514	3.4686	0.873	0.2865	1.4929	0.7138	2.0464	no	no	no		Shen et al 2018
Zygaenidae	Moth outgroup	Eterusia taiwana	wt	brown	green	rgb(72, 85, 50)	dorsal wing	4.793	8.763667	0.778667	0.174333333	3.068666667	1.664333	1.748666667	yes	no	no		Tamáska et al. 2013
Uraniidae	Moth outgroup	Chrysiridia rhipheus	wt	yellow	blue	rgb(140, 197, 175)	ventral wing	8.617667	12.08717	0.743167	0.2945	4.349166667	1.369667	2.377666667	no	yes	no		Tamáska et al. 2013

Table 3: Selected species, references, and average measurements done for both wildtype and mutant butterflies

Family	Species	Scale color	Iridescent color	Window area (µm^2)	Window perimeter (µm)	Window circularity	Crossrib thickness (µm)	Ridge to ridge distance (µm)	Trabeculae Length (µm)	Ridge elevation (µm)
Hesperiidae	*Carystoides escalantei*	white		1.168	3.968	0.933	0.607	2.029		
Hesperiidae	*Carystoides escalantei*	white		1.301	4.293	0.887	0.577	1.993		
Hesperiidae	*Carystoides escalantei*	white		1.088	3.917	0.891	0.381	2.036		
Hesperiidae	*Carystoides escalantei*	white		1.109	3.986	0.877	0.31	1.981		
Hesperiidae	*Carystoides escalantei*	white		1.035	3.933	0.841	0.296	1.723		
Hesperiidae	*Carystoides escalantei*	white		1.095	4.147	0.8	0.249	1.706		
Hesperiidae	*Carystoides escalantei*	white		1.047	3.969	0.835	0.202	1.733		
Hesperiidae	*Carystoides escalantei*	white		1.078	3.762	0.957	0.291	1.707		
Hesperiidae	*Carystoides escalantei*	white		1.014	3.806	0.879	0.345	1.492		
Hesperiidae	*Carystoides escalantei*	white		1.386	4.232	0.972	0.718	1.456		
Hesperiidae	*Carystoides escalantei*	white		1.176	4.01	0.918	0.35	1.431		
Hesperiidae	*Carystoides escalantei*	white		1.106	3.849	0.938	0.345	2.048		
Hesperiidae	*Carystoides escalantei*	white		1.425	4.36	0.942	0.293	1.984		
Hesperiidae	*Carystoides escalantei*	white		0.816	3.387	0.894	0.264	1.932		
Hesperiidae	*Carystoides escalantei*	white		0.966	3.598	0.938	0.283	1.993		
Hesperiidae	*Carystoides escalantei*	white		1.13	3.934	0.917	0.495	2.029		
Hesperiidae	*Carystoides escalantei*	white		1.098	3.769	0.971	0.239	1.521		
Hesperiidae	*Carystoides escalantei*	white		0.783	3.213	0.953	0.154	1.406		
Hesperiidae	*Carystoides escalantei*	white		1.094	3.802	0.951	0.256	2.023		
Hesperiidae	*Carystoides escalantei*	white		1.376	4.4	0.893	0.24	2.059		
Papilionidae	*Papilio xuthus*	cream		0.472	2.618	0.866	0.106	1.978	3.159	3.708
Papilionidae	*Papilio xuthus*	cream		0.306	2.184	0.807	0.152	1.97	3.079	3.878
Papilionidae	*Papilio xuthus*	cream		0.245	1.865	0.884	0.124	1.963	3.066	4.233
Papilionidae	*Papilio xuthus*	cream		0.283	1.961	0.926	0.117	1.993	3.122	4.205
Papilionidae	*Papilio xuthus*	cream		0.259	1.877	0.926	0.102	2.068	3.092	
Papilionidae	*Papilio xuthus*	cream		0.266	1.975	0.857	0.125	2.09	3.106	
Papilionidae	*Papilio xuthus*	cream		0.43	2.479	0.88	0.142	2.075	3.106	
Papilionidae	*Papilio xuthus*	cream		0.486	2.7	0.838	0.092	2.112	3.079	
Papilionidae	*Papilio xuthus*	cream		0.236	1.874	0.843	0.125	2.105	3.212	
Papilionidae	*Papilio xuthus*	cream		0.339	2.28	0.818	0.12	2.105	3.079	
Papilionidae	*Papilio xuthus*	cream		0.226	2.015	0.699	0.103	2.12		
Papilionidae	*Papilio xuthus*	cream		0.321	2.209	0.827	0.087	2.12		
Papilionidae	*Papilio xuthus*	cream		0.356	2.244	0.888	0.15	2.112		
Papilionidae	*Papilio xuthus*	cream		0.304	2.114	0.855	0.167	2.003		
Papilionidae	*Papilio xuthus*	cream		0.281	2.198	0.731	0.115	2.097		
Papilionidae	*Papilio xuthus*	cream		0.145	1.576	0.736	0.154	2.027		
Papilionidae	*Papilio xuthus*	cream		0.28	1.999	0.88	0.11	2.008		
Papilionidae	*Papilio xuthus*	cream		0.312	2.259	0.767	0.14	1.948		
Papilionidae	*Papilio xuthus*	cream		0.33	2.238	0.827	0.15	2.027		
Papilionidae	*Papilio xuthus*	cream		0.202	1.7	0.878	0.155	1.988		
Papilionidae	*Papilio xuthus*	orange		0.277	2.091	0.796	0.21	2.018	1.224	2.08
Papilionidae	*Papilio xuthus*	orange		0.194	1.624	0.925	0.175	2.013	1.184	2.378
Papilionidae	*Papilio xuthus*	orange		0.467	2.611	0.861	0.152	2.013	1.154	2.06
Papilionidae	*Papilio xuthus*	orange		0.195	1.673	0.877	0.248	1.958	1.234	2.15
Papilionidae	*Papilio xuthus*	orange		0.368	2.36	0.83	0.216	1.978	1.354	2.308
Papilionidae	*Papilio xuthus*	orange		0.613	3.163	0.77	0.241	1.954	1.224	2.328
Papilionidae	*Papilio xuthus*	orange		0.231	1.885	0.819	0.272	1.903	1.226	2.091
Papilionidae	*Papilio xuthus*	orange		0.685	3.26	0.81	0.141	1.903	1.493	2.1
Papilionidae	*Papilio xuthus*	orange		0.125	1.32	0.9	0.186	1.903	1.334	
Papilionidae	*Papilio xuthus*	orange		0.099	1.172	0.901	0.131	1.958		
Papilionidae	*Papilio xuthus*	orange		0.172	1.676	0.771	0.195	2.063		
Papilionidae	*Papilio xuthus*	orange		0.22	1.89	0.774	0.199	2.038		
Papilionidae	*Papilio xuthus*	orange		0.74	3.39	0.809	0.179	2.038		
Papilionidae	*Papilio xuthus*	orange		0.245	1.917	0.837	0.244	2.028		
Papilionidae	*Papilio xuthus*	orange		0.318	2.128	0.883	0.169	1.873		
Papilionidae	*Papilio xuthus*	orange		0.431	2.46	0.894	0.143	1.953		
Papilionidae	*Papilio xuthus*	orange		0.443	2.477	0.908	0.136	1.938		
Papilionidae	*Papilio xuthus*	orange		0.202	1.704	0.876	0.151	2.043		
Papilionidae	*Papilio xuthus*	orange		0.226	1.831	0.845	0.131	2.022		
Papilionidae	*Papilio xuthus*	orange		0.119	1.394	0.767	0.176	1.973		
Papilionidae	*Papilio xuthus*	black		0.191	1.633	0.902	0.093	1.85	0.956	1.836

Papilionidae	*Papilio xuthus*	black		0.389	2.316	0.911	0.09	1.828	0.963	1.575
Papilionidae	*Papilio xuthus*	black		0.097	1.164	0.903	0.166	1.76	0.978	1.515
Papilionidae	*Papilio xuthus*	black		0.119	1.325	0.855	0.079	1.753	0.933	1.642
Papilionidae	*Papilio xuthus*	black		0.161	1.533	0.86	0.109	1.7	0.724	1.522
Papilionidae	*Papilio xuthus*	black		0.199	1.734	0.833	0.243	1.678	0.955	1.598
Papilionidae	*Papilio xuthus*	black		0.117	1.27	0.91	0.202	1.7	1.037	
Papilionidae	*Papilio xuthus*	black		0.375	2.312	0.881	0.125	1.64	0.964	
Papilionidae	*Papilio xuthus*	black		0.206	1.731	0.866	0.086	1.633	1.001	
Papilionidae	*Papilio xuthus*	black		0.195	1.665	0.886	0.105	1.693	0.858	
Papilionidae	*Papilio xuthus*	black		0.127	1.317	0.921	0.097	1.618	1.005	
Papilionidae	*Papilio xuthus*	black		0.421	2.338	0.968	0.108	1.978	1.045	
Papilionidae	*Papilio xuthus*	black		0.101	1.242	0.824	0.109	1.985	0.747	
Papilionidae	*Papilio xuthus*	black		0.33	2.122	0.922	0.15	1.993	0.948	
Papilionidae	*Papilio xuthus*	black		0.063	1.122	0.626	0.169	1.993		
Papilionidae	*Papilio xuthus*	black		0.233	1.971	0.755	0.098	2.075		
Papilionidae	*Papilio xuthus*	black		0.233	1.971	0.755	0.11	2.06		
Papilionidae	*Papilio xuthus*	black		0.194	1.687	0.855	0.077	1.993		
Papilionidae	*Papilio xuthus*	black		0.154	1.561	0.796	0.097	1.933		
Papilionidae	*Papilio xuthus*	black		0.126	1.345	0.878	0.277	2.015		
Papilionidae	*Papilio xuthus*	blue	blue	1.151	4.44	0.734	0.199	2.537	0.732	1.986
Papilionidae	*Papilio xuthus*	blue	blue	0.657	3.417	0.707	0.177	2.467	0.985	2.067
Papilionidae	*Papilio xuthus*	blue	blue	0.189	1.596	0.931	0.236	2.437	0.948	1.903
Papilionidae	*Papilio xuthus*	blue	blue	0.309	2.281	0.747	0.173	2.547	0.925	2.022
Papilionidae	*Papilio xuthus*	blue	blue	0.223	1.777	0.886	0.223	2.557	0.978	1.888
Papilionidae	*Papilio xuthus*	blue	blue	0.82	3.89	0.681	0.18	2.337	0.987	1.963
Papilionidae	*Papilio xuthus*	blue	blue	1.386	4.689	0.792	0.137	2.367	1.1	2.019
Papilionidae	*Papilio xuthus*	blue	blue	0.263	1.936	0.883	0.107	2.367	0.986	
Papilionidae	*Papilio xuthus*	blue	blue	0.312	2.191	0.818	0.135	2.407	1.075	
Papilionidae	*Papilio xuthus*	blue	blue	0.472	2.548	0.914	0.132	2.437	0.785	
Papilionidae	*Papilio xuthus*	blue	blue	0.506	2.717	0.862	0.208	2.318	0.843	
Papilionidae	*Papilio xuthus*	blue	blue	1.121	4.188	0.803	0.196	2.507	0.985	
Papilionidae	*Papilio xuthus*	blue	blue	0.191	1.68	0.848	0.326	2.507		
Papilionidae	*Papilio xuthus*	blue	blue				0.112	2.367		
Papilionidae	*Papilio xuthus*	blue	blue				0.112	2.457		
Papilionidae	*Papilio xuthus*	blue	blue				0.106	2.527		
Papilionidae	*Papilio xuthus*	blue	blue				0.162	2.547		
Papilionidae	*Papilio xuthus*	blue	blue				0.15	2.467		
Papilionidae	*Papilio xuthus*	blue	blue				0.158	2.457		
Papilionidae	*Papilio xuthus*	blue	blue				0.19	2.697		
Papilionidae	*Papilio polytes*	white		0.447	2.422	0.958	0.181	2.529		
Papilionidae	*Papilio polytes*	white		0.193	1.619	0.923	0.149	2.514		
Papilionidae	*Papilio polytes*	white		0.943	3.742	0.846	0.162	2.588		
Papilionidae	*Papilio polytes*	white		0.784	3.364	0.871	0.11	2.577		
Papilionidae	*Papilio polytes*	white		0.501	2.621	0.916	0.165	2.602		
Papilionidae	*Papilio polytes*	white		0.704	3.242	0.842	0.128	2.401		
Papilionidae	*Papilio polytes*	white		1.137	3.873	0.952	0.165	2.534		
Papilionidae	*Papilio polytes*	white		0.378	2.251	0.939	0.206	2.483		
Papilionidae	*Papilio polytes*	white		0.362	2.204	0.936	0.233	2.317		
Papilionidae	*Papilio polytes*	white		0.683	3.099	0.894	0.207	2.107		
Papilionidae	*Papilio polytes*	white		0.325	2.105	0.923	0.174	2.12		
Papilionidae	*Papilio polytes*	white		1.088	3.93	0.885	0.151	2.055		
Papilionidae	*Papilio polytes*	white		0.74	3.196	0.911	0.241	2.09		
Papilionidae	*Papilio polytes*	white		0.894	3.511	0.912	0.199	2.408		
Papilionidae	*Papilio polytes*	white		0.404	2.366	0.907	0.192	2.551		
Papilionidae	*Papilio polytes*	white		0.8	3.294	0.927	0.222	2.294		
Papilionidae	*Papilio polytes*	white		0.294	2.038	0.89	0.213	2.305		
Papilionidae	*Papilio polytes*	white		1.235	4.097	0.924	0.2	2.467		
Papilionidae	*Papilio polytes*	white		0.722	3.155	0.911	0.191	2.36		
Papilionidae	*Papilio polytes*	white		0.578	2.896	0.866	0.198	2.519		
Papilionidae	*Graphium sarpedon*	white		0.947	3.772	0.836	0.13	1.761		
Papilionidae	*Graphium sarpedon*	white		0.605	3.021	0.834	0.125	1.673		
Papilionidae	*Graphium sarpedon*	white		0.131	1.343	0.916	0.144	1.709		
Papilionidae	*Graphium sarpedon*	white		0.78	3.334	0.881	0.115	1.702		

Papilionidae	*Graphium sarpedon*	white		0.365	2.624	0.665	0.118	1.694		
Papilionidae	*Graphium sarpedon*	white		0.557	2.942	0.808	0.167	1.687		
Papilionidae	*Graphium sarpedon*	white		0.976	3.841	0.831	0.206	1.694		
Papilionidae	*Graphium sarpedon*	white		1.299	4.186	0.932	0.288	1.901		
Papilionidae	*Graphium sarpedon*	white		0.972	3.866	0.817	0.28	1.923		
Papilionidae	*Graphium sarpedon*	white		0.147	1.439	0.891	0.269	1.732		
Papilionidae	*Graphium sarpedon*	white		1.006	3.761	0.894	0.137	1.694		
Papilionidae	*Graphium sarpedon*	white		0.127	1.411	0.801	0.265	1.797		
Papilionidae	*Graphium sarpedon*	white		0.652	3.134	0.834	0.228	1.797		
Papilionidae	*Graphium sarpedon*	white		0.655	3.104	0.853	0.291	1.797		
Papilionidae	*Graphium sarpedon*	white		0.116	1.327	0.824	0.217	1.797		
Papilionidae	*Graphium sarpedon*	white		0.821	3.343	0.924	0.191	1.878		
Papilionidae	*Graphium sarpedon*	white		0.134	1.523	0.728	0.195	1.856		
Papilionidae	*Graphium sarpedon*	white		0.21	1.837	0.782	0.156	1.871		
Papilionidae	*Graphium sarpedon*	white		0.811	3.302	0.935	0.184	1.702		
Papilionidae	*Graphium sarpedon*	white		0.569	3.013	0.788	0.144	1.702		
Papilionidae	*Graphium sarpedon*	glass	glass	0.162	1.476	0.933	1.703	2.564		
Papilionidae	*Graphium sarpedon*	glass	glass	0.033	0.663	0.947	0.465	2.619		
Papilionidae	*Graphium sarpedon*	glass	glass	0.04	0.737	0.924	1.116	2.431		
Papilionidae	*Graphium sarpedon*	glass	glass	0.038	0.719	0.927	1.282	2.53		
Papilionidae	*Graphium sarpedon*	glass	glass	0.03	0.634	0.951	0.807	2.464		
Papilionidae	*Graphium sarpedon*	glass	glass	0.014	0.424	0.949	0.405	2.564		
Papilionidae	*Graphium sarpedon*	glass	glass	0.049	0.831	0.898	1.426	2.519		
Papilionidae	*Graphium sarpedon*	glass	glass	0.03	0.631	0.939	0.564	2.519		
Papilionidae	*Graphium sarpedon*	glass	glass	0.074	0.991	0.954	0.619	2.586		
Papilionidae	*Graphium sarpedon*	glass	glass	0.045	0.816	0.855	0.965	2.597		
Papilionidae	*Graphium sarpedon*	glass	glass	0.071	0.981	0.924	0.398	2.575		
Papilionidae	*Graphium sarpedon*	glass	glass	0.122	1.355	0.835	0.344	2.409		
Papilionidae	*Graphium sarpedon*	glass	glass	0.029	0.647	0.873	1.271	2.564		
Papilionidae	*Graphium sarpedon*	glass	glass	0.13	1.309	0.952	2.354	2.475		
Papilionidae	*Graphium sarpedon*	glass	glass	0.031	0.632	0.972	1.394	2.476		
Papilionidae	*Graphium sarpedon*	glass	glass	0.02	0.546	0.86	0.964	2.508		
Papilionidae	*Graphium sarpedon*	glass	glass	0.063	0.916	0.942	0.862	2.486		
Papilionidae	*Graphium sarpedon*	glass	glass	0.012	0.406	0.895	0.955	2.663		
Papilionidae	*Graphium sarpedon*	glass	glass	0.009	0.355	0.912	0.796	2.475		
Papilionidae	*Graphium sarpedon*	glass	glass	0.017	0.475	0.938	1.127	2.497		
Papilionidae	*Battus philenor*	orange		0.118	1.356	0.805	0.199	2.489		
Papilionidae	*Battus philenor*	orange		0.097	1.22	0.818	0.209	2.524		
Papilionidae	*Battus philenor*	orange		0.215	1.81	0.826	0.228	2.531		
Papilionidae	*Battus philenor*	orange		0.046	0.819	0.862	0.263	2.53		
Papilionidae	*Battus philenor*	orange		0.18	1.625	0.858	0.218	2.517		
Papilionidae	*Battus philenor*	orange		0.046	0.881	0.744	0.182	2.517		
Papilionidae	*Battus philenor*	orange		0.197	1.745	0.813	0.223	2.496		
Papilionidae	*Battus philenor*	orange		0.081	1.191	0.714	0.218	2.447		
Papilionidae	*Battus philenor*	orange		0.115	1.308	0.841	0.299	2.447		
Papilionidae	*Battus philenor*	orange		0.15	1.467	0.878	0.232	2.496		
Papilionidae	*Battus philenor*	orange		0.159	1.565	0.819	0.213	2.392		
Papilionidae	*Battus philenor*	orange		0.26	1.882	0.923	0.228	2.489		
Papilionidae	*Battus philenor*	orange		0.116	1.434	0.711	0.177	2.447		
Papilionidae	*Battus philenor*	orange		0.103	1.252	0.825	0.212	2.44		
Papilionidae	*Battus philenor*	orange		0.117	1.292	0.879	0.235	2.496		
Papilionidae	*Battus philenor*	orange		0.116	1.27	0.903	0.187	2.489		
Papilionidae	*Battus philenor*	orange		0.186	1.857	0.677	0.202	2.523		
Papilionidae	*Battus philenor*	orange		0.092	1.203	0.797	0.209	2.579		
Papilionidae	*Battus philenor*	orange		0.082	1.083	0.882	0.206	2.531		
Papilionidae	*Battus philenor*	orange		0.073	1.097	0.766	0.205	2.426		
Papilionidae	*Battus philenor*	black	blue	0.058	0.875	0.956	0.519	2.253		
Papilionidae	*Battus philenor*	black	blue	0.018	0.504	0.885	0.395	2.346		
Papilionidae	*Battus philenor*	black	blue	0.02	0.512	0.939	0.146	2.429		
Papilionidae	*Battus philenor*	black	blue	0.039	0.733	0.904	0.33	2.356		
Papilionidae	*Battus philenor*	black	blue	0.06	0.886	0.959	0.484	2.357		
Papilionidae	*Battus philenor*	black	blue	0.015	0.443	0.944	0.173	2.346		
Papilionidae	*Battus philenor*	black	blue	0.058	0.891	0.921	0.411	2.118		
Papilionidae	*Battus philenor*	black	blue	0.083	1.053	0.939	0.213	2.139		

Papilionidae	*Battus philenor*	black	blue	0.069	1.006	0.86	0.292	2.087		
Papilionidae	*Battus philenor*	black	blue	0.034	0.675	0.936	0.131	2.097		
Papilionidae	*Battus philenor*	black	blue	0.152	1.473	0.88	0.285	2.097		
Papilionidae	*Battus philenor*	black	blue	0.037	0.733	0.87	0.312	2.107		
Papilionidae	*Battus philenor*	black	blue	0.048	0.795	0.964	0.26	2.129		
Papilionidae	*Battus philenor*	black	blue	0.012	0.404	0.92	0.234	2.107		
Papilionidae	*Battus philenor*	black	blue	0.089	1.089	0.948	0.171	2.107		
Papilionidae	*Battus philenor*	black	blue	0.017	0.479	0.932	0.223	2.377		
Papilionidae	*Battus philenor*	black	blue	0.015	0.447	0.929	0.254	2.377		
Papilionidae	*Battus philenor*	black	blue	0.1	1.158	0.939	0.183	2.346		
Papilionidae	*Battus philenor*	black	blue	0.013	0.439	0.866	0.14	2.128		
Papilionidae	*Battus philenor*	black	blue	0.034	0.676	0.933	0.126	2.346		
Papilionidae	*Papilio maackii*	black		0.341	2.211	0.877	0.19	2.145		
Papilionidae	*Papilio maackii*	black		0.199	1.947	0.66	0.172	2.08		
Papilionidae	*Papilio maackii*	black		0.154	1.498	0.864	0.181	2.048		
Papilionidae	*Papilio maackii*	black		0.059	0.89	0.934	0.192	2.039		
Papilionidae	*Papilio maackii*	black		0.241	1.895	0.844	0.195	1.991		
Papilionidae	*Papilio maackii*	black		0.227	2.054	0.678	0.173	2.08		
Papilionidae	*Papilio maackii*	black		0.21	1.852	0.768	0.2	2.155		
Papilionidae	*Papilio maackii*	black		0.23	1.922	0.784	0.195	1.963		
Papilionidae	*Papilio maackii*	black		0.246	1.905	0.852	0.171	2.01		
Papilionidae	*Papilio maackii*	black		0.225	1.747	0.925	0.172	2.098		
Papilionidae	*Papilio maackii*	black		0.271	2.022	0.832	0.216	2.006		
Papilionidae	*Papilio maackii*	black		0.239	1.868	0.859	0.216	2.155		
Papilionidae	*Papilio maackii*	black		0.277	2.001	0.87	0.213	2.124		
Papilionidae	*Papilio maackii*	black		0.163	1.504	0.908	0.223	2.127		
Papilionidae	*Papilio maackii*	black		0.216	1.771	0.867	0.248	2.122		
Papilionidae	*Papilio maackii*	black		0.27	2.05	0.807	0.207	2.098		
Papilionidae	*Papilio maackii*	black		0.149	1.418	0.929	0.192	1.987		
Papilionidae	*Papilio maackii*	black		0.15	1.43	0.922	0.2	2.127		
Papilionidae	*Papilio maackii*	black		0.103	1.349	0.709	0.24	1.953		
Papilionidae	*Papilio maackii*	black		0.239	1.854	0.876	0.234	1.778		
Papilionidae	*Papilio helenus*	black		0.321	2.312	0.755	0.154	2.421		
Papilionidae	*Papilio helenus*	black		0.108	1.313	0.787	0.131	2.557		
Papilionidae	*Papilio helenus*	black		0.32	2.251	0.794	0.17	2.424		
Papilionidae	*Papilio helenus*	black		0.264	2.054	0.788	0.17	2.5		
Papilionidae	*Papilio helenus*	black		0.246	2.106	0.697	0.153	2.481		
Papilionidae	*Papilio helenus*	black		0.223	1.747	0.918	0.13	2.537		
Papilionidae	*Papilio helenus*	black		0.199	1.888	0.7	0.141	2.517		
Papilionidae	*Papilio helenus*	black		0.16	1.64	0.748	0.149	2.452		
Papilionidae	*Papilio helenus*	black		0.262	2.167	0.702	0.205	2.406		
Papilionidae	*Papilio helenus*	black		0.346	2.362	0.779	0.171	2.489		
Papilionidae	*Papilio helenus*	black		0.356	2.311	0.837	0.205	2.527		
Papilionidae	*Papilio helenus*	black		0.16	1.662	0.727	0.177	2.574		
Papilionidae	*Papilio helenus*	black		0.205	1.765	0.826	0.234	2.387		
Papilionidae	*Papilio helenus*	black		0.245	2.071	0.718	0.177	2.377		
Papilionidae	*Papilio helenus*	black		0.213	1.703	0.923	0.196	2.415		
Papilionidae	*Papilio helenus*	black		0.181	2.048	0.543	0.131	2.406		
Papilionidae	*Papilio helenus*	black		0.174	1.911	0.598	0.177	2.453		
Papilionidae	*Papilio helenus*	black		0.277	2.228	0.701	0.151	2.405		
Papilionidae	*Papilio helenus*	black		0.248	1.89	0.871	0.194	2.294		
Papilionidae	*Papilio helenus*	black		0.305	2.06	0.902	0.136	2.303		
Papilionidae	*Papilio helenus*	black		0.227	1.91	0.782	0.14	2.294		
Papilionidae	*Papilio helenus*	black		0.235	1.827	0.883	0.139	2.266		
Papilionidae	*Papilio helenus*	black		0.165	1.627	0.784	0.123	2.275		
Papilionidae	*Papilio helenus*	black		0.271	1.916	0.928	0.152	2.286		
Papilionidae	*Troides aeacus*	black		0.117	1.398	0.753	0.166	1.152		
Papilionidae	*Troides aeacus*	black		0.152	1.67	0.684	0.096	1.184		
Papilionidae	*Troides aeacus*	black		0.117	1.32	0.845	0.133	1.33		
Papilionidae	*Troides aeacus*	black		0.177	1.568	0.906	0.117	1.323		
Papilionidae	*Troides aeacus*	black		0.157	1.478	0.902	0.144	1.369		
Papilionidae	*Troides aeacus*	black		0.221	1.992	0.699	0.151	1.409		
Papilionidae	*Troides aeacus*	black		0.221	1.749	0.906	0.115	1.569		
Papilionidae	*Troides aeacus*	black		0.154	1.717	0.657	0.144	1.478		

Papilionidae	*Troides aeacus*	black		0.153	1.525	0.827	0.139	1.466		
Papilionidae	*Troides aeacus*	black		0.2	1.706	0.864	0.151	1.44		
Papilionidae	*Troides aeacus*	black		0.165	1.769	0.662	0.092	1.465		
Papilionidae	*Troides aeacus*	black		0.222	1.842	0.823	0.136	1.382		
Papilionidae	*Troides aeacus*	black		0.184	1.714	0.788	0.148	1.393		
Papilionidae	*Troides aeacus*	black		0.209	1.759	0.849	0.155	1.404		
Papilionidae	*Troides aeacus*	black		0.117	1.294	0.877	0.199	1.398		
Papilionidae	*Troides aeacus*	black		0.137	1.495	0.77	0.202	1.359		
Papilionidae	*Troides aeacus*	black		0.201	1.67	0.907	0.106	1.386		
Papilionidae	*Troides aeacus*	black		0.183	1.704	0.794	0.195	1.394		
Papilionidae	*Troides aeacus*	black		0.127	1.405	0.81	0.193	1.277		
Papilionidae	*Troides aeacus*	black		0.112	1.346	0.776	0.19	1.301		
Papilionidae	*Troides aeacus*	black		0.148	1.726	0.625	0.129	1.171		
Papilionidae	*Troides aeacus*	black		0.31	2.309	0.73	0.207	1.29		
Papilionidae	*Troides aeacus*	black		0.214	1.811	0.821	0.157	1.292		
Papilionidae	*Trogonoptera brookiana*	white		0.352	2.283	0.848	0.173	2.156	1.619	2.54
Papilionidae	*Trogonoptera brookiana*	white		0.413	2.486	0.841	0.16	2.183	1.667	2.656
Papilionidae	*Trogonoptera brookiana*	white		0.227	1.794	0.886	0.198	2.239	1.785	2.19
Papilionidae	*Trogonoptera brookiana*	white		0.336	2.126	0.933	0.184	2.199	1.604	2.89
Papilionidae	*Trogonoptera brookiana*	white		0.301	2.09	0.867	0.166	2.214	2.086	2.829
Papilionidae	*Trogonoptera brookiana*	white		0.278	2.029	0.849	0.197	2.17	2.294	2.952
Papilionidae	*Trogonoptera brookiana*	white		0.367	2.281	0.885	0.179	2.305	2.398	3.054
Papilionidae	*Trogonoptera brookiana*	white		0.35	2.23	0.885	0.22	2.508	1.704	
Papilionidae	*Trogonoptera brookiana*	white		0.198	1.78	0.786	0.189	2.252	1.463	
Papilionidae	*Trogonoptera brookiana*	white		0.36	2.418	0.773	0.137	2.265	1.525	
Papilionidae	*Trogonoptera brookiana*	white		0.499	2.675	0.876	0.189	1.98	1.276	
Papilionidae	*Trogonoptera brookiana*	white		0.332	2.141	0.911	0.173	1.954	1.358	
Papilionidae	*Trogonoptera brookiana*	white		0.233	1.769	0.936	0.154	1.953		
Papilionidae	*Trogonoptera brookiana*	white		0.086	1.147	0.819	0.195	1.925		
Papilionidae	*Trogonoptera brookiana*	white		0.442	2.532	0.867	0.179	1.926		
Papilionidae	*Trogonoptera brookiana*	white		0.238	1.919	0.813	0.159	1.925		
Papilionidae	*Trogonoptera brookiana*	white		0.667	3.116	0.863	0.186	1.939		
Papilionidae	*Trogonoptera brookiana*	white		0.558	2.792	0.899	0.16	1.899		
Papilionidae	*Trogonoptera brookiana*	white		0.52	2.737	0.872	0.217	1.912		
Papilionidae	*Trogonoptera brookiana*	white		0.379	2.388	0.836	0.125	1.967		
Papilionidae	*Trogonoptera brookiana*	white		0.108	1.285	0.824	0.157	1.925		
Papilionidae	*Trogonoptera brookiana*	black		0.435	2.4	0.95	0.136	1.464		
Papilionidae	*Trogonoptera brookiana*	black		0.181	1.602	0.889	0.174	1.473		
Papilionidae	*Trogonoptera brookiana*	black		0.216	1.764	0.873	0.181	1.546		
Papilionidae	*Trogonoptera brookiana*	black		0.281	1.988	0.894	0.143	1.465		
Papilionidae	*Trogonoptera brookiana*	black		0.304	2.072	0.89	0.143	1.501		
Papilionidae	*Trogonoptera brookiana*	black		0.174	1.55	0.91	0.119	1.519		
Papilionidae	*Trogonoptera brookiana*	black		0.279	1.977	0.898	0.118	1.428		
Papilionidae	*Trogonoptera brookiana*	black		0.29	2.024	0.889	0.096	1.474		
Papilionidae	*Trogonoptera brookiana*	black		0.369	2.309	0.869	0.103	1.492		
Papilionidae	*Trogonoptera brookiana*	black		0.233	1.758	0.948	0.112	1.394		
Papilionidae	*Trogonoptera brookiana*	black		0.11	1.385	0.72	0.116	1.501		
Papilionidae	*Trogonoptera brookiana*	black		0.113	1.239	0.923	0.126	1.347		
Papilionidae	*Trogonoptera brookiana*	black		0.291	2.04	0.88	0.109	1.356		
Papilionidae	*Trogonoptera brookiana*	black		0.209	1.782	0.828	0.15	1.365		
Papilionidae	*Trogonoptera brookiana*	black		0.155	1.491	0.877	0.163	1.383		
Papilionidae	*Trogonoptera brookiana*	black		0.081	1.198	0.713	0.154	1.275		
Papilionidae	*Trogonoptera brookiana*	black		0.277	1.968	0.899	0.158	1.449		
Papilionidae	*Trogonoptera brookiana*	black		0.179	1.634	0.841	0.121	1.43		
Papilionidae	*Trogonoptera brookiana*	black		0.122	1.364	0.824	0.127	1.474		
Papilionidae	*Trogonoptera brookiana*	black		0.297	2.076	0.865	0.143	1.591		
Papilionidae	*Trogonoptera brookiana*	black		0.261	1.869	0.94	0.154	1.618		
Papilionidae	*Trogonoptera brookiana*	black		0.231	1.871	0.827	0.15	1.582		
Papilionidae	*Pachliopta aristolochiae*	black		0.276	1.923	0.937	0.061	1.766	1.346	2.603
Papilionidae	*Pachliopta aristolochiae*	black		0.088	1.167	0.815	0.051	1.773	1.232	2.488
Papilionidae	*Pachliopta aristolochiae*	black		0.151	1.687	0.666	0.074	1.782	0.891	2.405
Papilionidae	*Pachliopta aristolochiae*	black		0.179	1.628	0.849	0.099	1.688	1.53	2.71
Papilionidae	*Pachliopta aristolochiae*	black		0.193	1.777	0.768	0.042	1.676	1.619	2.337

Papilionidae	*Pachliopta aristolochiae*	black		0.083	1.222	0.7	0.064	1.66	1.761	2.376
Papilionidae	*Pachliopta aristolochiae*	black		0.14	1.416	0.88	0.115	1.699		
Papilionidae	*Pachliopta aristolochiae*	black		0.104	1.217	0.88	0.146	1.719		
Papilionidae	*Pachliopta aristolochiae*	black		0.227	1.846	0.838	0.08	1.793		
Papilionidae	*Pachliopta aristolochiae*	black		0.206	1.719	0.875	0.058	1.797		
Papilionidae	*Pachliopta aristolochiae*	black		0.132	1.474	0.766	0.082	1.82		
Papilionidae	*Pachliopta aristolochiae*	black		0.204	1.669	0.92	0.152	1.751		
Papilionidae	*Pachliopta aristolochiae*	black		0.304	2.144	0.83	0.046	1.696		
Papilionidae	*Pachliopta aristolochiae*	black		0.223	1.795	0.869	0.078	1.719		
Papilionidae	*Pachliopta aristolochiae*	black		0.154	1.64	0.719	0.055	1.758		
Papilionidae	*Pachliopta aristolochiae*	black		0.151	1.467	0.879	0.086	1.75		
Papilionidae	*Pachliopta aristolochiae*	black		0.141	1.517	0.772	0.047	1.715		
Papilionidae	*Pachliopta aristolochiae*	black		0.227	1.815	0.866	0.153	1.781		
Papilionidae	*Pachliopta aristolochiae*	black		0.21	1.771	0.84	0.067	1.793		
Papilionidae	*Pachliopta aristolochiae*	black		0.08	1.142	0.77	0.082	1.816		
Papilionidae	*Pachliopta aristolochiae*	brown		0.075	1.062	0.839	0.559	1.538		
Papilionidae	*Pachliopta aristolochiae*	brown		0.082	1.099	0.854	0.508	1.508		
Papilionidae	*Pachliopta aristolochiae*	brown		0.074	1.093	0.776	0.209	1.492		
Papilionidae	*Pachliopta aristolochiae*	brown		0.102	1.246	0.824	0.568	1.584		
Papilionidae	*Pachliopta aristolochiae*	brown		0.13	1.352	0.895	1.533	1.584		
Papilionidae	*Pachliopta aristolochiae*	brown		0.137	1.55	0.716	0.772	1.574		
Papilionidae	*Pachliopta aristolochiae*	brown		0.011	0.408	0.806	0.161	1.599		
Papilionidae	*Pachliopta aristolochiae*	brown		0.003	0.229	0.83	0.145	1.634		
Papilionidae	*Pachliopta aristolochiae*	brown		0.082	1.158	0.764	0.163	1.624		
Papilionidae	*Pachliopta aristolochiae*	brown		0.09	1.258	0.714	0.674	1.629		
Papilionidae	*Pachliopta aristolochiae*	brown		0.028	0.645	0.855		1.639		
Papilionidae	*Pachliopta aristolochiae*	brown		0.012	0.476	0.656		1.645		
Papilionidae	*Pachliopta aristolochiae*	brown		0.14	1.532	0.751		1.604		
Papilionidae	*Papilio nireus*	yellow	green	0.045	0.822	0.829	0.081	3.023	3.537	4.118
Papilionidae	*Papilio nireus*	yellow	green	0.064	0.982	0.838	0.083	3.039	3.555	4.241
Papilionidae	*Papilio nireus*	yellow	green	0.048	0.925	0.698	0.091	3.234	3.589	4.381
Papilionidae	*Papilio nireus*	yellow	green	0.043	0.952	0.601	0.077	3.247	3.572	4.241
Papilionidae	*Papilio nireus*	yellow	green	0.035	0.802	0.687	0.075	3.189	3.555	4.188
Papilionidae	*Papilio nireus*	yellow	green	0.042	0.89	0.671	0.067	3.249	3.555	4.4
Papilionidae	*Papilio nireus*	yellow	green	0.052	0.946	0.736	0.066	2.969	3.484	
Papilionidae	*Papilio nireus*	yellow	green	0.09	1.263	0.705	0.069	2.99	3.484	
Papilionidae	*Papilio nireus*	yellow	green	0.059	1.108	0.603	0.063	3.173	3.609	
Papilionidae	*Papilio nireus*	yellow	green	0.061	1.02	0.731	0.089	3.224	3.661	
Papilionidae	*Papilio nireus*	yellow	green	0.036	0.823	0.659	0.08	3.151		
Papilionidae	*Papilio nireus*	yellow	green	0.036	0.783	0.742	0.042	3.294		
Papilionidae	*Papilio nireus*	yellow	green	0.051	0.879	0.832	0.037	3.097		
Papilionidae	*Papilio nireus*	yellow	green	0.044	0.811	0.832	0.064	3.399		
Papilionidae	*Papilio nireus*	yellow	green	0.043	0.796	0.85	0.042	3.176		
Papilionidae	*Papilio nireus*	yellow	green	0.043	0.83	0.782	0.057	3.115		
Papilionidae	*Papilio nireus*	yellow	green	0.073	1.132	0.721	0.053	3.159		
Papilionidae	*Papilio nireus*	yellow	green	0.044	0.822	0.815	0.056	3.141		
Papilionidae	*Papilio nireus*	yellow	green	0.052	0.894	0.813	0.049	3.3		
Papilionidae	*Papilio nireus*	yellow	green	0.073	1.018	0.881	0.07	3.317		
Papilionidae	*Papilio nireus*	yellow	green	0.041	0.803	0.795	0.05			
Pieridae	*Catopsilia pomona*	yellow	green	0.765	3.465	0.801	0.062	1.505		
Pieridae	*Catopsilia pomona*	yellow	green	0.735	3.659	0.69	0.075	1.527		
Pieridae	*Catopsilia pomona*	yellow	green	0.608	3.353	0.679	0.070	1.635		
Pieridae	*Catopsilia pomona*	yellow	green	0.838	3.663	0.785	0.068	1.674		
Pieridae	*Catopsilia pomona*	yellow	green	0.854	3.663	0.8	0.059	1.712		
Pieridae	*Catopsilia pomona*	yellow	green	0.881	3.682	0.816	0.078	1.691		
Pieridae	*Catopsilia pomona*	yellow	green	0.716	3.542	0.717	0.093	1.634		
Pieridae	*Catopsilia pomona*	yellow	green	0.629	3.268	0.74	0.063	1.593		
Pieridae	*Catopsilia pomona*	yellow	green	0.524	3.024	0.72	0.067	1.59		
Pieridae	*Catopsilia pomona*	yellow	green	0.584	3.249	0.696	0.085	1.612		
Pieridae	*Catopsilia pomona*	yellow	green	0.725	3.501	0.743	0.070	1.676		
Pieridae	*Catopsilia pomona*	yellow	green	0.889	3.892	0.738	0.063	1.628		
Pieridae	*Catopsilia pomona*	yellow	green	0.93	3.902	0.768	0.088	1.681		
Pieridae	*Catopsilia pomona*	yellow	green	0.741	3.502	0.759	0.081	1.626		
Pieridae	*Catopsilia pomona*	yellow	green	0.642	3.468	0.671	0.057	1.702		

Pieridae	*Catopsilia pomona*	yellow	green	0.791	3.532	0.797	0.081	1.549		
Pieridae	*Catopsilia pomona*	yellow	green	0.585	3.335	0.661	0.070	1.652		
Pieridae	*Catopsilia pomona*	yellow	green	0.715	3.475	0.744	0.062	1.723		
Pieridae	*Catopsilia pomona*	yellow	green	0.72	3.463	0.754	0.075	1.606		
Pieridae	*Catopsilia pomona*	white	green	1.368	4.985	0.692	0.082	2.541		
Pieridae	*Catopsilia pomona*	white	green	1.812	5.634	0.717	0.106	2.118		
Pieridae	*Catopsilia pomona*	white	green	2.311	6.1	0.781	0.106	2.224		
Pieridae	*Catopsilia pomona*	white	green	2.656	6.444	0.804	0.112	2.518		
Pieridae	*Catopsilia pomona*	white	green	1.949	5.59	0.784	0.112	2.706		
Pieridae	*Catopsilia pomona*	white	green	2.64	6.24	0.852	0.106	2.518		
Pieridae	*Catopsilia pomona*	white	green	2.225	6.017	0.772	0.094	2.224		
Pieridae	*Catopsilia pomona*	white	green	2.342	6.145	0.779	0.106	2.153		
Pieridae	*Catopsilia pomona*	white	green	2.449	6.077	0.833	0.100	2.189		
Pieridae	*Catopsilia pomona*	white	green	1.466	4.815	0.795	0.100	2.553		
Pieridae	*Catopsilia pomona*	white	green	1.854	5.467	0.779	0.077	2.565		
Pieridae	*Catopsilia pomona*	white	green	1.528	4.909	0.797	0.100	2.471		
Pieridae	*Catopsilia pomona*	white	green	1.608	4.984	0.814	0.106	2.259		
Pieridae	*Catopsilia pomona*	white	green	1.727	5.439	0.734	0.100	2.224		
Pieridae	*Catopsilia pomona*	white	green	1.082	4.484	0.676	0.123	2.318		
Pieridae	*Catopsilia pomona*	white	green	1.799	5.464	0.757	0.121	2.612		
Pieridae	*Catopsilia pomona*	white	green	1.757	5.324	0.779	0.138	2.129		
Pieridae	*Catopsilia pomona*	white	green	1.097	4.634	0.642	0.106	2.176		
Pieridae	*Catopsilia pomona*	white	green	1.127	4.509	0.697	0.101	2.6		
Pieridae	*Catopsilia pomona*	white	green	1.754	5.423	0.749	0.100	2.294		
Pieridae	*Pieris rapae*	black		1.086	4.119	0.805	0.179	1.875		
Pieridae	*Pieris rapae*	black		0.712	3.736	0.641	0.168	1.859		
Pieridae	*Pieris rapae*	black		0.844	3.861	0.712	0.185	1.876		
Pieridae	*Pieris rapae*	black		0.822	3.951	0.661	0.157	1.881		
Pieridae	*Pieris rapae*	black		0.639	3.666	0.597	0.141	1.897		
Pieridae	*Pieris rapae*	black		0.705	3.76	0.627	0.173	1.892		
Pieridae	*Pieris rapae*	black		0.766	3.857	0.647	0.201	1.908		
Pieridae	*Pieris rapae*	black					0.163	1.805		
Pieridae	*Pieris rapae*	black						1.811		
Pieridae	*Pieris rapae*	black						1.773		
Pieridae	*Pieris rapae*	black						1.772		
Pieridae	*Pieris rapae*	black						1.805		
Pieridae	*Pieris rapae*	black						1.767		
Pieridae	*Pieris rapae*	black						1.81		
Pieridae	*Pieris rapae*	black						1.805		
Pieridae	*Pieris rapae*	black						1.81		
Pieridae	*Pieris rapae*	black						1.816		
Pieridae	*Pieris rapae*	black						1.81		
Pieridae	*Pieris rapae*	black						1.778		
Pieridae	*Pieris rapae*	black						1.854		
Pieridae	*Pieris rapae*	white		1.331	4.674	0.765		1.8	1.092	1.973
Pieridae	*Pieris rapae*	white		1.224	4.435	0.782		1.8	1.055	1.949
Pieridae	*Pieris rapae*	white		0.892	4.106	0.664		1.772	1.188	1.848
Pieridae	*Pieris rapae*	white		1.082	4.421	0.696		1.772	1.209	1.936
Pieridae	*Pieris rapae*	white		0.992	4.354	0.658		1.773	1.107	1.944
Pieridae	*Pieris rapae*	white					0.114	1.843	1.085	
Pieridae	*Pieris rapae*	white					0.125	1.827	1.136	
Pieridae	*Pieris rapae*	white					0.103	1.832	1.121	
Pieridae	*Pieris rapae*	white					0.130	1.794	1.199	
Pieridae	*Pieris rapae*	white					0.131	1.811		
Pieridae	*Pieris rapae*	white					0.087	1.81		
Pieridae	*Pieris rapae*	white					0.119	1.751		
Pieridae	*Pieris rapae*	white					0.136	1.745		
Pieridae	*Pieris rapae*	white					0.130	1.783		
Pieridae	*Pieris rapae*	white					0.114	1.808		
Pieridae	*Pieris rapae*	white						1.827		
Pieridae	*Pieris rapae*	white						1.821		
Pieridae	*Pieris rapae*	white						1.843		
Pieridae	*Pieris rapae*	white						1.832		
Pieridae	*Pieris rapae*	white						1.713		

Pieridae	*Anthocharis cardamines*	orange		1.011	3.955	0.812	0.077	1.472		
Pieridae	*Anthocharis cardamines*	orange		0.783	3.537	0.786	0.065	1.499		
Pieridae	*Anthocharis cardamines*	orange		0.743	3.465	0.777	0.086	1.54		
Pieridae	*Anthocharis cardamines*	orange		0.774	3.561	0.767	0.065	1.588		
Pieridae	*Anthocharis cardamines*	orange		1.04	3.84	0.886	0.070	1.588		
Pieridae	*Anthocharis cardamines*	orange		0.99	3.914	0.812	0.090	1.595		
Pieridae	*Anthocharis cardamines*	orange		0.716	3.466	0.749	0.080	1.479		
Pieridae	*Anthocharis cardamines*	orange		1.229	4.237	0.86	0.054	1.499		
Pieridae	*Anthocharis cardamines*	orange		0.743	3.51	0.758	0.069	1.561		
Pieridae	*Anthocharis cardamines*	orange					0.082	1.574		
Pieridae	*Anthocharis cardamines*	orange					0.078	1.588		
Pieridae	*Anthocharis cardamines*	orange					0.077	1.547		
Pieridae	*Anthocharis cardamines*	orange					0.090	1.54		
Pieridae	*Anthocharis cardamines*	orange					0.092	1.513		
Pieridae	*Anthocharis cardamines*	orange					0.086	1.513		
Pieridae	*Anthocharis cardamines*	orange					0.078	1.438		
Pieridae	*Anthocharis cardamines*	orange					0.090	1.567		
Pieridae	*Anthocharis cardamines*	orange					0.102	1.561		
Pieridae	*Anthocharis cardamines*	orange					0.110	1.513		
Pieridae	*Anthocharis cardamines*	orange					0.095	1.608		
Pieridae	*Delias nigrina*	white		0.747	3.631	0.712	0.104	1.646		
Pieridae	*Delias nigrina*	white		0.786	3.759	0.699	0.114	1.646		
Pieridae	*Delias nigrina*	white		0.655	3.519	0.665	0.117	1.682		
Pieridae	*Delias nigrina*	white		0.846	3.701	0.777	0.128	1.689		
Pieridae	*Delias nigrina*	white		0.854	3.72	0.775	0.113	1.658		
Pieridae	*Delias nigrina*	white		0.923	3.784	0.81	0.117	1.461		
Pieridae	*Delias nigrina*	white					0.103	1.447		
Pieridae	*Delias nigrina*	white					0.103	1.494		
Pieridae	*Delias nigrina*	white					0.100	1.472		
Pieridae	*Delias nigrina*	white						1.447		
Pieridae	*Delias nigrina*	white						1.71		
Pieridae	*Delias nigrina*	white						1.688		
Pieridae	*Delias nigrina*	white						1.653		
Pieridae	*Delias nigrina*	white						1.678		
Pieridae	*Delias nigrina*	white						1.667		
Pieridae	*Delias nigrina*	white						1.674		
Pieridae	*Delias nigrina*	white						1.649		
Pieridae	*Delias nigrina*	white						1.44		
Pieridae	*Delias nigrina*	white						1.496		
Pieridae	*Delias nigrina*	white						1.45		
Pieridae	*Colias crocea*	white		1.194	4.326	0.802	0.094	1.537		
Pieridae	*Colias crocea*	white		1.186	4.257	0.822	0.102	1.629		
Pieridae	*Colias crocea*	white		0.94	3.955	0.755	0.097	1.764		
Pieridae	*Colias crocea*	white		1	3.998	0.786	0.074	1.764		
Pieridae	*Colias crocea*	white		0.804	3.574	0.791	0.107	1.751		
Pieridae	*Colias crocea*	white		0.653	3.506	0.668	0.115	1.533		
Pieridae	*Colias crocea*	white		0.795	3.781	0.699	0.094	1.533		
Pieridae	*Colias crocea*	white		1.459	4.735	0.818	0.113	1.628		
Pieridae	*Colias crocea*	white		0.87	3.943	0.703	0.091	1.626		
Pieridae	*Colias crocea*	white		1.275	4.468	0.803	0.085	1.565		
Pieridae	*Colias crocea*	white		1.14	4.413	0.736	0.107	1.496		
Pieridae	*Colias crocea*	white		1.122	4.326	0.754	0.095	1.603		
Pieridae	*Colias crocea*	white		0.635	3.357	0.708	0.123	1.556		
Pieridae	*Colias crocea*	white					0.119	1.635		
Pieridae	*Colias crocea*	white					0.13	1.513		
Pieridae	*Colias crocea*	white					0.123	1.536		
Pieridae	*Colias crocea*	white					0.151	1.552		
Pieridae	*Colias crocea*	white					0.113	1.51		
Pieridae	*Colias crocea*	white					0.104	1.547		
Pieridae	*Colias crocea*	white					0.105	1.506		
Pieridae	*Colias crocea*	black		1.031	3.759	0.916	0.194	1.742		
Pieridae	*Colias crocea*	black		0.778	3.276	0.911	0.168	1.719		
Pieridae	*Colias crocea*	black		0.886	3.707	0.811	0.219	1.697		
Pieridae	*Colias crocea*	black		0.733	3.432	0.782	0.191	1.735		

Pieridae	*Colias crocea*	black		1.082	3.968	0.863	0.200	1.672		
Pieridae	*Colias crocea*	black		0.967	3.761	0.859	0.167	1.693		
Pieridae	*Colias crocea*	black		1.189	3.998	0.934	0.208	1.716		
Pieridae	*Colias crocea*	black		0.647	3.164	0.812	0.222	1.689		
Pieridae	*Colias crocea*	black		0.501	2.791	0.809	0.241	1.732		
Pieridae	*Colias crocea*	black		0.818	3.479	0.849	0.170	1.568		
Pieridae	*Colias crocea*	black		0.722	3.367	0.8	0.177	1.672		
Pieridae	*Colias crocea*	black		0.999	3.760	0.887	0.194	1.637		
Pieridae	*Colias crocea*	black		0.656	3.223	0.793	0.214	1.649		
Pieridae	*Colias crocea*	black		1.041	3.910	0.856	0.226	1.603		
Pieridae	*Colias crocea*	black		0.932	3.789	0.816	0.241	1.585		
Pieridae	*Colias crocea*	black					0.238	1.688		
Pieridae	*Colias crocea*	black					0.290	1.624		
Pieridae	*Colias crocea*	black					0.224	1.658		
Pieridae	*Colias crocea*	black					0.177	1.666		
Pieridae	*Colias crocea*	black					0.208	1.624		
Pieridae	*C. eurytheme*	white		0.603	3.097	0.79	0.066	1.346		
Pieridae	*C. eurytheme*	white		0.482	2.806	0.77	0.08	1.348		
Pieridae	*C. eurytheme*	white		0.52	2.997	0.728	0.076	1.402		
Pieridae	*C. eurytheme*	white		0.816	3.559	0.81	0.083	1.205		
Pieridae	*C. eurytheme*	white		0.741	3.356	0.827	0.099	1.265		
Pieridae	*C. eurytheme*	white		0.815	3.514	0.83	0.089	1.486		
Pieridae	*C. eurytheme*	white		1.004	3.876	0.839	0.076	1.427		
Pieridae	*C. eurytheme*	white		0.542	3.147	0.688	0.098	1.491		
Pieridae	*C. eurytheme*	white		1.125	4.064	0.856	0.071	1.341		
Pieridae	*C. eurytheme*	white		0.67	3.27	0.787	0.076	1.295		
Pieridae	*C. eurytheme*	white		0.491	2.889	0.74	0.063	1.265		
Pieridae	*C. eurytheme*	white		0.477	2.864	0.731	0.079	1.328		
Pieridae	*C. eurytheme*	white		0.909	3.696	0.837	0.076	1.275		
Pieridae	*C. eurytheme*	white		0.672	3.391	0.735	0.069	1.243		
Pieridae	*C. eurytheme*	white		0.902	3.772	0.796	0.067	1.311		
Pieridae	*C. eurytheme*	white		0.753	3.4	0.818	0.082	1.227		
Pieridae	*C. eurytheme*	white		0.728	3.365	0.808	0.07	1.36		
Pieridae	*C. eurytheme*	white		0.848	3.741	0.762	0.079	1.408		
Pieridae	*C. eurytheme*	white		0.838	3.595	0.815	0.076	1.479		
Pieridae	*C. eurytheme*	white		0.904	3.726	0.818	0.095	1.318		
Pieridae	*C. eurytheme*	orange		1.524	5.019	0.760	0.104	1.907		
Pieridae	*C. eurytheme*	orange		1.165	4.63	0.683	0.112	1.913		
Pieridae	*C. eurytheme*	orange		0.934	4.397	0.607	0.094	1.831		
Pieridae	*C. eurytheme*	orange		1.048	4.308	0.710	0.091	1.855		
Pieridae	*C. eurytheme*	orange		0.982	4.42	0.632	0.096	1.831		
Pieridae	*C. eurytheme*	orange		1.102	4.228	0.775	0.077	1.794		
Pieridae	*C. eurytheme*	orange		0.949	4.507	0.587	0.111	1.811		
Pieridae	*C. eurytheme*	orange		1.06	4.148	0.774	0.094	1.779		
Pieridae	*C. eurytheme*	orange		0.848	4.34	0.566	0.081	1.982		
Pieridae	*C. eurytheme*	orange		1.409	4.626	0.828	0.093	1.907		
Pieridae	*C. eurytheme*	orange		0.862	4.151	0.629	0.104	1.862		
Pieridae	*C. eurytheme*	orange		1.12	4.326	0.752	0.078	1.9		
Pieridae	*C. eurytheme*	orange		1.168	4.505	0.723	0.067	1.896		
Pieridae	*C. eurytheme*	orange					0.107	1.933		
Pieridae	*C. eurytheme*	orange					0.109	1.908		
Pieridae	*C. eurytheme*	orange					0.112	1.79		
Pieridae	*C. eurytheme*	orange					0.101	1.849		
Pieridae	*C. eurytheme*	orange					0.085	1.833		
Pieridae	*C. eurytheme*	orange					0.109	1.831		
Pieridae	*C. eurytheme*	orange					0.091	1.889		
Lycaenidae	*Polyommatus icarus*	brown	blue	1.125	3.92	0.92	0.115	1.626	0.819	1.543
Lycaenidae	*Polyommatus icarus*	brown	blue	1.095	3.867	0.92	0.106	1.648	0.833	1.459
Lycaenidae	*Polyommatus icarus*	brown	blue	0.966	3.628	0.922	0.094	1.569	0.796	1.453
Lycaenidae	*Polyommatus icarus*	brown	blue	0.955	3.657	0.897	0.104	1.552	0.763	1.516
Lycaenidae	*Polyommatus icarus*	brown	blue	0.897	3.617	0.862	0.12	1.554	0.827	1.426
Lycaenidae	*Polyommatus icarus*	brown	blue	0.776	3.467	0.811	0.121	1.511	0.776	1.506
Lycaenidae	*Polyommatus icarus*	brown	blue	0.891	3.594	0.867	0.115	1.655	0.758	
Lycaenidae	*Polyommatus icarus*	brown	blue	0.93	3.688	0.859	0.115	1.551	0.861	

Lycaenidae	*Polyommatus icarus*	brown	blue	0.932	3.706	0.853	0.111	1.501	0.878	
Lycaenidae	*Polyommatus icarus*	brown	blue	0.693	3.186	0.858	0.118	1.469	0.774	
Lycaenidae	*Polyommatus icarus*	brown	blue	0.711	3.28	0.83	0.101	1.485	0.835	
Lycaenidae	*Polyommatus icarus*	brown	blue	0.696	3.241	0.833	0.078	1.469		
Lycaenidae	*Polyommatus icarus*	brown	blue	0.929	3.694	0.856	0.098	1.48		
Lycaenidae	*Polyommatus icarus*	brown	blue	0.947	3.787	0.83	0.1	1.474		
Lycaenidae	*Polyommatus icarus*	brown	blue				0.104	1.479		
Lycaenidae	*Polyommatus icarus*	brown	blue				0.128	1.502		
Lycaenidae	*Polyommatus icarus*	brown	blue				0.11	1.487		
Lycaenidae	*Polyommatus icarus*	brown	blue				0.123	1.555		
Lycaenidae	*Polyommatus icarus*	brown	blue				0.115	1.599		
Lycaenidae	*Polyommatus icarus*	brown	blue				0.127	1.641		
Lycaenidae	*Polyommatus marcidus*	brown		0.518	3.35	0.581	0.165	1.513		
Lycaenidae	*Polyommatus marcidus*	brown		0.529	3.311	0.607	0.253	1.423		
Lycaenidae	*Polyommatus marcidus*	brown		0.448	3.08	0.594	0.232	1.455		
Lycaenidae	*Polyommatus marcidus*	brown		0.445	3.047	0.602	0.258	1.449		
Lycaenidae	*Polyommatus marcidus*	brown		0.579	3.363	0.644	0.224	1.518		
Lycaenidae	*Polyommatus marcidus*	brown		0.405	2.692	0.702	0.23	1.512		
Lycaenidae	*Polyommatus marcidus*	brown		0.608	3.591	0.593	0.238	1.497		
Lycaenidae	*Polyommatus marcidus*	brown		0.532	3.392	0.581	0.217	1.461		
Lycaenidae	*Polyommatus marcidus*	brown		0.498	3.378	0.548	0.24	1.404		
Lycaenidae	*Polyommatus marcidus*	brown		0.488	3.476	0.508	0.24	1.48		
Lycaenidae	*Polyommatus marcidus*	brown		0.526	3.15	0.666	0.233	1.421		
Lycaenidae	*Polyommatus marcidus*	brown		0.541	3.604	0.523	0.224	1.512		
Lycaenidae	*Polyommatus marcidus*	brown		0.487	3.196	0.6	0.205	1.489		
Lycaenidae	*Polyommatus marcidus*	brown		0.419	2.993	0.588	0.238	1.462		
Lycaenidae	*Polyommatus marcidus*	brown		0.592	3.527	0.598	0.222	1.529		
Lycaenidae	*Polyommatus marcidus*	brown		0.422	3.135	0.54	0.209	1.458		
Lycaenidae	*Polyommatus marcidus*	brown		0.589	3.471	0.614	0.253	1.435		
Lycaenidae	*Polyommatus marcidus*	brown		0.466	3.1	0.609	0.23	1.385		
Lycaenidae	*Polyommatus marcidus*	brown		0.525	3.165	0.658	0.241	1.352		
Lycaenidae	*Polyommatus marcidus*	brown		0.431	3.23	0.519	0.215	1.45		
Lycaenidae	*Thecla opisena*	brown	green	0.926	4.245	0.646	0.141	1.959		
Lycaenidae	*Thecla opisena*	brown	green	0.954	4.263	0.66	0.135	2.065		
Lycaenidae	*Thecla opisena*	brown	green	1.094	4.588	0.653	0.153	1.947		
Lycaenidae	*Thecla opisena*	brown	green	1.08	4.417	0.696	0.13	1.9		
Lycaenidae	*Thecla opisena*	brown	green	1.372	4.811	0.745	0.117	1.842		
Lycaenidae	*Thecla opisena*	brown	green	1.272	4.758	0.706	0.124	1.912		
Lycaenidae	*Thecla opisena*	brown	green	1.132	4.487	0.706	0.112	1.912		
Lycaenidae	*Thecla opisena*	brown	green	1.28	4.824	0.691	0.123	1.842		
Lycaenidae	*Thecla opisena*	brown	green	1.121	4.565	0.676	0.141	1.947		
Lycaenidae	*Thecla opisena*	brown	green	1.594	5.195	0.743	0.147	1.889		
Lycaenidae	*Thecla opisena*	brown	green	1.244	4.987	0.629	0.141	1.924		
Lycaenidae	*Thecla opisena*	brown	green	1.056	4.495	0.657	0.117	2.006		
Lycaenidae	*Thecla opisena*	brown	green	1.216	4.695	0.693	0.106	1.971		
Lycaenidae	*Thecla opisena*	brown	green	1.513	5.069	0.74	0.141	1.994		
Lycaenidae	*Thecla opisena*	brown	green	1.49	4.996	0.75	0.117	1.853		
Lycaenidae	*Thecla opisena*	brown	green	1.173	4.62	0.691	0.1	1.924		
Lycaenidae	*Thecla opisena*	brown	green	1.349	4.769	0.745	0.129	1.842		
Lycaenidae	*Thecla opisena*	brown	green	0.951	4.291	0.649	0.141	1.912		
Lycaenidae	*Thecla opisena*	brown	green	1.101	4.35	0.731	0.112	1.83		
Lycaenidae	*Thecla opisena*	brown	green	1.127	4.632	0.66	0.153	1.901		
Lycaenidae	*Albulina metallica*	brown	blue	1.042	4.169	0.753	0.124	2.007	1.006	1.368
Lycaenidae	*Albulina metallica*	brown	blue	0.906	4.003	0.711	0.103	1.96	1.092	1.474
Lycaenidae	*Albulina metallica*	brown	blue	0.894	3.997	0.703	0.109	1.937	1.019	1.415
Lycaenidae	*Albulina metallica*	brown	blue	0.761	3.827	0.653	0.137	1.975	0.991	1.298
Lycaenidae	*Albulina metallica*	brown	blue	0.971	4.009	0.759	0.124	1.947	1.014	1.355
Lycaenidae	*Albulina metallica*	brown	blue	0.825	3.786	0.723	0.104	2.057	1.091	
Lycaenidae	*Albulina metallica*	brown	blue	0.976	3.919	0.799	0.075	2.057	1.064	
Lycaenidae	*Albulina metallica*	brown	blue	0.852	3.905	0.702	0.096	2.015	1.009	
Lycaenidae	*Albulina metallica*	brown	blue	0.751	3.681	0.696	0.108	1.934	1.014	
Lycaenidae	*Albulina metallica*	brown	blue	0.901	3.813	0.778	0.108	1.95		
Lycaenidae	*Albulina metallica*	brown	blue	0.921	3.882	0.768	0.128	1.965		
Lycaenidae	*Albulina metallica*	brown	blue	0.795	3.605	0.768	0.082	1.918		

Lycaenidae	*Albulina metallica*	brown	blue	1.257	4.509	0.777	0.08	1.929		
Lycaenidae	*Albulina metallica*	gold	green	1.474	4.419	0.948	0.124	1.75	0.842	1.295
Lycaenidae	*Albulina metallica*	gold	green	0.973	3.935	0.789	0.118	1.685	0.9	1.262
Lycaenidae	*Albulina metallica*	gold	green	0.909	3.825	0.781	0.104	1.818	0.915	1.314
Lycaenidae	*Albulina metallica*	gold	green	1.159	4.134	0.852	0.09	1.785	0.862	1.23
Lycaenidae	*Albulina metallica*	gold	green	0.986	3.974	0.785	0.099	1.888	0.833	1.305
Lycaenidae	*Albulina metallica*	gold	green	0.802	3.712	0.732	0.091	1.643	0.972	1.31
Lycaenidae	*Albulina metallica*	gold	green	0.961	3.837	0.82	0.078	1.707	1.013	1.251
Lycaenidae	*Albulina metallica*	gold	green	0.852	4.017	0.664	0.118	1.693	0.952	1.285
Lycaenidae	*Albulina metallica*	gold	green	0.832	3.832	0.712	0.108	1.709	0.93	1.31
Lycaenidae	*Albulina metallica*	gold	green	1.619	4.979	0.821	0.101	1.658	0.921	1.212
Lycaenidae	*Albulina metallica*	gold	green							1.291
Lycaenidae	*atymna*	red		0.32	2.137	0.881	0.094	0.763		
Lycaenidae	*atymna*	red		0.215	1.895	0.752	0.093	0.72		
Lycaenidae	*atymna*	red		0.293	2.164	0.786	0.108	0.73		
Lycaenidae	*atymna*	red		0.306	2.147	0.833	0.084	0.71		
Lycaenidae	*atymna*	red		0.295	2.113	0.832	0.098	0.724		
Lycaenidae	*atymna*	red		0.328	2.281	0.792	0.084	0.884		
Lycaenidae	*atymna*	red		0.356	2.372	0.796	0.081	0.848		
Lycaenidae	*atymna*	red		0.266	2.057	0.789	0.086	0.886		
Lycaenidae	*atymna*	red		0.291	2.33	0.673	0.093	0.851		
Lycaenidae	*atymna*	red		0.277	1.998	0.872	0.104	0.76		
Lycaenidae	*atymna*	red		0.332	2.245	0.828		0.924		
Lycaenidae	*atymna*	red		0.265	2.236	0.667		0.954		
Lycaenidae	*atymna*	red		0.284	2.099	0.809		0.884		
Lycaenidae	*atymna*	red		0.299	2.23	0.756		0.865		
Lycaenidae	*atymna*	red		0.286	2.155	0.774		0.846		
Lycaenidae	*atymna*	red		0.331	2.469	0.683		0.929		
Lycaenidae	*atymna*	red		0.363	2.657	0.646		0.835		
Lycaenidae	*atymna*	red		0.289	2.18	0.764		0.873		
Lycaenidae	*atymna*	red		0.265	2.105	0.751		0.905		
Lycaenidae	*atymna*	red		0.28	2.174	0.744		0.929		
Nymphalidae	*Bicyclus anynana*	black		0.426	3.294	0.493	0.25	1.219		
Nymphalidae	*Bicyclus anynana*	black		0.437	3.31	0.501	0.25	1.24		
Nymphalidae	*Bicyclus anynana*	black		0.452	3.24	0.541	0.234	1.292		
Nymphalidae	*Bicyclus anynana*	black		0.521	3.297	0.602	0.219	1.281		
Nymphalidae	*Bicyclus anynana*	black		0.421	3.371	0.465	0.203	1.313		
Nymphalidae	*Bicyclus anynana*	black		0.508	3.28	0.593	0.224	1.323		
Nymphalidae	*Bicyclus anynana*	black		0.434	3.064	0.581	0.229	1.208		
Nymphalidae	*Bicyclus anynana*	black		0.473	3.284	0.551	0.188	1.156		
Nymphalidae	*Bicyclus anynana*	black		0.373	2.758	0.616	0.271	1.229		
Nymphalidae	*Bicyclus anynana*	black		0.419	3.091	0.551	0.214	1.156		
Nymphalidae	*Bicyclus anynana*	black		0.448	3.05	0.605	0.25	1.229		
Nymphalidae	*Bicyclus anynana*	black		0.428	3.099	0.56	0.261	1.219		
Nymphalidae	*Bicyclus anynana*	black		0.517	3.392	0.565	0.25	1.157		
Nymphalidae	*Bicyclus anynana*	black		0.452	3.351	0.505	0.229	1.208		
Nymphalidae	*Bicyclus anynana*	black		0.462	3.244	0.552	0.188	1.333		
Nymphalidae	*Bicyclus anynana*	black		0.41	3.144	0.521	0.229	1.323		
Nymphalidae	*Bicyclus anynana*	black		0.413	3.031	0.565	0.214	1.281		
Nymphalidae	*Bicyclus anynana*	black		0.559	3.369	0.619	0.25	1.333		
Nymphalidae	*Bicyclus anynana*	black		0.387	3.043	0.525	0.235	1.333		
Nymphalidae	*Bicyclus anynana*	black		0.38	3.048	0.514	0.227	1.344		
Nymphalidae	*Bicyclus anynana*	brown		0.557	3.513	0.567	0.31	1.196		
Nymphalidae	*Bicyclus anynana*	brown		0.58	3.602	0.562	0.28	1.126		
Nymphalidae	*Bicyclus anynana*	brown		0.974	4.157	0.708	0.261	1.166		
Nymphalidae	*Bicyclus anynana*	brown		0.448	3.137	0.572	0.33	1.151		
Nymphalidae	*Bicyclus anynana*	brown		0.591	3.594	0.575	0.241	1.063		
Nymphalidae	*Bicyclus anynana*	brown		0.635	3.868	0.534	0.207	1.078		
Nymphalidae	*Bicyclus anynana*	brown		0.658	3.839	0.561	0.192	1.181		
Nymphalidae	*Bicyclus anynana*	brown		0.591	3.472	0.616	0.271	1.151		
Nymphalidae	*Bicyclus anynana*	brown		0.609	3.647	0.576	0.221	1.181		
Nymphalidae	*Bicyclus anynana*	brown		0.682	3.834	0.583	0.236	1.196		
Nymphalidae	*Bicyclus anynana*	brown		0.572	3.493	0.589	0.192	1.181		
Nymphalidae	*Bicyclus anynana*	brown		0.604	3.578	0.593	0.182	1.166		

Nymphalidae	*Bicyclus anynana*	brown		0.544	3.406	0.589	0.162	1.122		
Nymphalidae	*Bicyclus anynana*	brown		0.532	3.247	0.634	0.202	1.122		
Nymphalidae	*Bicyclus anynana*	brown		0.503	3.04	0.684	0.212	1.122		
Nymphalidae	*Bicyclus anynana*	brown		0.471	3.122	0.608	0.241	1.093		
Nymphalidae	*Bicyclus anynana*	brown		0.608	3.708	0.556	0.207	1.092		
Nymphalidae	*Bicyclus anynana*	brown		0.497	3.412	0.536	0.207	1.23		
Nymphalidae	*Bicyclus anynana*	brown		0.511	3.453	0.538	0.218	1.22		
Nymphalidae	*Bicyclus anynana*	brown		0.485	3.112	0.629	0.204	1.181		
Nymphalidae	*Bicyclus anynana*	gold		0.411	3.277	0.481	0.217	1.063		
Nymphalidae	*Bicyclus anynana*	gold		0.308	2.803	0.492	0.285	1.064		
Nymphalidae	*Bicyclus anynana*	gold		0.342	2.912	0.507	0.204	1.027		
Nymphalidae	*Bicyclus anynana*	gold		0.307	3.154	0.388	0.224	1.042		
Nymphalidae	*Bicyclus anynana*	gold		0.368	2.793	0.592	0.249	1.038		
Nymphalidae	*Bicyclus anynana*	gold		0.377	2.732	0.635	0.154	1		
Nymphalidae	*Bicyclus anynana*	gold		0.275	2.818	0.434	0.241	0.99		
Nymphalidae	*Bicyclus anynana*	gold		0.323	3.006	0.448	0.227	1.039		
Nymphalidae	*Bicyclus anynana*	gold		0.348	2.852	0.538	0.256	0.956		
Nymphalidae	*Bicyclus anynana*	gold		0.458	3.187	0.566	0.227	0.956		
Nymphalidae	*Bicyclus anynana*	gold		0.4	2.843	0.623	0.218	0.975		
Nymphalidae	*Bicyclus anynana*	gold		0.384	2.747	0.64	0.236	0.975		
Nymphalidae	*Bicyclus anynana*	gold		0.287	2.462	0.596	0.265	0.907		
Nymphalidae	*Bicyclus anynana*	gold		0.387	2.992	0.543	0.245	0.995		
Nymphalidae	*Bicyclus anynana*	gold		0.357	3.025	0.49	0.322	0.995		
Nymphalidae	*Bicyclus anynana*	gold		0.421	3.173	0.526	0.234	1.004		
Nymphalidae	*Bicyclus anynana*	gold		0.557	3.579	0.546	0.278	0.936		
Nymphalidae	*Bicyclus anynana*	gold		0.405	2.826	0.637	0.278	0.956		
Nymphalidae	*Bicyclus anynana*	gold		0.392	3.004	0.546	0.183	0.995		
Nymphalidae	*Bicyclus anynana*	gold		0.381	2.989	0.536	0.249	0.943		
Nymphalidae	*Bicyclus anynana*	gold		0.383	2.953	0.553	0.25	1.024		
Nymphalidae	*Bicyclus anynana*	beige		0.933	4.304	0.633	0.215	1.053		
Nymphalidae	*Bicyclus anynana*	beige		0.616	3.514	0.627	0.166	1.053		
Nymphalidae	*Bicyclus anynana*	beige		0.648	3.342	0.729	0.215	1.038		
Nymphalidae	*Bicyclus anynana*	beige		0.523	3.394	0.57	0.236	1.068		
Nymphalidae	*Bicyclus anynana*	beige		0.684	3.584	0.67	0.241	1.053		
Nymphalidae	*Bicyclus anynana*	beige		0.56	3.126	0.72	0.241	1.06		
Nymphalidae	*Bicyclus anynana*	beige		0.555	3.319	0.634	0.263	0.965		
Nymphalidae	*Bicyclus anynana*	beige		0.638	3.224	0.772	0.2	0.973		
Nymphalidae	*Bicyclus anynana*	beige		0.397	3.101	0.519	0.215	1.009		
Nymphalidae	*Bicyclus anynana*	beige		0.659	3.261	0.779	0.197	0.995		
Nymphalidae	*Bicyclus anynana*	beige		0.526	3.263	0.621	0.219	0.98		
Nymphalidae	*Bicyclus anynana*	beige		0.527	3.138	0.673	0.19	0.987		
Nymphalidae	*Bicyclus anynana*	beige		0.716	3.871	0.601	0.201	1.112		
Nymphalidae	*Bicyclus anynana*	beige		0.637	3.763	0.566	0.205	1.09		
Nymphalidae	*Bicyclus anynana*	beige		0.608	3.405	0.659	0.224	1.112		
Nymphalidae	*Bicyclus anynana*	beige		0.761	3.637	0.723	0.182	1.097		
Nymphalidae	*Bicyclus anynana*	beige		0.617	3.702	0.566	0.214	1.082		
Nymphalidae	*Bicyclus anynana*	beige		0.658	3.597	0.639	0.199	1.038		
Nymphalidae	*Bicyclus anynana*	beige		0.63	3.3	0.726	0.196	1.082		
Nymphalidae	*Bicyclus anynana*	beige		0.65	3.39	0.711	0.293	1.075		
Nymphalidae	*Bicyclus anynana*	beige		0.554	3.305	0.637	0.249	1.06		
Nymphalidae	*Bicyclus anynana*	white		0.253	2.081	0.735	0.156	0.839		
Nymphalidae	*Bicyclus anynana*	white		0.21	2.194	0.547	0.166	0.897		
Nymphalidae	*Bicyclus anynana*	white		0.252	2.595	0.47	0.173	0.887		
Nymphalidae	*Bicyclus anynana*	white		0.354	2.281	0.856	0.176	0.873		
Nymphalidae	*Bicyclus anynana*	white		0.293	2.397	0.642	0.205	0.863		
Nymphalidae	*Bicyclus anynana*	white		0.31	2.525	0.611	0.171	0.853		
Nymphalidae	*Bicyclus anynana*	white		0.388	2.61	0.715	0.171	0.917		
Nymphalidae	*Bicyclus anynana*	white		0.275	2.364	0.618	0.166	0.887		
Nymphalidae	*Bicyclus anynana*	white		0.274	2.501	0.55	0.156	0.878		
Nymphalidae	*Bicyclus anynana*	white		0.302	2.407	0.655	0.171	0.897		
Nymphalidae	*Bicyclus anynana*	white		0.334	2.347	0.761	0.215	0.858		
Nymphalidae	*Bicyclus anynana*	white		0.286	2.541	0.556	0.161	0.887		
Nymphalidae	*Bicyclus anynana*	white		0.401	2.498	0.808	0.161	0.912		
Nymphalidae	*Bicyclus anynana*	white		0.357	2.63	0.648	0.196	0.858		

Nymphalidae	*Bicyclus anynana*	white		0.249	2.375	0.555	0.168	0.887		
Nymphalidae	*Bicyclus anynana*	white		0.37	2.654	0.661	0.155	0.897		
Nymphalidae	*Bicyclus anynana*	white		0.24	2.359	0.543	0.171	0.946		
Nymphalidae	*Bicyclus anynana*	white		0.319	2.573	0.606	0.185	0.951		
Nymphalidae	*Bicyclus anynana*	white		0.299	2.61	0.551	0.177	0.97		
Nymphalidae	*Bicyclus anynana*	white		0.301	2.32	0.703	0.195	0.956		
Nymphalidae	*Bicyclus anynana*	white		0.267	2.545	0.518	0.176	0.739		
Nymphalidae	*Heliconius telesiphe*	red		1.218	4.16	0.884	0.417	2.858		
Nymphalidae	*Heliconius telesiphe*	red		0.876	3.59	0.854	0.336	2.821		
Nymphalidae	*Heliconius telesiphe*	red		0.857	3.877	0.717	0.319	3.062		
Nymphalidae	*Heliconius telesiphe*	red		1.118	4.095	0.838	0.295	3.007		
Nymphalidae	*Heliconius telesiphe*	red		1.171	4.155	0.853	0.425	3.359		
Nymphalidae	*Heliconius telesiphe*	red		1.513	4.648	0.88	0.401	3.266		
Nymphalidae	*Heliconius telesiphe*	red		1.374	4.412	0.887	0.417	3.062		
Nymphalidae	*Heliconius telesiphe*	red		1.907	5.032	0.946	0.351	3.025		
Nymphalidae	*Heliconius telesiphe*	red		0.951	3.865	0.8	0.376	2.932		
Nymphalidae	*Heliconius telesiphe*	red		1.813	4.916	0.942	0.305	3.007		
Nymphalidae	*Heliconius telesiphe*	red		1.326	4.509	0.82	0.305	3.082		
Nymphalidae	*Heliconius telesiphe*	red		1.011	3.914	0.829	0.66	3.099		
Nymphalidae	*Heliconius telesiphe*	red		1.403	4.477	0.879	0.442	3.211		
Nymphalidae	*Heliconius telesiphe*	red		2.372	5.561	0.964	0.768	3.229		
Nymphalidae	*Heliconius telesiphe*	red		1.534	4.59	0.915	0.3	3.136		
Nymphalidae	*Heliconius telesiphe*	red		1.9	5.094	0.92	0.899	3.099		
Nymphalidae	*Heliconius telesiphe*	red		1.274	4.431	0.815	0.311	3.062		
Nymphalidae	*Heliconius telesiphe*	red		1.493	4.566	0.9	0.466	3.526		
Nymphalidae	*Heliconius telesiphe*	red		0.984	3.803	0.855	0.482	3.062		
Nymphalidae	*Heliconius telesiphe*	red		1.418	4.518	0.873	0.442	2.932		
Nymphalidae	*Heliconius sara*	yellow		2.223	5.613	0.887	0.391	3.516		
Nymphalidae	*Heliconius sara*	yellow		2.423	5.729	0.928	0.399	3.653		
Nymphalidae	*Heliconius sara*	yellow		1.771	5.165	0.834	0.331	3.625		
Nymphalidae	*Heliconius sara*	yellow		1.802	5.377	0.783	0.263	3.497		
Nymphalidae	*Heliconius sara*	yellow		2.06	5.57	0.834	0.349	3.322		
Nymphalidae	*Heliconius sara*	yellow		1.349	4.698	0.768	0.348	3.314		
Nymphalidae	*Heliconius sara*	yellow		3.405	6.685	0.957	0.399	3.313		
Nymphalidae	*Heliconius sara*	yellow		1.124	4.344	0.749	0.408	3.338		
Nymphalidae	*Heliconius sara*	yellow		1.595	4.994	0.804	0.314	3.134		
Nymphalidae	*Heliconius sara*	yellow		2.109	5.484	0.881	0.331	3.262		
Nymphalidae	*Heliconius sara*	yellow		2.569	5.95	0.912	0.425	3.313		
Nymphalidae	*Heliconius sara*	yellow		2.218	5.516	0.916	0.289	3.313		
Nymphalidae	*Heliconius sara*	yellow		2.86	6.091	0.969	0.442	3.185		
Nymphalidae	*Heliconius sara*	yellow		2.973	6.378	0.918	0.34	3.057		
Nymphalidae	*Heliconius sara*	yellow		1.718	5.221	0.792	0.544	2.93		
Nymphalidae	*Heliconius sara*	yellow		1.958	5.432	0.834	0.323	3.146		
Nymphalidae	*Heliconius sara*	yellow		2.278	5.606	0.911	0.315	3.185		
Nymphalidae	*Heliconius sara*	yellow		2.836	6.147	0.943	0.331	3.465		
Nymphalidae	*Heliconius sara*	yellow		3.325	6.65	0.945	0.289	2.956		
Nymphalidae	*Heliconius sara*	yellow		1.781	5.288	0.8	0.297	3.057		
Nymphalidae	*Hypolimnas salmacis*	white		0.788	3.663	0.738	0.072	1.423	0.839	2.107
Nymphalidae	*Hypolimnas salmacis*	white		1.082	4.04	0.833	0.078	1.482	1.534	1.675
Nymphalidae	*Hypolimnas salmacis*	white		0.984	3.92	0.804	0.075	1.384	1.827	2.132
Nymphalidae	*Hypolimnas salmacis*	white		0.675	3.311	0.773	0.066	1.342	1.485	2.611
Nymphalidae	*Hypolimnas salmacis*	white		1.308	4.349	0.869	0.063	1.357	1.765	2.624
Nymphalidae	*Hypolimnas salmacis*	white		0.898	3.605	0.868	0.071	1.297	0.838	2.743
Nymphalidae	*Hypolimnas salmacis*	white		0.933	3.807	0.809	0.062	1.446	1.227	2.723
Nymphalidae	*Hypolimnas salmacis*	white		1.117	4.055	0.854	0.098	1.347	1.362	2.762
Nymphalidae	*Hypolimnas salmacis*	white		1.077	3.954	0.866	0.066	1.388	1.146	1.681
Nymphalidae	*Hypolimnas salmacis*	white		0.814	3.538	0.817	0.079	1.332		
Nymphalidae	*Hypolimnas salmacis*	white						1.369		
Nymphalidae	*Hypolimnas salmacis*	white						1.403		
Nymphalidae	*Hypolimnas salmacis*	white						1.383		
Nymphalidae	*Hypolimnas salmacis*	white						1.48		
Nymphalidae	*Hypolimnas salmacis*	white						1.332		
Nymphalidae	*Hypolimnas salmacis*	white						1.445		
Nymphalidae	*Hypolimnas salmacis*	white						1.305		

Nymphalidae	*Hypolimnas salmacis*	white						1.428		
Nymphalidae	*Hypolimnas salmacis*	white						1.389		
Nymphalidae	*Hypolimnas salmacis*	brown		0.668	3.027	0.916	0.112	1.086	1.55	2.199
Nymphalidae	*Hypolimnas salmacis*	brown		0.703	3.082	0.93	0.126	1.15	1.565	2.211
Nymphalidae	*Hypolimnas salmacis*	brown		0.608	2.952	0.877	0.115	1.017	1.585	2.437
Nymphalidae	*Hypolimnas salmacis*	brown		0.506	2.736	0.85	0.091	1.019	1.304	2.497
Nymphalidae	*Hypolimnas salmacis*	brown		0.58	2.862	0.89	0.09	1.164	1.071	2.523
Nymphalidae	*Hypolimnas salmacis*	brown		0.613	2.895	0.92	0.085	1.217	1.852	1.97
Nymphalidae	*Hypolimnas salmacis*	brown		0.619	2.924	0.909	0.072	1.081	1.75E+00	1.505
Nymphalidae	*Hypolimnas salmacis*	brown		0.654	3.14	0.834	0.074	1.151	1.38E+00	2.556
Nymphalidae	*Hypolimnas salmacis*	brown		0.703	3.171	0.879	0.085	1.196	1.90E+00	
Nymphalidae	*Hypolimnas salmacis*	brown		0.604	2.823	0.953	0.084	1.197		
Nymphalidae	*Hypolimnas salmacis*	brown						1.067		
Nymphalidae	*Hypolimnas salmacis*	brown						1.092		
Nymphalidae	*Hypolimnas salmacis*	brown						1.111		
Nymphalidae	*Hypolimnas salmacis*	brown						1.072		
Nymphalidae	*Hypolimnas salmacis*	brown						1.179		
Nymphalidae	*Hypolimnas salmacis*	brown						1.173		
Nymphalidae	*Hypolimnas salmacis*	brown						1.099		
Nymphalidae	*Hypolimnas salmacis*	brown						1.137		
Nymphalidae	*Hypolimnas salmacis*	brown						1.057		
Nymphalidae	*Hypolimnas salmacis*	brown						1.074		
Nymphalidae	*Heliconius cydno*	black		0.599	2.953	0.862	0.059	1.204		
Nymphalidae	*Heliconius cydno*	black		0.409	2.679	0.716	0.081	1.142		
Nymphalidae	*Heliconius cydno*	black		0.608	3.045	0.824	0.066	1.185		
Nymphalidae	*Heliconius cydno*	black		0.514	2.854	0.793	0.081	1.199		
Nymphalidae	*Heliconius cydno*	black		0.392	2.709	0.671	0.106	1.07		
Nymphalidae	*Heliconius cydno*	black		0.52	2.772	0.851	0.074	1.116		
Nymphalidae	*Heliconius cydno*	black		0.449	2.695	0.776	0.082	1.251		
Nymphalidae	*Heliconius cydno*	black		0.611	2.993	0.857	0.078	1.158		
Nymphalidae	*Heliconius cydno*	black		0.593	2.918	0.875	0.12	1.266		
Nymphalidae	*Heliconius cydno*	black		0.499	2.812	0.793	0.074	1.075		
Nymphalidae	*Heliconius cydno*	black		0.358	2.398	0.783	0.083	1.142		
Nymphalidae	*Heliconius cydno*	black		0.343	2.419	0.737	0.109	1.112		
Nymphalidae	*Heliconius cydno*	black		0.42	2.599	0.782	0.116	1.189		
Nymphalidae	*Heliconius cydno*	black		0.489	2.815	0.775	0.12	1.055		
Nymphalidae	*Heliconius cydno*	black		0.393	2.501	0.79	0.105	1.071		
Nymphalidae	*Heliconius cydno*	black		0.561	2.798	0.901	0.12	1.098		
Nymphalidae	*Heliconius cydno*	black		0.571	2.911	0.847	0.126	1.113		
Nymphalidae	*Heliconius cydno*	black		0.403	2.672	0.709	0.116	1.19		
Nymphalidae	*Heliconius cydno*	black		0.463	2.676	0.812	0.12	1.168		
Nymphalidae	*Heliconius cydno*	black		0.455	2.735	0.765	0.119	1.158		
Nymphalidae	*Heliconius cydno*	white		0.075	0.992	0.965	0.399	1.053		
Nymphalidae	*Heliconius cydno*	white		0.084	1.05	0.958	0.146	0.966		
Nymphalidae	*Heliconius cydno*	white		0.123	1.286	0.932	0.244	0.981		
Nymphalidae	*Heliconius cydno*	white		0.061	0.917	0.916	0.494	0.994		
Nymphalidae	*Heliconius cydno*	white		0.129	1.328	0.918	0.7	0.754		
Nymphalidae	*Heliconius cydno*	white		0.121	1.349	0.836	0.27	0.828		
Nymphalidae	*Heliconius cydno*	white		0.124	1.319	0.894	0.239	0.868		
Nymphalidae	*Heliconius cydno*	white		0.075	1.018	0.904	0.237	0.872		
Nymphalidae	*Heliconius cydno*	white		0.108	1.258	0.855	0.44	0.887		
Nymphalidae	*Heliconius cydno*	white		0.1	1.162	0.932	0.365	0.922		
Nymphalidae	*Heliconius cydno*	white		0.091	1.126	0.904		0.9		
Nymphalidae	*Heliconius cydno*	white		0.097	1.134	0.947		1.025		
Nymphalidae	*Heliconius cydno*	white						0.833		
Nymphalidae	*Heliconius cydno*	white						0.888		
Nymphalidae	*Heliconius cydno*	white						0.813		
Nymphalidae	*Heliconius cydno*	white						0.864		
Nymphalidae	*Heliconius cydno*	white						0.88		
Nymphalidae	*Heliconius cydno*	white						0.876		
Nymphalidae	*Heliconius cydno*	white						0.986		
Nymphalidae	*Heliconius cydno*	white						0.869		
Nymphalidae	*Heliconius erato*	yellow		0.495	2.535	0.969	0.105	1.843		
Nymphalidae	*Heliconius erato*	yellow		0.381	2.246	0.948	0.181	1.812		

Nymphalidae	*Heliconius erato*	yellow		0.38	2.322	0.886	0.108	1.793		
Nymphalidae	*Heliconius erato*	yellow		0.361	2.175	0.957	0.126	1.765		
Nymphalidae	*Heliconius erato*	yellow		0.475	2.486	0.966	0.142	1.751		
Nymphalidae	*Heliconius erato*	yellow		0.271	1.926	0.918	0.093	1.693		
Nymphalidae	*Heliconius erato*	yellow		0.437	2.434	0.927	0.105	1.629		
Nymphalidae	*Heliconius erato*	yellow		0.446	2.404	0.969	1.42E-01	1.62		
Nymphalidae	*Heliconius erato*	yellow		0.327	2.115	0.919	1.64E-01	1.611		
Nymphalidae	*Heliconius erato*	yellow		0.349	2.208	0.9	0.118	1.599		
Nymphalidae	*Heliconius erato*	yellow		0.492	2.564	0.94	0.12	1.712		
Nymphalidae	*Heliconius erato*	yellow		0.313	2.067	0.92	7.50E-02	1.765		
Nymphalidae	*Heliconius erato*	yellow		0.353	2.144	0.965	1.38E-01	1.689		
Nymphalidae	*Heliconius erato*	yellow		0.45	2.459	0.935	1.16E-01	1.71		
Nymphalidae	*Heliconius erato*	yellow		0.383	2.302	0.908	0.082	1.84		
Nymphalidae	*Heliconius erato*	yellow		0.229	1.892	0.804	0.097	1.787		
Nymphalidae	*Heliconius erato*	yellow		0.285	1.969	0.925	0.135	1.785		
Nymphalidae	*Heliconius erato*	yellow		0.261	1.917	0.892	0.116	1.611		
Nymphalidae	*Heliconius erato*	yellow		0.255	1.866	0.919	0.091	1.699		
Nymphalidae	*Heliconius erato*	yellow		0.289	2.026	0.886		1.714		
Nymphalidae	*Heliconius erato*	black		0.185	1.679	0.826	0.086	0.759		
Nymphalidae	*Heliconius erato*	black		0.166	1.741	0.689	0.091	0.707		
Nymphalidae	*Heliconius erato*	black		0.157	1.703	0.681	0.096	0.685		
Nymphalidae	*Heliconius erato*	black		0.204	1.795	0.795	0.143	0.696		
Nymphalidae	*Heliconius erato*	black		0.163	1.992	0.516	0.118	0.815		
Nymphalidae	*Heliconius erato*	black		0.202	1.847	0.742	0.103	0.782		
Nymphalidae	*Heliconius erato*	black		0.186	1.858	0.678	0.089	0.77		
Nymphalidae	*Heliconius erato*	black		0.236	1.94	0.788	0.103	0.852		
Nymphalidae	*Heliconius erato*	black		0.17	1.918	0.581	0.086	0.811		
Nymphalidae	*Heliconius erato*	black		0.168	1.85	0.616	0.094	0.782		
Nymphalidae	*Heliconius erato*	black		0.185	1.751	0.757	0.121	0.844		
Nymphalidae	*Heliconius erato*	black		0.214	1.867	0.771	0.094	0.93		
Nymphalidae	*Heliconius erato*	black		0.162	1.838	0.604	0.108	0.919		
Nymphalidae	*Heliconius erato*	black		0.17	1.812	0.651	0.106	0.889		
Nymphalidae	*Heliconius erato*	black		0.171	1.745	0.706	0.108	0.948		
Nymphalidae	*Heliconius erato*	black		0.183	1.763	0.739	0.121	0.852		
Nymphalidae	*Heliconius erato*	black		0.188	1.82	0.712	0.101	0.808		
Nymphalidae	*Heliconius erato*	black		0.182	1.921	0.619	0.086	0.822		
Nymphalidae	*Heliconius erato*	black		0.195	1.951	0.645	0.111	0.789		
Nymphalidae	*Heliconius erato*	black		0.201	1.831	0.752	0.116	0.815		
Nymphalidae	*Heliconius erato*	red		0.466	2.577	0.882	0.228	0.894		
Nymphalidae	*Heliconius erato*	red		0.32	2.164	0.858	0.108	0.916		
Nymphalidae	*Heliconius erato*	red		0.346	2.405	0.752	0.234	0.929		
Nymphalidae	*Heliconius erato*	red		0.221	1.726	0.934	0.116	0.915		
Nymphalidae	*Heliconius erato*	red		0.285	1.99	0.904	0.166	0.726		
Nymphalidae	*Heliconius erato*	red		0.337	2.212	0.866	0.204	0.731		
Nymphalidae	*Heliconius erato*	red		0.286	2.011	0.89	0.095	0.942		
Nymphalidae	*Heliconius erato*	red		0.242	1.795	0.942	0.122	0.777		
Nymphalidae	*Heliconius erato*	red		0.273	1.982	0.874	0.202	0.944		
Nymphalidae	*Heliconius erato*	red		0.283	2.024	0.869	0.212	1.003		
Nymphalidae	*Heliconius erato*	red		0.379	2.438	0.802	0.144	0.967		
Nymphalidae	*Heliconius erato*	red		0.351	2.227	0.889	0.278	0.989		
Nymphalidae	*Heliconius erato*	red		0.343	2.168	0.916	0.23	0.953		
Nymphalidae	*Heliconius erato*	red		0.303	2.082	0.877	0.192	0.953		
Nymphalidae	*Heliconius erato*	red		0.328	2.284	0.79	0.182	0.944		
Nymphalidae	*Heliconius erato*	red		0.407	2.455	0.85	0.1	0.981		
Nymphalidae	*Heliconius erato*	red		0.273	1.968	0.885	0.132	0.686		
Nymphalidae	*Heliconius erato*	red		0.326	2.208	0.841	0.138	0.811		
Nymphalidae	*Heliconius erato*	red		0.453	2.578	0.855	0.12	0.929		
Nymphalidae	*Heliconius erato*	red		0.223	1.718	0.951	0.166	0.783		
Nymphalidae	*Morpho peleides*	brown		0.991	4.194	0.708	0.199	2.197		
Nymphalidae	*Morpho peleides*	brown		1.285	4.604	0.761	0.2	2.139		
Nymphalidae	*Morpho peleides*	brown		0.819	3.928	0.667	0.207	2.136		
Nymphalidae	*Morpho peleides*	brown		0.899	4.108	0.669	0.262	2.157		
Nymphalidae	*Morpho peleides*	brown		1.028	4.543	0.626	0.196	2.042		
Nymphalidae	*Morpho peleides*	brown		0.971	4.078	0.734	0.248	2.134		

Nymphalidae	*Morpho peleides*	brown		0.86	3.694	0.791	0.225	2.089		
Nymphalidae	*Morpho peleides*	brown		0.953	3.958	0.765	0.232	1.974		
Nymphalidae	*Morpho peleides*	brown		0.804	3.807	0.697	0.208	1.77		
Nymphalidae	*Morpho peleides*	brown		0.987	4.22	0.697	0.246	2.032		
Nymphalidae	*Morpho peleides*	brown		0.585	3.398	0.637	0.243	2.009		
Nymphalidae	*Morpho peleides*	brown		0.771	3.681	0.715	0.225	1.689		
Nymphalidae	*Morpho peleides*	brown		0.764	3.877	0.639	0.27	1.675		
Nymphalidae	*Morpho peleides*	brown		0.706	3.509	0.72	0.27	1.637		
Nymphalidae	*Morpho peleides*	brown		0.936	4.175	0.675	0.165	1.711		
Nymphalidae	*Morpho peleides*	brown		0.719	3.688	0.664	0.202	1.997		
Nymphalidae	*Morpho peleides*	brown		0.606	3.349	0.679	0.224	2.204		
Nymphalidae	*Morpho peleides*	brown		0.87	3.747	0.779	0.222	2.147		
Nymphalidae	*Morpho peleides*	brown		0.693	3.741	0.622	0.224	2.226		
Nymphalidae	*Morpho peleides*	brown		0.74	3.664	0.693	0.204	2.134		
Nymphalidae	*Morpho peleides*	black		0.264	1.99	0.836	0.244	1.422		
Nymphalidae	*Morpho peleides*	black		0.34	2.483	0.694	0.216	1.399		
Nymphalidae	*Morpho peleides*	black		0.336	2.491	0.68	0.222	1.433		
Nymphalidae	*Morpho peleides*	black		0.317	2.545	0.616	0.188	1.398		
Nymphalidae	*Morpho peleides*	black		0.266	2.179	0.704	0.194	1.41		
Nymphalidae	*Morpho peleides*	black		0.299	2.48	0.611	0.2	1.446		
Nymphalidae	*Morpho peleides*	black		0.362	2.39	0.798	0.172	1.375		
Nymphalidae	*Morpho peleides*	black		0.267	2.098	0.763	0.216	1.515		
Nymphalidae	*Morpho peleides*	black		0.388	2.555	0.747	0.222	1.435		
Nymphalidae	*Morpho peleides*	black		0.38	2.598	0.707	0.194	1.444		
Nymphalidae	*Morpho peleides*	black		0.386	2.361	0.869	0.173	1.471		
Nymphalidae	*Morpho peleides*	black		0.339	2.446	0.713	0.179	1.48		
Nymphalidae	*Morpho peleides*	black		0.411	2.688	0.715		1.48		
Nymphalidae	*Morpho peleides*	black		0.361	2.441	0.762		1.386		
Nymphalidae	*Morpho peleides*	black		0.304	2.338	0.698		1.411		
Nymphalidae	*Morpho peleides*	black		0.297	2.29	0.711		1.432		
Nymphalidae	*Morpho peleides*	black		0.47	2.842	0.731		1.41		
Nymphalidae	*Morpho peleides*	black		0.386	2.497	0.778		1.433		
Nymphalidae	*Morpho peleides*	black		0.405	2.666	0.716		1.398		
Nymphalidae	*Morpho peleides*	black		0.537	2.969	0.766		1.398		
Nymphalidae	*Danaus genutia*	yellow		0.769	3.89	0.639	0.254	1.642		
Nymphalidae	*Danaus genutia*	yellow		0.847	3.776	0.747	0.247	1.518		
Nymphalidae	*Danaus genutia*	yellow		0.638	3.882	0.532	0.255	1.557		
Nymphalidae	*Danaus genutia*	yellow		0.515	3.772	0.455	0.247	1.572		
Nymphalidae	*Danaus genutia*	yellow		0.814	3.983	0.645	0.274	1.635		
Nymphalidae	*Danaus genutia*	yellow		0.713	3.869	0.599	0.219	1.58		
Nymphalidae	*Danaus genutia*	yellow		0.963	4.114	0.715	0.231	1.595		
Nymphalidae	*Danaus genutia*	yellow		0.757	3.967	0.604	0.216	1.642		
Nymphalidae	*Danaus genutia*	yellow		0.64	3.72	0.581	0.239	1.618		
Nymphalidae	*Danaus genutia*	yellow		0.562	3.543	0.563	0.301	1.642		
Nymphalidae	*Danaus genutia*	yellow		0.907	3.858	0.766	0.239	1.557		
Nymphalidae	*Danaus genutia*	yellow		0.731	3.819	0.63	0.239	1.48		
Nymphalidae	*Danaus genutia*	yellow		0.838	3.887	0.696	0.278	1.58		
Nymphalidae	*Danaus genutia*	yellow		0.603	3.637	0.573	0.221	1.704		
Nymphalidae	*Danaus genutia*	yellow		0.7	3.603	0.678	0.247	1.657		
Nymphalidae	*Danaus genutia*	yellow		0.565	3.733	0.51	0.185	1.634		
Nymphalidae	*Danaus genutia*	yellow		0.654	3.456	0.688	0.257	1.534		
Nymphalidae	*Danaus genutia*	yellow		0.627	3.725	0.568	0.264	1.603		
Nymphalidae	*Danaus genutia*	yellow		0.662	3.757	0.589	0.216	1.603		
Nymphalidae	*Danaus genutia*	yellow		0.706	3.933	0.574	0.262	1.603		
Nymphalidae	*Melanitis leda*	brown		0.806	4.946	0.414	0.183	2.004		
Nymphalidae	*Melanitis leda*	brown		0.959	5.246	0.438	0.228	2.032		
Nymphalidae	*Melanitis leda*	brown		0.813	4.678	0.467	0.216	1.976		
Nymphalidae	*Melanitis leda*	brown		0.586	4.915	0.305	0.207	2.118		
Nymphalidae	*Melanitis leda*	brown		0.786	4.788	0.431	0.338	2.164		
Nymphalidae	*Melanitis leda*	brown		0.899	5.319	0.399	0.278	2.104		
Nymphalidae	*Melanitis leda*	brown		0.993	5.705	0.383	0.238	2.063		
Nymphalidae	*Melanitis leda*	brown		0.939	5.478	0.393	0.288	2.026		
Nymphalidae	*Melanitis leda*	brown		1.006	5.2	0.468	0.266	2.013		
Nymphalidae	*Melanitis leda*	brown		0.873	5.137	0.416	0.252	2.018		

Nymphalidae	*Melanitis leda*	brown		0.999	5.583	0.403	0.306	2.038		
Nymphalidae	*Melanitis leda*	brown		1.179	5.619	0.469	0.225	2.168		
Nymphalidae	*Melanitis leda*	brown		0.86	5.765	0.325	0.224	2.266		
Nymphalidae	*Melanitis leda*	brown		0.926	5.856	0.339	0.255	2.131		
Nymphalidae	*Melanitis leda*	brown		0.853	5.43	0.363	0.261	2.056		
Nymphalidae	*Melanitis leda*	brown		0.84	5.378	0.365	0.237	1.995		
Nymphalidae	*Melanitis leda*	brown		0.733	5.387	0.317	0.265	2.01		
Nymphalidae	*Melanitis leda*	brown		1.019	4.984	0.516	0.265	2.032		
Nymphalidae	*Melanitis leda*	brown		0.786	4.635	0.46	0.324	2.091		
Nymphalidae	*Melanitis leda*	brown		0.733	5.188	0.342	0.32	2.104		
Nymphalidae	*Melanitis leda*	brown		0.746	4.618	0.44	0.434	1.937		
Nymphalidae	*Melanitis leda*	brown		0.733	4.374	0.481	0.3	2.177		
Nymphalidae	*Melanitis leda*	orange		1.546	5.111	0.744	0.231	1.847		
Nymphalidae	*Melanitis leda*	orange		1.153	5.376	0.501	0.26	1.828		
Nymphalidae	*Melanitis leda*	orange		1.419	5.257	0.645	0.328	1.741		
Nymphalidae	*Melanitis leda*	orange		0.946	4.848	0.506	0.317	1.761		
Nymphalidae	*Melanitis leda*	orange		1.046	5.107	0.504	0.272	1.762		
Nymphalidae	*Melanitis leda*	orange		1.059	5.014	0.53	0.174	1.837		
Nymphalidae	*Melanitis leda*	orange		1.113	5.011	0.557	0.26	1.683		
Nymphalidae	*Melanitis leda*	orange		1.306	5.092	0.633	0.232	1.744		
Nymphalidae	*Melanitis leda*	orange		1.199	5.251	0.547	0.242	1.683		
Nymphalidae	*Melanitis leda*	orange		1.326	5.672	0.518	0.242	1.943		
Nymphalidae	*Melanitis leda*	orange		1.159	5.434	0.493	0.272	1.831		
Nymphalidae	*Melanitis leda*	orange		1.086	4.915	0.565	0.261	1.974		
Nymphalidae	*Melanitis leda*	orange		1.173	5.012	0.587	0.28	1.876		
Nymphalidae	*Melanitis leda*	orange		1.146	5.269	0.519	0.241	1.888		
Nymphalidae	*Melanitis leda*	orange		1.259	4.833	0.678	0.253	1.799		
Nymphalidae	*Melanitis leda*	orange		1.286	5.424	0.549	0.241	1.82		
Nymphalidae	*Melanitis leda*	orange		1.153	5.22	0.532	0.212	1.831		
Nymphalidae	*Melanitis leda*	orange		0.979	4.766	0.542	0.272	1.886		
Nymphalidae	*Melanitis leda*	orange		1.453	5.221	0.67	0.289	1.706		
Nymphalidae	*Melanitis leda*	orange		1.053	4.92	0.547	0.215	1.791		
Nymphalidae	*Melanitis leda*	orange		1.279	4.981	0.648	0.231	1.84		
Nymphalidae	*Melanitis leda*	orange		1.433	5.653	0.563	0.261	1.741		
Nymphalidae	*Melanitis leda*	black		0.8	5.129	0.382	0.302	2.216		
Nymphalidae	*Melanitis leda*	black		0.773	4.821	0.418	0.317	2.218		
Nymphalidae	*Melanitis leda*	black		0.78	4.536	0.476	0.317	2.152		
Nymphalidae	*Melanitis leda*	black		0.773	4.822	0.418	0.332	2.089		
Nymphalidae	*Melanitis leda*	black		0.786	4.808	0.427	0.285	2.099		
Nymphalidae	*Melanitis leda*	black		0.973	4.906	0.508	0.32	2.151		
Nymphalidae	*Melanitis leda*	black		0.666	4.888	0.35	0.292	2.071		
Nymphalidae	*Melanitis leda*	black		0.733	4.836	0.394	0.332	2.155		
Nymphalidae	*Melanitis leda*	black		0.653	4.738	0.366	0.31	2.085		
Nymphalidae	*Melanitis leda*	black		0.573	4.753	0.319	0.311	2.06		
Nymphalidae	*Melanitis leda*	black		0.806	4.884	0.425	0.236	2.075		
Nymphalidae	*Melanitis leda*	black		0.54	4.553	0.327	0.358	1.974		
Nymphalidae	*Melanitis leda*	black		0.56	3.63	0.534	0.306	2.078		
Nymphalidae	*Melanitis leda*	black		0.626	4.54	0.382	0.256	2.049		
Nymphalidae	*Melanitis leda*	black		0.766	4.782	0.421	0.329	2.111		
Nymphalidae	*Melanitis leda*	black		0.726	4.969	0.37	0.3	2.018		
Nymphalidae	*Melanitis leda*	black		0.806	4.881	0.425	0.349	1.976		
Nymphalidae	*Melanitis leda*	black		0.906	4.991	0.457	0.316	2.011		
Nymphalidae	*Melanitis leda*	black		0.673	4.692	0.384	0.301	2.012		
Nymphalidae	*Melanitis leda*	black		0.8	4.81	0.434	0.356	1.995		
Nymphalidae	*Melanitis leda*	black		0.906	5.239	0.415	0.279	1.979		
Nymphalidae	*Melanitis leda*	black		0.54	4.631	0.316	0.365	2.034		
Nymphalidae	*Melanitis leda*	white		1.546	5.848	0.568	0.279	2.176		
Nymphalidae	*Melanitis leda*	white		1.832	5.981	0.644	0.231	2.282		
Nymphalidae	*Melanitis leda*	white		1.373	5.104	0.662	0.294	2.193		
Nymphalidae	*Melanitis leda*	white		1.712	5.842	0.63	0.242	2.081		
Nymphalidae	*Melanitis leda*	white		1.446	5.374	0.629	0.183	2.143		
Nymphalidae	*Melanitis leda*	white		1.499	5.833	0.554	0.279	2.32		
Nymphalidae	*Melanitis leda*	white		1.506	5.942	0.536	0.262	1.995		
Nymphalidae	*Melanitis leda*	white		1.626	6.012	0.565	0.291	2.15		

Nymphalidae	*Melanitis leda*	white		1.599	5.997	0.559	0.313	2.186		
Nymphalidae	*Melanitis leda*	white		1.353	5.534	0.555	0.261	2.199		
Nymphalidae	*Melanitis leda*	white		1.866	5.75	0.709	0.213	2.209		
Nymphalidae	*Melanitis leda*	white		1.226	5.564	0.498	0.283	2.261		
Nymphalidae	*Melanitis leda*	white		1.359	5.39	0.588	0.27	2.195		
Nymphalidae	*Melanitis leda*	white		1.393	5.321	0.618	0.241	2.197		
Nymphalidae	*Melanitis leda*	white		1.259	5.551	0.514	0.26	2.196		
Nymphalidae	*Melanitis leda*	white		1.459	5.498	0.607	0.231	2.239		
Nymphalidae	*Melanitis leda*	white		1.559	5.537	0.639	0.289	2.158		
Nymphalidae	*Melanitis leda*	white		1.712	5.668	0.67	0.27	2.18		
Nymphalidae	*Melanitis leda*	white		1.672	6.135	0.558	0.302	2.11		
Nymphalidae	*Melanitis leda*	white		1.926	6.105	0.649	0.269	2.258		
Nymphalidae	*Melanitis leda*	white		1.732	5.812	0.645	0.351	2.227		
Nymphalidae	*Melanitis leda*	white		1.632	5.887	0.592	0.253	2.212		
Nymphalidae	*Penthema adelma*	black		0.872	5.604	0.674	0.25	1.735		
Nymphalidae	*Penthema adelma*	black		2.003	5.631	0.794	0.258	1.758		
Nymphalidae	*Penthema adelma*	black		0.924	4.198	0.659	0.258	1.742		
Nymphalidae	*Penthema adelma*	black		1.85	5.555	0.753	0.348	1.811		
Nymphalidae	*Penthema adelma*	black		1.025	4.658	0.593	0.243	1.743		
Nymphalidae	*Penthema adelma*	black		1.392	5.022	0.694	0.227	1.727		
Nymphalidae	*Penthema adelma*	black		1.144	4.434	0.731	0.288	1.69		
Nymphalidae	*Penthema adelma*	black		0.978	4.584	0.585	0.305	1.591		
Nymphalidae	*Penthema adelma*	black		1.566	5.073	0.765	0.235	1.727		
Nymphalidae	*Penthema adelma*	black		1.453	4.918	0.755	0.25	1.66		
Nymphalidae	*Penthema adelma*	black		1.599	5.285	0.719	0.19	1.712		
Nymphalidae	*Penthema adelma*	black		0.905	4.431	0.579	0.273	1.743		
Nymphalidae	*Penthema adelma*	black		1.065	4.485	0.666	0.265	1.668		
Nymphalidae	*Penthema adelma*	black		1.301	4.826	0.702	0.258	1.697		
Nymphalidae	*Penthema adelma*	black		1.159	4.602	0.688	0.223	1.651		
Nymphalidae	*Penthema adelma*	black		1.393	4.832	0.75	0.334	1.834		
Nymphalidae	*Penthema adelma*	black		0.947	4.525	0.582	0.303	1.811		
Nymphalidae	*Penthema adelma*	black		0.922	4.044	0.709	0.311	1.819		
Nymphalidae	*Penthema adelma*	black		1.6	4.965	0.815	0.259	1.864		
Nymphalidae	*Penthema adelma*	black		0.902	4.471	0.567	0.326	1.841		
Saturniidae	*Bunaea alcinoe*	brown		1.106	3.954	0.889	0.237	1.324	0.63	2.54
Saturniidae	*Bunaea alcinoe*	brown		1.217	4.087	0.916	0.24	1.387	0.779	2.335
Saturniidae	*Bunaea alcinoe*	brown		0.894	3.478	0.929	0.358	1.335	0.5	1.879
Saturniidae	*Bunaea alcinoe*	brown		0.957	3.604	0.926	0.291	1.423	0.883	1.891
Saturniidae	*Bunaea alcinoe*	brown		0.605	2.999	0.845	0.236	1.491	0.791	2.068
Saturniidae	*Bunaea alcinoe*	brown		0.861	3.615	0.828	0.303	1.539	0.649	1.962
Saturniidae	*Bunaea alcinoe*	brown		1.018	3.73	0.92	0.231	1.614	0.822	2.185
Saturniidae	*Bunaea alcinoe*	brown		0.669	3.119	0.865	0.32	1.684	0.557	1.742
Saturniidae	*Bunaea alcinoe*	brown		0.637	3.282	0.743	0.37	1.632	0.696	1.771
Saturniidae	*Bunaea alcinoe*	brown		0.55	2.818	0.869	0.279	1.5	0.831	2.091
Saturniidae	*Bunaea alcinoe*	brown		0.473	2.565	0.902	0.268	1.559		
Saturniidae	*Bunaea alcinoe*	brown		0.712	3.124	0.917	0.325	1.577		
Saturniidae	*Bunaea alcinoe*	brown		0.876	3.484	0.906	0.224	1.606		
Saturniidae	*Bunaea alcinoe*	brown		0.716	3.239	0.858	0.237	1.694		
Saturniidae	*Bunaea alcinoe*	brown		0.545	3.132	0.699	0.251	1.53		
Saturniidae	*Bunaea alcinoe*	brown		0.863	3.462	0.904	0.299	1.455		
Saturniidae	*Bunaea alcinoe*	brown		0.536	2.922	0.789	0.328	1.425		
Saturniidae	*Bunaea alcinoe*	brown		0.557	2.903	0.831	0.268	1.364		
Saturniidae	*Bunaea alcinoe*	brown		0.512	3.163	0.644	0.279	1.391		
Saturniidae	*Bunaea alcinoe*	brown		0.568	3.138	0.725	0.289	1.401		
Saturniidae	*Bunaea alcinoe*	brown		0.638	3.066	0.853	0.322	1.682		
Lycaenidae	*Cyanoprys remus*	blue		0.18	1.687	0.797	0.107	1.851	1.434	2.11
Lycaenidae	*Cyanoprys remus*	blue		0.124	1.471	0.72	0.095	2.028	1.426	2.139
Lycaenidae	*Cyanoprys remus*	blue		0.265	1.93	0.894	0.063	1.97	1.445	2.168
Lycaenidae	*Cyanoprys remus*	blue		0.111	1.339	0.779	0.156	2.067	1.437	2.15
Lycaenidae	*Cyanoprys remus*	blue		0.21	1.73	0.883	0.088	2.088	1.468	2.148
Lycaenidae	*Cyanoprys remus*	blue		0.151	1.501	0.84	0.079	1.884	1.413	2.094
Lycaenidae	*Cyanoprys remus*	blue		0.129	1.413	0.812	0.1	1.935	1.397	2.107
Lycaenidae	*Cyanoprys remus*	blue		0.138	1.529	0.743	0.063	1.893	1.39	2.135
Lycaenidae	*Cyanoprys remus*	blue		0.116	1.431	0.712	0.087	1.898	1.321	2.171

Lycaenidae	*Cyanoprys remus*	blue		0.15	1.586	0.749	0.1	1.928	1.33	2.215
Lycaenidae	*Cyanoprys remus*	blue		0.215	1.813	0.824	0.083	1.777	1.315	2.177
Lycaenidae	*Cyanoprys remus*	blue		1.19E-01	1.367	0.799	0.09	2.093	1.383	1.782
Lycaenidae	*Cyanoprys remus*	blue		1.35E-01	1.409	0.857	0.114	1.983	1.638	
Lycaenidae	*Cyanoprys remus*	blue		0.29	2.007	0.905	0.11	1.973	1.611	
Lycaenidae	*Cyanoprys remus*	blue		1.47E-01	1.497	0.822	0.131	1.691	1.532	
Lycaenidae	*Cyanoprys remus*	blue		1.90E-01	1.692	0.832	0.117	1.979	1.289	
Lycaenidae	*Cyanoprys remus*	blue		1.37E-01	1.456	0.812	0.119	2.067	1.453	
Lycaenidae	*Cyanoprys remus*	blue		2.27E-01	1.775	0.906	0.119	1.833	1.413	
Lycaenidae	*Cyanoprys remus*	blue		2.10E-01	1.749	0.864	0.133	1.925	1.381	
Lycaenidae	*Cyanoprys remus*	blue		0.285	2.059	0.844	0.099	1.863	1.569	
Lycaenidae	*Callophrys rubi*	brown	green	1.317	4.905	0.688	0.121	1.993	1.967	3.466
Lycaenidae	*Callophrys rubi*	brown	green	0.929	4.309	0.629	0.137	1.997	1.714	3.472
Lycaenidae	*Callophrys rubi*	brown	green	1.388	5.118	0.666	0.169	2.004	2.096	3.52
Lycaenidae	*Callophrys rubi*	brown	green	1.125	4.526	0.69	0.166	1.981	1.647	3.544
Lycaenidae	*Callophrys rubi*	brown	green	1.084	4.596	0.645	0.166	2.007	2.184	3.501
Lycaenidae	*Callophrys rubi*	brown	green	1.141	4.705	0.648	0.141	2.055	2.381	3.572
Lycaenidae	*Callophrys rubi*	brown	green	1.991	5.743	0.759	0.176	2.082	1.938	3.531
Lycaenidae	*Callophrys rubi*	brown	green	1.093	4.655	0.634	0.143	2.067	2.476	3.549
Lycaenidae	*Callophrys rubi*	brown	green	0.975	4.431	0.624	0.153	2.093	2.738	2.126
Lycaenidae	*Callophrys rubi*	brown	green	1.273	4.811	0.691	0.175	2.056	2.587	2.277
Lycaenidae	*Callophrys rubi*	brown	green	0.932	4.236	0.653	0.143	2.095	2.664	2.127
Lycaenidae	*Callophrys rubi*	brown	green	1.31E+00	5.09	0.636	0.175	2.157	2.714	3.528
Lycaenidae	*Callophrys rubi*	brown	green	1.01E+00	4.556	0.61	0.142	2.025	2.943	3.511
Lycaenidae	*Callophrys rubi*	brown	green	0.928	4.142	0.679	0.143	2.042	2.583	3.539
Lycaenidae	*Callophrys rubi*	brown	green	1.28E+00	4.982	0.65	0.154	1.975	2.75	3.53
Lycaenidae	*Callophrys rubi*	brown	green	1.33E+00	4.756	0.74	0.145	1.972		
Lycaenidae	*Polyommatus daphnis*	brown	blue	1.542	4.718	0.871	0.12	1.962	0.692	1.575
Lycaenidae	*Polyommatus daphnis*	brown	blue	1.482	4.589	0.884	0.112	1.837	0.674	1.593
Lycaenidae	*Polyommatus daphnis*	brown	blue	1.135	4.06	0.865	0.106	1.917	0.681	1.58
Lycaenidae	*Polyommatus daphnis*	brown	blue	1.06	4.031	0.82	0.107	1.915	0.654	1.591
Lycaenidae	*Polyommatus daphnis*	brown	blue	1.068	4.331	0.716	0.093	1.923	0.66	1.622
Lycaenidae	*Polyommatus daphnis*	brown	blue	1.097	4.092	0.824	0.085	1.944	0.668	1.565
Lycaenidae	*Polyommatus daphnis*	brown	blue	1.249	4.307	0.846	0.106	2.007	0.682	1.645
Lycaenidae	*Polyommatus daphnis*	brown	blue	1.518	4.923	0.787	0.128	1.932	0.648	1.636
Lycaenidae	*Polyommatus daphnis*	brown	blue	1.031	3.998	0.811	0.138	2.03	0.649	1.64
Lycaenidae	*Polyommatus daphnis*	brown	blue	1.596	4.698	0.909	0.106	1.983	0.69	1.658
Uraniidae	*Chrysiridia rhipheus*	yellow	blue	7.157	10.918	0.755	0.323	4.299	1.408	2.443
Uraniidae	*Chrysiridia rhipheus*	yellow	blue	8.168	11.682	0.752	0.356	4.407	1.354	2.299
Uraniidae	*Chrysiridia rhipheus*	yellow	blue	9.447	12.631	0.744	0.316	4.228	1.384	2.292
Uraniidae	*Chrysiridia rhipheus*	yellow	blue	8.366	11.382	0.812	0.285	4.345	1.391	2.329
Uraniidae	*Chrysiridia rhipheus*	yellow	blue	8.945	13.296	0.636	0.213	4.475	1.349	2.416
Uraniidae	*Chrysiridia rhipheus*	yellow	blue	9.623	12.614	0.76	0.274	4.341	1.332	2.487
Lycaenidae	*Albulina metallica*	brown	blue	2.41	6.226	0.781	0.203	2.989	1.025	1.576
Lycaenidae	*Albulina metallica*	brown	blue	2.303	6.189	0.756	0.204	2.94	0.964	1.644
Lycaenidae	*Albulina metallica*	brown	blue	1.973	5.671	0.771	0.287	3.027	1.091	1.56
Lycaenidae	*Albulina metallica*	brown	blue	2.94	6.739	0.814	0.259	3.003	0.927	1.627
Lycaenidae	*Albulina metallica*	brown	blue	2.179	5.782	0.819	0.249	3.095	0.881	1.436
Lycaenidae	*Albulina metallica*	brown	blue	2.929	6.859	0.782	0.199	2.847	0.976	1.436
Lycaenidae	*Albulina metallica*	brown	blue	2.032	5.887	0.737	0.206	2.854	1.078	1.422
Lycaenidae	*Albulina metallica*	brown	blue	3.055	6.929	0.8	0.236	2.808	0.887	1.397
Lycaenidae	*Albulina metallica*	brown	blue	2.56	6.226	0.83	0.25	2.882	1.078	1.627
Lycaenidae	*Albulina metallica*	brown	blue	1.822	5.769	0.688	0.266	3.076	1.105	1.452
Lycaenidae	*Albulina metallica*	brown	blue	2.377	6.078	0.809	0.176	3.086	1.009	
Lycaenidae	*Albulina metallica*	brown	blue	1.51E+00	5.237	0.694	0.157	2.717	1.087	
Lycaenidae	*Albulina metallica*	brown	blue	3.22E+00	6.907	0.847	0.199	2.929	1.033	
Zygaenidae	*Eterusia taiwana*	brown	green	4.784	9.026	0.738	0.107	3.155	2.051	1.722
Zygaenidae	*Eterusia taiwana*	brown	green	3.877	8.136	0.736	0.143	3.02	1.418	1.772
Zygaenidae	*Eterusia taiwana*	brown	green	5.718	9.129	0.862	0.273	3.031	1.524	1.752

Table 4: Raw data table of all the measurements across all our datasets for wild type butterfly scales

Family	Specie	Scale color pre manipulation	Scale color post manipulation	Gene knocked out	Manipulation	Window area (µm^2)	Window perimeter (µm)	Window circularity	Crossrib thickness (µm)	Ridge to ridge distance (µm)
Nymphalidae	Bicyclus anynana	black	brown	yellow	CRISPR	0.382	2.879	0.579	0.165	1.425
Nymphalidae	Bicyclus anynana	black	brown	yellow	CRISPR	0.376	2.979	0.532	0.149	1.383
Nymphalidae	Bicyclus anynana	black	brown	yellow	CRISPR	0.345	3.034	0.472	0.151	1.37
Nymphalidae	Bicyclus anynana	black	brown	yellow	CRISPR	0.473	3.227	0.57	0.157	1.303
Nymphalidae	Bicyclus anynana	black	brown	yellow	CRISPR	0.467	3.427	0.499	0.183	1.412
Nymphalidae	Bicyclus anynana	black	brown	yellow	CRISPR	0.473	3.377	0.521	0.173	1.397
Nymphalidae	Bicyclus anynana	black	brown	yellow	CRISPR	0.367	3.093	0.482	0.154	1.404
Nymphalidae	Bicyclus anynana	black	brown	yellow	CRISPR	0.424	3.33	0.481	0.14	1.597
Nymphalidae	Bicyclus anynana	black	brown	yellow	CRISPR	0.406	3.387	0.445	0.153	1.439
Nymphalidae	Bicyclus anynana	black	brown	yellow	CRISPR	0.354	3.065	0.474	0.158	1.445
Nymphalidae	Bicyclus anynana	black	brown	yellow	CRISPR	0.403	3.4	0.438	0.152	1.431
Nymphalidae	Bicyclus anynana	black	brown	yellow	CRISPR	0.394	3.076	0.523	0.099	1.397
Nymphalidae	Bicyclus anynana	black	brown	yellow	CRISPR	0.518	3.313	0.593	0.166	1.424
Nymphalidae	Bicyclus anynana	black	brown	yellow	CRISPR	0.354	3.295	0.41	0.172	1.459
Nymphalidae	Bicyclus anynana	black	brown	yellow	CRISPR	0.421	3.278	0.492	0.131	1.431
Nymphalidae	Bicyclus anynana	black	brown	yellow	CRISPR	0.551	3.888	0.458	0.172	1.357
Nymphalidae	Bicyclus anynana	black	brown	yellow	CRISPR	0.397	3.222	0.48	0.117	1.398
Nymphalidae	Bicyclus anynana	black	brown	yellow	CRISPR	0.445	3.066	0.596	0.152	1.314
Nymphalidae	Bicyclus anynana	black	brown	yellow	CRISPR	0.454	3.237	0.545	0.161	1.363
Nymphalidae	Bicyclus anynana	brown	yellow	yellow	CRISPR	1.479	4.738	0.828	0.125	1.661
Nymphalidae	Bicyclus anynana	brown	yellow	yellow	CRISPR	0.685	4.079	0.517	0.198	1.635
Nymphalidae	Bicyclus anynana	brown	yellow	yellow	CRISPR	1.133	4.742	0.633	0.165	1.681
Nymphalidae	Bicyclus anynana	brown	yellow	yellow	CRISPR	0.988	4.537	0.603	0.166	1.735
Nymphalidae	Bicyclus anynana	brown	yellow	yellow	CRISPR	0.833	4.336	0.557	0.175	1.67
Nymphalidae	Bicyclus anynana	brown	yellow	yellow	CRISPR	0.906	4.298	0.616	0.188	1.661
Nymphalidae	Bicyclus anynana	brown	yellow	yellow	CRISPR	0.924	5.023	0.46	0.132	1.615
Nymphalidae	Bicyclus anynana	brown	yellow	yellow	CRISPR	1.045	4.817	0.566	0.154	1.697
Nymphalidae	Bicyclus anynana	brown	yellow	yellow	CRISPR	0.664	4.333	0.444	0.209	1.661
Nymphalidae	Bicyclus anynana	brown	yellow	yellow	CRISPR	0.579	3.46	0.607	0.22	1.67
Nymphalidae	Bicyclus anynana	brown	yellow	yellow	CRISPR	0.945	3.948	0.762	0.128	1.661
Nymphalidae	Bicyclus anynana	brown	yellow	yellow	CRISPR	0.803	4.298	0.546	0.127	1.652
Nymphalidae	Bicyclus anynana	brown	yellow	yellow	CRISPR	0.657	4.461	0.415	0.103	1.66
Nymphalidae	Bicyclus anynana	brown	yellow	yellow	CRISPR	0.782	4.48	0.489	0.138	1.675
Nymphalidae	Bicyclus anynana	brown	yellow	yellow	CRISPR	0.885	4.457	0.56	0.165	1.658
Nymphalidae	Bicyclus anynana	brown	yellow	yellow	CRISPR	1.26	4.539	0.769	0.193	1.652
Nymphalidae	Bicyclus anynana	brown	yellow	yellow	CRISPR	0.727	4.204	0.517	0.193	1.725
Nymphalidae	Bicyclus anynana	brown	yellow	yellow	CRISPR	0.8	4.252	0.556	0.183	1.744
Nymphalidae	Bicyclus anynana	brown	yellow	yellow	CRISPR	0.712	4.011	0.556	0.248	1.679
Nymphalidae	Bicyclus anynana	brown	yellow	yellow	CRISPR	0.757	4.092	0.568	0.122	1.624
Nymphalidae	Bicyclus anynana	gold	yellow	yellow	CRISPR	0.476	3.422	0.51	0.227	1.555
Nymphalidae	Bicyclus anynana	gold	yellow	yellow	CRISPR	0.5	3.346	0.561	0.151	1.493
Nymphalidae	Bicyclus anynana	gold	yellow	yellow	CRISPR	0.597	3.714	0.544	0.172	1.5
Nymphalidae	Bicyclus anynana	gold	yellow	yellow	CRISPR	0.421	3.258	0.498	0.179	1.5
Nymphalidae	Bicyclus anynana	gold	yellow	yellow	CRISPR	0.591	3.715	0.538	0.2	1.5
Nymphalidae	Bicyclus anynana	gold	yellow	yellow	CRISPR	0.685	4.188	0.491	0.193	1.454
Nymphalidae	Bicyclus anynana	gold	yellow	yellow	CRISPR	0.473	3.59	0.461	0.158	1.528
Nymphalidae	Bicyclus anynana	gold	yellow	yellow	CRISPR	0.691	4.057	0.527	0.166	1.652
Nymphalidae	Bicyclus anynana	gold	yellow	yellow	CRISPR	0.527	3.381	0.58	0.202	1.673
Nymphalidae	Bicyclus anynana	gold	yellow	yellow	CRISPR	0.503	3.935	0.408	0.187	1.631
Nymphalidae	Bicyclus anynana	gold	yellow	yellow	CRISPR	0.673	3.681	0.624	0.193	1.701
Nymphalidae	Bicyclus anynana	gold	yellow	yellow	CRISPR	0.43	3.062	0.576	0.186	1.713
Nymphalidae	Bicyclus anynana	gold	yellow	yellow	CRISPR	0.648	3.995	0.511	0.193	1.727
Nymphalidae	Bicyclus anynana	gold	yellow	yellow	CRISPR	0.521	3.627	0.498	0.207	1.714
Nymphalidae	Bicyclus anynana	gold	yellow	yellow	CRISPR	0.406	3.228	0.489	0.208	1.642
Nymphalidae	Bicyclus anynana	gold	yellow	yellow	CRISPR	0.542	3.621	0.52	0.227	1.638
Nymphalidae	Bicyclus anynana	gold	yellow	yellow	CRISPR	0.645	3.744	0.579	0.255	1.674
Nymphalidae	Bicyclus anynana	gold	yellow	yellow	CRISPR	0.545	3.678	0.507	0.201	1.576
Nymphalidae	Bicyclus anynana	gold	yellow	yellow	CRISPR	0.515	3.326	0.585	0.238	1.617
Nymphalidae	Bicyclus anynana	gold	yellow	yellow	CRISPR	0.548	3.829	0.47	0.22	1.521
Nymphalidae	Bicyclus anynana	beige	yellow	yellow	CRISPR	0.851	4.131	0.627	0.184	1.865
Nymphalidae	Bicyclus anynana	beige	yellow	yellow	CRISPR	0.788	4.074	0.596	0.248	1.863
Nymphalidae	Bicyclus anynana	beige	yellow	yellow	CRISPR	0.939	4.381	0.615	0.248	1.835
Nymphalidae	Bicyclus anynana	beige	yellow	yellow	CRISPR	0.854	4.478	0.535	0.23	1.807
Nymphalidae	Bicyclus anynana	beige	yellow	yellow	CRISPR	0.664	3.779	0.584	0.183	1.862
Nymphalidae	Bicyclus anynana	beige	yellow	yellow	CRISPR	0.857	3.995	0.675	0.22	1.798
Nymphalidae	Bicyclus anynana	beige	yellow	yellow	CRISPR	0.77	3.922	0.629	0.269	1.881
Nymphalidae	Bicyclus anynana	beige	yellow	yellow	CRISPR	0.96	4.446	0.611	0.18	1.872
Nymphalidae	Bicyclus anynana	beige	yellow	yellow	CRISPR	0.876	4.221	0.618	0.174	1.783
Nymphalidae	Bicyclus anynana	beige	yellow	yellow	CRISPR	0.751	3.985	0.595	0.217	1.725

Nymphalidae	Bicyclus anynana	beige	yellow	yellow	CRISPR	1.048	4.464	0.661	0.13	1.807
Nymphalidae	Bicyclus anynana	beige	yellow	yellow	CRISPR	1.15E+00	4.677	0.66	0.167	1.671
Nymphalidae	Bicyclus anynana	beige	yellow	yellow	CRISPR	8.88E-01	4.29	0.606	0.138	1.756
Nymphalidae	Bicyclus anynana	beige	yellow	yellow	CRISPR	0.906	4.266	0.625	0.175	1.726
Nymphalidae	Bicyclus anynana	beige	yellow	yellow	CRISPR	6.21E-01	3.841	0.529	0.192	1.679
Nymphalidae	Bicyclus anynana	beige	yellow	yellow	CRISPR	9.21E-01	4.65	0.535	0.202	1.807
Nymphalidae	Bicyclus anynana	beige	yellow	yellow	CRISPR	9.00E-01	4.289	0.615	0.165	1.652
Nymphalidae	Bicyclus anynana	beige	yellow	yellow	CRISPR	7.15E-01	4.16	0.519	0.175	1.725
Nymphalidae	Bicyclus anynana	beige	yellow	yellow	CRISPR	6.88E-01	4.178	0.495	0.174	1.62
Nymphalidae	Bicyclus anynana	beige	yellow	yellow	CRISPR	0.894	4.164	0.648	0.22	1.708
Nymphalidae	Bicyclus anynana	white	yellow	yellow	CRISPR	0.454	3.174	0.566	0.154	1.45
Nymphalidae	Bicyclus anynana	white	yellow	yellow	CRISPR	0.323	2.844	0.502	0.14	1.487
Nymphalidae	Bicyclus anynana	white	yellow	yellow	CRISPR	0.553	3.553	0.551	0.184	1.459
Nymphalidae	Bicyclus anynana	white	yellow	yellow	CRISPR	0.435	2.976	0.618	0.156	1.48
Nymphalidae	Bicyclus anynana	white	yellow	yellow	CRISPR	0.503	3.25	0.599	0.133	1.487
Nymphalidae	Bicyclus anynana	white	yellow	yellow	CRISPR	0.472	2.918	0.697	0.168	1.468
Nymphalidae	Bicyclus anynana	white	yellow	yellow	CRISPR	0.503	3.234	0.605	0.179	1.534
Nymphalidae	Bicyclus anynana	white	yellow	yellow	CRISPR	0.438	3.086	0.578	0.168	1.459
Nymphalidae	Bicyclus anynana	white	yellow	yellow	CRISPR	0.357	2.505	0.716	0.194	1.412
Nymphalidae	Bicyclus anynana	white	yellow	yellow	CRISPR	0.429	2.532	0.84	0.21	1.478
Nymphalidae	Bicyclus anynana	white	yellow	yellow	CRISPR	0.41	2.786	0.664	0.205	1.449
Nymphalidae	Bicyclus anynana	white	yellow	yellow	CRISPR	3.64E-01	2.348	0.829	0.184	1.403
Nymphalidae	Bicyclus anynana	white	yellow	yellow	CRISPR	2.55E-01	2.753	0.423	0.182	1.515
Nymphalidae	Bicyclus anynana	white	yellow	yellow	CRISPR	0.283	2.304	0.669	0.158	1.357
Nymphalidae	Bicyclus anynana	white	yellow	yellow	CRISPR	3.11E-01	2.454	0.649	0.139	1.348
Nymphalidae	Bicyclus anynana	white	yellow	yellow	CRISPR	3.29E-01	2.533	0.645	0.188	1.505
Nymphalidae	Bicyclus anynana	white	yellow	yellow	CRISPR	4.51E-01	2.734	0.757	0.169	1.468
Nymphalidae	Bicyclus anynana	white	yellow	yellow	CRISPR	3.39E-01	2.367	0.76	0.157	1.442
Nymphalidae	Bicyclus anynana	white	yellow	yellow	CRISPR	4.57E-01	3.164	0.574	0.175	1.459
Nymphalidae	Bicyclus anynana	white	yellow	yellow	CRISPR	0.398	2.799	0.638	0.175	1.459
Nymphalidae	Bicyclus anynana	black	grey	DDC	CRISPR	0.333	2.833	0.521	0.165	1.124
Nymphalidae	Bicyclus anynana	black	grey	DDC	CRISPR	0.463	3.098	0.607	0.086	1.338
Nymphalidae	Bicyclus anynana	black	grey	DDC	CRISPR	0.224	3.113	0.29	0.208	1.283
Nymphalidae	Bicyclus anynana	black	grey	DDC	CRISPR	0.805	3.342	0.906	0.177	1.32
Nymphalidae	Bicyclus anynana	black	grey	DDC	CRISPR	0.242	2.832	0.38	0.149	1.162
Nymphalidae	Bicyclus anynana	black	grey	DDC	CRISPR	0.14	2.273	0.34	0.168	1.432
Nymphalidae	Bicyclus anynana	black	grey	DDC	CRISPR	0.5	2.7	0.863	0.168	0.967
Nymphalidae	Bicyclus anynana	black	grey	DDC	CRISPR	0.255	2.646	0.457	0.168	1.255
Nymphalidae	Bicyclus anynana	black	grey	DDC	CRISPR	0.255	2.675	0.448	0.132	1.329
Nymphalidae	Bicyclus anynana	black	grey	DDC	CRISPR	0.482	3.474	0.502	0.186	1.366
Nymphalidae	Bicyclus anynana	black	grey	DDC	CRISPR	0.441	2.873	0.672	0.133	1.256
Nymphalidae	Bicyclus anynana	black	grey	DDC	CRISPR	3.98E-01	2.872	0.606	0.145	1.108
Nymphalidae	Bicyclus anynana	black	grey	DDC	CRISPR	4.23E-01	3.374	0.467	0.201	1.273
Nymphalidae	Bicyclus anynana	black	grey	DDC	CRISPR	0.42	3.209	0.512	0.204	1.357
Nymphalidae	Bicyclus anynana	black	grey	DDC	CRISPR	4.10E-01	3.412	0.443	0.195	1.385
Nymphalidae	Bicyclus anynana	black	grey	DDC	CRISPR	2.11E-01	2.255	0.522	0.168	1.264
Nymphalidae	Bicyclus anynana	black	grey	DDC	CRISPR	2.36E-01	2.806	0.377	0.15	1.18
Nymphalidae	Bicyclus anynana	black	grey	DDC	CRISPR	6.00E-01	3.026	0.823	0.195	1.218
Nymphalidae	Bicyclus anynana	black	grey	DDC	CRISPR	1.34E-01	2.6	0.248	0.149	1.113
Nymphalidae	Bicyclus anynana	black	grey	DDC	CRISPR	0.168	2.829	0.263	0.168	1.1
Nymphalidae	Bicyclus anynana	black	grey	DDC	CRISPR	4.10E-01	3.118	0.53	0.187	1.181
Nymphalidae	Bicyclus anynana	brown	white	DDC	CRISPR	1.433	5.36	0.627	0.301	2.205
Nymphalidae	Bicyclus anynana	brown	white	DDC	CRISPR	1.097	5.243	0.501	0.256	2.052
Nymphalidae	Bicyclus anynana	brown	white	DDC	CRISPR	1.364	4.921	0.708	0.178	2.051
Nymphalidae	Bicyclus anynana	brown	white	DDC	CRISPR	0.426	4.675	0.245	0.195	1.882
Nymphalidae	Bicyclus anynana	brown	white	DDC	CRISPR	1.57	5.543	0.642	0.125	2.149
Nymphalidae	Bicyclus anynana	brown	white	DDC	CRISPR	1.063	4.726	0.598	0.321	2.244
Nymphalidae	Bicyclus anynana	brown	white	DDC	CRISPR	1.147	5.376	0.499	0.252	2.37
Nymphalidae	Bicyclus anynana	brown	white	DDC	CRISPR	1.51	5.015	0.755	0.298	2.16
Nymphalidae	Bicyclus anynana	brown	white	DDC	CRISPR	0.768	4.901	0.402	0.349	2.191
Nymphalidae	Bicyclus anynana	brown	white	DDC	CRISPR	1.035	4.952	0.53	0.313	2.153
Nymphalidae	Bicyclus anynana	brown	white	DDC	CRISPR	0.519	4.956	0.266	0.268	2.24
Nymphalidae	Bicyclus anynana	brown	white	DDC	CRISPR	3.67E-01	5.656	0.144	0.339	2.133
Nymphalidae	Bicyclus anynana	brown	white	DDC	CRISPR	9.91E-01	4.97	0.504	0.197	2.244
Nymphalidae	Bicyclus anynana	brown	white	DDC	CRISPR	0.845	5.031	0.42	0.181	2.175
Nymphalidae	Bicyclus anynana	brown	white	DDC	CRISPR	1.32E+00	5.401	0.566	0.181	2.286
Nymphalidae	Bicyclus anynana	brown	white	DDC	CRISPR	9.91E-01	5.14	0.472	0.195	2.204
Nymphalidae	Bicyclus anynana	brown	white	DDC	CRISPR	9.63E-01	4.884	0.508	0.294	2.206
Nymphalidae	Bicyclus anynana	brown	white	DDC	CRISPR	1.32E+00	5.148	0.626	0.237	2.107
Nymphalidae	Bicyclus anynana	brown	white	DDC	CRISPR	1.20E+00	5.46	0.504	0.362	2.039
Nymphalidae	Bicyclus anynana	brown	white	DDC	CRISPR	1.507	5.115	0.724	0.197	2.428
Nymphalidae	Bicyclus anynana	gold	yellow	DDC	CRISPR	1.085	4.623	0.638	0.168	1.771

Nymphalidae	Bicyclus anynana	gold	yellow	DDC	CRISPR	0.463	4.319	0.312	0.179	1.783
Nymphalidae	Bicyclus anynana	gold	yellow	DDC	CRISPR	0.796	4.266	0.549	0.177	1.742
Nymphalidae	Bicyclus anynana	gold	yellow	DDC	CRISPR	0.65	3.79	0.568	0.168	1.87
Nymphalidae	Bicyclus anynana	gold	yellow	DDC	CRISPR	0.889	4.451	0.564	0.192	1.901
Nymphalidae	Bicyclus anynana	gold	yellow	DDC	CRISPR	0.668	4.273	0.46	0.224	1.807
Nymphalidae	Bicyclus anynana	gold	yellow	DDC	CRISPR	0.911	4.358	0.602	0.186	1.823
Nymphalidae	Bicyclus anynana	gold	yellow	DDC	CRISPR	1.066	4.639	0.622	0.149	1.831
Nymphalidae	Bicyclus anynana	gold	yellow	DDC	CRISPR	0.957	4.266	0.661	0.177	1.879
Nymphalidae	Bicyclus anynana	gold	yellow	DDC	CRISPR	0.761	4.819	0.412	0.205	1.728
Nymphalidae	Bicyclus anynana	gold	yellow	DDC	CRISPR	0.678	4.055	0.518	0.15	1.786
Nymphalidae	Bicyclus anynana	gold	yellow	DDC	CRISPR	1.09E+00	4.768	0.6	0.183	1.793
Nymphalidae	Bicyclus anynana	gold	yellow	DDC	CRISPR	9.01E-01	4.297	0.613	0.142	1.803
Nymphalidae	Bicyclus anynana	gold	yellow	DDC	CRISPR	0.656	3.831	0.561	0.337	1.868
Nymphalidae	Bicyclus anynana	gold	yellow	DDC	CRISPR	6.50E-01	3.791	0.568	0.142	1.85
Nymphalidae	Bicyclus anynana	gold	yellow	DDC	CRISPR	9.42E-01	4.608	0.557	0.26	1.582
Nymphalidae	Bicyclus anynana	gold	yellow	DDC	CRISPR	9.32E-01	4.527	0.572	0.286	2.165
Nymphalidae	Bicyclus anynana	gold	yellow	DDC	CRISPR	6.40E-01	4.269	0.442	0.224	2.346
Nymphalidae	Bicyclus anynana	gold	yellow	DDC	CRISPR	9.88E-01	4.61	0.584	0.255	2.448
Nymphalidae	Bicyclus anynana	gold	yellow	DDC	CRISPR	0.988	4.754	0.55	0.231	2.177
Nymphalidae	Bicyclus anynana	beige	white	DDC	CRISPR	1.576	5.24	0.721	0.227	2.132
Nymphalidae	Bicyclus anynana	beige	white	DDC	CRISPR	1.159	5.635	0.459	0.168	2.174
Nymphalidae	Bicyclus anynana	beige	white	DDC	CRISPR	1.594	5.322	0.707	0.194	2.066
Nymphalidae	Bicyclus anynana	beige	white	DDC	CRISPR	0.674	4.791	0.369	0.154	2.063
Nymphalidae	Bicyclus anynana	beige	white	DDC	CRISPR	1.274	4.634	0.746	0.195	2.021
Nymphalidae	Bicyclus anynana	beige	white	DDC	CRISPR	0.951	4.721	0.536	0.142	2.021
Nymphalidae	Bicyclus anynana	beige	white	DDC	CRISPR	1.05	4.558	0.636	0.139	1.951
Nymphalidae	Bicyclus anynana	beige	white	DDC	CRISPR	0.948	4.812	0.514	0.19	2.049
Nymphalidae	Bicyclus anynana	beige	white	DDC	CRISPR	1.234	5.187	0.576	0.211	2.063
Nymphalidae	Bicyclus anynana	beige	white	DDC	CRISPR	0.97	4.943	0.499	0.21	2.035
Nymphalidae	Bicyclus anynana	beige	white	DDC	CRISPR	1.377	5.145	0.654	0.461	2.119
Nymphalidae	Bicyclus anynana	beige	white	DDC	CRISPR	7.89E-01	4.558	0.478	0.237	2.135
Nymphalidae	Bicyclus anynana	beige	white	DDC	CRISPR	8.70E-01	4.819	0.471	0.168	2.105
Nymphalidae	Bicyclus anynana	beige	white	DDC	CRISPR	1.016	4.497	0.631	0.139	2.01
Nymphalidae	Bicyclus anynana	beige	white	DDC	CRISPR	1.51E+00	5.757	0.574	0.21	2.05
Nymphalidae	Bicyclus anynana	beige	white	DDC	CRISPR	2.02E+00	5.318	0.899	0.195	2.021
Nymphalidae	Bicyclus anynana	beige	white	DDC	CRISPR	4.72E-01	5.17	0.222	0.251	1.952
Nymphalidae	Bicyclus anynana	beige	white	DDC	CRISPR	1.01E+00	4.767	0.557	0.227	1.94
Nymphalidae	Bicyclus anynana	beige	white	DDC	CRISPR	1.19E+00	5.3	0.533	0.153	1.927
Nymphalidae	Bicyclus anynana	beige	white	DDC	CRISPR	1.063	4.887	0.559	0.101	1.996
Pieridae	Colias crocea	white	orange	BarH-1	CRISPR	1.398	4.833	0.752	0.131	2.074
Pieridae	Colias crocea	white	orange	BarH-1	CRISPR	1.152	4.359	0.762	0.122	2.057
Pieridae	Colias crocea	white	orange	BarH-1	CRISPR	1.033	4.123	0.764	0.134	2.081
Pieridae	Colias crocea	white	orange	BarH-1	CRISPR	0.782	3.735	0.705	0.138	2.01
Pieridae	Colias crocea	white	orange	BarH-1	CRISPR	0.939	4.021	0.73	0.131	1.998
Pieridae	Colias crocea	white	orange	BarH-1	CRISPR	1.034	4.208	0.734	0.122	1.869
Pieridae	Colias crocea	white	orange	BarH-1	CRISPR	0.931	3.962	0.745	0.099	1.998
Pieridae	Colias crocea	white	orange	BarH-1	CRISPR	0.73	3.583	0.714	0.074	1.962
Pieridae	Colias crocea	white	orange	BarH-1	CRISPR	0.785	3.611	0.756	0.122	1.987
Pieridae	Colias crocea	white	orange	BarH-1	CRISPR	0.717	3.518	0.728	0.114	2.025
Pieridae	Colias crocea	white	orange	BarH-1	CRISPR	0.96	4.05	0.735	0.13	1.993
Pieridae	Colias crocea	white	orange	BarH-1	CRISPR	9.62E-01	4.07	0.73	0.155	1.957
Pieridae	Colias crocea	white	orange	BarH-1	CRISPR	1.03E+00	4.207	0.728	0.106	1.914
Pieridae	Colias crocea	white	orange	BarH-1	CRISPR	0.812	3.712	0.741	0.138	1.88
Pieridae	Colias crocea	white	orange	BarH-1	CRISPR	6.80E-01	3.399	0.74	0.14	1.861
Pieridae	Colias crocea	white	white	BarH-1	CRISPR	1.814	5.85	0.666	0.188	2.243
Pieridae	Colias crocea	white	white	BarH-1	CRISPR	1.561	5.087	0.758	0.163	2.231
Pieridae	Colias crocea	white	white	BarH-1	CRISPR	1.693	5.09	0.821	0.157	2.331
Pieridae	Colias crocea	white	white	BarH-1	CRISPR	1.639	5.5	0.681	0.177	2.251
Pieridae	Colias crocea	white	white	BarH-1	CRISPR	1.418	4.665	0.819	0.221	2.27
Pieridae	Colias crocea	white	white	BarH-1	CRISPR	1.199	4.715	0.678	0.188	2.237
Pieridae	Colias crocea	white	white	BarH-1	CRISPR	1.721	5.412	0.738	0.145	2.18
Pieridae	Colias crocea	white	white	BarH-1	CRISPR	1.064	4.27	0.733	0.226	2.249
Pieridae	Colias crocea	white	white	BarH-1	CRISPR	1.179	4.366	0.777	0.172	2.141
Pieridae	Colias crocea	orange	white		chemical removal c	1.065	4.107	0.793	0.26	1.986
Pieridae	Colias crocea	orange	white		chemical removal c	1.19	4.179	0.856	0.272	1.93
Pieridae	Colias crocea	orange	white		chemical removal c	1.079	4.189	0.773	0.179	1.886
Pieridae	Colias crocea	orange	white		chemical removal c	0.92	3.819	0.792	0.165	1.799
Pieridae	Colias crocea	orange	white		chemical removal c	1.987	5.364	0.868	0.19	1.794
Pieridae	Colias crocea	orange	white		chemical removal c	0.94	3.791	0.822	0.253	1.804
Pieridae	Colias crocea	orange	white		chemical removal c	0.443	2.951	0.639	0.168	1.834
Pieridae	Colias crocea	orange	white		chemical removal c	0.617	3.069	0.824	0.165	1.706
Nymphalidae	Heliconius cydno	black	brown	AI1	CRISPR	0.459	2.558	0.882	0.373	2.298

Nymphalidae	Heliconius cydno	black	brown	Al1	CRISPR	0.382	2.412	0.824	0.152	2.31
Nymphalidae	Heliconius cydno	black	brown	Al1	CRISPR	0.435	2.586	0.818	0.212	2.224
Nymphalidae	Heliconius cydno	black	brown	Al1	CRISPR	0.384	2.512	0.764	0.2	2.057
Nymphalidae	Heliconius cydno	black	brown	Al1	CRISPR	0.5	2.706	0.859	0.251	2.014
Nymphalidae	Heliconius cydno	black	brown	Al1	CRISPR	0.378	2.462	0.785	0.278	2.015
Nymphalidae	Heliconius cydno	black	brown	Al1	CRISPR	0.648	2.92	0.955	0.513	2.036
Nymphalidae	Heliconius cydno	black	brown	Al1	CRISPR	0.156	1.65	0.718	0.222	2.077
Nymphalidae	Heliconius cydno	black	brown	Al1	CRISPR	0.461	2.523	0.911	0.202	2.097
Nymphalidae	Heliconius cydno	black	brown	Al1	CRISPR	0.418	2.568	0.796	0.205	2.292
Nymphalidae	Heliconius cydno	black	brown	Al1	CRISPR	0.472	3.027	0.648	0.259	2.38
Nymphalidae	Heliconius cydno	black	brown	Al1	CRISPR	3.51E-01	2.826	0.553	0.252	2.468
Nymphalidae	Heliconius cydno	black	brown	Al1	CRISPR	3.47E-01	2.552	0.67	0.233	1.875
Nymphalidae	Heliconius cydno	black	brown	Al1	CRISPR	0.774	3.226	0.934	0.272	1.704
Nymphalidae	Heliconius cydno	black	brown	Al1	CRISPR	5.29E-01	2.857	0.815	0.214	1.787
Nymphalidae	Heliconius cydno	black	brown	Al1	CRISPR	5.70E-01	2.989	0.801	0.204	1.972
Nymphalidae	Heliconius cydno	black	brown	Al1	CRISPR	8.16E-01	3.429	0.872	0.238	1.992
Nymphalidae	Heliconius cydno	black	brown	Al1	CRISPR	8.24E-01	3.511	0.84	0.255	1.838
Nymphalidae	Heliconius cydno	black	brown	Al1	CRISPR	5.24E-01	2.858	0.805	0.25	2.326
Nymphalidae	Heliconius cydno	black	brown	Al1	CRISPR	0.603	2.909	0.895	0.235	0.49

Table 5: Data on genetically modified or chemically altered butterfly scales

References

1. Abu-Shaar, M., Ryoo, H. D., & Mann, R. S. (1999). Control of the nuclear localization of Extradenticle by competing nuclear import and export signals. Genes & Development 13(8), 935-945.

2. Ando, T., & Fujiwara, H. (2012). Electroporation-mediated somatic transgenesis for rapid functional analysis in insects. Development, 140, 454-458.

3. Ando, T., Fujiwara, H., & Kojima, T. (2018). The pivotal role of aristaless in development and evolution of diverse antennal morphologies in moths and butterflies. BMC Evolutionary Biology, 18(8).

4. Beermann, A., & Schroder, R. (2004). Functional stability of the aristaless gene in appendage tip formation during evolution. Dev Gnes Evol 214, 303-308.

5. Brakefield, P. M., Beldade, P., & Zwaan, B. J. (2009). Fixation and dissection of embryos from the African butterfly Bicyclus anynana. Cold Spring Harbor Protocols, 4(5).

6. Campbell, G., & Tomlinson, A. (1988). The roles of the homeobox aristaless and Distal-less in patterning the legs and wings of Drosophila. Development 125, 4483-4493.

7. Campbell, G., Weaver, T., & Tomllnson, A. (1993). Axis Specification in the Developing Drosophila Appendage: The Role of wingless, decapentaplegic, and the Homeobox Gene aristaless . Cell 74, 1113-1123.

8. Carrel, J. E., & Nijhout, H. F. (1992). The Development and Evolution of Butterfly Wing Patterns. Annals of the Entomological Society of America, 85(6), 808–809. https://doi.org/10.1093/AESA/85.6.808

9. Chamberlain, N. L., Hill, R. I., Kapan, D. D., Gilbert, L. E., & Kronforst, M. (2009). Polymorphic butterfly reveals the missing link in ecological speciation . Science, 326 (5954), 847-850.

10. Davis, A. L., Nijhout, H. F., & Johnsen, S. (2020). Diverse nanostructures underlie thin ultra-black scales in butterflies. Nature Communications 2020 11:1, 11(1), 1–7. https://doi.org/10.1038/s41467-020-15033-1

11. Deshmukh, R., Baral, S., Gandhimathu, A., Kuwalekar, M., & Kunte, K. (2017). Mimicry in butterflies: co-option and a bag of magnificent developmental genetic tricks. Wires, Developmental Biology 7.

12. Dinwiddie, A., Null, R., Pizzano, M. C., Krup, L. A., & Patel, N. H. (2014). Dynamics of F-actin prefigure the structure of butterfly wing scales. Developmental Biology, 392, 404-418.

13. Fujiwara, H., & Nishikawa, H. (2016). Funtional analysis of gene involved in color pattern formation in lepidoptera. Corrent opinion in insect science, 17, 16-23.

14. Finkbeiner, S. D., Fishman, D. A., Osorio, D., & Briscoe, A. D. (2017). Ultraviolet and yellow reflectance but not fluorescence is important for visual discrimination of conspecifics by Heliconius erato. Journal of Experimental Biology, 220, 1267-1276. https://doi.org/10.1242/jeb.153593

15. Finkbeiner, S. D., & Briscoe, A. D. (2021). True UV color vision in a female butterfly with two UV opsins. The Journal of Experimental Biology, 224(18). https://doi.org/10.1242/JEB.242802

16. Galant, R., Skeath, J. B., Paddock, S., Lewis, D. L., & Carroll, S. B. (1998). Expression pattern of a butterfly achaete-scute homolog reveals the homology of butterfly wing scales and insect sensory bristles. Current Biology 8(14), 807-813.

17. Ghiradella, H. (1991). Light and color on the wing: structural colors in butterflies and moths. Applied Optics, Vol. 30, Issue 24, Pp. 3492-3500, 30(24), 3492–3500. https://doi.org/10.1364/AO.30.003492

18. Ghiradella, H. (2010). Insect Cuticular Surface Modifications: Scales and Other Structural Formations. Advances in Insect Physiology, 38(C), 135–180. https://doi.org/10.1016/S0065-2806(10)38006-4\

19. Gilbert, L. E., Forrest, H. S., Schultz, T. D., & Harvey, D. J. (1988). Correlation of Ultrastructure and Pigmentation Suggest How Genes Control Development of Wing Scales of Heliconius. Journal of Research on the Lepidoptera, 26, 141-160.

20. Hines, H. M., Papa, R., Ruiz, M., Papanicolaou, A., Wang, C., Nijhout, H. F., . . . Reed, R. D. (2012). Transcriptome analysis reveals novel patterning and pigmentation genes underlying Heliconius butterfly wing pattern variation. BMC Genomics, 13 (288).

21. Janssen, J. M., Monteiro, A., & Brakefield, P. M. (2001). Correlations between scale structure and pigmentation in butterfly wings. Evolution & Development, 3(6), 415–423. https://doi.org/10.1046/J.1525-142X.2001.01046.X

22. Koch, B. F., Lorenz, U., Brakefield, P. M., & ffrench-Constant, R. H. (2000). Butterfly wing pattern mutants: developmental heterochrony and co-ordinately regulated phenotypes . Dev Genes Evol, 210, 536-544.

23. Kronforst, M. R., Barsh, G. S., Kopp, A., Mallet, J., Monteiro, A., Mullen, S. P., Protas, M., Rosenblum, E. B., Schneider, C. J., & Hoekstra, H. E. (2012). Unraveling the thread of nature's tapestry: The genetics of diversity and convergence in animal pigmentation. Pigment Cell and Melanoma Research, 25(4), 411–433. https://doi.org/10.1111/J.1755-148X.2012.01014.X/FORMAT/PDF

24. Kronforst, M. R., & Papa, R. (2015). The Functional Basis of Wing Patterning in Heliconius Butterflies: The Molecules Behind Mimicry . Genetics, 200, 1-19.

25. Kronforst, M. R., Young, L. G., Kapan, D. D., McNeely, C., O'Neill, R. J., & Gilbert, L. E. (2006). Linkage of butterfly mate preference and wing color preference cue at the genomic location of wingless. PNAS, 103 (17), 6575-6580.

26. Künnapuu, J., Björkgren, I., & Shimmi, O. (2009). The Drosophila DPP signal is produced by cleavage of its proprotein at evolutionary diversified furin-recognition sites. PNAS, 106(21), 8501-8506.

27. Livraghi, L., Hanly, J. J., van Bellghem, S. M., Montejo-Kovacevich, G., van der Heijden, E. S. , … Jiggins, C. D. (2021). Cortex cis-regulatory switches establish scale color identity and pattern diversity in Heliconius. ELife, 10.

28. Mallarino, R., Henegar, C., Mirasierra, M., Manceau, M., Scharadin, C., Vallejo, B. S., . . . Hoekstra, H. E. (2016). Developmental Mechanisms of Stripe Patterns in Rodents . Nature, 539, 518-523.

29. Martin, A., & Reed, R. (2010). wingless and aristaless2 Define a Developmental Ground Plan fo Moth and Butterfly Wing Pattern Evolution. Mol. Biol. Evol., 27 (12), 2864-2878.

30. Martin, A., McCulloch, K. J., Patel, N. H., Briscoe, A. D., Gilbert, L. E., & Reed, R. D. (2014). Multiple recent co-options of Optix associated with novel traits in adaptive butterfly wing radiations. EvoDevo 5(7).

31. Martin, A., Papa, R., Nadeau, N. J., Hill, R. I., Counterman, B. A., Halder, G., . . . Reed, R. D. (2012). Diversification 0f complex butterfly wing patterns by repeated regulatory evolution of a Wnt ligand . PNAS, 109 (31), 12632-12637.

32. Mazo-Vargas, A., Concha, C., Livraghi, L., Massardo, D., Wallbank, R. W., Papador, J. D., . . . Martin, A. (2017). Macroevolutionary shifts of WntA function potentiate butterfly wing-pattern diversity . PNAS 114(40), 10701-10706.

33. McMillan, W. O., Livraghi, L., Concha, C., & Hanly, J. J. (2020). From Patterning Genes to Process: Unraveling the Gene Regulatory Networks That Pattern Heliconius Wings. *Frontiers in Ecology and Evolution*, *8*, 221. https://doi.org/10.3389/FEVO.2020.00221/BIBTEX

34. Miyawaki, K., Inoue, Y., Mito, T., Fujumoto, T., Matsushima, K., Shinmyo, Y., . . . Noji, S. (2002). Expression patterns of aristaless in developing appendages of Gryllus bimaculatus (cricket). Mechanisms of Development, 113, 181-184.

35. Moczek, A. P. (2005). The Evolution and Development of Novel Traits, or How Beetles Got Their Horns. BioScience, 55 (11), 937-951.

36. Nadeau, N. J. (2016). The gene cortex controls mimicry and crpsis in butterflies and moths. Nature, 534, 106-110.

37. Nijhout, F (1991). The Development and Evolution of Butterfly Wing Patterns. *Smithsonian Institution Scholarly Press*. https://doi.org/10.1086/417849

38. Oliveira, M. B., Liedholm, S. E., Lopez, J. E., Lochte, A. A., Pazio, M., Martin, J. P., Mörch, P.

39. R., Salakka, S., York, J., Yoshimoto, A., & Janssen, R. (2014). Expression of arthropod distal limb-patterning genes in the onychophoran Euperipatoides kanangrensis. Development Genes and Evolution, 224(2), 87–96. https://doi.org/10.1007/S00427-014-0466-Z

40. Ozawa, H., Ashizawa, S., Naito, M., Yanagihara, M., Ohnishi, N., Maeda, T., . . . Hatakeyama, M. (2004). Paired-like homeodomain protein ESXR1 possesses a cleavable C-terminal region that inhibits cyclin degradation. Oncogene, 23(39), 6590-6602.

41. Prum, R. O., Quinn, T., & Torres, R. H. (2006). Anatomically diverse butterfly scales all produce structural colours by coherent scattering. Journal of Experimental Biology, 209(4), 748–765. https://doi.org/10.1242/JEB.02051

42. Ramos, D., & Monteiro, A. (2007). In situ Protocol for Butterfly Pupal Wings Using Riboprobes . J Vis Exp., 4.

43. Reed, R. D., McMillan, W. O., & Nagy, L. M. (2008). Gene expression underlying adaptive variation inHeliconiuswing patterns: non-modular regulationof overlapping cinnabar and vermilion prepatterns. Proc. R. Soc. B 275, 37-45.

44. Reed, R. D., Papa, R., Martin, A., Hines, H. M., Counterman, B. A., Pardo-Díaz, C., . . . McMillan, W. O. (2011). optix Drives the Repeated Convergent Evolution of Butterfly Wing Pattern Mimicry . Science 333, 1137-1141.

45. Schneitz, K., Spielmann, P., & Noll, M. (1993). Molecular genetics of aristaless, a prd-type homeo box gene involved in the morphogenesis of proximal and distal pattern elements in a subset of appendages in Drosophila. Genes and Development 7(1), 114-129.

46. Tajiri, R., Tsuji, T., Ueda, R., Saigo, K., & Kojima, T. (2007). Fate determination of Drosophila leg distal regions by trachealess and tango through repression and stimulation, respectively, of Bar homeobox gene expression in the future pretarsus and tarsus. *Developmental Biology*, *303*(2), 461–473. https://doi.org/10.1016/J.YDBIO.2006.11.026

47. Van Belleghem, S. M., Rastas, P., Papanicolaou, A., Martin, S. H., Arias, C. F., Supple, M. A., . . . Papa, R. (2017). Complex modular architecture around a simple toolkit of wing pattern genes. Nature ecology & evolution, 1, 1-12.

48. Westerman, E., VanKuren, N., Massardo, D., Tenger-Trolander, A., Zhang, W., Hill, R. I., . . . Kronforst, M. R. (2018). Aristaless Controls Butterfly Wing Color Variation Used in Mimicry and Mate Choice. Current Biology 28(21), 3469-3474.

49. Wittkopp, P. J., & Beldade, P. (2009). Development and evolution of insect pigmentation: Genetic mechanisms and the potential consequences of pleiotropy. *Seminars in Cell & Developmental Biology*, *20*, 65–71. https://doi.org/10.1016/j.semcdb.2008.10.002

50. Zhang, L., Mazo-Vargas, A., & Reed, R. D. (2017). Single master regulatory gene coordinates the evolution and development of butterfly color and iridescence. PNAS 114(40), 10707-10712.